

Volume 219

David M. Whitacre *Editor*

Reviews of Environmental Contamination and Toxicology

 Springer

Reviews of
Environmental Contamination
and Toxicology

VOLUME 219

For further volumes:
<http://www.springer.com/series/398>

Reviews of Environmental Contamination and Toxicology

Editor
David M. Whitacre

Editorial Board

Maria Fernanda Cavieres, Valparaiso, Chile • Charles P. Gerba, Tucson, Arizona, USA
John Giesy, Saskatoon, Saskatchewan, Canada • O. Hutzinger, Bayreuth, Germany
James B. Knaak, Getzville, New York, USA
James T. Stevens, Winston-Salem, North Carolina, USA
Ronald S. Tjeerdema, Davis, California, USA • Pim de Voogt, Amsterdam, The Netherlands
George W. Ware, Tucson, Arizona, USA

Founding Editor
Francis A. Gunther

VOLUME 219

 Springer

Coordinating Board of Editors

DR. DAVID M. WHITACRE, *Editor*
Reviews of Environmental Contamination and Toxicology

5115 Bunch Road
Summerfield, North Carolina 27358, USA
(336) 634-2131 (PHONE and FAX)
E-mail: dmwhitacre@triad.rr.com

DR. HERBERT N. NIGG, *Editor*
Bulletin of Environmental Contamination and Toxicology

University of Florida
700 Experiment Station Road
Lake Alfred, Florida 33850, USA
(863) 956-1151; FAX (941) 956-4631
E-mail: hnn@LAL.UFL.edu

DR. DANIEL R. DOERGE, *Editor*
Archives of Environmental Contamination and Toxicology

7719 12th Street
Paron, Arkansas 72122, USA
(501) 821-1147; FAX (501) 821-1146
E-mail: AECT_editor@earthlink.net

ISSN 0179-5953

ISBN 978-1-4614-3280-7

e-ISBN 978-1-4614-3281-4

DOI 10.1007/978-1-4614-3281-4

Springer New York Dordrecht Heidelberg London

© Springer Science+Business Media, LLC 2012

All rights reserved. This work may not be translated or copied in whole or in part without the written permission of the publisher (Springer Science+Business Media, LLC, 233 Spring Street, New York, NY 10013, USA), except for brief excerpts in connection with reviews or scholarly analysis. Use in connection with any form of information storage and retrieval, electronic adaptation, computer software, or by similar or dissimilar methodology now known or hereafter developed is forbidden.

The use in this publication of trade names, trademarks, service marks, and similar terms, even if they are not identified as such, is not to be taken as an expression of opinion as to whether or not they are subject to proprietary rights.

Printed on acid-free paper

Springer is part of Springer Science+Business Media (www.springer.com)

Foreword

International concern in scientific, industrial, and governmental communities over traces of xenobiotics in foods and in both abiotic and biotic environments has justified the present triumvirate of specialized publications in this field: comprehensive reviews, rapidly published research papers and progress reports, and archival documentations. These three international publications are integrated and scheduled to provide the coherency essential for nonduplicative and current progress in a field as dynamic and complex as environmental contamination and toxicology. This series is reserved exclusively for the diversified literature on “toxic” chemicals in our food, our feeds, our homes, recreational and working surroundings, our domestic animals, our wildlife, and ourselves. Tremendous efforts worldwide have been mobilized to evaluate the nature, presence, magnitude, fate, and toxicology of the chemicals loosed upon the Earth. Among the sequelae of this broad new emphasis is an undeniable need for an articulated set of authoritative publications, where one can find the latest important world literature produced by these emerging areas of science together with documentation of pertinent ancillary legislation.

Research directors and legislative or administrative advisers do not have the time to scan the escalating number of technical publications that may contain articles important to current responsibility. Rather, these individuals need the background provided by detailed reviews and the assurance that the latest information is made available to them, all with minimal literature searching. Similarly, the scientist assigned or attracted to a new problem is required to glean all literature pertinent to the task, to publish new developments or important new experimental details quickly, to inform others of findings that might alter their own efforts, and eventually to publish all his/her supporting data and conclusions for archival purposes.

In the fields of environmental contamination and toxicology, the sum of these concerns and responsibilities is decisively addressed by the uniform, encompassing, and timely publication format of the Springer triumvirate:

Reviews of Environmental Contamination and Toxicology [Vol. 1 through 97 (1962–1986) as Residue Reviews] for detailed review articles concerned

with any aspects of chemical contaminants, including pesticides, in the total environment with toxicological considerations and consequences.

Bulletin of Environmental Contamination and Toxicology (Vol. 1 in 1966) for rapid publication of short reports of significant advances and discoveries in the fields of air, soil, water, and food contamination and pollution as well as methodology and other disciplines concerned with the introduction, presence, and effects of toxicants in the total environment.

Archives of Environmental Contamination and Toxicology (Vol. 1 in 1973) for important complete articles emphasizing and describing original experimental or theoretical research work pertaining to the scientific aspects of chemical contaminants in the environment.

Manuscripts for Reviews and the Archives are in identical formats and are peer reviewed by scientists in the field for adequacy and value; manuscripts for the Bulletin are also reviewed, but are published by photo-offset from camera-ready copy to provide the latest results with minimum delay. The individual editors of these three publications comprise the joint Coordinating Board of Editors with referral within the board of manuscripts submitted to one publication but deemed by major emphasis or length more suitable for one of the others.

Coordinating Board of Editors

Preface

The role of Reviews is to publish detailed scientific review articles on all aspects of environmental contamination and associated toxicological consequences. Such articles facilitate the often complex task of accessing and interpreting cogent scientific data within the confines of one or more closely related research fields.

In the nearly 50 years since *Reviews of Environmental Contamination and Toxicology* (formerly *Residue Reviews*) was first published, the number, scope, and complexity of environmental pollution incidents have grown unabated. During this entire period, the emphasis has been on publishing articles that address the presence and toxicity of environmental contaminants. New research is published each year on a myriad of environmental pollution issues facing people worldwide. This fact, and the routine discovery and reporting of new environmental contamination cases, creates an increasingly important function for *Reviews*.

The staggering volume of scientific literature demands remedy by which data can be synthesized and made available to readers in an abridged form. Reviews addresses this need and provides detailed reviews worldwide to key scientists and science or policy administrators, whether employed by government, universities, or the private sector.

There is a panoply of environmental issues and concerns on which many scientists have focused their research in past years. The scope of this list is quite broad, encompassing environmental events globally that affect marine and terrestrial ecosystems; biotic and abiotic environments; impacts on plants, humans, and wildlife; and pollutants, both chemical and radioactive; as well as the ravages of environmental disease in virtually all environmental media (soil, water, air). New or enhanced safety and environmental concerns have emerged in the last decade to be added to incidents covered by the media, studied by scientists, and addressed by governmental and private institutions. Among these are events so striking that they are creating a paradigm shift. Two in particular are at the center of everincreasing media as well as scientific attention: bioterrorism and global warming. Unfortunately, these very worrisome issues are now superimposed on the already extensive list of ongoing environmental challenges.

The ultimate role of publishing scientific research is to enhance understanding of the environment in ways that allow the public to be better informed. The term “informed public” as used by Thomas Jefferson in the age of enlightenment conveyed the thought of soundness and good judgment. In the modern sense, being “well informed” has the narrower meaning of having access to sufficient information. Because the public still gets most of its information on science and technology from TV news and reports, the role for scientists as interpreters and brokers of scientific information to the public will grow rather than diminish. Environmentalism is the newest global political force, resulting in the emergence of multinational consortia to control pollution and the evolution of the environmental ethic. Will the new politics of the twenty-first century involve a consortium of technologists and environmentalists, or a progressive confrontation? These matters are of genuine concern to governmental agencies and legislative bodies around the world.

For those who make the decisions about how our planet is managed, there is an ongoing need for continual surveillance and intelligent controls to avoid endangering the environment, public health, and wildlife. Ensuring safety-in-use of the many chemicals involved in our highly industrialized culture is a dynamic challenge, for the old, established materials are continually being displaced by newly developed molecules more acceptable to federal and state regulatory agencies, public health officials, and environmentalists.

Reviews publishes synoptic articles designed to treat the presence, fate, and, if possible, the safety of xenobiotics in any segment of the environment. These reviews can be either general or specific, but properly lie in the domains of analytical chemistry and its methodology, biochemistry, human and animal medicine, legislation, pharmacology, physiology, toxicology, and regulation. Certain affairs in food technology concerned specifically with pesticide and other food-additive problems may also be appropriate.

Because manuscripts are published in the order in which they are received in final form, it may seem that some important aspects have been neglected at times. However, these apparent omissions are recognized, and pertinent manuscripts are likely in preparation or planned. The field is so very large and the interests in it are so varied that the editor and the editorial board earnestly solicit authors and suggestions of underrepresented topics to make this international book series yet more useful and worthwhile.

Justification for the preparation of any review for this book series is that it deals with some aspect of the many real problems arising from the presence of foreign chemicals in our surroundings. Thus, manuscripts may encompass case studies from any country. Food additives, including pesticides, or their metabolites that may persist into human food and animal feeds are within this scope. Additionally, chemical contamination in any manner of air, water, soil, or plant or animal life is within these objectives and their purview.

Manuscripts are often contributed by invitation. However, nominations for new topics or topics in areas that are rapidly advancing are welcome. Preliminary communication with the editor is recommended before volunteered review manuscripts are submitted.

Contents

Parameters for Pyrethroid Insecticide QSAR and PBPK/PD Models for Human Risk Assessment	1
James B. Knaak, Curtis C. Dary, Xiaofei Zhang, Robert W. Gerlach, R. Tornero-Velez, Daniel T. Chang, Rocky Goldsmith, and Jerry N. Blancato	
Appendix A: Nomenclature	115
Appendix B: Pyrethroids, Pyrethroids Isomers and Technical Products	121
Appendix C: Chromatographic Separation of Pyrethroids and Their Isomers	131
Appendix D: Chemical Structures, Physical Parameters, and Tissue: Partition Coefficients of Parent Pyrethroids and Metabolites	141
Appendix E: Metabolic Pathways and Preliminary Metabolic Rate Constants (V_{max} and K_m) for the Metabolism of Parent Pyrethroids and Metabolites	213
Appendix F: Allethrin PBPK/PD Model	251
Index	253

Parameters for Pyrethroid Insecticide QSAR and PBPK/PD Models for Human Risk Assessment

James B. Knaak, Curtis C. Dary, Xiaofei Zhang,
Robert W. Gerlach, R. Tornero-Velez, Daniel T. Chang,
Rocky Goldsmith, and Jerry N. Blancato

1 Introduction

This pyrethroid insecticide parameter review is an extension of our interest in developing quantitative structure–activity relationship–physiologically based pharmacokinetic/pharmacodynamic (QSAR-PBPK/PD) models for assessing health risks, which interest started with the organophosphorus (OP) and carbamate insecticides (Knaak et al. 2004, 2008). The parameters shown in Table 1 (Blancato et al. 2000) are needed for developing pyrethroid PBPK/PD models, as is information on the metabolic pathways of specific pyrethroids in laboratory test animals and humans. Parameters may be obtained by fitting the output from models to experimental data gathered from in vivo studies (Zhang et al. 2007; Nong et al. 2008), in conjunction with using (1) experimental data obtained from in vitro studies, (2) quantitative structure–activity relationships (QSAR) and (3) other mathematical models, such as the mechanistic Poulin-Theil (2000; 2002a; b) algorithms for obtaining blood:tissue partition coefficients.

J.B. Knaak (✉)

Department of Pharmacology and Toxicology, School of Medicine and Biomedical Sciences,
SUNY at Buffalo, 3435 Main Street, Buffalo, NY 14214, USA
e-mail: jbknaak@aol.com

C.C. Dary

Human Exposure and Atmospheric Sciences Division, U.S. Environmental Protection Agency,
944 East Harmon Avenue, Las Vegas, NV 89193-3478, USA

X. Zhang • R.W. Gerlach

General Dynamics Information Technology, 181 North Arroyo Grande Boulevard, Suite 105A,
Henderson, NV 89074-1624, USA

R. Tornero-Velez • D.T. Chang • R. Goldsmith • J.N. Blancato

National Exposure Research Laboratory, U.S. Environmental Protection Agency, 109 T.W.
Alexander Drive, Research Triangle Park, NC 27709, USA

Table 1 Biological parameters required for pyrethroid insecticide physiologically based pharmacokinetic/pharmacodynamic (PBPK/PD) models^a

Biological process	Compartment	Parameter	Units
Absorption	GI tract		h^{-1}
	Respiratory tract	Blood: air PC ^b	Unitless
	Skin	Permeability constant	$\text{cm} \cdot \text{h}^{-1}$
Distribution	Desired compartments	Blood: tissue PC ^b	Unitless
Metabolism, P450 Cytochromes, etc.	Liver	V_{\max}	$\mu\text{mol} \cdot \text{h}^{-1} \cdot \text{kg}^{-1} \text{ bwt}^c$
		K_m	$\mu\text{mol} \cdot \text{kg}^{-1}$
Excretion	Kidney	V_{\max}	$\mu\text{mol} \cdot \text{h}^{-1} \cdot \text{kg}^{-1} \text{ bwt}^c$
		K_m	$\mu\text{mol} \cdot \text{kg}^{-1}$
Toxicity	Central and peripheral nervous systems, Heart	Inhibition of VGSC	$\mu\text{mol} \cdot \text{kg}^{-1} \text{ bwt}$

Please refer to Appendix A, Table A1 for definitions of acronyms and abbreviations, and Table A2 for a key to chemical and mathematical expressions

^a Source: Blancato et al. (2000), revised for pyrethroids

^b PC partition coefficients

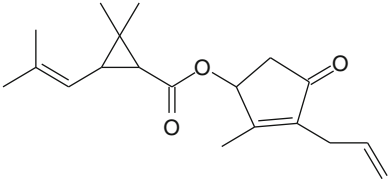
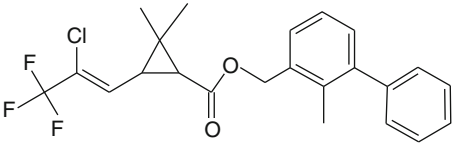
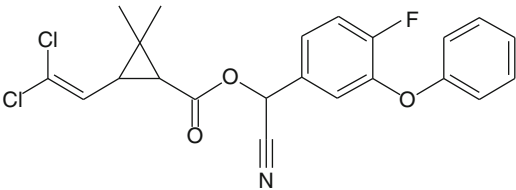
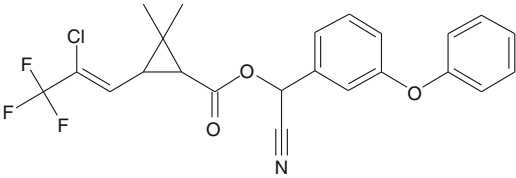
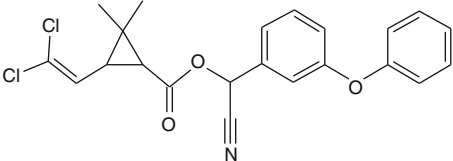
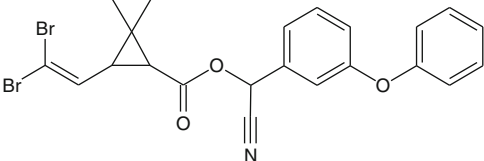
^c bwt body weight

In this review, we have concentrated on the development of (1) *in vivo* metabolic data (i.e., V_{\max} and K_m , etc.), (2) QSAR, and (3) mechanistic models and their application for building PBPK/PD models. The development of the pyrethroid insecticides for agricultural and home use is complicated by their chemistry, in that they each possess one to four chiral centers, increasing the number of isomeric forms by a factor of 2^n (where n = the number of chiral centers). Isomer mixtures and individual isomers are commonly both subjected to testing for insecticidal activity. The fewer the number of active forms, the easier it is to test them for insecticidal activity, toxicity, and to build PBPK/PD models for them. The pyrethroids on which we focus in this review are presented in Table 2, along with their trivial and CAS names and their structures. Table A1 (Appendix A) defines the acronyms and abbreviations used in the text, while Table A2 (Appendix A) defines the chemical and mathematical expressions that are presented in this review.

2 Nature of Pyrethrin and Pyrethroid Insecticides

LaForge and Haller (1936) were the first to elucidate the structure of natural pyrethrum, in which they demonstrated constituted esters of chrysanthemic acid (CA). The natural pyrethrins (I and II), depicted in Figs. 1 and 2, are structures comprised of cyclopropanecarboxylic acids esterified with alkenylmethyl cyclopentenolones. All natural pyrethrins contain the cyclopropanecarboxylic acid moiety that is substituted in various ways at the 3'-position of the cyclopropane ring (A position) and at the carboxylic acid (B position). Unlike the substituent at the A position (C-3 of cyclopropane ring), the gem-dimethyl at position C-2 of the ring is critical to insect toxicity. Pyrethrin I/II and allethrin (Figs. 1, 2 and Table 2 (2.1)) each contains a chiral carbon at the CH or 7'-position of the cyclopentenolone ring.

Table 2 The structures and key information on the pyrethroids of interest, their trivial and CAS names for stereoisomer lists are collected in Appendix B

Structure	Trivial name: CAS name
	(2.1) Allethrin: Cyclopropanecarboxylic acid, 2,2-dimethyl-3-(2-methyl-1-propen-1-yl)-, (RS)- α -2-methyl-4-oxo-3-(2-propen-1-yl)-2-cyclopenten-1-yl ester, (1RS,3RS;1RS,3SR)- CAS no. 584-79-2 Type I (see Appendix B, Table B1)
	(2.2) Bifenthrin: Cyclopropanecarboxylic acid, 3-[(1Z)-2-chloro-3,3,3-trifluoro-1-propen-1-yl]-2,2-dimethyl-, (2-methyl [1, 1'-biphenyl]-3-yl) methyl ester, (1RS,3RS;1RS,3SR)- CAS no. NA Type I (see Appendix B, Table B3)
	(2.3) Cyfluthrin: Cyclopropanecarboxylic acid, 3-(2,2-dichloroethenyl)-2,2-dimethyl-, (RS)- α -cyano (4-fluoro-3-phenoxyphenyl) methyl ester, (1RS,3RS;1RS,3SR)- CAS no. 68359-37-5 Type II (see Appendix B, Table B5)
	(2.4) Cyhalothrin: Cyclopropanecarboxylic acid, 3-[(1Z)-2-chloro-3,3,3-trifluoro-1-propen-1-yl]-2,2-dimethyl-, (RS)- α -cyano (3-phenoxyphenyl) methyl ester, (1RS,3RS;1RS,3SR)-rel- CAS no. 68085-85-8 Type II (see Appendix B, Table B7)
	(2.5) Cypermethrin: Cyclopropanecarboxylic acid, 3-(2,2-dichloroethenyl)-2,2-dimethyl-, (RS)- α -cyano (3-phenoxyphenyl) methyl ester, (1RS,3RS;1RS,3SR)- CAS no. 52315-07-8 Type II (see Appendix B, Table B9)
	(2.6) Deltamethrin: Cyclopropanecarboxylic acid, 3-(2,2-dibromoethenyl)-2,2-dimethyl-, (RS)- α -cyano (3-phenoxyphenyl)methyl ester, (1RS,3RS;1RS,3SR)- CAS no. 52820-00-5 Type II (see Appendix B, Table B11)

(continued)

Table 2 (continued)

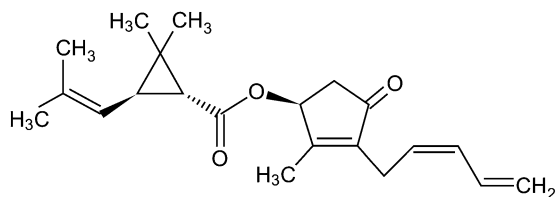
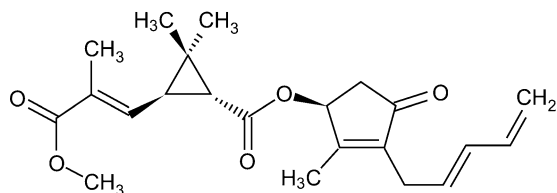
Structure	Trivial name: CAS name
	(2.7) Fenvalerate: Benzeneacetic acid, 4-chloro- α -(1-methylethyl)-, (RS)- α -cyano (3-phenoxy phenyl) methyl ester, (RS)- CAS no. 51630-58-1 Type II (see Appendix B, Table B13)
	(2.8) Fenpropathrin: Cyclopropanecarboxylic acid, 2,2,3,3-tetramethyl-, (RS)- α -cyano (3-phenoxyphenyl) methyl ester CAS no. 584-79-2 Type I/II (see Appendix B, Table B15)
	(2.9) Fluvalinate: DL-valine, N-[2-chloro-4-(trifluoromethyl) phenyl]-, (RS)- α -cyano (3-phenoxyphenyl) methyl ester CAS no. 69409-94-5 Type II (see Appendix B, Table B17)
	(2.10) Permethrin: Cyclopropanecarboxylic acid, 3-(2,2-dichloroethenyl)-2,2-dimethyl-, (3-phenoxyphenyl) methyl ester, (1RS,3RS;1RS,3SR)- CAS no. 52645-53-1 Type I (see Appendix B, Table B19)
	(2.11) Phenothrin: Cyclopropanecarboxylic acid, 2,2-dimethyl-3-(2-methyl-1-propen-1-yl)-, (3-phenoxyphenyl) methyl ester, (1RS,3RS;1RS,3SR)- CAS no. 26002-80-2 Type I (see Appendix B, Table B21)
	(2.12) Resmethrin: Cyclopropanecarboxylic acid, 2,2-dimethyl-3-(2-methyl-1-propen-1-yl)-, (5-(phenylmethyl)-3-furanyl) methyl ester, (1RS,3RS;1RS,3SR)- CAS no. 10453-86-8 Type I (see Appendix B, Table B23)
	(2.13) Tefluthrin: Cyclopropanecarboxylic acid, 2,2-dimethyl-3-[(1Z)-2-chloro-3,3,3-trifluoro-1-propen-1-yl]-, (2,3,5,6-tetrafluoro-4-methyl phenyl)methyl ester, (1RS,3RS;1RS,3SR)- CAS no. NA Type I (see Appendix B, Table B25)

(continued)

Table 2 (continued)

Structure	Trivial name: CAS name
	(2.14) Tetramethrin: Cyclopropanecarboxylic acid, 2,2-dimethyl-3-(2-methyl-1-propen-1-yl)-, (1, 3, 4, 5, 6, 7-hexahydro-1,3-dioxo-2 <i>H</i> -isoindol-2-yl) methyl ester, (1 <i>R</i> ,3 <i>S</i>);(1 <i>R</i> ,3 <i>R</i>)
	CAS no. 7696-12-0 Type I (see Appendix B, Table B27)
	(2.15) Tralomethrin: Cyclopropanecarboxylic acid, 2,2-dimethyl-3-[(<i>R</i>)-1,2,2,2-tetrabromoethyl]-, (<i>R</i>)- α -cyano-(3-phenoxyphenyl) methyl ester, (1 <i>R</i> ,3 <i>R</i>);(1 <i>R</i> ,3 <i>S</i>)
	CAS no. 66841-25-6 Type II (see Appendix B, Table B29)

NA not available

**Fig. 1** Pyrethrin I: cyclopropanecarboxylic acid, 2,2-dimethyl-3-(2-methyl-1-propen-1-yl)-, (1*S*)-2-methyl-4-oxo-3-[(2*Z*)-2,4-pentadien-1-yl]-2-cyclopenten-1-yl ester, (1*R*,3*R*). (Please refer to Appendix A, Table A1, for definitions of acronyms or abbreviations)**Fig. 2** Pyrethrin II: cyclopropanecarboxylic acid, 3-[(1*E*)-3-methoxy-2-methyl-3-oxo-1-propen-1-yl]-2,2-dimethyl-, (1*S*)-2-methyl-4-oxo-3-[(2*E*)-2,4-pentadien-1-yl]-2-cyclopenten-1-yl ester, (1*R*,3*R*)

2.1 Discovery

The synthetic era for the pyrethroids began with the replacement of the cyclopentenolone groups with other alcohol moieties, which resulted in the production of several household use products, and this success was followed by replacing the cyclopropane ring with a number of other acid functional groups. The cyclopropane ring changes were intended to produce pyrethroids beneficial for outdoor and agricultural insect control. The last changes to be made involved modifying the ester linkages (e.g., ethers, oximes, alkanes, and alkenes) (Katsuda 1999). According to Nishizawa (1971), the natural pyrethrin compounds are optically active, whereas the synthetic pyrethroids used in the early studies were optically inactive. Optically active pyrethroids prepared from (+)-*trans*-chrysanthemic acid were superior to those prepared from optically inactive (\pm)-*cis*-, *trans*-compounds. Racemization and isomerization were used to convert the ($-$)-*trans* and (\pm)-*cis* isomers into the desired (+)-*trans* isomer.

The change in the alcohol moiety to allethrine led to the development of the first synthetic pyrethroid, allethrin. It also led to improved chemical stability of the natural pyrethrins and to reduced cost, because the original pyrethrins had been sourced from natural products (LaForge and Soloway 1947). The stability of allethrin made it superior to the natural pyrethrins in both kill and knock-down effects against mosquitoes. Allethrin's successful discovery was followed by the development of other successful pyrethroids, to wit, tetramethrin (Kato et al. 1965) (1965, patent appl date) from tetrahydrophthalimide, resmethrin (Elliott et al. 1967) (1967, patent appl date) from 5-benzyl-3-furylmethyl alcohol and phenothrin (Fujimoto et al. 1973) (1968, patent appl date) by changing α -benzylfuran to phenoxyphenyl.

Additional changes to the acid moiety led to the development of fenpropathrin (Matsuo et al. 1976) (1971, patent appl date), permethrin, cypermethrin and deltamethrin (Elliott et al. 1974) (1972, patent appl date), fenvalerate (Ohno et al. 1974) (1973, patent appl date), fluvalinate (Henrick 1977) (1975, 1977 patent appl dates; Katsuda 1975), tralomethrin (Martel 1976) (1976, patent appl date), and cyhalothrin (Huff 1978) (1977, patent appl date). Unfortunately, patent application dates were unavailable for cyfluthrin, tefluthrin, or bifenthrin (Katsuda 1999).

Resmethrin was the first synthetic pyrethroid insecticide that possessed insecticidal activity approaching the potency of pyrethrin I. In resmethrin, the furan ring replaced the cyclopentenone ring of pyrethrin I, and the benzene ring replaced the diene side chain of pyrethrin I. The success of resmethrin (four isomers, two *cis*- and two *trans*-) led to the synthesis of a form that was less toxic to mammals, bioresmethrin (1*R-trans* isomer). Unfortunately, bioresmethrin per se was not more photostable than were the earlier synthetic pyrethroids, because both the furan ring and isobutenyl side chain were sites vulnerable to degradation.

The bioresmethrin work led to the development of biopermethrin (new alcohol side chain and dihalovinyl group), and later to the introduction of an α -cyano group to yield cypermethrin. Insect activity is the greatest when the side chain is *cis* to the ester group. Deltamethrin was discovered by replacing a bromine for a chlorine

atom in the acid side chain, making it possible to isolate a single crystalline product ([1R, *cis*] α -S isomer) with all three centers resolved (Elliott et al. 1974). Permethrin, cypermethrin, and deltamethrin were introduced by Elliott et al. (1974, 1978), Elliott and Janes (1978), Elliott (1989), and Fisher et al. (1983). Phenothrin contains four optical and stereo isomers, with only the [1R, *trans*] and [1R, *cis*] isomers being insecticidally active. Metabolism studies were carried out with these individual isomers (Izumi et al. 1984; Kaneko et al. 1981a, 1984; Miyamoto et al. 1974; Suzuki et al. 1976). The discovery of fenpropathrin, with its relatively simple structure, was first announced in 1973 by Sumitomo Chemical Co., and was commercially introduced as an acaricide in 1980. Sumitomo Chemical Co. introduced esters of the substituted phenyl acetic acids in 1974, replacing the cyclopropane pyrethroids. This led to the first commercial pyrethroid that was photostable, viz., fenvalerate. The racemic mixture of this product was followed in 1986 by the single (S, S) isomer, esfenvalerate.

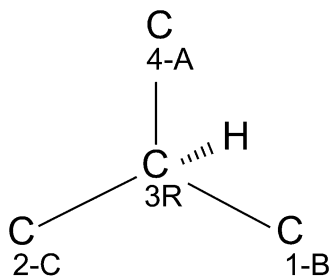
The development of fenvalerate and later esfenvalerate led to the synthesis and commercial marketing of fluvalinate, which is active against spider mites (Henrick et al. 1980). Fuchs synthesized all of the seven possible fluoro-substituted isomers of cypermethrin (e.g., 2, 4, 5, 6, 2', 3' and 4') (Hamman and Fuchs 1981). Substitution at the 4'-position produced the most active compound, cyfluthrin. Activity was almost eliminated when chlorine was substituted for fluorine in the 4'-position. Tefluthrin has a higher vapor pressure than most of the other pyrethroids and is active against soil pests such as the corn root worm (Jutsum et al. 1986). Bifenthrin is an ester with alcoholic components whose activity is not enhanced by an alpha-cyano substituent. Bifenthrin is active against insects (aphids) and mites (Plummer et al. 1983).

2.2 *Isomers and Technical Products*

The pyrethroids addressed in this review are esters of chiral acids (e.g., dimethylcyclopropane-carboxylic acid, chrysanthemic acid) and alcohols (e.g., (S) cyclopentenolones, 3-phenoxybenzyl, α -cyano-3-phenoxybenzyl). These pyrethroids possess $n =$ one to four chiral centers resulting in 2^n isomers per pyrethroid. The pesticidal activity of each isomer varies, with only one or two of the isomers being active against insect pests. The stereochemistry and structure of these isomers may be mentioned in the literature when they were subjected to biological study. However, a complete listing of the isomers by chemical name or by CAS numbers rarely appears in either published biological studies, or in analytical studies involving chromatographic separations. Terms such as enantiomers and diastereoisomers and their definitions are often used in conjunction with studies involving these isomers, particularly in the case of analytical, biological, or toxicological studies. At best many of these terms are confusing to the reader and the use of some of the terms in the literature may be incorrect.

From one to all possible isomers exist in technical pyrethroid products sold by manufacturers of these pyrethroids, and their combined content is given as a

Fig. 3 Stereodescriptors for the 3R position of pyrethrin I, clockwise sequence



percentage. Technical products are used by companies to formulate finished products that are used in and around homes and gardens. Regulators require the development of appropriate analytical methods to identify both registered “actives” and the “toxic” metabolites that appear in urine and tissues or in edible crops. However, it is common for multiple different chromatographic methods to be used for the analysis of pesticide mixtures (Eadsforth and Baldwin 1983). For pyrethroids, methods adequate to trace the *cis* vs. *trans* isomer content are important, and depend on the nature of the registered “active” or technical products and also on the nature of their biotransformation products.

In Appendix B, Tables B1–B30, we provide depictions of and CAS numbers for the chiral isomers for each of the 15 pyrethroids addressed in this review. The stereoisomer codes (A, B, C, etc.) were used in these tables to specify chiral configurations (i.e., (1R, 3S) (α S)), optical rotation, *cis/trans* and enantiomers pairs, and CAS no. The Chemical Abstracts Index Guide, (Appendix IV 2002) provides a discussion of the stereochemical descriptors found in the CAS index names. The CAS rules are consistent with IUPAC recommendations and produce readily interpreted stereochemical names. R and S are employed for chiral elements possessing either absolute or relative stereochemistry. E and Z are used primarily to describe geometrical isomerism about double bonds. The relative terms *cis*, *trans*; α and β are used as alternatives to R and S. The absolute terms R and S are based on the Cahn–Ingold–Prelog Sequence rule (Cahn et al. 1966) and depend on the ranking of atoms or groups attached to the stereochemical element or chiral atom. R is assigned to a clockwise sequence, whereas S denotes a counterclockwise sequence of atoms represented by a, b, c, and d about the chiral center. For example, 3R of pyrethrin I (Fig. 1) is represented by the rule in Fig. 3, wherein the least preferred atom or group “H” is considered to be below the plane of the paper, while the other groups project outward toward the viewer. The structure for pyrethrin I (Fig. 1, 1R, 3R) indicates that 1R is *trans* to the 3'-position as shown in Fig. 4.

Where they exist, we also identify enantiomeric pairs. A molecule with n stereogenic centers has 2^n stereoisomers (except when special symmetry conditions are present). When two stereoisomers are mirror images of each other they form an enantiomer pair. Each stereoisomer has only one enantiomer. Any other pairing of stereoisomers is considered to be a diastereomer pair. Thus, when there are

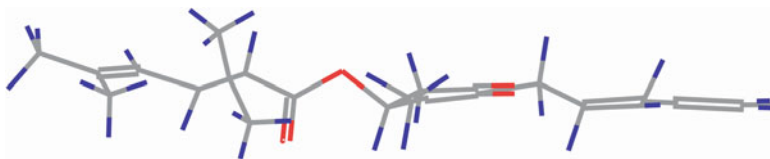


Fig. 4 Stereochemistry of pyrethrin I, showing the group at position 1 on the cyclopropane ring being *trans* to the groups about position 3 on the ring. The stereochemistry of pyrethrin I may be written as (1*R*, *trans*) or (1*R*, 3*R*)

3-stereogenic centers, one has 8 stereoisomers that can be arranged into 4 enantiomer pairs and 24 diastereomer pairs. For the above example that has eight stereoisomers, each stereoisomer is associated with one enantiomer and six diastereomers. Each stereoisomer is simultaneously an enantiomer and a diastereomer, unless the discussion is limited to just one pair of stereoisomers. The literature becomes difficult to understand and interpret when discussions of stereoisomers blur the above definitions and are unclear as to which stereoisomer or stereoisomer pair is being reported on. One should not report on a diastereomer unless its paired stereoisomer is also identified, and enantiomers should only be discussed as a pair of compounds.

A geometric isomer contribution from the presence of double bonds does not qualify as a stereocenter. When double bonds affect stereochemistry, the enantiomers are due only to chiral differences associated with a stereocenter. The enantiomers are always paired with identical configurations about the double bond. Both isomers must be *cis*- or *trans*- to meet the mirror image requirement that defines an enantiomer pair.

2.3 Stereochemistry

The following paragraphs describe the stereochemistry of the 15 pyrethroids addressed in this review.

Allethrin: Table B1, Appendix B, gives the chiral configurations of the eight individual isomers of allethrin, their optical rotation, *cis/trans* configurations, CAS number for absolute stereochemistry, and enantiomer pairs. The structure of each stereoisomer is coded A through H making it easier to identify (label) each isomer. In Table B2, Appendix B, the common and proprietary names used by registrants for technical products are presented. Each product contains more than one isomer, except for *dl-trans*-allethrin, which is 100% “H” isomer. The “B” isomer is the most pesticidal isomer of the eight allethrin isomers.

Bifenthrin: Table B3, Appendix B, gives the chiral configurations of the four individual isomers of bifenthrin having a *Z*-configuration for the double bond, their optical rotation, *cis/trans* configurations, and CAS no. for absolute stereochemistry. The structure of each stereoisomer is coded A through D making it easier to identify (label) each isomer. In Table B4, Appendix B, the common name of one technical product sold by registrants is listed. The Technical product contains isomers A and D, comprising 100% of the active ingredients.

Cyfluthrin: Table B5, Appendix B, gives the chiral configurations of the eight individual isomers of cyfluthrin, their optical rotation, *cis/trans* configurations, CAS no. for absolute stereochemistry, and the four enantiomer pairs (mirror images). The structure of each stereoisomer is coded A through H making it easier to identify (label) each isomer.

In Table B6, Appendix B, the common name of two technical products sold by registrants is listed. Cyfluthrin is a mixture of all eight isomers. The *cis/trans* isomers (B and G, D and E) comprise up to 95% of the active ingredients in beta-cyfluthrin.

Cyhalothrin: Table B7, Appendix B, gives the chiral configurations of eight individual isomers of cyhalothrin having a *Z*-configuration about the double bond, their optical rotation, *cis/trans* configurations, and CAS no. for absolute stereochemistry. The structure of each stereoisomer is coded A through H making it easier to identify (label) each isomer. In Table B8, Appendix B, the common name of two technical products sold by registrants is listed. Cyhalothrin is a mixture of four *cis* isomers (A, B, G and H), while the most used technical product, lambda cyhalothrin, is a mixture of isomers B and G. Gamma cyhalothrin contains only one isomer, the “B” isomer.

Cypermethrin: Table B9, Appendix B, gives the chiral configurations of the eight individual isomers of cypermethrin, their optical rotation, *cis/trans* configurations, CAS no. for absolute stereochemistry, and the four enantiomer pairs (mirror images). The structure of each stereoisomer is coded A through H making it easier to identify (label) each isomer. In Table B10, Appendix B, the common name of five technical products sold by registrants is listed. Cypermethrin is a mixture of all eight *cis/trans* isomers (A–H); however, the most used technical product, α -cypermethrin, is a mixture of the *cis* isomers B and G. Theta-cypermethrin contains the two *trans* isomers, D and E, whereas β -cypermethrin is a 2:3 mixture of α - and θ -cypermethrin.

Deltamethrin: Table B11, Appendix B, gives the chiral configurations of the eight individual isomers of deltamethrin, their optical rotation, *cis/trans* configurations, the CAS no. for absolute stereochemistry and enantiomer pairings. The structure of each stereoisomer is coded A through H making it easier to identify (label) each isomer. In Table B12, Appendix B, deltamethrin is shown as the name for the technical product containing only stereoisomer B. Small quantities of the other isomers are most likely present in technical deltamethrin.

Esfenvalerate/fenvalerate: Table B13, Appendix B, gives the chiral configurations of the four individual isomers of fenvalerate, their optical rotation, *cis/trans* configurations, CAS no. for absolute stereochemistry and the two enantiomer pairs (mirror images). The structure of each stereoisomer is coded A through D making it easier to identify (label) each isomer. In Table B14, Appendix B, esfenvalerate and fenvalerate (Pydrin) are listed as the two technical products sold by registrants. These two technical products contain all four isomers, with esfenvalerate having isomer “D” as the major component. Fenvalerate (pydrin) contains equal amounts of each of the four isomers.

Fenpropathrin: Table B15, Appendix B, gives the chiral configurations of the two individual isomers of fenpropathrin, their optical rotation, and CAS no. for absolute stereochemistry. The structure of each stereoisomer is coded A and B making it easier to identify (label) each isomer. In Table B16, Appendix B, fenpropathrin is identified as the only technical product sold by registrants. This technical product contains both isomers.

Fluvalinate: Table B17, Appendix B, gives the chiral configurations of the four individual isomers of fluvalinate, their CAS no. for absolute stereochemistry, and enantiomer pairs. The structure of each stereoisomer is coded A-D making it easier to identify (label) each isomer. In Table B18, Appendix B, fluvalinate and *tau*-fluvalinate are listed as the only technical products sold by registrants. Technical fluvalinate contains all four isomers, while *tau*-fluvalinate is limited to isomers “A” and “B”.

Permethrin: Table B19, Appendix B, gives the chiral configurations of the four individual isomers of permethrin, their optical rotation, CAS no. for absolute stereochemistry, and enantiomer pairs. The structure of each stereoisomer is coded A-D making it easier to identify (label) each isomer. Table B20, Appendix B, lists permethrin, *cis*-permethrin, *trans*-permethrin, and biopermethrin as technical products sold by registrants. Technical permethrin contains all four isomers, while *cis/trans* permethrin contains isomers A, D and B, C, respectively. Biopermethrin contains only isomer “B”.

Phenothrin: Table B21, Appendix B, gives the chiral configurations of the four individual isomers of phenothrin, their optical rotation, CAS no. for absolute stereochemistry, and enantiomer pairs. The structure of each stereoisomer is coded A–D making it easier to identify (label) each isomer. In Table B22, Appendix B, phenothrin, *cis*-phenothrin, *trans*-phenothrin, and sumithrin are listed as technical products sold by registrants. Technical sumithrin contains one isomer (A), while *trans/cis* phenothrin contain isomers A, D and B, C, respectively.

Resmethrin: Table B23, Appendix B, gives the chiral configurations of the four individual isomers of resmethrin, their optical rotation, CAS no. for absolute stereochemistry, and enantiomer pairs. The structure of each stereoisomer is coded A–D making it easier to identify (label) each isomer. In Table B24, Appendix B, resmethrin, *cis*-resmethrin, *trans*-resmethrin, bioresmethrin, and cismethrin are listed as technical products sold by registrants. Technical bioresmethrin contains one isomer (A), while *trans/cis* resmethrin contains isomers A, D and B, C, respectively.

Tefluthrin: Table B25, Appendix B, gives the chiral configurations of the four individual isomers of tefluthrin having “Z” configuration at the chiral double bond and CAS no. for absolute stereochemistry. The structure of each stereoisomer is coded A–D making it easier to identify (label) each isomer. In Table B26, Appendix B, tefluthrin is identified as the only technical product sold by

registrants. Technical tefluthrin contains two *cis*-isomers (A, D). Isomer A is the main active component.

Tetramethrin: Table B27, Appendix B, gives the chiral configurations of the four individual isomers of tetramethrin, their CAS no. for absolute stereochemistry, and enantiomer pairs. The structure of each stereoisomer is coded A–D making it easier to identify (label) each isomer. In Table B28, Appendix B, tetramethrin is identified as the technical products sold by registrants. Technical (+)-*cis*-tetramethrin contains one *cis* isomer (B). D-tetramethrin is composed of isomers A and B in a 4:1 ratio.

Tralomethrin: Table B29, Appendix B, gives the chiral configurations of the 16 individual isomers of tralomethrin, their CAS no. for absolute stereochemistry, and enantiomer pairs. The structure of each stereoisomer is coded A–P making it easier to identify (label) each isomer. In Table B30, Appendix B, tralomethrin (isomers G and H) is listed as the only technical product sold by registrants.

2.4 Analytical Methods for Pyrethroid Isomers

The US EPA requires registrants of pesticides to provide suitable analytical methods to affirm the identity of the pesticides they test. Such methods are needed for: acute and chronic toxicology studies, special studies (i.e., metabolism, pharmacokinetic, human exposure, animal residues, etc.), product and environmental chemistry studies, efficacy, health effects testing (i.e., functional observation battery, peripheral nerve function) and for pesticide residue enforcement efforts. In the past, registrants provided gas chromatographic methods for each active ingredient (i.e., permethrin, cypermethrin, etc.), with all the isomers chromatographing as a single component. Gas chromatography (GC), performed with open tube or packed columns containing polar (carbowax) or nonpolar (silicones, polysiloxane) phases, was the primary instrument used in the 1950s–1960s to analyze environmental samples for pesticide residues, including pyrethroids such as permethrin. The GC columns then available did not separate the stereoisomers present, because their partition coefficients are so similar. Low-pressure columns packed with alumina or silica gel were often used to clean up samples prior to gas chromatography, but were not routinely used for chromatographic analysis of pesticide residues. Thin-layer chromatographic (TLC) plates (e.g., silica gel 60 F254) were used by Kaneko et al. (1981a, b, c, 1984), Ruzo and Casida (1977), and Ruzo et al. (1978, 1979) for separating and identifying radiolabeled parent pyrethroids and their metabolites. The resolution achieved on these plates, by using two-dimensional chromatography and up to seven solvent systems (Kaneko et al. 1981a, b, c, 1984), was quite remarkable considering the nonpolar and polar nature of the products being separated.

The introduction of capillary gas chromatographic columns (30 m × 0.53 mm) in about 1970 that were run in split and splitless modes provided a means for separating greater numbers of pesticides. However, analyses by gas chromatography, in which only conventional achiral stationary phases in capillary columns are used, are not capable of separating the pyrethroid isomers. Gas chromatographic analysis of the pyrethroid isomers is best achieved by hydrolysis of the pyrethroid, methylation of the acids or alcohols, followed by GC chromatographic analysis.

Because of the problems encountered in separating the pyrethroid isomers by gas chromatography, chiral specific phase (CSP) HPLC (High Pressure Liquid Chromatography) columns were developed. These utilized a base support such as silica along with large groups such as (R)-phenylglycine and 3, 5-dinitrobenzoic acid-amide linkages attached to Si groups. These groups are varied so that they can be matched to the nature of the analytes being separated.

The chiral columns used for liquid chromatography may also be used for supercritical fluid chromatography (SFC). SFC offers important advantages over HPLC and GC in the separation of enantiomers. First, SFC provides a higher resolution per unit of time than does LC, because the diffusion rates in the mobile phase and linear velocities are higher. Second, SFC chromatography is carried out at temperatures well below those used in GC. LC and GC detectors, such as FID (flame ionized detectors) and mass spectrometry (MS), may also be applied to SFC (Chamberlain et al. 1998).

A search of the literature involving application of chiral chromatographic columns for separating pyrethroid isomers turned up the information that is summarized in Appendix C, Tables C1–C15. This information (i.e., chiral columns, isomers chromatographed, solvent systems, and results) includes recent work performed on the separation of the isomers of the 15 pyrethroids we address in this review. A brief history of this work is reviewed in the following sections for each of the pyrethroids.

Allethrin: D-allethrin has eight isomers ($2^3 = 8$), four *cis* (C, D, E, and F) and four *trans* (A, B, G, H) isomers. Mancini et al. (2004) separated *cis/trans* isomers from each other on an achiral silica HPLC column using *n*-hexane:*tert*-butyl methyl ether (96:4) (v/v) as the mobile phase (Table C1, Appendix C). The *trans* isomers were separated (G, H, A, B, respectively) from each other on a CHIRAL-CEL OJ using *n*-hexane:*tert*-butyl methyl ether (90:10) (v/v). This same column was used to separate the *cis* isomers (F, D, C, and E, respectively) using *n*-hexane:isopropanol (99.3:0.7) (v/v). Kutter and Class (1992) were able to separate the *trans* allethrin isomers on a chiral β -cyclodextrin RP-HPLC column, but were unable to separate the *cis* isomers.

Bifenthrin: Bifenthrin has four isomers ($2^2 = 4$) with the Z configuration about the double bond. Technical bifenthrin is comprised of two *cis* isomers, A and D (Table B3, Appendix B). Liu et al. (2005a) separated the two isomers on a β -cyclodextrin-coated BGB-172 gas chromatographic column with “A” chromatographing first (54.3 min) followed by “D” (55.5 min) (Table C2, Appendix C). Chromatography on a Sumichiral OA-2500-1 HPLC column using *n*-hexane, isopropanol, and ethanol (99.9/0.6/0.14) reduced the retention time down to 10.57 min for “A” and 11.25 min for “D” (Liu et al. 2005b).

Cyfluthrin: Cyfluthrin has eight isomers ($2^3 = 8$). Liu et al. (2005b) separated all eight stereoisomers in the order A, H, G, B, C, F, E, and D using a Chirex 00G-3019-DO HPLC column (Phenomenex; Torrance, CA) (Table C3, Appendix C). The mobile phase consisted of *n*-hexane:1, 2-dichloroethane:ethanol (500:10:0.05, v/v/v). Li et al. (2003) separated four stereoisomers (enantiomer pairs II and IV) on a Chiralcel OD HPLC column; mobile phase *n*-hexane:2-propanol (100 + 2, v/v). All four isomers were baseline separated, with *cis* isomers eluting prior to *trans* isomers. Faraoni et al. (2004) used a dual-column approach to successfully separate all eight stereoisomers. Enantiomer pairs were separated using a CNP silanized silica gel HPLC column with *n*-hexane:2-propanol, (99.0:0.1, v/v). One sample split was analyzed with a Chiralcel OD-H HPLC column, *n*-hexane:2-propanol (99.4:0.5) (v/v), giving peak separation for stereoisomers A, G, H, B, E, and D, in that order. A second split was routed through a Pirkle-type CSP (DNBPG) HPLC column (Aldrich-Chimica, Milan, IT) with *n*-hexane:2-propanol (99.9:0.1, v/v), separating peaks C and F.

Cyhalothrin: Cyhalothrin has eight isomers ($2^3 = 8$). The *cis* isomers are generally more toxic than the corresponding *trans* isomers. In practice, cyhalothrin is produced only in the *Z* and *cis* forms, reducing the number of isomers to four. These comprise two pairs of isomers: pair A and H: (*Z*), (1*R*, 3*R*), *R*- α -cyano and (*Z*), (1*S*, 3*S*) *S*- α -cyano and pair B and G: (*Z*), (1*R*, 3*R*), *S*- α -cyano and (*Z*), (1*S*, 3*S*) *R*- α -cyano. Pure γ -cyhalothrin is a racemic mixture of isomers B and G. A normal phase Nucleosil Sherisorb CN column (Shimadzu, Kyoto, Japan) was used to separate this mixture. The mobile phase was *n*-hexane:tetrahydrofuran:2-propanol (99:0.9:0.1, v/v/v) (Rao et al. 2004) (Table C4, Appendix C). The isomers chromatographed in the following order: B, G, H, and A. The major isomers in λ -cyhalothrin were B and G with small quantities of A and H. Yang et al. (2004) separated the principal isomers (B and G) of commercially produced λ -cyhalothrin on a CHIRALCEL OD-R column using acetonitrile:water (30:70, v/v). The elution order was not indicated by the authors.

CHIRALCEL OD and three other chiral columns CHIRALCEL (OJ), CHIRALPAK (AD), and CHIRALPAK (AS) were used to chromatograph and separate the two isomers of λ -cyhalothrin, B + G (Xu et al. 2007). The order (B or G first) in which they chromatographed was not indicated by the authors.

Cypermethrin: Cypermethrin has eight isomers ($2^3 = 8$). Liu et al. (2005b) and Tan et al. (2007) used two Chirex OOG-3019-OD columns to separate the eight isomers in the following order: A, H, G, B, C, F, E, and D. *Cis* isomers chromatographed before the *trans* isomers (Table C5, Appendix C). Tan et al. (2007) used *n*-hexane:1, 2-dichloromethane:2-propanol (96.8:3:0.2, v/v/v) as the mobile phase, while Liu et al. (2005b) used *n*-hexane:1, 2-dichloroethane:ethanol (500:30:0.15, v/v/v) to separate the isomers. A CHIRALCEL OD column was used by Li et al. (2003) to separate the (1:1 *cis/trans*) isomers in β -cypermethrin. The solvent system consisting of *n*-hexane:2-propanol (100 + 2, v/v) separated β -cypermethrin into four peaks, B (*cis*), D (*trans*), G (*cis*) and E (*trans*), in their respective order. This order was unusual, based on the studies of Liu et al. (2005b) and Tan et al. (2007), wherein

the *cis* isomers chromatographed before the *trans* isomers. Wang et al. (2004) prepared a chiral stationary phase by bonding cellulose-tris (3, 5-dimethylphenyl-carbamate) on aminopropylsilica that separated seven of eight stereoisomers in less than 25 min. A Partisil silica column separated the eight isomers of cypermethrin into four enantiomer pairs (A + H; B + G; C + F; D + E). The mobile phase was *n*-hexane: diethyl ether (500:10, v/v) (Wang et al. 2004).

Deltamethrin: Deltamethrin has eight isomers ($2^3 = 8$). According to Cayley and Simpson (1986), a cyano-bonded column was capable of chromatographic separation of deltamethrin (isomer B) from isomer A, by using 0.1% 2-propanol in *n*-hexane as the mobile phase (Table C6, Appendix C). Technical deltamethrin contains only one isomer, "B." Yang et al. (2004) used a Chiralpak AD HPLC column (GROM, Herrenberg-Kayh, Germany), with a mobile phase of ethanol: water (85:15, v/v), to separate isomer B from isomer G. A new analytical method for the determination of deltamethrin in TC, WP, EC, UL, and DP was adopted by CIPAC (Collaborative International Pesticides Analytical Council), with provisional status, in 2004. This HPLC method used a cyano-column and detection at 230 nm (WHO, Deltamethrin 2005a). No chromatographic procedures were found that separated all seven isomers of deltamethrin from deltamethrin per se (isomer B).

Fenvalerate: Fenvalerate has four isomers ($2^2 = 4$). A CHIRALCEL OD column separated the enantiomer pair I (isomers A + D) from II (isomers B + C) (Li et al. 2006) (Table C7, Appendix C). Of the four individual isomers, the first and second peaks were only partially resolved (Li et al. 2009). Huang et al. (1991) resolved fenvalerate into four well-separated peaks on a Pirkle-type 1-A chiral HPLC column using 99.9:0.1 hexane/isopropanol (v/v) as the mobile phase. The respective elution order was B, C, D, and A. The enantiomer pair II eluted before pair I.

Esfenvalerate consists primarily of isomer D. Tan et al. (2007) reported on the complete separation of the four fenvalerate isomers by using a novel CSP prepared by connecting (R)-1-phenyl-2-(4-methylphenyl)ethylamine (PTE) amide derivative of (S)-isoleucine to aminopropyl silica gel, through a 2-amino-3,5-dinitro-1-carboxamido-benzene unit. The mobile phase was hexane 1, 2-dichloroethane 2-propanol (97.45:2.50:0.05). The order of elution was C, B, A, and D, respectively. In an earlier study, Papadopoulou-Mourkidou (1985) used a chiral column (BAKERBOND) and a mobile phase of 0.1% methanol, 0.3% 2-propanol, and 99.6% hexane (by volume) to separate all four isomers of fenvalerate.

Fenpropathrin: Fenpropathrin has two isomers ($2^1 = 2$) by virtue of possessing one chiral center. Tan et al. (2007) reported the separation of the two isomers of fenpropathrin with a CSP column (that is described in the above paragraph as having also separated the four isomers of fenvalerate) (Table C8, Appendix C). The mobile phase was *n*-hexane 1, 2-dichloroethane 2-propanol (96.8:3.0:0.2). The "A" isomer chromatographed prior to the "B" isomer.

Fluvalinate: Fluvalinate has two enantiomer pairs and four isomers ($2^2 = 4$). Gao et al. (1998) separated the enantiomer pairs (I, A + D; II, B + C) on a Pirkle-type chiral phase HPLC column (Table C9, Appendix C). Yang et al. (2004) used a CHIRALCEL

OJ column (250 × 2 mm ID) to separate the two isomers of tau-fluvalinate (A + B) with *n*-hexane ethanol (90:10, v/v) as the mobile phase. The CHIRALCEL OJ column was purchased from GROM (Herrenberg-Kayh, Germany).

Permethrin: Permethrin has two enantiomer pairs and four isomers ($2^2 = 4$). Liu et al. (2005) separated A + D (*cis* isomers) and B + C (*trans* isomers) on a Sumichiral OA-2500-I column by using *n*-hexane, isopropanol, and ethanol (99.9:0.6:0.14, v/v) as the mobile phase (Table C10, Appendix C). The *cis* isomers chromatographed before the *trans* isomers, in the order of A, D, B, and C, respectively. A CHIRALCEL OJ column was used by Ulrich et al. (2008) to separate all four isomers of permethrin, with isopropanol and ethanol (2–5%) in *n*-hexane as the mobile phase. The isomers chromatographed in the order of D, A, B, and C, respectively. The *cis* isomers (A + D) chromatographed before the *trans* isomers (B + C).

Phenothrin: Phenothrin has two enantiomer pairs and four isomers ($2^2 = 4$). Girelli et al. (2002) separated *cis*-1R-phenothrin (B) and *trans*-1R-phenothrin (A) on a CHIRALCEL OD-H column by using *n*-hexane:2-propanol (99.97:0.03, v/v) (Table C11, Appendix C). The (+) optical isomer (*cis*) chromatographed prior to the (–), or *trans* isomer. Separating these two isomers were also achieved by using a Chirex (S)-leu/(S)-NEA column or a 3, 5-DNB- α -phenylglycine column. The Chiralcel OD-H and Chirex (S)-leu/(S)-NEA columns were purchased from Daicel (Tokyo, Japan) and Chemtex Analytical (Bologna, Italy), respectively. The 3, 5-DNB- α -phenylglycine column was obtained by treating an Econosphere NH₂-5 column (Alltech, Italy) with 3,5-DNBPG ((–) (R)-N-(3,5-dinitrobenzoyl) α -phenylglycine). The four optical isomers of phenothrin were separated to the enantiomer level by using a covalently bonded Pirkle-type 1-A HPLC column, and a mobile phase of 0.25–1% diethyl ether in hexane. Enantiomer separation was achieved by adding a second column that utilized a reverse phase Regis Pirkle-type 1-A ionic stationary phase (Deeside, UK), and *n*-hexane:2-propanol (99.975:0.025, v/v) mobile phase (Cayley and Simpson 1986).

Resmethrin: Resmethrin has two enantiomer pairs and four isomers ($2^2 = 4$). The columns employed by Girelli et al. (2002) to separate the *cis* and *trans* 1R-phenothrin isomers were also used to separate *cis*- from *trans*-resmethrin [enantiomer pairs: (B + C; A + D)] (Table C12, Appendix C). The method used by Cayley and Simpson (1986) for phenothrin also separated the resmethrin isomers in the order B, C, A, and D. And, the method described by Oi et al. (1990) for phenothrin also separated all four resmethrin isomers.

Tefluthrin: Tefluthrin has eight isomers ($2^3 = 8$), but only the *Z*-configuration is used in commercial products, giving four isomers of interest. A search of the literature turned up no published studies that addressed the chromatographic separation of the isomers (Table C13, Appendix C). Tefluthrin was developed by Syngenta Crop Protection and is based on the same *Z*-*cis*-acid that is used to produce λ -cyhalothrin. Tefluthrin is sold as a racemic mixture that contains equal amounts of the A and D isomers; the A isomer is the most active component.

Tetramethrin: Tetramethrin has four isomers ($2^2 = 4$). Base line separation of these four isomers was achieved by Zhe et al. (2008) by their use of a Chiralpak AD-H column (amylose 3,5-dimethylphenyl-carbamate) and a solvent system consisting of *n*-hexane:ethanol:2-propanol (99.0:0.9:0.1, v/v/v) (Table C14, Appendix C). The column was purchased from Daicel Chemical Industries Ltd., Japan. The isomers elute in the order of B, D, A, and C, respectively. The *trans* isomers (D and A) yielded the largest peaks, because the sample of tetramethrin used was *trans*-isomer enriched. Zhe et al. (2008) used a UV detector in conjunction with a polarimeter to identify the isomers. According to Kurihara et al. (1997a, b), all of the 1R isomers give positive (+) peaks in the polarimeter.

Tralomethrin: Tralomethrin has four possible chiral centers (1C, 3C, α C, and CBr), giving rise to 16 possible isomers ($2^4 = 16$). The commercial product contains: G, (1R, 3S, α S, BrR) tralomethrin and H, (1R, 3S, α S, BrS) tralomethrin. Loss of bromide ion results in the formation of deltamethrin. A LiChroCART 125-4 Superspher 100 RP-18 column (Hewlett-Packard) was used by Valverde et al. (2001) to separate and detect the two diastereoisomers (G and H) of tralomethrin by LC-ES-MS (Table C15, Appendix C).

2.5 Pyrethrins, Pyrethroids, and Their Chiral Components

In the natural pyrethrin esters, the presence of two asymmetric cyclopropane carbons implies the possible existence of four stereoisomers (Deltamethrin Monograph 1982). However, in the natural pyrethrins, only the (1R, 3R) configuration exists. This fact limits the number of acids (isomers) that need to be considered in developing analytical methods for detecting pyrethrin residues in food products, or animal tissues and fluids (i.e., blood, urine, and feces). For the alcohol component, three alcohols exist: pyrethrolone, cinerolone and jasmolone, and all three possess an asymmetric center that has an (S) configuration.

The discovery of the synthetic pyrethroid insecticides presented chemists/biologists with the challenge of separating and identifying the isomers possessing the highest insecticidal activity. The esterification of allethrone with chrysanthemic acid, without resolution of the asymmetric centers, resulted in the formation of 2^3 (eight isomers) of which only the stereoisomers having the (S) configuration of allethrone were active insecticides. The most active isomer, (S)-bioallethrin (1R, 3R, α -S), has the same asymmetric centers as does the pyrethrins, and is currently manufactured in large quantities.

The same synthetic approach (i.e., varying the acid, alcohol, or both) resulted in the development of the commercially successful active pyrethroid insecticides covered in this review; this same approach also produced a host of relatively inactive isomers. The most potent constituent of resmethrin is the 1R, 3R isomer (bioresmethrin), and is formed during the esterification of (+) *cis*-, *trans*-chrysanthemic acid with 5-benzyl-3-furylmethyl alcohol to produce bioresmethrin and three other stereoisomers. Of greater interest to most chemists/biologists is the

development of the eight isomers of deltamethrin, and specifically the active 1R, 3R, α -S isomer (Deltamethrin Monograph 1982), which was resolved from the isomer mixture by crystallization.

The lack of standardization, good analytical methods, and a clear understanding of the chemistry of these pyrethroids has prevented interested parties from easily studying the details of the metabolism, pharmacokinetics, toxicity, and environmental fate of the individual isomers.

2.6 *Isomers of Chrysanthemic Acids*

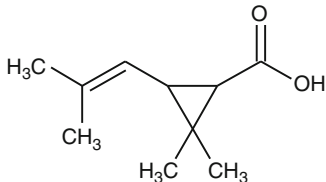
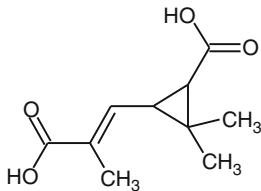
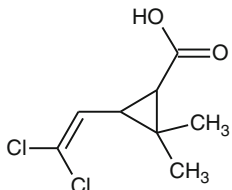
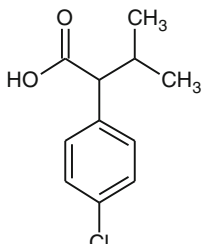
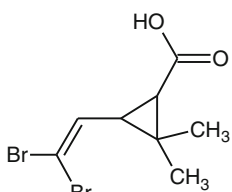
In Table 3, we present the structures and names of the chrysanthemic acids that are used in the synthesis of allethrin, cyfluthrin, deltamethrin, permethrin, fenvalerate, phenothrin, resmethrin, and tetramethrin. These acids (isomers), depicted in Tables B31–B35, Appendix B, are released during metabolism and are excreted in the urine of exposed animals. A short discussion of each acid and their isomers is presented in the following paragraphs.

1. Chrysanthemic acid: Table B31, Appendix B, gives the four isomers, two *trans* and two *cis* isomers for chrysanthemic acid along with their optical rotation. These four isomers are the products of the hydrolysis of the allethrin, phenothrin, and resmethrin.
2. Chrysanthemum dicarboxylic acid: In Table B32, Appendix B, the four isomers arising from the oxidation/hydrolysis of allethrin, fenpropathrin, phenothrin, and resmethrin are listed. Oxidation of the parent molecule may occur prior to hydrolysis, or hydrolysis may occur followed by oxidation.
3. Permethrinic acid: Table B33, Appendix B, gives the four isomers arising from the hydrolysis of the four isomers of permethrin and the eight isomers of cypermethrin and cyfluthrin.
4. Esfenvaleric acid/Fenvaleric acid: Table B34, Appendix B, gives the two isomers arising from the hydrolysis of esfenvalerate/fenvalerate.
5. Decamethrinic acid: Table B35, Appendix B, gives the four isomers arising from the hydrolysis of deltamethrin.

2.7 *Analytical Chemistry, Acid Components*

Chrysanthemic acid has $n = 2$ enantiomer pairs and four isomers ($2^n = 4$) (Table C16, Appendix C). Oi et al. (1995) and Oi (2005) readily separated these isomers on an HPLC CHIREX column Phase 3010 by using a mobile phase of 0.1 M ammonium acetate in water/tetrahydrofuran (60:40). The four individual isomers of chrysanthemic acid are given in Table B31; Appendix B. Table 3 shows the generic structure of chrysanthemic acid. This moiety is the acid leaving group for allethrin,

Table 3 The structures and CAS names for the acids presented in Appendix B

Structure	Trivial name: CAS name
	(3.1): Chrysanthemic acid: Cyclopropanecarboxylic acid, 2,2-dimethyl-3-(2-methyl-1-propen-1-yl)-, (1R,3S)- CAS no. 10453-89-1 (generic) Allethrin, phenothrin, resmethrin and tetramethrin
	(3.2): Chrysanthemum dicarboxylic acid: Chrysanthemum dicarboxylic acid, 3-[(1E)-2-carboxyprop-1-enyl]-2,2-dimethylcyclopropanecarboxylic acid CAS no. 497-95-0 (generic)
	(3.3): Permethrinic acid: Cyclopropanecarboxylic acid, 3-(2,2-dichloroethenyl)-2,2-dimethyl-, (1R,3R)- CAS no. 55701-05-8 (generic) Cyfluthrin, permethrin
	(3.4): Esfenvaleric/Fenvaleric acid: 2-(4-chlorophenyl)-3-methylbutanoic acid CAS no. 2012-74-0 (generic) Fenvalerate and esfenvalerate
	(3.5): Decamethrinic acid: Cyclopropanecarboxylic acid, 3-(2,2-dibromoethenyl)-2,2-dimethyl-, (1R, 3R) or 1R-trans CAS no. 53179-78-5 abs Deltamethrin

phenothrin, resmethrin, and tetramethrin, which is further oxidized to *E-cis/trans* chrysanthemum dicarboxylic acid (Elflein et al. 2003). The isomers of the dicarboxylic acid are given in Table B32, Appendix B. Elflein et al. (2003) separated the esterified esters of chrysanthemum dicarboxylic acid (four isomers) by gas chromatography into two separated peaks (enantiomer peaks), probably the *cis* and

trans isomers of the dicarboxylic acid (Table C17, Appendix C). Column and analysis conditions were not provided.

Permethrinic acid has two enantiomer pairs and four isomers ($2^n = 4$) (Table B33, Appendix B). The acid leaving group for permethrin, cypermethrin, and cyfluthrin is permethrinic acid. The structure of this acid is given in Table 3. Angerer and Ritter (1997) separated the methyl esters of *cis*- and *trans*-permethrinic acid on a polysiloxane capillary column by GC (Table C18, Appendix C). The carboxylic acids of several of these pyrethroids were also listed as *trans*- or *cis*-3-(2, 2-dichlorovinyl)-2, 2-dimethyl cyclopropane carboxylic acid. The acids may be separated on a CHIREX phase 3005 column (Phenomenex, 2320 W 205th Street, Torrance, CA 90501) by HPLC.

Esfenvaleric/fenvaleric acids are present in two isomeric forms as shown in Table B34, Appendix B. The structures of these acids are identical and displayed in Table 3. Li et al. (2006) separated the methyl esters of the two isomers (R and S) on a chiral column by GC (Table C19, Appendix C).

Decamethrinic acid is the acid leaving group of deltamethrin and exists in four isomeric forms as shown in Table B35, Appendix B. The acid possesses two bromines as shown in Table 3. The *cis* and *trans* methyl esters were separated from the esters of permethrinic acid by Angerer and Ritter (1997) by GC chromatography on a siloxane column (Table C20, Appendix C).

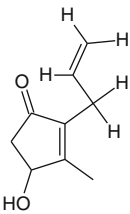
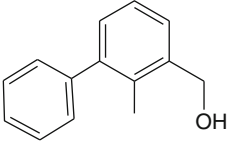
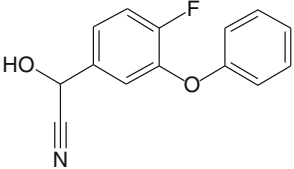
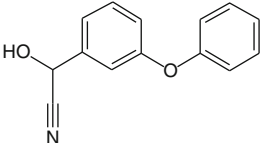
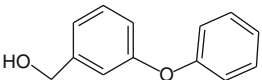
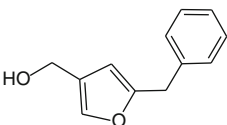
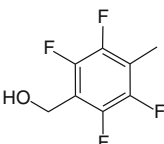
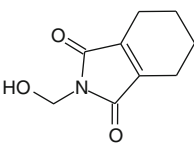
2.8 Alcohol Components

The alcohol moieties used in the synthesis of the 15 pyrethroids are shown in Table 4. A discussion of the synthesis of each alcohol (i.e., stereochemistry, etc.) is beyond the scope of this review, although allethrine and 5-(phenylmethyl)-3-furanmethanol have been mentioned in the discovery section. Information on the synthesis of α -hydroxy- α -(3-phenoxyphenyl) acetonitrile (R, S forms) (cyanohydrin of phenoxyphenyl aldehyde) and the resolution of the desired S form that produces (1R, 3R, α -S) deltamethrin may be found in Chap. 2 of the Deltamethrin Monograph (1982). The alcohols and their metabolites are readily separated by partition chromatography on GC or HPLC columns. Ruzo and Casida (1977) and Ruzo et al. (1978, 1979) used TLC to separate and identify the alcohol metabolites.

2.9 Mammalian Toxicity

The mammalian toxicity of the pyrethroids is highly dependent upon the structure of the parent pyrethroid (e.g., does it have an α -cyano group or not), nature of the isomer mixture, and whether one or more of the isomers have been enriched. Appendix B, Tables B1–B30, provide information on the nature of each of the

Table 4 The structures, scientific names, and CAS names for the alcohols presented in Appendix B

Structure	Trivial name: CAS name
	(4.1): Allethronol: 2-cyclopenten-1-one, 4-hydroxy-3-methyl-2-(2-propen-1-yl)- CAS no. 29605-88-7 Alcohol for allethrin
	(4.2): NA: [1,1'-biphenyl]-3-methanol, 2-methyl- CAS no. 76350-90-8 Alcohol for bifenthrin
	(4.3): NA: benzeneacetonitrile, 4-fluoro- α -hydroxy-3-phenoxy- CAS no. 76783-44-3 Alcohol for cyfluthrin
	(4.4): NA: benzeneacetonitrile, α -hydroxy-3-phenoxy- CAS no. 39515-47-4 Alcohol for cyhalothrin, cypermethrin, deltamethrin, fenvalerate, fenpropathrin, fluvalinate and tralomethrin
	(4.5): NA: benzenemethanol, 3-phenoxy- CAS no. 13826-35-2 Alcohol for permethrin and phenothrin
	(4.6): NA: 3-furanmethanol, 5-(phenylmethyl)- CAS no. 20416-09-5 Alcohol for resmethrin
	(4.7): NA: benzenemethanol, 2,3,5,6-tetrafluoro-4-methyl- CAS no. 79538-03-7 Alcohol for tefluthrin
	(4.8): NA: 1H-isoindole-1,3(2H)-dione, 4,5,6,7-tetrahydro-2-(hydroxymethyl)- CAS no. 4887-42-7 Alcohol for tetramethrin

NA not available

Table 5 Acute oral toxicities of the pyrethroid insecticides to rats

Pyrethroid	LD ₅₀ (mg/kg)		References
	Male	Female	
Bioallethrin	395	410	Furnax and Audegond (1985a)
S-Bioallethrin	370	320	Furnax and Audegond (1985b)
Bifenthrin	70.1	53.8	Freeman (1982)
Lambda cyhalothrin	79	56	Southwood (1985a)
	299 ^a	433 ^a	Allen and Leah (1990)
Cyfluthrin	155	160	Heimann (1987)
Cypermethrin	297	372	Freeman (1987)
	7,654 ^a	7,180 ^a	Rand (1983)
Zeta-cypermethrin	134	86	Freeman (1989)
Deltamethrin	95	87	Varsho (1996)
	>5,000 ^a	>5,000 ^a	Myer (1989)
Fenpropathrin	70.6	66.7	Hiromori et al. (1983, unpublished) ^b
Fenvalerate	~370	~370	Bilsback et al. (1984)
Esfenvalerate	87	87	Bilsback et al. (1984)
Permethrin	1,200	1,200	Killeen (1975)
	8,900 ^a	8,900 ^a	Killeen (1975)
Pyrethrum	710	320	Gabriel (1992)
Resmethrin	1695	1640	Glomot (1979)
Tefluthrin	21.8	34.6	Southwood (1985b)
Tralomethrin	99	157	Audegond et al. (1981a)
	>1,000 ^a	>1,000 ^a	Audegond et al. (1981b)
	<5000 ^a	<500 ^a	

All pyrethroids were administered in corn or sesame oil

Source: Soderlund et al. 2002 (published with permission)

^aAqueous suspension

^bHiromori T, Misaki Y, Seki T, Hosokawa S, Miyamoto J (1983) Acute oral toxicity of S-3206 (91.8%) in rats. Sumitomo Chemical, America

pyrethroids listed in Table 5. For example, bioallethrin is composed largely of isomers A and B (46% each), whereas S-bioallethrin constitutes largely one isomer, B (>90%). The administration of the pyrethroid in water vs. corn- or sesame-oil greatly decreases the rat oral toxicity (LD₅₀) of the pyrethroids.

Figure 5, obtained from Wolansky and Harrill (2008), shows the acute toxicity (LD₅₀) values in rats for the parent pyrethroids and one or more of their enriched isomers. Structural information on the compounds tested and their purity was limited to a few of the more commonly used pyrethroids (i.e., allethrin, resmethrin, bifenthrin permethrin, deltamethrin, cypermethrin). The authors recognized the need to standardize test materials, the pyrethroid isomers used in the tests, and their purity for improving the value of information obtained from toxicological studies.

The Office of Pesticide Programs (OPP), EPA, Washington, DC, has a complete file on the acute and chronic toxicity of the registered pyrethroids. Information on

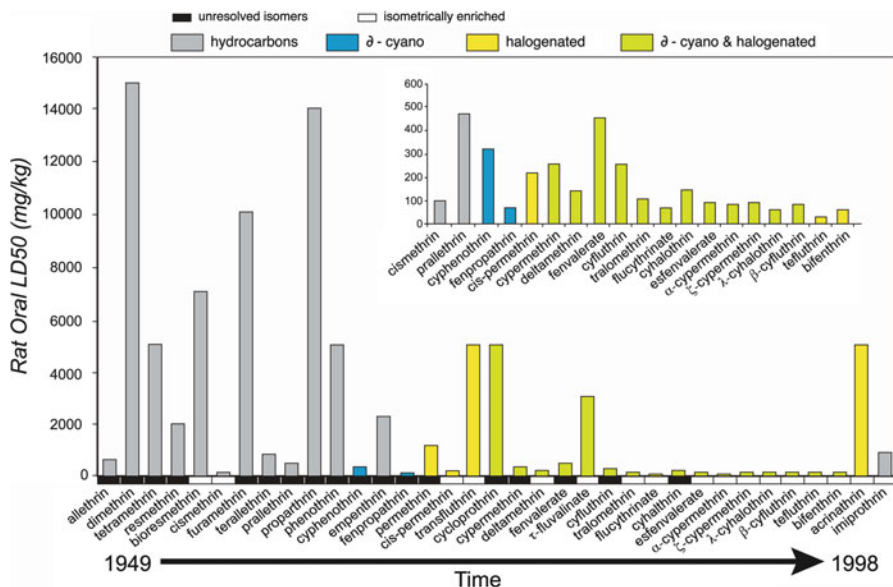


Fig. 5 Oral LD₅₀s in rats following acute exposure to the pyrethroid insecticides. Compounds are ordered chronologically according to the approximated date of the original patent application (Gray and Soderlund 1985; Katsuda 1999; Khambay 2002; Naumann 1998). Only pyrethroids with central ester bonds are included. Milestones in the development of the structural properties of synthetic pyrethroids are denoted by the colored or shaded bars. Pyrethroid preparations that are isomerically enriched are denoted by white boxes lining the *x*-axis, while formulations that constitute unresolved mixtures of many isomers are denoted by *black boxes*. All pyrethroids that have LD₅₀ values < 500 mg · kg⁻¹ are pictured in the *inset*. Values for dimethrin, tetramethrin, bioresmethrin, phenothrin, empenethrin, and transluthrin correspond to the maximal doses tested in literature studies, because true LD₅₀s could not be determined. LD₅₀ values for a typical permethrin formulation (i.e., 40:60 *cis:trans* ratio) and a permethrin preparation enriched in *cis*-isomers (i.e., *cis*-permethrin) were taken from McGregor (1999). Taken from EC-HCPDG (2002); Miyamoto (1976); PMRA (2005); White et al. (1976); WHO (1965); and WHO (2005b). This figure is reproduced from Wolansky and Harrill (2008), with permission

these pyrethroids may be obtained from OPP through the “Freedom of Information Act.” Some of the toxicology information on file in OPP is also available online in “Summary form” from the state of California’s Department of Pesticide Regulation (CALEPA.ca.gov). The summaries are in *.pdf format and may be downloaded. However, no information was available in this database for allethrin, cyhalothrin, or tefluthrin, and the data involving tralomethrin were found under deltamethrin. The organization of the database containing these files may be found in Knaak et al. (1993). The technical pyrethroid products (percent purity given) tested for toxicity were largely *cis/trans* mixtures (percentages given in the reports). No information was found concerning the nature of the individual isomers in the surveyed reports.

3 Experimentally-Derived Absorption Parameters Used in PBPK/PD Models

The set of parameters shown in Table 1 are required to run the PBPK/PD models. In addition, the models for the organophosphate, carbamate and pyrethroid pesticide classes may require additional compartments and or parameters to properly predict the fate (absorption, distribution, metabolism, and elimination, or ADME) of pesticides in food, or amounts that will dissolve in a minimum volume of corn oil or polyethylene glycol 400 (PEG 400) for oral administration in toxicity tests. In general, pyrethroid insecticides that are ingested are rapidly and nearly completely absorbed by the small intestine, with small percentages being eliminated in feces and the remainder as metabolites in urine. In some cases, the events that occur are easily modeled and require a modest number of compartments (i.e., blood, brain, liver, kidney, rapidly and slowly perfused tissue, skin, and GI tract) and parameters (i.e., partition coefficients, absorption, hepatic metabolism, metabolic, and elimination rate constants). The pyrethroid insecticides (Type I/II) may require additional compartments (e.g., full gastrointestinal submodel) and parameters (e.g., protein plasma binding constants, plasma:tissue equilibrium dialysis constants, plasma partition coefficients, multidrug efflux P-glycoprotein (Pgp) permeability constants, and microsomal V_{max} and K_m values in liver or GI lumen) to properly model amounts ingested.

Environmental (e.g., surface and crop leaf residues) and work-place exposures (e.g., mixer-loaders, applicators, etc.) may result in the transfer of pyrethroids to skin where they may be absorbed. Dermal PBPK/PD models require compartment/submodels and additional parameters (e.g., K_p , permeation constants, exposed surface area, evaporation rates, washoff fractions, etc.) to model the fate of pyrethroids deposited on the skin.

The following sections address the development of parameters that are key to these models.

3.1 *Gastrointestinal Absorption/Metabolism*

A series of rate constants (k_s , h^{-1}) are currently used in physiologically based models to describe the transfer of a dose to the stomach and then its distribution to the various regions of the small intestine. This compartmental approach was used by Timchalk et al. (2002) to predict the ADMET (absorption, distribution, metabolism, elimination, and toxicity) of chlorpyrifos in rats and humans. Zhang et al. (2007) chose a compartmental transit and absorption GI model for carbofuran. The model incorporated the majority of the GI, including colon, duodenum, lower small intestine, and stomach lumen (food flow, $L \cdot h^{-1}$, and volumes, L) and walls (volume, percent). Yu et al. (1996) developed one of the first compartmental absorption and transit (CAT) models that were described by a set of differential

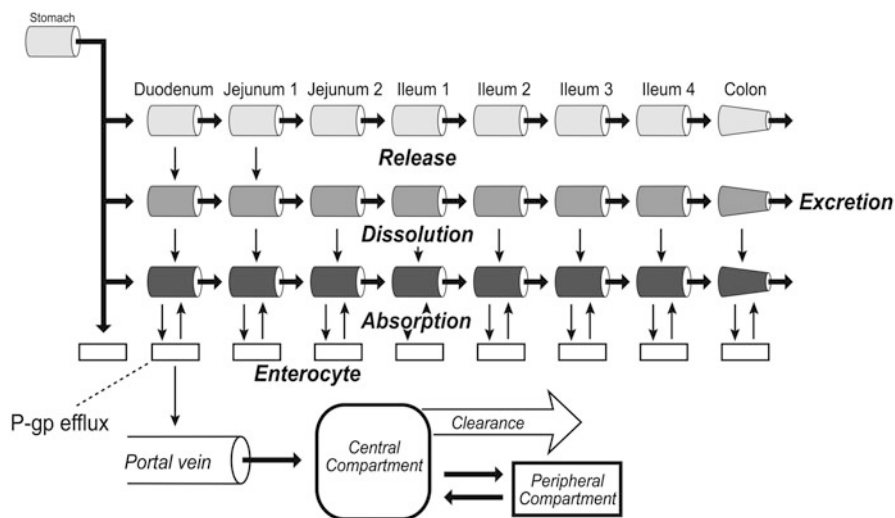


Fig. 6 This schematic is an illustration of the GIT advanced compartmental transit model (stomach, seven small intestine compartments, colon, and nine enterocytes). The administered drug, after dissolution, becomes available for passive absorption and efflux secretion. The rate of drug transfer into and out of enterocyte compartments for each GIT lumen compartment is calculated by using the concentration gradient across the apical and basolateral membranes. This figure is published with permission (Agoram et al. 2001)

equations and kinetic rate constants. The division of the GI tract into seven regional pH-, volume- and permeability-compartments gave the best fit to the experimental results of the small intestinal transit time vs. percent of dose that reached the colon.

The original CAT model (Yu et al. 1996) and modifications thereof (ACAT; Advanced Compartmental Absorption and Transit) by SimulationsPlus Inc. (Lancaster, CA) are being used to simulate the absorption of drugs through the gastrointestinal tract (Agoram et al. 2001). This dynamic physiological model, ACAT, requires parameters (e.g., length, radius, transit time, and pH for GI tract, regional effective drug permeability (P_{eff}), solubility, absorption scale factors (ASF model; effect of $\log D$ values on absorption) and metabolism (enzyme, metabolic rate constants, and transporter expression)) for each compartment of the gastrointestinal tract (e.g., stomach, intestine, and colon). Figure 6 provides a schematic representation of an ACAT model for Talinolol (CAS no. 57460-41-0) (Tubic et al. 2006).

The effective permeability (P_{eff}) in human intestine (GastroPlus Manual, version 6.0) may be calculated by measuring the rate of disappearance of a drug from a section of the GI tract at steady state as shown in (1):

$$P_{\text{eff}} = \frac{Q(C_{\text{in}} - C_{\text{out}})}{2\pi RLC_{\text{out}}}, \quad (1)$$

where Q is the volumetric flow rate, C_{in} and C_{out} are the concentrations at the input and output posts, and R and L are the radius and length of the perfused section.

Equation (1) may be rearranged to give:

$$\frac{dM}{dt} = P_{\text{eff}} \times \alpha \times M, \quad (2)$$

where

$$\alpha = \frac{(\text{cylinder surface}) \times 2\pi RL}{(\text{cylinder volume}) \times \pi R^2 L} = \frac{2}{R}, \quad (3)$$

and

$$k_a = P_{\text{eff}} \times \alpha, \quad (4)$$

$$\frac{dM(i)_{\text{absorbed}}}{dt} = k_a'(i)V(i)C(i)_{\text{lumen}} - C(i)_{\text{enterocyte}}, \quad (5)$$

where $dM(i)_{\text{absorbed}}/dt$ is the rate of absorption, $k_a'(i)$ is the absorption rate coefficient, $C(i)_{\text{lumen}}$ is the concentration in the lumen, $C(i)_{\text{enterocyte}}$ is the concentration of drug in the enterocyte subcompartment, and i indicates a particular compartment.

Intestinal drug flux mediated by P-glycoprotein was measured in terms of flux by Stephens et al. (2001) as shown in the following equation (Eq. 6):

$$J = \frac{J_{\text{min}} + (J_{\text{max}} - J_{\text{min}})}{(1 + ((C/EC_{50})^{-P}))}, \quad (6)$$

where J is the net flux, C is donor concentration, P is a constant (the Hill slope), and EC_{50} (K_m , μM) is the concentration at which half-maximal flux was achieved. J_{max} values range from 3.0 to 13.0 $\text{nmol} \cdot \text{h}^{-1} \cdot \text{cm}^{-2}$.

Permeability may be measured using Caco-2 cells or isolated intestine in Ussing chambers (Stephens et al. 2001). Caco-2 cell (immortalized human colon adenocarcinoma cell line) monolayers are widely used to evaluate the intestinal absorption of drugs because they incorporate both passive transport (transcellular or paracellular route) and active transporters, such as the peptide transporter (PepT1), monocarboxylic transporter (MCT), and the efflux pump P-glycoprotein (P-gp) (Liang et al. 1995; Tamai et al. 1995; Ueda et al. 1986). The Caco-2 assay is a relatively low-throughput method, as a result of its 3-week growth period and the requirement for regular maintenance feeding. The apparent permeability, P_{app} , values in $\text{cm} \cdot \text{s}^{-1}$, was calculated by Irvine et al. (1999) using (7):

$$P_{\text{app}} = \frac{dQ}{dt} \frac{1}{C_0} \frac{1}{A}, \quad (7)$$

where dQ/dt is the permeability rate (nmol s^{-1}), C_0 is the initial concentration (μM) in the donor compartment, and A is the surface area (cm^2) of the filter.

The use of a faster-growing cell line, MDCK (Madin-Darby canine kidney) cells, appears to be a good replacement for Caco-2 cells (Irvine et al. 1999). The parallel artificial membrane permeation assay (PAMPA) is a rapid in vitro assay, in which transcellular permeation is evaluated (Kansy et al. 1998). PAMPA may also be used to predict oral absorption, blood-brain barrier penetration, and human skin permeability (Fujikawa et al. 2007) by using QSAR models. To our knowledge, neither PAMPA, Caco-2 cell monolayers nor MDCK cells have been used to examine the absorption/permeability of the pyrethroids. The advantages and limitations of the Caco-2 model were reviewed by Artursson et al. (1996) and Delie and Rubas (1997).

3.2 Enterohepatic Circulation

The need for dynamic enterohepatic circulation (EHC) models and parameters has been established for the carbamate pesticides (Zhang et al. 2007) and may also be needed for certain pyrethroids. Zhang et al. (2007) modeled the enterohepatic circulation of glucuronides formed during the metabolism of carbofuran in the rat. A bile to duodenum partition coefficient was used to describe the transfer of glucuronides from bile to the contents of the duodenum for reabsorption. Pyrethroid-based QSAR models are currently generating parameters for dynamic models involving liver metabolism (e.g., microsomal, CYP, and carboxylesterase (CaE) activity), percutaneous absorption, protein binding, and tissue-blood partitioning. These predictive QSAR models are addressed in the next sections along with models that involve toxicity.

3.3 Gut Metabolism/Transport

The total rate of gut metabolism includes all the enzymes (i.e., individual CYPs and CYP abundances, index i) that exist in the gut enterocyte compartments (index j) (Gastroplus 5.0, SimulationsPlus, Inc., Lancaster, CA). The CYP450 enzymes are present in the gut in smaller quantities (~ 20 times less) than in the liver; however, in some cases their contribution to metabolism is similar to what occurs in the liver. This is true for drugs that are highly bound to plasma proteins and have limited access to liver hepatocyte enzymes (Agoram et al. 2001). GastroPlus Manual version 6.0 describes the metabolic activity of all gut enzymes in (8).

$$\text{Gut metabolic rate} = \sum_j \sum_i \frac{V_{\max}^i \text{SF}_{V_{\max}} \text{ESF}_{i,j} C_{\text{ent}f_{\text{ue}}}^j}{K_m^i \text{SF}_{K_m} + C_{\text{ent}f_{\text{ue}}}^j}, \quad (8)$$

where C_{ent} is the concentration of the drug in the enterocyte compartment j , f_{ue} is the unbound fraction of drug in the enterocytes, V_{max} is the maximum velocity, and K_m is the Michaelis–Menten constant (enzyme i), $\text{SF}_{V_{\text{max}}}$ and SF_{K_m} are the overall scale factors for all gut metabolic enzymes, ESF_{ij} are the gut enzyme distribution factors for enzyme i in compartment j .

The same V_{max} and K_m from a hepatic enzyme may be used for the gut so long as the regional distribution of enzymes in the GI tract is expressed as an amount relative to the whole liver amount of the same enzyme.

3.3.1 Saturable Carrier-Mediated Transport (P-glycoprotein)

Transport Rate = Influx – Efflux as described by GastroPlus Manual version 6.0, (9) and (10).

$$\text{Gut influx rate} = \sum_j \sum_i \frac{V_{\text{max}}^i \text{SF}_{V_{\text{max}}}^{\text{In}} \text{ESF}_{i,j} C_{\text{lumen}}^j}{K_m^i \text{SF}_{K_m}^{\text{In}} + C_{\text{lumen}}^j}, \quad (9)$$

$$\text{Gut efflux rate} = \sum_j \sum_i \frac{V_{\text{max}}^i \text{SF}_{V_{\text{max}}}^{\text{Ef}} \text{ESF}_{i,j} C_{\text{ent}}^j f_e}{K_m^i \text{SF}_{K_m}^{\text{Ef}} + C_{\text{ent}}^j f_e}, \quad (10)$$

where i is the index for i -th influx/efflux transporter, j is the index for j -th lumen compartment, $V_{\text{max}(i)}$ is the maximum transport rate for influx/efflux transporter i , C_{lumen}^j is the concentration of drug in lumen compartment j , C_{ent}^j is the concentration of drug in enterocyte compartment j , $K_{m(i)}$ is the Michaelis–Menten constant (concentration at V_{max}) for transporter i , $\text{ESF}_{(i,j)}$ is the scale factor for maximum transport rate for transporter i in compartment j , $\text{SF}_{V_{\text{max}}}^{\text{Int}}$ is the overall influx transport scale factor, $\text{SF}_{V_{\text{max}}}^{\text{Ef}}$ is the overall efflux transport scale factor, $\text{SF}_{K_m}^{\text{In}}$ is the overall scale factor for K_m for influx transporters, $\text{SF}_{K_m}^{\text{Ef}}$ is the overall scale factor for K_m efflux transporters.

The efflux transport calculations are based on concentrations in the apical membrane of the enterocytes, while the influx transport calculations are based on concentrations in the lumen. Drugs that enter the enterocyte are subject to metabolism by CYP3A4, or those not so metabolized may be effluxed back into the lumen by P-glycoprotein to be reabsorbed and again metabolized.

In liver and kidney, P-glycoprotein is localized on the luminal membrane of hepatic canaliculi facing the bile duct lumen or on the luminal brush-border membrane of renal proximal tubular cells facing the renal tubule lumen. This means P-glycoprotein is localized at the exit site of hepatocytes and renal epithelial cells and contacts only drug molecules after cellular uptake, intracellular distribution and metabolism in the liver and kidney. In contrast to the liver and kidney, P-glycoprotein is localized at the entrance site of epithelial cells of intestines. Drug molecules are exposed to P-glycoprotein prior to intracellular

distribution and metabolism. The distribution of P-glycoprotein in the intestine strongly supports the role of P-glycoprotein in enhancement of CYP3A4-mediated metabolism.

P-glycoprotein appears to have a greater impact on limiting cellular uptake of drugs from blood circulation into brain and from the intestinal lumen into epithelial cells than on enhancing drug elimination from hepatocytes and renal tubules (Lin and Yamazaki 2003). The process of drug (e.g., vinblastine and digoxin) efflux via Caco-2 cells by P-glycoprotein has been demonstrated to be saturable, with Michaelis–Menten constants (K_m values) of 26 and 58 μM , respectively, for vinblastine and digoxin (CAS no. 865-21-4 and 20830-75-5). Permeation studies indicate the following relationship:

$$\begin{aligned} &\text{Dose passing through intestinal cells} = \text{influx} \\ &\quad \times (\text{passive diffusion and/or active uptake}) - \text{efflux and metabolism.} \end{aligned}$$

Drug elimination is enhanced by the formation of glucuronic acid conjugates. The uridine 5'-diphosphate-(UDP)-glucuronosyltransferase (UGT) family of enzymes, comprising 14 functional “isoforms” (1A1, 1A3, 1A4, 1A6, 1A7, 1A8, 1A9, 1A10, 2A1, 2B4, 2B7, 2B15, 2B17, and 2B28) catalyze the conjugation of chemicals containing a suitable nucleophilic atom (i.e., aliphatic or aromatic hydroxyl, carboxyl or amino groups) with glucuronic acid. The structural features of substrates that confer isoform selectivity are not well understood. For almost all UGT isoforms, an aromatic ring attached to the nucleophilic atom increases the susceptibility of the nucleophilic atom to glucuronidation.

UGT is a membrane-bound protein with a poorly defined 3-dimensional structure (Sorich et al. 2006). According to Chang and Benet (2005), the V_{\max} and K_m constants for naphthol glucuronidation by human liver microsomes are $20.2 \text{ nmol} \cdot \text{min}^{-1} \cdot \text{mg}^{-1}$ and 216 μM , respectively. Little if any of the hydroxylated intact pyrethroids are conjugated prior to being eliminated. The importance of the activities of transporters and metabolizing enzymes in the ADME of pyrethroids has yet to be established. Inhibitors of these systems may be used to study their effect on ADME (Lau et al. 2003).

3.4 Skin Absorption

Until the beginning of the last century, the skin was believed to be an impervious layer, except perhaps for some permeability to inert gases (Scheuplein and Blank 1971). In 1877, Fleischer concluded that the intact skin of man was totally impermeable to all substances (Fleischer 1877). This belief was dispelled by Schwenkenbecker (1904) and others who demonstrated the relative permeability of skin to lipid-soluble substances and water.

3.5 Skin Permeability

It took almost 50 years after Schwenkenbecker's work to establish that the stratum corneum (horny layer) was the barrier that prevented water permeability of skin. The water permeability experiments of Berenson and Burch (1951) on isolated epidermis and stratum corneum provided evidence that the horny layer was, indeed, the permeability barrier. The permeability of water through skin is $0.2\text{--}0.4 \text{ mg} \cdot \text{cm}^{-2} \cdot \text{h}^{-1}$ at 30°C according to Baker and Kligman (1967). The process of percutaneous absorption is described as being the adsorption onto the stratum corneum, diffusion through it and through the viable epidermis, and finally through the papillary dermis and into the microcirculation (Scheuplein and Blank 1971). The stratum corneum acts as a passive diffusion medium, with the degree of hydration, swelling, diameters of sweat ducts and hair follicles playing a role in the absorption process.

From using both in vivo or in vitro studies, human skin has been found to be more impermeable than the skin of other species such as the cat, dog, rat, mouse, or guinea pig (Wester and Maibach 1977, 1993; Wester and Noonan 1980). Pig or guinea pig skin is favored for use in studies involving diffusion cells (Bronaugh et al. 1986; Harrison et al. 1984; Reifenrath and Kampainen 1991) over other animal skin types, whereas skin from the forearm or back is favored in live monkey studies and in studies performed on human volunteers (Feldmann and Maibach 1974). The degree of percutaneous absorption has been determined by using the isolated perfused rabbit ear (Bast et al. 1997), and other models have employed porcine skin flaps for the same purpose (Riviere and Monteiro-Riviere 1991; Riviere et al. 1986; Nicoli and Santi 2007). These methods are described in reviews authored by Bronaugh et al. (1982), Wester and Maibach (1993), and Barbero and Frasch (2009).

Work by Maibach et al. (1971), Serat (1973), Serat and Bailey (1974), and Serat et al. (1975) ignited interest in percutaneous studies involving worker exposure to cholinesterase-inhibiting organophosphorus pesticides in California. Two reviews by Knaak et al. (1989, 2002) detailed the history of the hazards posed by reentry into pesticide-treated foliage, laboratory and field exposure studies, and solutions for solving problems that included establishing pesticide reentry intervals in California. The use of blood cholinesterases as biomarkers of effect in field studies was reviewed by Nigg and Knaak (2000). (Ellison et al. 2011), Farahat et al. (2011), and Crane et al. (2011) reported on the effects of chlorpyrifos (CAS no. 2921-86-2) exposure to cotton-field workers in Egypt. Excellent agreement was obtained between cumulative urinary TCPy (CAS no. 6515-38-4) elimination, blood AChE and ButyrylChE inhibition, using a PBPK/PD model (Ellison et al. 2011). The field workers in this Egyptian study were first exposed to chlorpyrifos, then cypermethrin (CAS no. 52315-07-8) and later profenofos (CAS no. 41198-08-7), during the 2008 pesticide application season. Workers having had contact with cypermethrin on their hands and arms during mixing and spraying reported a tingling sensation (Farahat, personal communication).

3.6 Relationship Between K_p (Permeation Constant), Skin: Air, and Skin: Vehicle Partition Coefficients

The mathematical relationship between a dose applied to the skin and its absorption has been addressed by several authors (Scheuplein and Blank 1971; Guy et al. 1987; Potts and Guy 1992, 1995; Mattie et al. 1994; Moss et al. 2002; Geinoz et al. 2004). The steady-state flux (J_s , $\mu\text{g} \cdot \text{cm}^{-2} \cdot \text{h}^{-1}$) of solute through a simple inert membrane is described in (11) in terms of Fick's equation.

$$\text{Flux} = Dk_m C/l = K_p C, \quad (11)$$

where D is the diffusion coefficient ($\text{cm}^{-2} \cdot \text{h}^{-1}$), K_m is the partition coefficient of the chemical in skin (unit less), C is the concentration of the chemical in skin ($\mu\text{g} \cdot \text{cm}^{-3}$), l is the thickness of the skin (cm), and K_p is the permeability constant ($\text{cm} \cdot \text{h}^{-1}$). Flux takes on units of $\mu\text{g} \cdot \text{cm}^{-2} \cdot \text{h}^{-1}$ in the overall equation, depending upon whether or not C is in μg or μmols , or some other unit of measurement.

For chemicals such as the glycol ethers (Boatman and Knaak 2001) or pesticides, and when vehicles such as water or air are used, skin:air and skin:water partition coefficients must be determined and used in this equation to account for the higher concentrations in skin caused by partitioning.

K_p , area, and concentration per unit area are routinely used in PBPK/PD models that describe the absorption of a dermal dose to workers (Ellison et al. 2011), as shown in (12):

$$\text{Dose} (\mu\text{g}) = \text{Area} (\text{cm}^2) \times C (\mu\text{g} \text{cm}^{-3}) \times K_p (\text{cm} \text{h}^{-1}) \times \text{time} (\text{h}). \quad (12)$$

3.7 Skin:Blood Partition Coefficients

Mechanistic models for determining the partitioning of a pesticide between skin and blood are addressed in Sect. 4.4. In this section, blood plasma protein binding (F_{up}) was included in the Poulin–Theil model (2000; 2002a; b) to calculate tissue: blood partition coefficients. This procedure greatly reduces the amount of unbound pesticide in blood that is available for partitioning into adipose tissues. A laboratory method, such as the one developed by Jepson et al. (1992, 1994) and reviewed by Knaak et al. (2008), may be used to determine whether predicted values are correct.

3.8 Dermal Dose-Response, Pharmacokinetic, and Metabolism Studies

Sidon et al. (1988) developed 7- or 14-days dermal absorption data in Rhesus monkeys and Sprague–Dawley rats using permethrin (*cis* and *trans* isomers) labeled

with ^{14}C in the alcohol and cyclopropyl groups. Permethrin was applied to the forehead or forearm of the monkey and to the mid-lumbosacral region of the rat. An intramuscular dose was employed to correct for urinary recovery. The forehead skin (24–28%) of the monkey was more permeable to both isomers than was forearm skin (14–21%). No significant difference in dermal absorption was observed between the *cis*- and *trans*-isomers. For the rat, absorption was greater than in monkeys, with 46 and 43% of the *cis*- and *trans*-isomers being absorbed, respectively. In a similar study in six human volunteers, Wester et al. (1994) applied ^{14}C -pyrethrin in a formula containing 0.3% pyrethrin ($5.5 \mu\text{g} \cdot \text{cm}^{-2}$ of skin) and 3.0% of the insecticidal synergist, piperonyl butoxide ($75.8 \mu\text{g} \cdot \text{cm}^{-2}$ of skin) to the ventral forearm. The forearms were washed with soap and water 30 min after the application. The absorbed dose was determined by analysis of urine samples collected over a 7-days period. The volunteers absorbed 1.9% of the applied dose of pyrethrin. The authors calculated that 7.5% of the pyrethrin dose applied to the scalp was absorbed.

The effect on skin absorption of several insecticides was tested after *in vivo* pretreatment of the skin with either a 3% fenvalerate or 3% parathion in ethanol solution (Chang et al. 1995). The insecticides tested were carbaryl, fenvalerate, lindane, and parathion and their absorption was studied using a pig skin *in vitro* approach. Concentrations of 40 or 400 $\mu\text{g} \cdot \text{cm}^{-2}$ of carbaryl, fenvalerate, lindane, and parathion were used. Pretreatment with an ethanol control, or fenvalerate and parathion increased the total absorption of these insecticides proportionally with dose. In a study by Hotchkiss et al. (1992), ethanol was again shown to increase the percutaneous absorption of chemicals.

In an *in vitro* percutaneous study performed on rodent and pig skin with DEET (diethyl-m-toluamide; CAS no. 134-62-3), permethrin and carbaryl; results were that no permethrin was absorbed. It was believed by the authors that DEET inhibited the absorption of permethrin (Baynes et al. 1997). Bast et al. (1997) studied the percutaneous absorption of permethrin through the isolated perfused rabbit ear. Permethrin was applied in isopropyl myristate (reference ointment) or in ethanol. The ethanol was evaporated off skin, and the skin was covered with 1.5 (w/w) methyl cellulose in water. The authors measured the appearance rates ($\text{pmol} \cdot \text{min}^{-1} \cdot \text{cm}^{-2}$) of 3-phenoxy benzene methanol (CAS no. 13826-35-2) and 3-phenoxybenzoic acid (CAS no. 3739-38-6) in the effusate after dermal application ($3.61 \mu\text{mol} \cdot \text{cm}^{-2}$ of skin). No permethrin *per se* was found in the effusate. The metabolites were believed to be from impurities in the permethrin. From the concentration that permethrin constitutes in a pharmaceutical brand (Ambush[®]) and from detection limits, Bast et al. (1997) calculated a K_p of $2.63 \times 10^{-8} \text{ cm} \cdot \text{h}^{-1}$.

Other investigators (Eadsforth et al. 1988; van der Rhee et al. 1989; Woollen et al. 1992) reported percutaneous absorption rates of 1% or more of applied cypermethrin, the metabolites of which appeared in urine, and may have originated from impurities in the cypermethrin.

Percutaneous absorption studies with cypermethrin by Scott and Ramsay (1987) indicated that 1% of an *in vivo* dose to rats was absorbed after an 8-h exposure; however, no absorption was detected *in vitro* using human and rat skin after 8 h. A K_p was not calculated from the information obtained in the *in vivo* study.

4 Mechanistic Models for Determining Tissue: Blood Partition Coefficients

4.1 Tissue Partition Coefficients/Distribution

Pyrethroid physiologically based pharmacokinetic (PBPK) models require tissue: blood partition coefficients to describe the biological fate of chemicals in humans and animals. Partitioning into blood is determined by the solubility in the water and lipid components, and by protein binding. The effects of protein binding are more extensive in rat blood than in human blood for volatile organic chemicals of moderate or high lipophilicity (Payne and Kenny 2002). Compared with protein molecules in solution, as in blood, solid protein in tissues that have strong intermolecular interactions are expected to have a much reduced capacity for binding low molecular weight volatile organic compounds. The accuracy of such predictions is greater for human tissues than for rat tissues, because of the difficulties in modeling the very large protein-binding effects in rat blood. In this regard, Payne and Kenny (2002) cautioned from their work that no single equation can be applied to all circumstances.

4.2 Partition Coefficients From In Vitro Data

Knaak et al. (2008) reviewed the literature pertaining to in vitro methods for developing tissue: blood partition coefficients for PBPK models. The experimental work of Jepson et al. (1992, 1994) is significant. Ultrafiltration was used to develop tissue: saline and tissue: blood partition coefficients. No new studies of this nature were found during the preparation of this review on pyrethroids. Automated laboratory methods are still needed and must be developed to insure the partition coefficients obtained from the use of mechanistic or QSAR models are reasonable (Payne and Kenny 2002; Rowland, personal communication).

4.3 Selection of $P_{o:w}$ and Log $D_{o:w}$ Values

There are many log P /log D QSAR models (Knaak et al. 2008) published in the literature. The key to using the mechanistic (Poulin and Theil 2000, 2000a, b) approach to determining partition coefficients is the selection of a log P /log D model that adequately predicts values for the 15 pyrethroids targeted in this review, and their metabolites (ionized and nonionized species). Simulations Plus, Inc. (Lancaster, CA) uses built-in equations or data bases in GastroPlus to provide log P /log D values. On the basis of the findings in a carbamate review (Knaak et al. 2008), ACD Log D

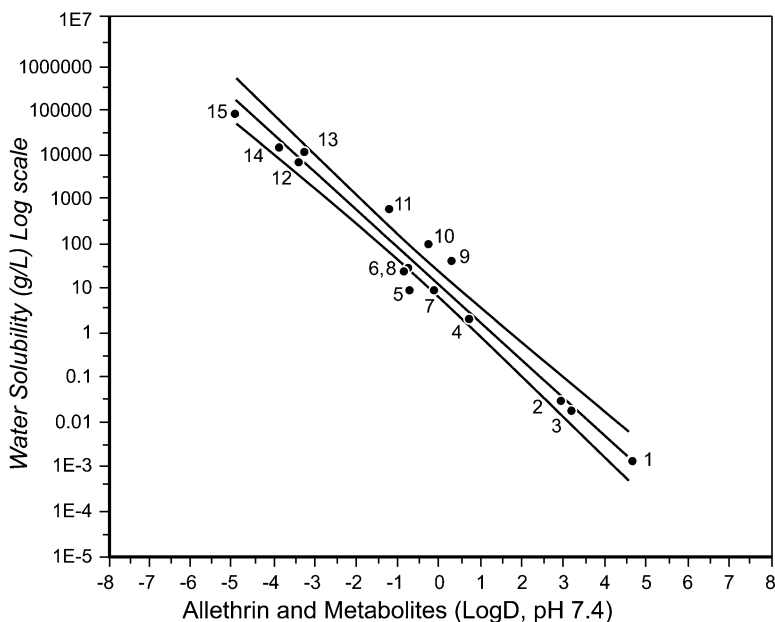


Fig. 7 The water solubility ($\text{g} \cdot \text{L}^{-1}$, Eq. 13) of allethrin and metabolites is plotted as a function of ACD Log $D_{\text{pH } 7.4}$. Allethrin and metabolites are identified in Table D1 (Appendix D). Outer bounds represent the 95% confidence interval (adj $R^2 = 0.95$)

Suite, Version 12.0 (ACD, Advance Chemistry Development, Toronto, Ontario, Canada) was selected for predicting pK_a , $\log P$, $\log D$, and water solubility (WS) values for the individual pyrethroids and their metabolites (see Appendix D and tables).

As part of the selection of a program for calculating $\log D$, the WS for each of the pyrethroids and their metabolites were individually plotted against $\log D_{\text{pH } 7.4}$ values to determine whether a linear, but inverse, relationship existed, based on the knowledge that metabolism significantly increases the water solubility of administered pesticides, drugs, and other chemicals. Water solubility was calculated using the equation (13) of Meylan and Howard (1994a, b), where:

$$\log(S \text{ mol} \cdot \text{L}^{-1}) = 0.796 - 0.854 \cdot \log(K_{\text{o:w}}) - 0.00728 \cdot \text{MW} + \text{corrections.} \quad (13)$$

ACD Log D values were used in the equation rather than $\log K_{\text{o:w}}$ values to calculate water solubilities. This procedure yielded linear plots with r^2 values greater than 0.9 for all 15 pyrethroids and their metabolites. Figures 7 and 8 show the plots for allethrin and cypermethrin. The numbers on the points in the two plots correspond to the numbers in Appendix D, Table D1, for allethrin and Table D5 for cypermethrin.

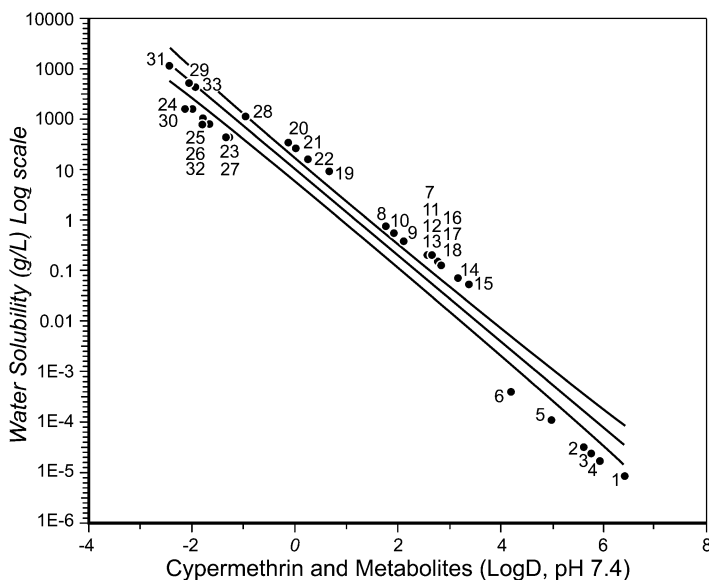


Fig. 8 The water solubility ($\text{g} \cdot \text{L}^{-1}$, Eq. 13) of cypermethrin and metabolites is plotted as a function of ACD Log $D_{\text{pH } 7.4}$. Cypermethrin and metabolites are identified in Table D5 (Appendix D). Outer bounds represent the 95% confidence interval (adj $R^2 = 0.95$)

Allethrin (pt 1) is at the bottom right-hand corner of Fig. 7, while allethrine (pt 9) and allethrine glucuronic acid (pt 12), allethrine sulfate (pt 13) are at the top left-hand corner with the glucuronics of Met B (pt 14) and Met A (pt 15). The unconjugated aglycones (pts 10, 11) appear below the conjugates. Point 4 belongs to allethrin acid.

Water solubilities $>10,000 \text{ g} \cdot \text{L}^{-1}$ were calculated by the Meylan and Howard (1994a, b) equation for conjugated pyrethroids metabolites, but were not determined by the ACD Log D suite. Cypermethrin (pt 1) appears at the lower right-hand corner of the plot followed by the ring hydroxylated cypermethrins (pts 2, 3, 4, 5 and 6). The metabolites in the middle of the plot are the cyanohydrins (pts 7, 8, 9 and 10), aldehydes (pts 11, 12, 13 and 14), and alcohols (pts 15, 16, 17 and 18). The metabolites at the upper end of the plot (pts 19–33) are the aminoacetic acids (glycine conjugates), benzoic acids, and conjugates of glucuronic and sulfuric acids.

4.4 Tissue:Blood Partition Coefficients

Knaak et al. (2008) used the Poulin and Theil (2000, 2002a, b) equations to obtain partition coefficients for a series of carbamate insecticides and their metabolites. Protein binding was not considered for carbamates because binding constants were

not readily available. Binding was included for chemicals in the equations used by GastroPlus™, SimulationsPlus, Inc., Lancaster, CA (www.simulations-plus.com) (Berezhkovskly (2004a, b, 2007); Poulin and Theil (2000, 2002a, b); Rodgers et al. (2005, 2007), Rodgers and Rowland (2006, 2007)) to calculate partition coefficients, while SimCYP™ (www.simcyp.com) modified the Poulin and Theil (2000, 2002a, b) equations for nonadipose tissues from:

$$P_{t:p} = \frac{[P_{o:w}(V_{nlt} + 0.3V_{pht})] + [(V_{wt} + 0.7V_{pht})]}{[P_{o:w}(V_{nlp} + 0.3V_{php})] + [(V_{wp} + 0.7V_{php})]} \times \frac{f_{up}}{f_{ut}} \quad (14)$$

to:

$$P_{t:p} = \frac{[P_{o:w}(V_{nlt} + 0.3V_{pht})] + [(V_{wt}/f_{ut} + 0.7V_{pht})]}{[P_{o:w}(V_{nlp} + 0.3V_{php})] + [(V_{wp}/f_{up} + 0.7V_{php})]}, \quad (15)$$

and for adipose tissue from:

$$P_{t:p} = \frac{[D_{vo:w}(V_{nlt} + 0.3V_{pht})] + [(V_{wt} + 0.7V_{pht})]}{[D_{vo:w}(V_{nlp} + 0.3V_{php})] + [(V_{wp} + 0.7V_{php})]} \times \frac{f_u}{1} \quad (16)$$

to:

$$P_{t:p} = \frac{[D_{vo:w}(V_{nlt} + 0.3V_{pht})] + [V_{wt} + 0.7V_{pht})]}{[D_{vo:w}(V_{nlp} + 0.3V_{php})] + [(V_{wt}/f_{up} + 0.7V_{php})]}, \quad (17)$$

based on the work of Berezhkovskly (2004a, b, 2007).

The Berezhkovskly (2004b) equation for obtaining tissue:plasma and tissue:blood partition coefficients is as follows:

$$P_{t-p}^0 = \frac{[K_{vo-w}(V_{tn} + 0.3V_{tph}) + 0.7V_{tph} + V_{tw}/F_{ut}]}{[K_{vo-w}(V_{pn} + 0.3V_{pph}) + 0.7V_{pph} + V_{pw}/F_{up}]}, \quad (18)$$

where F_{ut} and F_{up} are the unbound (free) drug fractions for tissue and plasma. The derivation of equation (18) is given in the paper by Berezhkovskly (2004b). Berezhkovskly points out that his definition of F_{ut} and F_{up} differs from the commonly used definitions f_{ut} and f_{up} of unbound fractions in tissue and plasma. The parameter F_{ut} describes only the protein binding through the values of the equilibrium dissociation constants K_{dj} (k_{dj}^-/k_{onj}) and protein concentrations P_j , while f_{ut} and f_{up} include both protein binding and partitioning. Equations (18)–(20) describe the relationships for F_{ut} and f_{ut} .

$$F_{ut} = 1 / \left(1 + \sum P_j / K_{dj} \right), \quad (19)$$

where,

$$\sum P_j/K_{dj} = \sum k_{ij}^+/k_{ij}^- = 1/F_{ut} - 1, \text{ and } k_{ij}^+ = k_{onj}P_j$$

while the equation for f_{ut} is as follows:

$$f_{ut} = 1 / \left(\sum P_{ij-w} v_{ij} + v_{tw}/F_{ut} \right), \quad (20)$$

where $v_{tw} = V_{tw}/V_t$; $v_{ij} = V_{ij}/V_t$ and $P_{ij-w} = (k_{ij}^+/k_{ij}^-)(v_{tw}/v_{ij})$.

In summary, the tissue-plasma partition coefficient calculated in (21) takes us back to (18) in the Berezhkovskly paper.

$$P_{t-p}^o = \frac{f_{up}}{f_{ut}} = \frac{\left(\sum P_{ij-w} v_{ij} + v_{tw}/F_{ut} \right)}{\left(\sum P_{pj-w} v_{pj} + v_{pw}/F_{up} \right)}. \quad (21)$$

On the basis of the work by Berezhkovskly, Poulin-Theil, and the GastroPlus User Manual (SimulationsPlus, Inc., Lancaster, CA), the binding equations [(22) and (23)] for the input parameters (f_{up} , f_{ut} , f_{up}/f_{ut}) were added to Table 6 for calculating partition coefficients for the 15 pyrethroids and their metabolites that we have targeted in this review. Table 6 was derived from Table 6 in Knaak et al. (2008). Equation (22) for calculating f_{up} was obtained from the GastroPlus User Manual. This equation requires values for F_{up} (% unbound in plasma). F_{up} values were determined using a QSAR program for predicting K_{hsa} values for the pyrethroids and their metabolites [Chang et al. (2009) F_{up} values derived from K_{hsa} values using QikProp, Unpublished results].

$$f_{up} = \frac{1}{10^{\log D_{7.4}} \left(\frac{V_{lipid}}{V_{water}} \right) + 1 + \frac{1-F_{up,exp}}{F_{up,exp}}}, \quad (22)$$

$$f_{ut} = \frac{1}{\left(1 + \left\{ \left[(1 - f_{up})/f_{up} \right] \times RA_t \right\} \right)}. \quad (23)$$

RA_t is the ratio of albumin concentration found in tissue over plasma. When using Poulin's method for adipose tissue, we assume that $RA_t = 0.15$; for other tissues we assume that $RA_t = 0.5$.

Equation (23) for calculating f_{ut} was already available in the Excel spreadsheet (Table 6; Knaak et al. 2008) used to calculate the Poulin-Theil partition coefficients for the carbamates Knaak et al. (2008). To correct for protein binding, the nonadipose and adipose tissue equations [(14) and (16)] of Poulin-Theil were both multiplied by f_{up}/f_{ut} . The revised Excel spreadsheets were used to calculate rat and human partition coefficients for the pyrethroids and their metabolites in Appendix D.

The users of the GastroPlus 5.0 program (SimulationsPlus, Inc., Lancaster, CA) are provided with a series of methods for calculating partition coefficients for perfusion- and permeability-limited tissues, when running PBPK models.

Table 6 An example of a spreadsheet used to calculate the partition coefficients (14) and (16) for cypermethrin (inTable D5; Appendix D)

Input parameters	Adipose		Nonadipose		Source
$\log D_{\text{pH}7.4 \text{ oxw}}$	-		6.41		ACD
pH^{a}	-		-		ACD
pK^{a}	-		-		ACD
$\log D_{\text{vo:w}}^*$	5.797		-		$\log D_{\text{vo:w}} = \log D_{\text{vo:w}}^*$
$\log D_{\text{vo:w}}$	5.797		-		$\log D_{\text{vo:w}} = 1.115 \log D_{\text{pH}7.4 \text{ oxw}} - 1.35$
f_{lip}	6.62E-4		1.6E-4		Equation (22)
f_{t}	4.4E-3		3.2E-4		Equation (23)
$f_{\text{ip}}/f_{\text{it}}$	1.505E-1		5.00E-1		Multiplier, (14) and (16)
F_{ip}	0.1064		0.1064		Chang (2009, unpublished)

Rat tissue	Eq. # ^a	Tissue (V_{t}) ^b	Water (V_{w}) ^b	Lipids		Numerator ^d	P_{cb}^{e}	P_{ip}^{f}	$V_{\text{t}}^*F_{\text{ip}}^{\text{g}}$
				Neutral (V_{nl}) ^b	Phospho (V_{pl}) ^b				
Adipose	16	0.0761	0.120	0.853	0.0020	53,5062.5	66.7	73.5	5.59
Adipose	14	0.0761	0.120	0.853	0.0020				
Bone	14	0.0415	0.446	0.0273	0.0027	72,355.3	7.38	7.80	0.324
Brain	14	0.0057	0.788	0.0392	0.0533	142,039.5	14.4	15.3	0.087
Gut	14	0.0270	0.749	0.0292	0.0138	85,867.4	8.76	9.26	0.250
Heart	14	0.0033	0.779	0.0140	0.0118	45,085.5	4.60	4.86	0.016
Kidney	14	0.0073	0.771	0.0123	0.0284	53,691.1	5.48	5.79	0.042
Liver	14	0.0366	0.705	0.0138	0.0303	59,901.8	6.11	6.46	0.236
Lung	14	0.005	0.790	0.0219	0.0140	67,267.1	6.86	7.25	0.036
Muscle	14	0.404	0.756	0.0100	0.0090	32,644.8	3.33	3.52	1.422
Skin	14	0.190	0.651	0.0239	0.0180	75,460.7	7.70	8.14	1.546
Spleen	14	0.002	0.771	0.0077	0.0136	30,280.0	3.09	3.27	0.007
Plasma	14	0.0449	0.960	0.00147	0.00083	4,636.9			9.639 ^h
Plasma ($D^*\text{vo/w}$)	16	0.0449	0.960	0.00147	0.00083				
Whole blood	14	0.0816	0.840	0.0013	0.002	1,096.7 ^g			
Whole blood ($D^*\text{vo/w}$)	16	0.0816	0.84	0.0013	0.002	4,900.6 ^f			
Erythrocytes	14	0.0367	NU ⁱ	NU	NU	1,207.8 ^e			

Human tissue	Eq. # ^a	Tissue (V_t) ^b	Water (V_w) ^b	Lipids			Numerator ^d	P_{tb}^j	P_{tp}^k	$V_t^*P_{tp}^l$
				Neutral (V_n) ^b	Phospho (V_p) ^b	$D_{pH\ 7.4\ o.w.}^c$				
Adipose	16	0.1196	0.18	0.79	0.002	495,575.6	31.1	28.5	3.408	
Adipose	14	0.1196	0.18	0.79	0.002					
Bone	14	0.0856	0.439	0.074	0.0011	191,057.9	8.68	7.86	0.673	
Brain	14	0.02	0.77	0.051	0.0565	174,659.2	7.94	7.18	0.144	
Gut	14	0.0171	0.718	0.0487	0.0163	137,748.2	6.26	5.67	0.097	
Heart	14	0.0047	0.758	0.0115	0.0166	42,360.9	1.92	1.74	0.008	
Kidney	14	0.0044	0.783	0.0207	0.01622	65,715.5	2.99	2.70	0.012	
Liver	14	0.026	0.751	0.0348	0.0252	108,882.7	4.95	4.48	0.116	
Lung	14	0.0076	0.811	0.003	0.009	14,652.1	0.67	0.60	0.005	
Muscle	14	0.4	0.76	0.0238	0.0072	66,728.2	3.03	2.74	1.098	
Skin	14	0.0371	0.718	0.0284	0.0111	81,559.4	3.71	3.35	0.124	
Spleen	14	0.0026	0.788	0.0201	0.0198	66,933.9	3.04	2.75	0.007	
Plasma	14	0.0424	0.945	0.0035	0.00225	12,159.5			5.734 ^b	
Plasma (D*vo/w)	16	0.0424	0.945	0.0035	0.00225	2,617.9 ^l				
Whole blood	14	0.0771	0.82	0.0032	0.002	11,006.7 ^k				
Whole blood (D*vo/w)	16	0.0771	0.82	0.0032	0.002	2,398.4 ^l				
Erythrocytes	14	0.0347	NU	NU	NU					
All tissue less plasma		0.956								

^aEquation number used to calculate partition coefficients: P_{tb} and P_{tp}

^bValues used in (14) and (16) as presented in Poulin and Thiel (2002a). Values for (6) in Poulin and Thiel (2002a) are: E: P (erythrocyte; plasma in vivo) = 1,

B:P (blood; plasma in vitro) = 1, and Ht (hematocrit in blood) = 0.45

^cAntilog $D_{pH\ 7.4\ o.w.}$, $\log D_{pH\ 7.4\ v.o.w.}$ and $\log D_{pH\ 7.4\ v.o.w}$

^dNumerator value from (14) or (16) depending on tissue

^eDenominator value used in (14) or (16) for P_{tb} in the rat

^fDenominator value used in (14) or (16) for P_{tp} in the rat

^gDenominator value used in (14) or (16) for $V_t^*P_{tp}$ in the rat

^hVolume distribution at steady state (V_{dss} ; $L\ kg^{-1}$)

ⁱNU = Not used in Poulin and Thiel (2002a)

^jDenominator value used in (14) or (16) for P_{tb} in the human

^kDenominator value used in (14) or (16) for P_{tp} in the human

^lDenominator value used in (14) or (16) for $V_t^*P_{tp}$ in the human

The Poulin and Theil (homogeneous and extracellular), Berezhkovskly and Rodgers, Leahy, and Rowland methods for calculating partition coefficients are among those available in the program. The Poulin and Theil and Berezhkovskly models take into consideration the volume fractions of water, phospholipids, neutral lipids, and unbound protein fractions in tissues and plasma (f_{ut} and f_{up}). The Poulin and Theil models do not take into consideration unbound proteins.

Rodgers et al. (2005, 2007) and Rodgers and Rowland (2006, 2007) incorporated drug ionization and the interaction of strong bases with acidic phospholipids in calculating partition coefficients (K_p) for drugs, where $K_p = K_{pu} \times f_u$. The basic equation for the calculation of unbound tissue–plasma partition coefficient, K_{pu} , is shown in (24) as it has been rewritten by Simulations-Plus, Inc., Lancaster, CA in their GastroPlus user manual (version 6.0).

Strong bases and group I zwitterions (compounds with at least one base $pK_a \geq 7$)

$$K_{pu} = V_{ewt} + \left(\frac{(1/X_{[D],IW})}{(1/X_{[D],P})} V_{iwt} \right) + \left(\frac{K_a [AP]_T ((1/X_{[D],IW}) - 1)}{(1/X_{[D],P})} \right) + \left(\frac{K \cdot V_{nlt} + (0.3K + 0.7)V_{pht}}{(1/X_{[D],P})} \right), \quad (24)$$

where V_{nlt} , V_{pht} , V_{ewt} , V_{iwt} are the volume fraction of neutral lipids, phospholipids, intracellular and extracellular water in tissues, K_a is the association constant of basic compound with acidic phospholipids, $[AP]_T$ is the concentration of acidic phospholipids in individual tissues, $X_{[D], IW}$, $X_{[D], P}$ are the fraction of neutral drug species in intracellular space (pH = 7.0) and plasma (pH = 7.4), and K is the solvent/water partition coefficient for the drug (vegetable oil/water partition coefficient for adipose and yellow marrow; 1-octanol/water partition coefficient for all other tissues).

The term $((K_a [AP]_T ((1/X_{[D],IW}) - 1)) / (1/X_{[D],P}))$ represents the interactions of bases with acidic phospholipids.

The equation for the calculation of unbound tissue–plasma partition coefficients, K_{pus} , for neutral pyrethroids and their acidic metabolites is shown in (25).

Acids, neutrals, weak bases, and group 2 zwitterions (all $pK_{as} < 7$)

$$K_{pu} = \left(\frac{(1/X_{[D],IW})V_{iwt}}{(1/X_{[D],P})} \right) + V_{ewt} + \left(\frac{K \cdot V_{nlt} + (0.3K + 0.7)V_{pht}}{(1/X_{[D],P})} \right) + \left(\frac{1}{f_{up}} - 1 - \frac{K \cdot V_{nlp} + (0.3K + 0.7)V_{php}}{(1/X_{[D],P})} \right) \times RA_t, \quad (25)$$

where V_{nlt} , V_{pht} , V_{ewt} , V_{iwt} are the volume fraction of neutral lipids, phospholipids, intracellular and extracellular water in tissues, V_{nlp} , V_{php} are the

volume fraction of neutral lipids and phospholipids in plasma, RA_t is the ratio of albumin (for nonionizable compounds) or lipoprotein (for ionizable compounds) concentration found in tissue over plasma, $X_{[D],IW}$, $K_{[D],p}$ are the fraction of neutral drug species in intracellular space (pH = 7) and plasma (pH = 7.4), K is the solvent/water partition coefficient for the drug (vegetable oil/water partition coefficient for adipose and yellow marrow; 1-octanol/water partition coefficient for all other tissues), f_{up} is the fraction of unbound in plasma.

For all types of compounds, the final K_p is calculated as:

$$K_p = K_{pu} \times f_{up}$$

Two equations (24) and (25) were combined in GastroPlus by SimulationsPlus, Inc. into a single equation (26) to provide a continuous shift from neutral and acid compounds, which bind almost exclusively to albumin, to strong bases that bind almost exclusively to acidic phospholipids,

$$\begin{aligned} K_{pu} = & V_{ew} + \left(\frac{1/X_{[D],iw}}{1/X_{[D],p}} V_{iw} \right) + \left(\frac{P \cdot V_{nlt} + (0.3 \cdot P + 0.7) \cdot V_{pht}}{1/X_{[D],p}} \right) \\ & + (F_n + F_a) \cdot \left[\frac{1}{f_{up}} - 1 - \left(\frac{P \cdot V_{nlp} + (0.3 \cdot P + 0.7) \cdot V_{php}}{1/X_{[D],p}} \right) \right] \cdot RA_{tp} \\ & + (F_c) \cdot \left(\frac{K_a \cdot [AP]_T \cdot ((1/X_{[D],IW}) - 1)}{(1/X_{[D],p})} \right), \end{aligned} \quad (26)$$

where $(F_n + F_a)$ is the fraction of drug without positive charge in plasma and F_c is the fraction of drug with positive charge in plasma. The remaining parameters have the same meaning as in the original two Rodgers equations.

4.5 Partition Coefficients for Pyrethroids and Metabolites

The spreadsheet in Table 6 was used to calculate the partition coefficients for allethrin and cypermethrin which are depicted in Figs. 9 and 10 (Appendix D, Tables D1, and D5).

4.5.1 Graphs of $\log D_{pH\ 7.4}$ vs. Adipose Tissue: Blood and Liver: Blood Partition Coefficients

The plots of $\log D_{o:w}$ (pH 7.4) vs. $PC_{t;b-liver}$ and $\log D_{vo:w}^*$ (pH 7.4) vs. $PC_{t;b-adipose}$ for allethrin and cypermethrin are shown in Figs. 9 and 10. In these two figures, the water-soluble metabolites, with $\log D_{pH\ 7.4} < 2$, all have $PC_{t;b-liver}$ and $PC_{t;b-adipose}$ values ≤ 2.0 at the bottom of each plot; in contrast, the parent pyrethroid and their neutral metabolites, with $\log D_{pH\ 7.4} > 0$, have $PC_{t;b}$ values ranging from 1.0 to 80.0 extending up in a sigmoid curve to the right side of each plot.

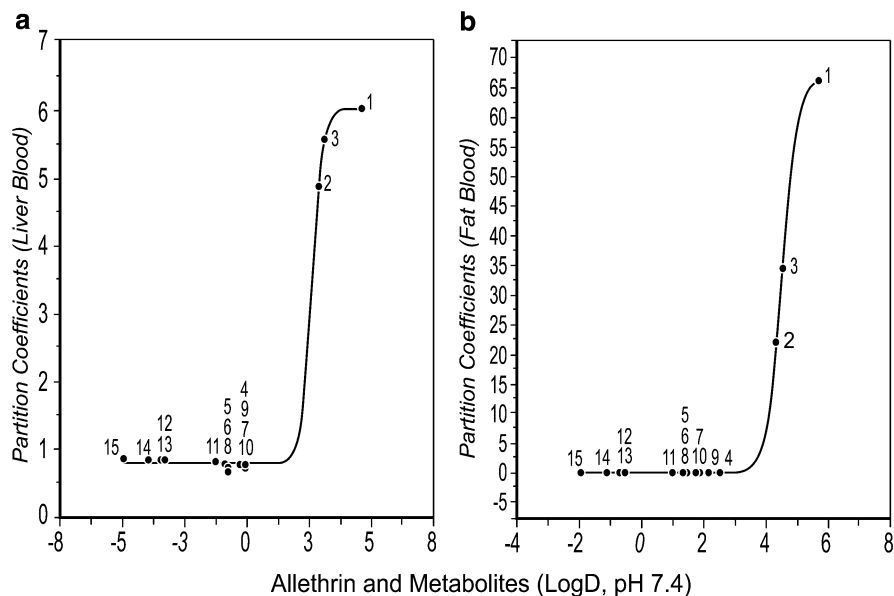


Fig. 9 Liver: blood and fat blood partition coefficients of allethrin and metabolites are plotted as a function of ACD Log $D_{pH\ 7.4}$. Equation (14), involving ACD Log $D_{pH\ 7.4}$, was used to calculate the partition coefficients for liver. Equation (16), involving the conversion of ACD Log $D_{pH\ 7.4}$ to log $D^*_{vo:w}$, was used to calculate the partition coefficients for fat. To correct for protein binding, the nonadipose and adipose tissue equations (14) and (16) were multiplied by f_{up}/f_{ut} derived from equations (22) and (23) (see Table 6). The Henderson-Hasselbach equations were not used. Allethrin and its metabolites are identified in Table D1 (Appendix D)

5 In Vivo Metabolism of 15 Pyrethroid Insecticides

The metabolic pathways for each of the 15 pyrethroids addressed in this review are given in Tables E1–E17 (see Appendix E). The tables were developed from available pathway data published in the literature (Anadon et al. 1996; Cole et al. 1982; Crawford and Hutson 1977; Hutson and Logan 1986; Izumi et al. 1984; Kaneko et al. 1987; Kaneko and Miyamoto 2001; Miyamoto et al. 1974; Nakamura et al. 2007; Ruzo et al. 1978; Staiger and Quistad 1984; Tomigahara et al. 1994a,b,c, 1996, 1997; Ueda et al. 1975) and from physiological models (Mirfazaelian et al. 2006) developed from the pathways.

A preliminary physiological model for allethrin is presented in Fig. 1F, Appendix F. Preliminary ACSL-based physiological models were also written for deltamethrin, *cis/trans* permethrin, and *cis/trans* resmethrin (Knaak, unpublished). A PBPK model was developed for deltamethrin (Mirfazaelian et al. 2006; Godin et al. 2010; Tornero-Velez et al. 2010) to assess internal dose levels in various organs and tissues of rats and humans. Deltamethrin was selected to represent the disposition of the pyrethroids, because it is structurally similar to other commercial

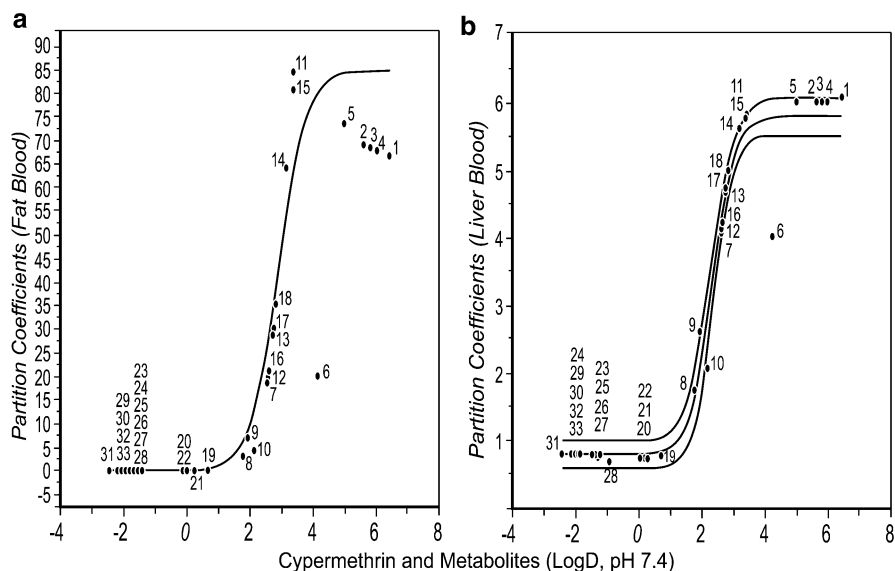


Fig. 10 Liver: blood and fat: blood partition coefficients of cypermethrin and metabolites are plotted as a function of ACD Log $D_{pH\ 7.4}$. Equation (14), involving log $D_{pH\ 7.4}$, was used to calculate partition coefficients for liver. Equation (16), involving the conversion of ACD Log $D_{pH\ 7.4}$ to log $D^*_{vo,w}$, was used to calculate the partition coefficients for fat. To correct for protein binding, the nonadipose and adipose tissue equations (14) and (16) were multiplied by f_{u_p}/f_u , derived from equations (22) and (23) (see Table 6). The Henderson-Hasselbach equations were not used. Cypermethrin and its metabolites are identified in Table D5 (Appendix D)

pyrethroids and is formulated as a single isomer ((S)-cyano-3-phenoxybenzyl (1R, 3R)-cis-3-(2, 2-dibromovinyl)-2, 2-dimethylcyclopropane carboxylate). This minimized any complexities introduced by the presence of multiple isomers. An important characteristic of these models is that they incorporate diffusion-limited kinetics. Godin et al. (2010) proposed diffusion-limited kinetics in all tissues, while Mirfazaelian et al. (2006) and Tornero-Velez et al. (2010) proposed mixed-flow and diffusion-limited kinetics. Based on a finding of apparent first-order kinetic behavior, Godin et al. (2010) applied a first-order clearance structure in modeling the biotransformation of deltamethrin.

In the past, industry sold most pyrethroids as isomer mixtures; however, in recent years the active isomer or isomers are being made and sold under different, but similar product names (e.g., biopermethrin, cismethrin, bioresmethrin, and deltamethrin). This reflects the fact that the manufactures were able to economically produce one, or primarily one isomer. It is, therefore, reasonable to now develop PBPK models for these active isomers, rather than to try to construct them to only reflect the metabolism of mixtures. As a result of our having reviewed the metabolism of the 15 pyrethroids of interest in this paper, we have attempted to point out the isomers of each product that were studied (e.g., labeled with ^{14}C), and to provide their relative insecticidal activities. In Appendix D, Tables D1–D15, we

present the chemical structures (generic), physical parameters, and tissue partition coefficients of the parent pyrethroids and their metabolites. The stereochemistry of these pyrethroids was presented in Appendix B (see Tables B1–B30).

5.1 Allethrin

Casida et al. (1971a, b); Yamamoto et al. (1971); and Elliott et al. (1972) analyzed the rat urinary metabolites resulting from the administration of ^{14}C -allethrin (CAS no. 584-79-2). Allethrin was oxidized at the chrysanthemate isobutenyl moiety to a *trans*-2-carboxy-1-propen-1-yl group and at the allyl group to derivatives of 1-hydroxy-2-propenyl-1-yl and 2, 3-dihydroxypropyl. A methyl group on the cyclopropyl moiety was hydroxylated to give the hydroxymethyl derivative. Chrysanthemum dicarboxylic acid (CAS no. 497-95-0) and allethrolone (CAS no. 29605-88-7) were found as hydrolysis products in urine. The major metabolites in rats were the diol of allethrin carboxylic acid (CAS no. 31338-05-3), allethrin monohydroxy acid (CAS no. 31338-06-4), and allethrin hydroxymethyl acid (CAS no. 36912-77-3). The last two metabolites were found by Class et al. (1990) in urine to partly exist as conjugates. Metabolites were tentatively identified by chemical ionization mass spectrometry, following treatment with diazomethane or diazoethane and trimethylsilylacetamide and high-resolution GC. According to Yamamoto et al. (1971), allethrin is eliminated primarily as intact esters, with small amounts of the chrysanthemum dicarboxylic acid being present in urine. In Table D1, Appendix D, we give the structure and technical name of allethrin. No information was found concerning the stereochemistry of the allethrin used in the metabolic studies and the position of the label(s).

5.2 Bifenthrin

A complete metabolic pathway for bifenthrin in the rat is given in Table D2, Appendix D. Intact bifenthrin is first hydroxylated on the biphenyl ring or one of the dimethyls on the cyclopropane ring before being hydrolyzed to yield alcohols (e.g., CAS no. 76350-90-8) and TFP acid (CAS no. 74609-46-4). This metabolism information was obtained from Figs. 58.2 and 76.2, Kaneko and Miyamoto (2001) and Kaneko (2010), respectively.

Bifenthrin and cyhalothrin both possess the 2-chloro-3, 3, 3-trifluoropropenyl group; however, they differ by cyhalothrin having a cyano group and a phenoxyphenyl ring, while bifenthrin has a 1, 1'-biphenyl ring and no cyano group. Bifenthrin (100% *cis*) contains two isomers (A + D) and is the primary commercial product in use. No information was given by Kaneko (2010) regarding the stereochemistry of the bifenthrin used in the metabolism studies.

In a rat study involving the two isomers of bifenthrin, the major metabolites found in rat plasma (Smith et al. 2002; Tullman 1987) were the parent compound, the hydrolysis product, 2-MBP alcohol, [1'1-biphenyl]-3-methanol, 2-methyl (CAS no. 76350-90-8), and the oxidized product of the alcohol, 2-MBP acid, [1,1'-biphenyl]-3-carboxylic acid (CAS no. 115363-11-6). The 2-MBP acid compound is analogous to 3-phenoxybenzoic acid (CAS no. 3739-38-6), the hydrolysis product of cypermethrin, deltamethrin, permethrin, and fenvalerate (Huckle et al. 1981a, b, 1984; IARC 1991; Woollen et al. 1992). In addition to these ester-cleaved products, 4'-OH, 2-MBP alcohol (CAS no. 115340-46-0) and 4'-OH, 2-MBP acid (CAS no. NA) were found. According to Kaneko (2010), these metabolites are metabolically converted to dimethoxy 2-MBP alcohol and dimethoxy 2-MBP acid.

In another study (Wheelock et al. 2006), the 2-methyl group of bifenthrin was reported to be hydroxylated to give 2-hydroxymethyl bifenthrin. The 4'- and 2'-positions of 1, 1' biphenyl were also hydroxylated to give the 4'OH and 2'OH pyrethroids before hydrolysis by carboxylesterases. According to Wheelock et al. (2006), bifenthrin is resistant to attack by carboxylesterases.

5.3 Cyfluthrin

The metabolic pathway data presented in Table D3, Appendix D, and Table E3, Appendix E, were obtained from Figs. 58.4 and 76.4 in Kaneko and Miyamoto (2001) and Kaneko (2010), respectively. The structure and stereochemistry of cyfluthrin is given in Table 2. Cyfluthrin is a Type II pyrethroid and possesses a cyano group. β -Cyfluthrin (CAS no. 68359-37-5) contains both the *cis* (30–40%) and *trans* (57–67%) isomers of cyfluthrin and is the primary commercial-use product. The *cis* and *trans* forms each contain two isomers (B+G) and (D+E) as shown in Appendix B, Table B5. The other four forms (A+H) and (C+F) comprise ~5% of β -cyfluthrin. No information was given by Kaneko (2010) regarding the stereochemistry of the cyfluthrin used in metabolic studies.

In rat studies, the 4-fluoro-3-phenoxyphenyl group of cyfluthrin is hydroxylated in the 2', 4'- and 5'-position, while one of the 2, 2-dimethyl groups is hydroxylated to form a 2-hydroxymethyl derivative. Hydrolysis of the ester(s) yields the cyanohydrins of phenoxybenzeneacetonitrile (e.g., CAS no. 76783-44-3), which are further converted to alcohols, acids, and ultimately are conjugated with glucuronic acid, sulfuric acid or glycine. The liberated dichlorocyclopropanecarboxylic acids (DCCA; 3-(2, 2-dichloroethenyl)-2, 2-dimethyl-cyclopropanecarboxylic acid and 2-OHMeDCCA; 3-(2, 2-dichloroethenyl)-2-(hydroxymethyl)-2-methyl-cyclopropanecarboxylic acid) are eliminated per se, or as conjugates with glucuronic acid prior to excretion in urine.

In a human inhalation study by Leng et al. (1997), nine male volunteers were exposed to an aerosol containing cyfluthrin at mean concentrations of 160 and 40 $\mu\text{g}/\text{m}^3$. The main urinary metabolites of cyfluthrin were *cis/trans* DCCA

and 4-fluoro-3-phenoxybenzoic acid (FPBA). The same metabolites were found in the urine of pesticide applicators applying cyfluthrin in Germany (Hardt and Angerer 2003).

The urinary biomarker FPBA was also found in the urine of humans exposed to indoor residential cyfluthrin residues during a Jazzercise™ exercise program (Williams et al. 2003).

5.4 Cyhalothrin

The nature of the metabolites of cyhalothrin are listed in Table D4, Appendix D, and are shown in Figs. 58.5 and 76.5 as taken from Kaneko and Miyamoto (2001) and Kaneko (2010), respectively. γ -Cyhalothrin (CAS no. 76703-62-3) is the most insecticidally active of the eight possible chiral isomers (16 involving the double bond) of cyhalothrin. Cyclopropyl- C^{14} -labeled γ -cyhalothrin (position 1) was prepared by Johnson (2007) for studying the metabolism and the environmental fate of this pyrethroid. This pyrethroid is currently marketed by Pytech Chemicals GmbH (joint venture between Dow AgroSciences and Cheminova A/S). Information on the metabolism of cyhalothrin and bifenthrin is scanty. According to the literature, the CF_3 (dihalovinyl) group is stable and the double bond (vinyl group) does not undergo hydroxylation. Cytochrome P450 enzymes hydroxylate the alcohol (benzenemethanol, 2-phenoxy-) in the 4'-position and perhaps in the 2'-position, and in the 5'-position as well, before hydrolysis by carboxylesterases.

According to Kaneko (2010), the major metabolic reaction is ester hydrolysis followed by hydroxylation of the alcohol moiety and its subsequent oxidation to an acid. The cyano group of the alcohol, benzeneacetonitrile, α -hydroxy-3-phenoxy (CAS no. 39515-47-4) is converted to an SCN ion. The major metabolites of the acid moiety are cyclopropylcarboxylic acid and its glucuronide, while the alcohol moiety is converted to PB acid (benzoic acid, 3-phenoxy) (CAS no. 3739-38-6), 4'-OH PB acid (benzoic acid, 3-(4-hydroxyphenoxy)) (CAS no. 35065-12-4), and the sulfate of 4'-OH-PB acid (benzoic acid, 3-[4-(sulfooxy)phenoxy]) (CAS no. 58218-91-0).

5.5 Cypermethrin

Table D5, Appendix D, shows the metabolites of cypermethrin as defined by Kaneko and Miyamoto (2001) and Kaneko (2010). Cypermethrin (eight stereoisomers) typically contains 20–40% α -cypermethrin (CAS no. 67375-30-8; B+G isomers). The two isomers, B+G are the most toxicologically active isomers in cypermethrin.

Crawford et al. (1981a) orally administered separate *cis* and *trans* isomer mixtures or *cis-trans* mixtures of radiolabeled cypermethrin (cyclopropyl- ^{14}C ,

benzyl- ^{14}C , or cyano- ^{14}C) individually to male and female rats ($1\text{--}5\text{ mg kg}^{-1}$), in a mass balance and tissue retention study. The cypermethrin isomers were analyzed on a column of 5- μm Hypersil (Shandon Southern Products Ltd., Runcorn, UK) (20 cm \times 4.5 mm) using hexane in 30% water-saturated dichloromethane (4:1 v/v). The isomers eluted as follows: 1R, *cis*- αR and 1S, *cis*- αS isomers; 1R, *cis*- αS and 1S, *cis*- αR isomers; 1S, *trans*- αS and 1R, *trans*- αR isomers; 1S, *trans*- αR and 1R, *trans*- αS isomers. Single oral doses of *cis*- and *trans*-cypermethrin (benzyl- ^{14}C label) were rapidly eliminated in urine with the exception of the *cis* isomer in female rats, in which the 0–24 output was 53% for males and 35% for females. A sex difference was not observed for the *trans*-isomers.

A total of 98.9% of the label from the *cis*-isomers was recovered in 8 days and 103.2% for the *trans*- isomers was recovered in 3 days. No respiratory $^{14}\text{CO}_2$ was eliminated. The radioactivity from (cyclopropyl- ^{14}C)-*cis*, *trans*-cypermethrin (mixture) was eliminated in the urine of both male (55.8%) and female (66.5%) rats. Fecal elimination amounted to 28.7% by male and 27.0% by female rats. Less than 0.1% of the dose was eliminated as respiratory carbon dioxide. The radioactivity from the (cyano- ^{14}C)-*cis*, *trans*-cypermethrin (mixture) was different from the other two labels as the α -cyano group was released and converted to thiocyanate ion, which was slowly eliminated from the body. The majority of the administered radiocarbon was recovered in the feces (42.0–57.2%) with lesser amounts in urine (8.3–9.6%). Respiratory carbon dioxide contained 1–2% of the administered radioactivity. Tissue residues from (benzyl- ^{14}C) *cis*-cypermethrin were highest in fat (0.83–1.46 $\mu\text{g/g}$) of male and female rats, 8 days after administration.

Information on the nature of the excreted metabolites was published by Crawford et al. (1981b). The major metabolic reactions were hydrolysis of *trans*- and *cis*-cypermethrin, hydroxylation of a geminal dimethyl on the cyclopropane ring, and hydroxylation of the phenoxy group at the 4'-position. The unlabeled standard compounds used for metabolite identification were described by Ruzo and Casida (1981), Ruzo et al. (1978), and Unai and Casida (1977). Separation and identification of metabolites was achieved on F254 silica gel 60 TLC chromatoplates (Cole et al. 1982).

In the just mentioned 1982 study by Cole et al., metabolites from ^{14}C -acid (geminal dimethyl), ^{14}C -alcohol (benzyl methine), and ^{14}CN (cyano) labeled (1R, αS)-*cis* cypermethrin preparations and their percentages were identified in urine and feces. Cole et al. (1982) recovered 100% of a ^{14}C -benzyl-labeled dose (0.12 mg/kg) of cypermethrin [(1R, αS)-*cis* cypermethrin (CAS no. 65731-84-2)] in the urine (62.9%), feces (33.8%) and tissue (3.3%) of rats. Cypermethrin is metabolized in the rat to the 4'-OH ester (CAS no. 64691-63-0) (4.1%), PB acid (CAS no. 3739-38-6) (5.9%), 4'-OH PB acid (CAS no. 35065-12-4) (3.0%), the glucuronides of PB alcohol (CAS no. 65658-93-7) (15.4%), PB acid (CAS no. 57991-35-2) (0.1%), 4'-OH PB acid (CAS no. 66858-01-7) (5.4%), the sulfates of 4'-OH PB acid (CAS no. 58218-91-0) (28.7%), 2'-OH PB acid (CAS no. 61183-26-4) (3.3%), and the glycine conjugate of PB acid (CAS no. 57991-36-3) (1.5%). Products retaining the ester linkage were found in feces, while hydrolysis products

were present in urine. The findings by Cole et al. (1982) are in agreement with those of Crawford et al. (1981a, b) and Ruzo et al. (1978).

Hutson and Logan (1986) reported on the metabolic fate in rats of WL85871, which was a mixture of two isomers of cypermethrin [(1R, *cis*) α S and (1S, *cis*) α R]. Approximately 20% of the ingested compound was not absorbed and was eliminated unchanged in the feces. There was no evidence for any racemization of the chiral centers of WL85871 either in the intestine, the feces, or in fat. Approximately 40% of a 2.0 mg/kg dose was eliminated in urine as 3-(4-hydroxyphenoxy) benzoic acid sulfate (CAS no. 58218-91-0). Some hydroxylation occurred before hydrolysis. The small proportion of the dose stored in adipose tissue was eliminated by biphasic kinetics (2–3 days and 17–26 days).

Humans eliminated conjugates of 3-phenoxybenzoic acid (CAS no. 3739-38-6), 3-(4'-hydroxyphenoxy) benzoic acid (CAS no. 35065-12-4), and cyclopropane-carboxylic acid (DCCA; CAS no. 55701-05-8) in urine according to Woollen et al. (1992). In the Woollen et al. study, cypermethrin was administered orally to six male volunteers as a single dose (3.3 mg; *cis:trans* 1:1) and dermally to six volunteers at a dose of 31 mg/800 cm² (*cis:trans* 56:44) of skin. Cypermethrin was orally absorbed between 27 and 57% (mean of 36%) based on the elimination of DCCA and four times greater based on the recovery of benzoic acid conjugates. In the case of the dermal studies, 1.2% of the applied dose was recovered in urine as benzoic acid conjugates.

5.6 Deltamethrin

Table D6, Appendix D, gives the metabolites of deltamethrin as presented in Figs. 58.8 and 76.8, respectively, by Kaneko and Miyamoto (2001) and Kaneko (2010). Deltamethrin (CAS no. 52918-63-5) is sold as a single chiral isomer [(1R, α S)-*cis* deltamethrin].

Cole et al. (1982) recovered 100% of a ¹⁴C-benzyl-labeled dose of deltamethrin [(1R, α S)-*cis* deltamethrin, CAS no. 52918-63-5] administered to rats (0.32 mg/kg), in urine (65.2%), feces (32.6%), and tissues (2.2%). These recovery values are quite similar to those obtained using radiolabeled cypermethrin. Metabolites from acid-¹⁴C, alcohol-¹⁴C, and ¹⁴CN-labeled preparations and their percentages were identified in urine and feces by Cole et al. (1982). Products retaining ester linkage were found in feces, and hydrolysis products were present in urine. The Cole et al. (1982) findings are in agreement with those of Crawford et al. (1981a, b) and Ruzo et al. (1978). Staiger and Quistad (1984) reviewed the nature of the urinary metabolites of deltamethrin resulting from the administration of 0.32 mg kg⁻¹ to rats. The same alcohol-¹⁴C- and ¹⁴CN-labeled metabolites were eliminated by rats receiving deltamethrin (0.32 mg kg⁻¹) as those receiving cypermethrin (0.12 mg kg⁻¹). The percentages of each of the metabolites varied somewhat, particularly by showing differences in the percentage of each of the glucuronides or sulfates. The glucuronide of PB alcohol from deltamethrin was lower (4.1%

vs. 15.4%) than the corresponding one from cypermethrin. The sulfate of 4'-OH PB acid arising from the administration of deltamethrin was higher (47.5%) than from cypermethrin (28.7%). The significance of this difference is unknown and may not be very important, because overall recoveries and urinary elimination were very similar.

5.7 Fenvalerate

Table D7, Appendix D, gives the chemical structure of parent pyrethroid and metabolites of fenvalerate (Kaneko and Miyamoto 2001; Kaneko 2010). Fenvalerate or Pydrin (CAS no. 51630-58-1) contain equal amounts of the four chiral isomers (Appendix B, Table B14), while esfenvalerate (CAS no. 66230-04-4), shown in Table B14, is comprised of 84% of the D isomer.

Ohkawa et al. (1979) recovered 100% of α - ^{14}C -benzyl-labeled dose of fenvalerate (CAS no. 51630-58-1), administered to rats (8.0 mg/kg), in urine (63.9%), feces (31.7%) and tissue (4.4%) at the end of the study. Staiger and Quistad (1984) identified the urinary metabolites of fenvalerate resulting from the administration of 8.0 mg kg⁻¹ to rats. The primary metabolites were the 4'-OH ester (5.6%), the sulfates of 4'-OH PB acid (40%) and 2'-OH PB acid (3.7%) and unconjugated aglycones (5.2%). The glucuronides of these acids and PB acid were present at considerably lower percentages (~2.3%).

5.8 Fenpropathrin

Table D8, Appendix D, provides the chemical structures of parent pyrethroid and metabolites of fenpropathrin from the work of Kaneko and Miyamoto (2001) and Kaneko (2010).

Crawford and Hutson (1977) studied the metabolism of a 1.5 mg/kg oral dose of benzyl- ^{14}C -labeled fenpropathrin in the rat. The stereochemistry of fenpropathrin was not indicated. Fifty-seven percent of the administered dose was eliminated in urine and 40% in feces within 48 h. Fenpropathrin was hydroxylated on the phenyl ring to form 4'-OH fenpropathrin and at a *trans* methyl group on the cyclopropane ring. The intact hydroxylated esters and fenpropathrin were cleaved by carboxylesterase action and eliminated as the glucuronide of tetramethyl CPCA (2, 2, 3, 3-tetramethyl cyclopropanecarboxylic acid; CAS no. 15641-58-4), 2-OH, trimethyl CPCA (2-(hydroxymethyl)-2, 3, 3-trimethyl-cyclopropanecarboxylic acid; CAS no. 97280-65-4), and the O-sulfates of the oxidized 3-phenoxybenzene moiety.

For ^{14}C -acid- and ^{14}C -alcohol-labeled fenpropathrin, Kaneko et al. (1987) reported that 58–70% and 54–71%, respectively, of an administered dose (2.4–26.8 mg kg⁻¹) was recovered in feces and 27–44% and 26–43%, respectively, in urine. Fenpropathrin per se was readily hydrolyzed by carboxylesterases or hydroxylated at the methyl group of the acid moiety and at the 4'-position of the

alcohol prior to hydrolysis. The sulfate of PB acid was the major urinary metabolite along with the glucuronides 2, 2, 3, 3-tetramethylcyclopropanecarboxylic acid (TMPA) and its hydroxymethyl derivatives. Intact esters were the major fecal metabolites with hydroxylation at the 4'-position of the alcohol and the *trans*-methyl group of the acid.

5.9 Fluralinate

Table D9, Appendix D, gives the chemical structures of the parent pyrethroid and metabolites of fluralinate (CAS no. 69409-94-5) (Kaneko and Miyamoto 2001; Kaneko 2010). Quistad et al. (1983) prepared (α RS, 2R)-[benzyl-U-ring- 14 C] tau-fluralinate (CAS no. 102851-06-9) to study the fate of the alcohol moiety. Rats were given single oral doses (0.7 and 60 mg/kg) by gavage in corn oil. Previous studies by Quistad et al. (1983) involved the administration of 14 CF-labeled (α R, 2R), (α S, 2S), (α R, 2S), and (α S, 2R) isomers (23%, 25%, 28%, and 24%, respectively) of fluralinate (CAS no. 69409-94-5) (1 mg/kg) in corn oil. Urinary metabolites from the ring-labeled study of Quistad et al. (1983) included PB acid (3.9%), 4'-OH BP acid (2.3%), PB acid glycine (9.0%), and 4'-OH PB acid sulfate (72.0%). The metabolites analyzed in 1-day urine samples represented 57.0% of the single oral dose, while fecal extracts contained 75.9% fluralinate (33.4% of administered dose), with lesser amounts of PB acid (3.1%), PB alcohol (4.0%), and 4'-OH PB acid (1.7%). No conjugates of PB acid (cholic, CAS no. 82186-87-6), (taurocholic, CAS no. 82186-90-1) or (taurochenodeoxycholic acids, CAS no. 82186-91-2) were found in feces. The presence of the 4'-OH derivative of fluralinate was not detected in feces or urine as was shown for other pyrethroids, suggesting that hydroxylation of the phenoxy ring occurred after cleavage.

Quistad et al. (1983), studied the elimination of 14 CF-labeled fluralinate, and discovered that the hydroxy acid (CAS no. 82186-86-5), anilino acid (CAS no. 76338-73-3), glycine conjugate of the anilino acid, haloaniline (CAS no. 39885-50-2) and the sulfate of hydroxyhaloaniline (CAS no. 84960-10-1) were excreted in urine. Fluralinate, hydroxyacid, anilino acid, and anilino acid conjugates were found in feces. According to Quistad et al. (1983), the ratio of fecal to urinary elimination is higher for fluralinate than for fenvalerate (Kaneko et al. 1981b; Ohkawa et al. 1979), deltamethrin (Cole et al. 1982; Ruzo et al. 1978), cypermethrin (Cole et al. 1982), and tralomethrin (Cole et al. 1982).

5.10 Permethrin

Table D10, Appendix D, gives the physical/chemical and partition coefficient data for *trans*- and *cis*-permethrin (chirality not shown) and metabolites. See Tables 2 and D10 for the structures and technical names of these. According to Michael-Rocky Goldsmith (EPA, personal communication), chirality does not change

the values $\log P/D$. The metabolites were taken from Fig. 58.17, the metabolic pathways for permethrin, as reported by Kaneko and Miyamoto (2001) and from Fig. 76.19 of the Kaneko (2010) study. The pathway takes into consideration differences in the carboxylesterase catalyzed hydrolysis rates of *trans*- and *cis*-permethrin, with more hydrolysis products being formed from the *trans* isomer.

Permethrin (CAS no. 52645-53-1) is a mixture of the (1RS, *trans*) and (1RS, *cis*) isomers. Gaughan et al. (1977) studied the metabolism of (1R, *trans*)-, (1RS, *trans*)-, (1R, *cis*)-, and (1RS, *cis*)-permethrin administered orally to rats at dosages of 1.6–4.8 mg · kg⁻¹. In their study, labeled permethrins and metabolites (1–10) were used: (1R, *trans*; 1R, *cis*) permethrin labeled in the acid (Cl₂C* = CH) moiety (metabolites 1,3); (1R, *trans*; 1R, *cis*) permethrin uniformly labeled (UL) in the phenoxy ring (metabolites 2, 4); (1RS, *trans*; 1RS, *cis*) permethrin labeled in the acid moiety (C* = O) (metabolites 5,7), and (1RS, *trans*; 1RS, *cis*) and permethrin labeled in the α -OH carbon (metabolites 6, 8). Two metabolites were radiolabeled, one in the acid moiety (¹⁴C)-CPA (metabolite 9) and one in the alcohol moiety [(¹⁴C)-PB alcohol] (metabolite 10). The (1R, *trans*) permethrin and (1R, *cis*) permethrin are each single isomers, while the (1RS, *trans*) permethrin and (1RS, *cis*) permethrin are each mixtures of two isomers.

Male rats were individually administered the ten compounds, with the rats administered carbonyl-labeled (5, 7) (1RS, *trans*; 1RS, *cis*) and phenoxy-labeled (2, 4) (1RS, *trans*; 1RS, *cis*) permethrin being placed in all glass metabolism cages for up to 12 days, which permitted the complete collection of urine, feces, and carbon dioxide (Gaughan et al. 1977). The other six test groups were housed in metal cages for the same period of time. The metabolites retaining the ester linkage were compared by TLC to those from the administration of (1R, *trans*) permethrin, labeled in the acid (¹⁴C)-DCCA and (¹⁴C)-PB alcohol moieties. Products retaining the ester linkage were hydrolyzed and the degradation products recovered and identified. Conjugates were cleaved by enzyme, acid and base, and then were chromatographed.

Lactonization occurred during treatment with strong acids or as artifacts of TLC separations. The glucuronides were partially converted to lactone derivatives when dilute methanolic HCL solutions were evaporated to dryness. Ninety-seven to hundred percent of the two mixed *cis*-permethrin isomers and the two mixed *trans* isomers (¹⁴C-acid and alcohol labeled) were recovered in urine and feces. The hydrolysis products of (¹⁴C-acid-1R, *trans*) and (¹⁴C-alcohol-1R, *trans*) permethrin were largely eliminated in urine (81–90%), while only 45–54% from *cis*-permethrin appeared in urine. The glucuronide of Cl₂CA was the principal metabolite found in the urines of (1R, *trans*; 56.1%) and (1RS, *trans*; 41.9%) permethrin-treated rats, while a lesser amount were found in the urines of (1R, *cis*; 18.5%) and (1RS, *cis*; 13.8%) permethrin-administered rats. For rats administered the ¹⁴C-alcohol-labeled permethrin, the principal metabolite was 4-OH PB acid sulfate in urine of rats administered (1R, *trans*; 30.7%) and (1RS, *trans*; 42.8%) permethrin. Less of this metabolite was found in urine of rats administered the (1R, *cis*; 19.5%) and (1RS, *cis*; 29.3%) permethrin.

In summary, the five principal sites of metabolism on permethrin are ester cleavage, oxidation at the *trans* or *cis* methyl group of the geminal dimethyl moiety, and oxidation at the 2'- or 4'-position of the phenoxy group. Considerable attention was paid by Gaughan et al. (1977) to the oxidation of the geminal dimethyl moieties; they found only a small percentage (0.3–1.4%) of the *trans*-methyl groups were oxidized, with an equivalent amount of oxidation (1.5–4.7%) on the *cis*-methyl group.

The importance of the oxidation of the geminal dimethyl moieties appears to disappear in some of the later studies with pyrethroids. The reason for this may be difficulties in obtaining appropriate synthesized standards and setting up good chromatographic procedures for identifying such compounds in urine. The alternative explanation is that hydroxylation of the methyl group does not occur to any extent in the other pyrethroids.

According to Anadon et al. (1996), the oral bioavailability of permethrin in the rat was 60.69%. Permethrin was administered orally and intravenously at dosages of 460 and 46 mg kg⁻¹ to male Sprague–Dawley rats. The maximum amount of permethrin found respectively in cerebellum, hippocampus, caudate putamen, frontal cortex, hypothalamus, and sciatic nerve were respectively about 1.5, 2.2, 2.7, 4.8, and 7.5 times higher than in plasma. Certain metabolites of permethrin, PB alcohol, and PB acid were detected in plasma and selected tissues 48 h after dosing.

Choi and Soderlund (2006) identified human alcohol (ADH) and aldehyde dehydrogenases (ALDH) as the enzymes involved in the oxidation of PB alcohol (phenoxybenzyl alcohol) from *trans*-permethrin to PB acid (phenoxybenzoic acid) via phenoxybenzaldehyde. *Cis*-Permethrin was not metabolized to any extent in human liver fractions. Cytochrome P450 isoforms were not involved either in the hydrolysis of *trans*-permethrin or in the oxidation of the PB alcohol to the PB acid.

5.11 Phenothrin

Table D11, Appendix D, gives the metabolites for *cis*- and *trans*-phenothrin as presented in Figs. 58.19 and 76.20, respectively, from Kaneko and Miyamoto (2001) and Kaneko (2010). The structure and technical name for phenothrin is presented in Table 2.

The chiral structures (stereochemistry) are not shown in Table D11. The *trans*-isomers are more readily hydrolyzed than are the *cis*-isomers by carboxylesterases and are perhaps more readily hydroxylated by P450 isozymes. Kaneko et al. (1984) studied the metabolism of six isomer preparations [(1R-*trans*), (1RS-*trans*), (1S-*trans*), (1R-*cis*), (1RS-*cis*), and (1S-*cis*)] of phenothrin after single oral administration of each ¹⁴C-labeled isomer or isomer mixture at 10 mg kg⁻¹ to rats and mice. There was no significant difference between the elimination of the (1R-*trans*) and (1RS-*trans*) or the (1R-*cis*) and (1RS-*cis*) isomers. However, the (1S-*trans*) and (1S-*cis*) isomers were eliminated to a greater extent in urine than were the (1R-) and (1RS-) *trans*- and *cis*-isomers, respectively (Izumi et al. 1984).

The alcohol moiety of (1*R-trans*)- and (1*R-cis*)-phenothrin is rapidly metabolized and eliminated, with the major excreted metabolite being either free or conjugated 4-OH PB acid (CAS no. 35065-12-4) (Miyamoto et al. 1974; Miyamoto 1976). Intact esters of (1*R, cis*) phenothrin were excreted in feces, one being 4-OH phenothrin (CAS no. NA), another carboxy phenothrin (CAS no. 79897-38-4) and carboxy 4'-OH phenothrin (CAS no. 79861-56-6). Oxidation of one of the geminal dimethyl groups has also been reported (Miyamoto 1976). According to Elliott et al. (1976), phenothrin is metabolized like permethrin except for alterations on the isobutenyl group not seen for the dichlorovinyl side chain of permethrin.

5.12 Resmethrin

Table D12, Appendix D, gives the metabolites for *trans*- and *cis*-resmethrin. The metabolism of *trans*- and *cis*-resmethrin was presented by Kaneko and Miyamoto (2001) and Kaneko (2010), respectively in Figs. 58.22 and 76.23 of their publications. See Table 2 for resmethrin's structure and technical name. Bioresmethrin and cismethrin are (1*R-trans*) and (1*R-cis*) isomers of resmethrin, respectively.

Miyamoto et al. (1971) and Ueda et al. (1975) studied the rat metabolism of (1*RS-trans*), (1*R-trans*), or (1*R-cis*)-resmethrin that was individually labeled with ¹⁴C at the carbonyl group of the acid moiety or the phenyl group of the alcohol moiety. The purity of the *trans-cis* isomers was determined by gas chromatography to be >99.5%. Authentic standards of unlabeled (–)-*cis*-chrysanthemic acid and 5-(phenylmethyl)-3-furanmethanol (CAS no. 20416-09-5) were used for tentative identification of resmethrin metabolites. Five additional compounds, BF acid (CAS no. 24313-22-2), α -keto BF acid (CAS no. 37744-71-1), α -OH BF acid (CAS no. 37744-70-0), 4-methoxy BF alcohol, and 4-methoxy BF acid, were prepared according to the methods of Miyamoto et al. (1971). In reviews authored by Ueda et al. (1975) and Miyamoto (1976), it was reported that (+)-*trans*-resmethrin is readily hydrolyzed by carboxylesterases and eliminated as oxidized products of 5-(phenylmethyl)-3-furanmethanol (BF alcohol) and CPCA. The oxidative degradation of (+)-*cis*-resmethrin by cytochrome P450 was also reported (Suzuki and Miyamoto 1974; Ueda et al. 1975) to produce geometric isomers (E- and Z-isomers) of chrysanthemic acid products (i.e., alcohol, aldehyde, and acid). The proposed metabolic pathways indicate that intact resmethrin is not oxidized (hydroxylated) on one of the phenyl or furan rings of 5-(phenylmethyl)-3-furanmethanol, or at the isobutenyl methyl group, prior to hydrolysis. Table D12, Appendix D, shows the metabolic pathway for resmethrin as it was proposed by Kaneko and Miyamoto (2001), and as it was revised by Kaneko (2010). These pathways are similar, except that resmethrin per se in Table D12 was hydroxylated at the 4'-position of the phenyl and furan ring, and at the phenylmethyl group, before hydrolysis. Hydrolysis of resmethrin and these three resmethrin derivatives by carboxylesterases, followed by the oxidation of their alcohol leaving groups

would explain the presence of their respective acids in urine. This begs the question as to why one of the methyls of the isobutenyl or gem-dimethyl group in the intact ester is not oxidized to a carboxylic acid, or to an alcohol, as shown for phenothrin prior to hydrolysis. The reason may be the rapid hydrolysis of the *trans* isomer, but this does not explain why these groups are not oxidized by cytochrome P450s prior to hydrolysis as is the case of the *cis* isomer. Bioresmethrin (1*R-trans*) was hydrolyzed more rapidly by the carboxylesterases in rat liver microsomes (RLM) than cismethrin (1*R-cis*). The carboxylesterases in plasma did not show this *cis-trans* relationship (White et al. 1976).

5.13 Tefluthrin

Table D13, Appendix D, gives the metabolites of the two *cis* isomers of tefluthrin (PP993), (1*R*, 3*R*), and (1*S*, 3*S*) tefluthrin (CAS no. 79538-32-2 rel) (Prout et al. 1985a, 1986; Prout and Howard 1985b). In the Prout et al. (1985a) studies, oral doses of 1.0 mg/kg of [¹⁴C]-cyclopropane ring (acid)-labeled tefluthrin and [¹⁴C]-alcohol-labeled tefluthrin were individually administered in corn oil to four male and four female Alpk:APfSD strain rats. The rats were individually housed in metabolism cages over a period of 7 days to collect daily urine and feces. Tissues and carcasses were harvested at the end of the 7-days period for radioanalysis. One additional male and female rat each was administered 1.0 mg/kg of [¹⁴C] alcohol-labeled tefluthrin for collection of respiratory ¹⁴CO₂ over a 48-h period. The animals were then terminated and embedded in paraffin blocks for whole-body autoradiography. A higher percentage of the dose was excreted in feces (53.9–66.6%) than in urine (20.1–33.4%). There were no pronounced differences in the excretion profiles of the alcohol or acid ¹⁴C-labeled tefluthrin. Negligible amounts of radioactivity were eliminated as respiratory ¹⁴CO₂. In the autoradiograph, the radioactivity was located largely in the gastrointestinal tract, liver, and brown fat.

In a second study by Prout and Howard (1985b), the tissue distribution and excretion of [¹⁴C]-alcohol-labeled tefluthrin was followed after the oral administration of 10 mg/kg to four male and four female rats in corn oil. The animals were individually housed in metabolism cages for daily collections of urine and feces over a 7-days period. Rats were terminated at the end of 7 days and individual tissues harvested for the determination of radioactivity. A further set of two males and two females were administered an oral dose of 1.0 mg/kg [¹⁴C] alcohol-labeled tefluthrin, after bile duct cannulation. Urine, bile, and feces were collected for a period of 48 h. Signs of acute toxicity were observed in the 10 mg/kg rats. Males excreted slightly less in urine (26% vs. 33%) and more in feces (68% vs. 63%) than females. In the bile duct study, males excreted 5–16% and females 8–10% of total radioactivity.

In the third Prout et al. (1986) study, urinary metabolites from tefluthrin ([¹⁴C]-acid or -alcohol labeled) orally administered to rats at 1.0 mg/kg or [¹⁴C]-alcohol labeled at 10 mg/kg were isolated by solvent extraction. The extracts were

chromatographed by a combination of TLC, HPLC, and GLC techniques to identify metabolites. The glucuronide conjugates were hydrolyzed using glucuronidase or 6M HCL at 100°C. The metabolites were identified by mass spectroscopy and by co-chromatography with reference standards. The [¹⁴C]-alcohol metabolites were identified as the glucuronides of tetrafluoro-1, 4-benzenediol (CAS no. 142209-31-2), and tefluthrin alcohol, 18–37% and 13–28%, respectively. Additional metabolites in urine were 10–18% tetrafluoro-4-OH methyl benzoic acid (CAS no. 107900-84-5), and 12–28% tetrafluoro-4-methyl-benzoic acid (CAS no. 652-32-4). The characterized [¹⁴C]-acid-tefluthrin metabolites in urine were the lactone of 2-OH methyl TFP acid (CAS no. 107900-83-4) and TFP acid (CAS no. 74609-46-4) and its glucuronide (CAS no. 120851-78-7).

The bile contained the glucuronides of two metabolites, tefluthrin alcohol (CAS no. 79538-03-7) and tetrafluoro-1, 4-benzenediol (CAS no. 142209-31-2). No parent compound was found in the bile. Analysis of fecal extracts from the rats administered the [¹⁴C]-alcohol label contained mostly unchanged or unabsorbed tefluthrin. Metabolites consisted of 4-OH methyl tefluthrin (CAS no. 120851-77-6), 2-OH methyl tefluthrin (CAS no. 120808-42-6) and 2-OH methyl, 4-OH methyl tefluthrin (CAS no. NA). Several minor metabolites were found, two of which were tetrafluoro-4-OH methyl benzoic acid (CAS no. 107900-84-5) and tetrafluoro-4-methyl benzoic acid (CAS no. 652-32-4).

5.14 Tetramethrin

In Table D14, Appendix D, the metabolites of *trans*- and *cis*-tetramethrin are given. The metabolic pathway in this table was taken from the work of Kaneko and Miyamoto (2001) and Kaneko (2010), Figs. 58.23 and 76.24, respectively. Tetramethrin is a 4:1:1:4 mixture of four isomers with the two *trans* isomers (1R, 3R) and (1S, 3S) being more abundant than the two *cis* isomers. Only the metabolism of the (1R, 3R) and (1R, 3S) isomers were studied by Kaneko et al. (1981c). The oxidized and sulfonic acid intermediates were not shown in the Kaneko and Miyamoto (2001) review, were added to Table D14.

Kaneko et al. (1981c) identified the metabolites of ¹⁴C carboxyl-, and alcohol-labeled (1R)-*trans*- (CAS no. 1166-46-7) and (1R)-*cis*-tetramethrin (CAS no. 51348-90-4) in the urine of rats. A small amount of the *cis* isomer or its ester metabolites were eliminated in feces. No *trans*-isomer or ester metabolites were found in feces. TPI (3,4,5,6-tetrahydrophthalimide; CAS no. 4720-86-9), its glucuronide (CAS no. 81951-66-8), HPI (CAS no. 1444-94-6), and its 3a-hydroxy (CAS no. 81951-68-0), 4-hydroxy (CAS no. 17605-52-6), and 5-hydroxy derivatives (CAS no. 81951-69-1), THAM (CAS no. 81951-65-7) and carbon dioxide were identified as ring metabolites of *trans*- and *cis*-tetramethrin. The chrysanthemetic acid metabolites found were three dicarboxylic acids, (1R, 3R)-E isomer (CAS no. 72120-98-0), (1R, 3R)-Z isomer (CAS no. 56390-95-5), (1R, 3S)-E isomer (56390-97-7), and three hydroxymethyl monoacids, (1R, 3R)-E isomer (CAS no.

54324-84-4), (1R, 3S)-E isomer (CAS no. 54276-09-4), and (1R, 3S)-Z isomer (CAS no. 56390-96-6).

Tomigahara et al. (1994b) administered ^{14}C -alcohol-labeled (1RS)-*trans* or (1RS)-*cis* tetramethrin to rats orally at doses of 2 and 250 mg/kg. In 7 days, 38–56 and 42–58% of the ^{14}C *trans*-isomer was recovered in feces and urine, respectively. These same values for the *cis* isomer were 66–91 and 9–31% of the ^{14}C in feces and urine, respectively. In feces, the main metabolites were sulfonate derivatives, and in urine, the alcohol and dicarboxylic acid derivatives from the 3,4,5,6-tetrahydrophthalimide moiety. Two of the five sulfonic acids (*trans*-acid-3-OH-NPY-SA and TPI-SA) were detected in urine. The sulfonic acids were believed to have been formed in the intestinal tract, because the sulfonic acids were not detected in the urine of bile duct-cannulated rats.

5.15 Tralomethrin

Tralomethrin differs from deltamethrin in having 3-tetrahaloethyl substituent instead of 3-dihalovinyl groups. The 1R, α S-*cis* configuration (CAS no. 66818-66-4 and 66841-22-3) confers the highest insecticidal potency and esters with the R and S configurations at the 1' center of the 3 side chain are comparable in activity (Ackermann et al. 1980). Tralomethrin is rapidly converted to deltamethrin in insects (Ruzo and Casida 1981). The metabolic pathway in Appendix D, Table D15, was taken from Kaneko and Miyamoto (2001; Fig. 58.24) and Kaneko (2010).

(1'S)-Tralomethrin administered orally to mice undergoes 25% debromination in the stomach within the first hour after dosing. The metabolic pathway then involves two starting products, tralomethrin and deltamethrin, with deltamethrin being the final starting product. Tralomethrin is readily debrominated by tissue thiols, such as glutathione. Cole et al. (1982) orally administered ^{14}C -alcohol (benzylic methane), ^{14}C -acid (geminal dimethyl), and ^{14}C -CN (cyano)-labeled tralomethrin [(S)-cyano(3-phenoxyphenyl)methyl (1R,3R)-2,2-dimethyl-3-[(1S)-1,2,2,2-tetrabromoethyl]cyclopropanecarboxylate] (CAS no. 68198-90-3) individually to rats (0.32 mg kg⁻¹) and recovered the ^{14}C -alcohol-labeled dose in urine (42.6%), feces (56.0%), and tissues (1.4%) at the end of the study. These recovery values are quite similar to those obtained using radiolabeled deltamethrin. Metabolites from acid- ^{14}C , alcohol- ^{14}C and ^{14}CN -labeled preparations and their percentages were identified in urine and feces by Cole et al. (1982). Products retaining ester linkage were found in feces, while hydrolysis products were present in urine. Tralomethrin is not normally detected in feces per se or as hydroxylated products. No X₄CA (carboxylic acid) was detected in excreta. The evolution of $^{14}\text{CO}_2$ from the ^{14}C -alcohol compounds is a minor event, as is the case for $^{14}\text{CO}_2$ from ^{14}CN - (Ohkawa et al. 1979) labeled pyrethroids. Staiger and Quistad (1984) also reported on the nature of the urinary metabolites of tralomethrin resulting from the administration of 0.32 mg kg⁻¹ to rats. The same metabolites were eliminated

by rats receiving deltamethrin (0.32 mg kg^{-1}) as were those receiving tralomethrin (0.32 mg kg^{-1}). The sulfate of 4'-OH PB acid arising from the administration of deltamethrin was higher (47.5%) than from tralomethrin (24.3%).

6 Metabolic Enzymes, Carboxylesterases, and Cytochrome P450s

6.1 Carboxylesterases and Their Multiple Forms

According to Hosokawa et al. (1987, 1990), and Satoh and Hosokawa (1998), Carboxylesterases (CEs) are members of the α/β hydrolase family of enzymes. The family provides a stable scaffold for the active sites of the enzymes. The catalytic residues constitute a highly conserved triad consisting of a nucleophile (serine, cysteine, or aspartic acid), an orientating acid, glutamate, and a histidine residue. The nucleophile is located in a sharp turn, called the “nucleophile elbow,” where it is easily approached by the substrate, as well as by the hydrolytic water molecule (Nardini and Dijkstra 1999). The α/β hydrolase fold family is the first example of enzymes with a glutamate residue. The acidic member is located in a reverse turn, usually following strand $\beta 7$. The histidine residue is the site that is absolutely conserved. The loop may differ considerably in shape and length among the various members of the family.

Mammalian liver CEs are encoded by multiple genes. The isozymes were initially classified by their substrate specificities and pI (isoionic point). The two major human liver isozymes, hCE-1 and hCE-2, belong to two classes: CES1 and CES2, while rat CEs belong to two classes, hydrolases A and B. CEs may currently be classified into five major groups, CES1–CES5, according to the homology of their amino acid sequence (Satoh and Hosokawa 1998, 2010). The CES1 family includes the major form of CE isozymes which may be subdivided into eight subfamilies: CES1A, CES1B, CES1C, CES1D, CES1E, CES1F, CES1G, and CES1H. Most of the CES1 family, except for CES1G, is expressed in the liver. The CES1A subfamily includes the major forms of human CEs. A high level of CES1 activity is present in the blood of rats and mice with no activity present in human blood. In contrast to CES1, the CES2 family is mainly expressed in the small intestine. Stok et al. (2004) identified a pyrethroid-hydrolyzing carboxylesterase from mouse liver microsomes by mass spectral sequence analysis of the protein. Two peptide sequences were identical to sequences in a putative carboxylesterase (NCBI accession number BAC-36707). A third peptide also corresponded to the same putative carboxylesterase with one amino acid difference from the reported sequences. Stok et al. (2004) also found that, during the expression and purification of carboxylesterase, the protein was not as closely associated with the microsomes; 63% was found in the cytosol and only 11% in the microsomes.

Analysis of human CE by Northern blot shows a single band of approximately 2.1 kilobases (kb) (Riddles et al. 1991), and three bands of approximately 2-, 3-, and 4.2-kb occurring with hCE-2 (Schwer et al. 1997). The intensities of the 2.1-kb band were liver \gg heart > stomach > testis \geq kidney = spleen > colon > other tissues. For hCE-2, the 2-kb band was located in liver > colon > small intestine > heart, the 3-kb band in liver > small intestine > colon > heart, and the 4.2-kb band in brain, testis, and kidney only. Analysis of substrate structure versus efficiency for ester (pyrethroid substrates) revealed that the two CEs recognize different structural features of the substrate (i.e., acid, alcohol, etc.). The catalytic mechanism involves the formation of an acyl-enzyme on an active serine. While earlier studies of pyrethroid metabolism were primarily performed in rodents, knowledge of the substrate structure–activity relationships and the tissue distribution of hCEs are critical for predicting the metabolism and pharmacokinetics of pesticides in humans. Wheelock et al. (2003) used a chiral mixture of the fluorescent substrate cyclopropanecarboxylic acid, 3-(2,2-dichloroethenyl)-2,2-dimethyl-, cyano(6-methoxy-2-naphthalenyl)methyl ester (CAS No. 395645-12-2) to study the hydrolytic activity of human liver microsomes. Microsomal activity against this substrate was considered to be low (average value of ten samples: $2.04 \pm 0.68 \text{ nmol} \cdot \text{min}^{-1} \text{ mg}^{-1}$), when compared to p-nitrophenyl acetate (CAS No. 830-03-5) at $3,700 \pm 2,100 \text{ nmol min}^{-1} \cdot \text{mg}^{-1}$.

6.2 Cytochrome P450s and Their Multiple Forms

CYP450 was first shown to be a hemoprotein by Omura and Sato (1964). It has a noncovalently bound iron protoporphyrin IX prosthetic group, similar to the heme in b-type cytochromes, hemoglobin, and myoglobin. The heme prosthetic groups may be removed from the protein by acidic acetone, alkali, or pyridine. The binding of carbon monoxide provides a means for their analysis and quantification. The enzymes of the CYP-dependent monooxygenase system are embedded in the endoplasmic reticulum of liver hepatocytes and the cells of other organs. The endoplasmic reticulum is harvested from a cell homogenate by centrifugation at $16,000 \times g$ to remove large particles and then at $105,000 \times g$ to pelletize the microsomes (endoplasmic reticulum) from the supernatant (Lu and West 1980). The P450 enzymes are distributed between the two surfaces of the microsomal bilayer with the NADPH-CYP reductase and P450 facing the cytoplasm of the cell. Therefore, the monooxygenase system is composed of three components: reductase protein, a lipid fraction, and CYP protein. The purification of rat and human liver P450s is described by Guengerich and Martin (1998). Estimation of protein concentrations provides a means for evaluating the progress of purification. The content of CYP heme should be about 18 nmol mg^{-1} protein.

Multiple forms of CYPs exist in liver microsomes. These forms play a role in the oxidation (i.e., hydroxylation of aromatic, aliphatic, and alkyl groupings) of pyrethroid insecticides. The major isoforms in human liver include CYP 1A2, 2A6,

2B6, 2C8, 2C19, 2E1, 3A4, 3A5, and 3A7 (fetal livers). There are large individual variations in the microsomal content of these forms in human liver. A calculator for determining the content of these P450 isozymes in human liver (ages 1–18 year) was presented by Foxenberg et al. (2007). The recombinant human CYPs are available from a Baculovirus-insect cell expression system along with the coexpression of NADPH-CYP reductase (Supersomes; Gentest, Woburn, MA). Yields range from 50 to 250 pmol P450 mg⁻¹ microsomal protein as determined by CO difference spectral analysis (Hood et al. 1998). The major isoforms in rat liver include CYP1A1, 1A2; 2A1; 2B1; 2C6, 11, 12, 13; 2D1, 2D2; 3A1, and 3A2 (Supersomes, BD Biosciences (Woburn, MA)). It is important to note that human and rat CYPs exhibit significant differences in protein structure as well as catalytic activity. Thus, there is a critical need to conduct future studies of pyrethroid metabolism with human CYPs and CEs, since most researchers who have published in the literature have utilized rodent models.

6.3 Hydrolysis of Pyrethroids by CEs

Ross et al. (2006) studied the hydrolytic metabolism of Type I pyrethroids (bioresmethrin, 1RS *trans*-permethrin, and 1RS *cis*-permethrin) and several Type II pyrethroids (alpha-cypermethrin and deltamethrin) by pure human CEs (hCE-1 and hCE-2), a rabbit CE (rCE), and two rat CEs (Hydrolases A and B). Hydrolysis rates were based on the formation of 3-phenoxybenzyl alcohol (PBAlc) (CAS no. 13826-36-2) for the *cis* and *trans* isomers of permethrin. For bioresmethrin, hydrolysis was based on the production of the *trans*-chrysanthemic acid (CPCA) (CAS no. 10453-89-1). For alpha-cypermethrin and deltamethrin, hydrolysis was based on the formation of *cis*-permethrinic acid (DCCA) (CAS no. 57112-16-0) and 3-phenoxybenzyl aldehyde (PBAlc; CAS no. 39515-51-0), respectively. Human CE-1 and hCE-2 hydrolyzed *trans*-permethrin 8- and 28-fold more efficiently (based on k_{cat}/K_m values) than did *cis*-permethrin, respectively. The kinetic parameters (V_{max} , K_m) for the hydrolysis of *trans*- and *cis*-permethrin, bioresmethrin and alpha-cypermethrin by rat, mouse, and human hepatic microsomes are given in Table 7. The *trans*- isomer of permethrin is more readily hydrolyzed by rat, mouse and human hepatic microsomal carboxylesterase than *cis*-permethrin (13.4, 85.5 and 56.0 times, respectively). However, the lower K_m for hydrolysis of *cis*-permethrin in human microsomes suggests that there are both stereoisomer and species-specific differences in metabolism kinetics.

The relative levels of hCE-1 protein were measured in human microsomes by immunoblotting to determine if variation in hydrolytic metabolism was related to the abundance of hCE-1 in the microsomes. Human CE-1 levels did not correlate ($r = 0.294$) well with V_{max} values for the hydrolysis of *trans*-permethrin. Esterases other than hCE-1 are believed to be responsible for the different V_{max} values. CDMB (1,2-ethanedione, 1-(2-chlorophenyl)-2-(3,4-dimethoxyphenyl)-(CAS no. 56159-70-7)) was used to inhibit the activity of hCE-2 (Wadkins et al. 2005).

Table 7 Hydrolysis catalyzed via the hepatic microsomal carboxylesterases

Parameter	Pyrethroid	Rat	Mouse	Human
K_m , μM^a	<i>trans</i> -Permethrin	19.16	20.95	20.66
	<i>cis</i> -Permethrin	30.78	41.5	2.49
	Bioresmethrin	46.6	53.98	33.39
	alpha-Cypermethrin	13.16	6.62	9.22
V_{\max} , $\text{nmol} \cdot \text{min}^{-1} \cdot \text{mg}^{-1}$ microsomal protein ^a	<i>trans</i> -Permethrin	1.34	1.71	1.12
	<i>cis</i> -Permethrin	0.1	0.02	0.02
	Bioresmethrin	4.54	6.62	2.57
	alpha-Cypermethrin	0.51	0.09	0.14

V_{\max} and K_m values and calculations by species are presented for selected pyrethroids

^a Source: Table 4, Ross et al. 2006 (published with permission)

The results suggested that a significant portion of the microsomal activity was catalyzed by hCE-2. An antibody was not available for detecting or measuring hCE-2. Turnover numbers (k_{cat}/K_m , $\text{mM}^{-1} \cdot \text{min}^{-1}$) indicate that *trans*-permethrin is as efficiently hydrolyzed by hCE-1 as it is for hCE-2. Bioresmethrin is not hydrolyzed by hCE-2 suggesting that metabolism is primarily mediated by hCE-1. The rates of hydrolytic metabolism by rabbit carboxylesterase followed the order: bioresmethrin > *trans*-permethrin > *cis*-permethrin > deltamethrin > alpha-cypermethrin. Ross et al. (2006) did not extrapolate hydrolytic in vitro V_{\max} values ($\text{nmol} \cdot \text{min}^{-1} \cdot \text{mg}^{-1}$ of microsomal protein) into in vivo values ($\mu\text{mol} \cdot \text{h}^{-1} \cdot \text{kg}^{-1}$ of body weight (bwt)) for use in PBPK models.

Crow et al. (2007) examined the catalytic activity of carboxylesterase (rCE proteins: hCE-1 and hCE-2) on Type I pyrethroids (i.e., 1RS *trans*-permethrin (98% pure, 93% *trans* and 5% *cis*), 1RS *cis*-permethrin (99% pure), 1R *trans*-resmethrin (bioresmethrin, 99% pure, 97% *trans* and 2% *cis*)); Type II pyrethroids (i.e., alpha-cypermethrin (99% pure, mixture of isomers), lambda-cyhalothrin (99% pure, mixture of isomers), and deltamethrin (99% pure)).

Human intestinal microsomes effectively hydrolyzed *trans*-permethrin; however, bioresmethrin, and deltamethrin were not metabolized in the intestine to any appreciable extent. Human hepatic microsomes and cytosol contained both hCE-1 and hCE-2 when examined by native PAGE (polyacrylamide gel electrophoresis); human intestine contained only hCE-2. Table 8 gives the kinetic parameters obtained by Crow et al. (2007) with *trans*-permethrin and liver and intestinal carboxylesterases.

Rat serum was found capable of hydrolyzing the six pyrethroids studied by Crow et al. (2007), with bioresmethrin and *trans*-permethrin being hydrolyzed the fastest and *cis*-permethrin, deltamethrin and esfenvalerate the slowest. Humans lack detectable amounts of CEs in blood. On this basis, the rat should be considered a poor surrogate animal for human health risk assessment at the environmentally low levels at which the pyrethroids normally exist (Crow et al. 2007).

Table 8 Kinetic parameters of *trans*-permethrin hydrolysis catalyzed by human and rat hepatic subcellular fractions (microsomes and cytosols) and intestinal carboxylesterases

Species (fraction)	<i>trans</i> -Permethrin		
	K_m , μM	V_{\max} ($\text{nmol} \cdot \text{min}^{-1} \cdot \text{mg}^{-1}$)	Cl_{int}^a ($\text{nmol} \cdot \text{min}^{-1} \cdot \text{mg}^{-1} \cdot \text{mM}^{-1}$)
Hepatic			
Rat (microsomes) ^b	19.2	1.3	67.7
Rat (cytosol) ^b	24.6	0.56	22.8
Human (microsomes) ^c	20.7	1.1	53.1
Human (cytosol) ^d	3.4	0.47	138.2
Intestinal human (microsomes) ^e	–	1.88	–

$$^a Cl_{\text{int}} = V_{\max} \cdot K_m^{-1}$$

^b Rat microsomes and cytosol (pooled) were prepared from another study (Ross et al. 2006). Values (\pm SE) were obtained by non-linear regression of kinetic plots. The microsomal kinetic data are from Ross et al. (2006). The cytosol kinetic data are from this study

^c Pooled sample ($n = 18$ individuals)

^d Pooled sample ($n = 20$ individuals)

Source: Table 1, Crow et al. 2007, published with permission

6.4 In Vitro Metabolism

Scollon et al. (2009) studied the in vitro metabolism of bifenthrin (100% *cis*), S-bioallethrin (100% *trans*), bioresmethrin (96% *trans*/2% *cis*), β -cyfluthrin (67% *trans*/33% *cis*), γ -cyhalothrin (100% *cis*), cypermethrin (49% *cis*/51% *trans*), *cis*-permethrin (100% *cis*), *trans*-permethrin (96% *trans*/4% *cis*), and resmethrin (30% *cis*/70% *trans*) by rat and human liver microsomes and cytochrome P450 isozymes. Rat liver microsomes (Long-Evans males, 275–299 g) were prepared from a pool of livers from six animals. Three samples of mixed gender pool human adult liver microsomes were purchased from three different sources (CellzDirect, Phoenix, AZ; Cedra, Austin, TX; and XenoTech, LLC, Lenexa, KS). Each pool was used in a separate study. Assays were conducted by measuring the total disappearance of parent compounds over 10 min with and without NADPH. Pyrethroids were added in 25 μL of methanol at time 0 to obtain incubation concentrations of 0.1, 1.5, 10, 20, or 50 μM . Aliquots were removed at 0, 2, 6, 8, and 10 min for analysis using HPLC/tandem mass spectrometry and the results converted to moles of substrate remaining. Substrate remaining was converted to product formed and plotted versus time to produce a reaction velocity. Reaction velocities were plotted against initial concentrations to yield estimates of K_m and V_{\max} (JMP version 6; SAS Institute, Cary, NC) for each pyrethroid. The results are given in Table 9.

The metabolism of bifenthrin, S-bioallethrin, and *cis*-permethrin in rat and human hepatic microsomes was the result of oxidative processes, while the metabolism of bioresmethrin and cypermethrin in human hepatic microsomes was hydrolytic (not shown in Table 8). Cypermethrin and bioresmethrin were metabolized by oxidation and hydrolysis in rat hepatic microsomes. *Trans*-permethrin and β -cyfluthrin were metabolized by both pathways in human and rat hepatic microsomes.

Table 9 V_{\max} and K_m values^a are presented for Type I pyrethroids incubated with rat liver microsomes

Pyrethroid	Isomer	K_m , μM	V_{\max} , $\text{nmol min}^{-1} \text{mg}^{-1}$ microsomal protein	Percentage oxidative in presence of NADPH
S-Bioallethrin	100% <i>trans</i>	31.11	4.40	100
Bifenthrin	100% <i>cis</i>	5.42	0.64	100
<i>cis</i> -permethrin	100% <i>cis</i>	3.70	0.14	100
<i>trans</i> -permethrin	96% <i>trans</i> , 4% <i>cis</i>	9.03	0.97	35
Bioresmethrin	96% <i>trans</i> , 2% <i>cis</i>	3.87	0.32	57

^aSource: Table 2, Scollon et al. 2009 (published with permission)

In addition to the microsomal studies, Scollon et al. (2009) purchased rat and human Supersomes (containing P450 reductase) from BD Biosciences (Woburn, MA) to use in pyrethroid metabolism studies. The individual Supersomes contained rat CYP1A1, 1A2; 2A1; 2B1; 2C6, 11, 12, 13; 2D1, 2D2; 3A1, 3A2 and human CYP1A1, 1A2; 2B6; 2C8, 2C9*1, 2C9*2, 2C9*3, 2C19; and 3A4 P450 isoforms. The P450 content ranged from 1,000 to 2,000 pmol/mL. Nine pyrethroids (six of Type I and three of Type II) were screened for metabolism with or without NADPH in the incubation medium. The rat isoforms that showed activity were CYP1A1 (9/9 pyrethroids), 1A2 (3/9), 2C6 (9/9), 2C11 (8/9), 2D1 (1/9), 3A1 (8/9), and 3A2 (6/9), with human isoforms CYP1A1 (1/9 pyrethroids), 1A2 (1/9), 2B6 (1/9), 2C8 (3/9), 2C9*1 (4/9), 2C9*2 (2/9), 2C19 (9/9), and 3A4 (2/9) showing activity. The percentage of each parent pyrethroid metabolized during a 10-min incubation period was presented, while no isoform V_{\max} or K_m values were determined in the study. The results suggest that human CYP2C19 is the most important mediator of CYP-dependent metabolism and highlights the need to assess species- and CYP-isozyme-specific metabolism of pyrethroids.

Godin et al. (2006) used an Agilent 1100 series LC/MSD VL ion trap mass spectrometer in their *in vitro* studies involving the metabolism of deltamethrin and esfenvalerate by human and rat microsomes and purified carboxylesterases. Pyrethroids were 98%+ pure; deltamethrin was obtained from Bayer Crop Sciences (Research Triangle Park, NC) and esfenvalerate from Dupont (Johnston, IA). The kinetics of hydrolysis of deltamethrin by hCE-1 (human) and hydrolase A (rat) were measured based on the release of PBAlD (CAS no. 39515-51-0), which is spontaneously formed from the cyanohydrin (Wheelock et al. 2003). The metabolism of deltamethrin and esfenvalerate from rat liver microsomes occurred primarily via NADPH-dependent pathways (P450s). The independent-NADPH pathway was 20% in the case of deltamethrin and 11% for esfenvalerate. TEPP (diphosphoric acid, P, P, P', P'-tetraethyl ester, CAS no. 107-49-3) was used to inhibit the NADPH independent hydrolytic pathway catalyzed by carboxylesterases. In contrast to the rat, human liver microsomes metabolize deltamethrin by the NADPH-independent hydrolytic pathway, while esfenvalerate was metabolized by the CYP-dependent pathway. The high level of hydrolysis of deltamethrin reported in Tables 10 and 11 (particularly for hCE-1) appear to be consistent with the human k_{cat} values reported in Table 11 and Figs. 11 and 12.

Table 10 Clearance rates for deltamethrin and esfenvalerate from rat and human liver microsomes

	Clearance rate	
	+NADPH	–NADPH
	pmol · min ⁻¹ · mg ⁻¹ microsomal protein	
Deltamethrin		
Rat microsomes	30.4 ± 7.3	8.8 ± 0.23
Rat microsomes + TEPP ^a	24.6 ± 3.7	N.D.
Human microsomes	52.8 ± 6.2	58.0 ± 3.0
Human microsomes + TEPP ^a	5.8 ± 5.4	N.D.
Esfenvalerate		
Rat microsomes	45.3 ± 2.4	4.8 ± 1.4
Rat microsomes + TEPP ^a	23.4 ± 9.0	N.D.
Human microsomes	20.9 ± 4.4	2.6 ± 1.6
Human microsomes + TEPP ^a	18.9 ± 2.7	N.D.

+NADPH total clearance (oxidative and hydrolytic) of parent chemical from microsomal assay, –NADPH NADPH-independent hydrolytic clearance of parent chemical from microsomal incubation, N.D. no detectable elimination

^aTEPP (CAS no. 107-49-3) (200 μM) was used to inhibit hydrolytic metabolism

Source: Table 2, Godin et al. 2006. Published with permission

Table 11 Hydrolysis of deltamethrin: kinetic parameters of human and rat carboxylesterases

	K_m , μM	V_{max} , nmol · min ⁻¹ · mg ⁻¹	k_{cat} , min ⁻¹	k_{cat}/K_m , min ⁻¹ · mM ⁻¹
Human CE-1	22.6 ± 3.7	21.4 ± 7.2	1.3 ± 0.4	56.3
Human CE-2	1.6 ± 1.6	0.6 ± 0.1	0.035 ± 0.003	21.1
Rat hydrolase A	6.3 ± 0.4	4.5 ± 0.8	0.27 ± 0.04	42.7
Rat hydrolase B	2.0 ± 4.9	1.1 ± 0.3	0.07 ± 0.02	35.2

Parameters are the means ± S.D. obtained from three independent kinetic experiments
Eight different concentrations of deltamethrin were assayed (5–100 μM) in each kinetic experiment, rates are based on the formation of 3-phenoxybenzaldehyde

$V_{max} \cdot \text{nmol} \cdot \text{min}^{-1} \cdot \text{mg}^{-1} \cdot 60,000 \cdot \text{mg} \cdot \text{mmol}^{-1} \cdot \text{mmol} \cdot 10^{-6} \cdot \text{nmol}^{-1} = k_{cat} \cdot \text{min}^{-1}$

Source: Table 4, Godin et al. 2006. Published with permission

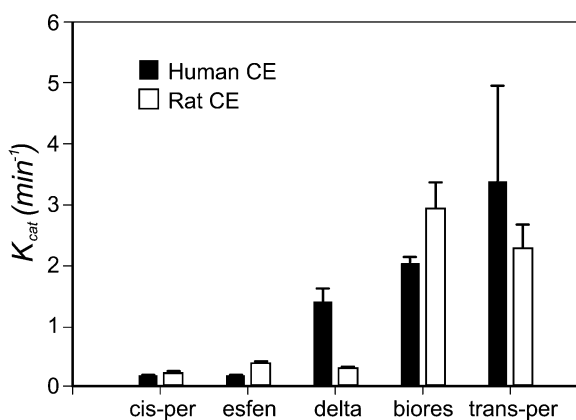


Fig. 11 Comparison of the turnover numbers (k_{cat}) for human CE (hCE-1) and rat CE (hydrolase A). Hydrolysis of *cis*-permethrin, *trans*-permethrin, and bioresmethrin are from Ross et al. (2006), while similar information for esfenvalerate and deltamethrin are from Godin et al. (2006). This figure is published with permission (Godin et al. 2006)

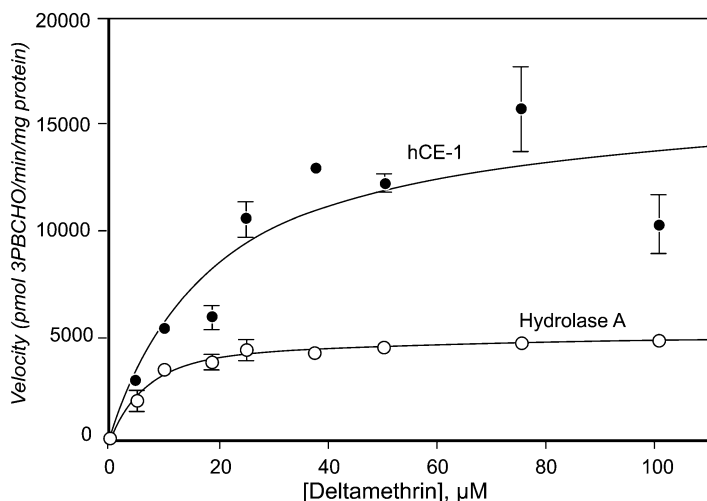


Fig. 12 Kinetics of deltamethrin hydrolysis by hCE-1 and hydrolase A. Velocity was measured by the amount of PBald (phenoxy benzaldehyde) released during the reaction. Data (symbols) were fit to the Michaelis–Menten equation and the nonlinear regression lines plotted. Each point represents the mean \pm S.D. ($n = 3$). This figure is published with permission (Godin et al. 2006)

In their work to extrapolate the in vitro clearance to in vivo clearance (Cl_{int}) on a per kilogram basis, Godin et al. (2006) assumed humans and rats have 40 and 25.7 g of liver per kg of body weight, respectively (Davies and Morris 1993). The microsomal content of the livers was assumed to be 52.5 and 45 mg of microsomal protein per g of liver for humans (Iwatsubo et al. 1997) and rats (Houston 1994), respectively.

In another study by Godin et al. (2007), the rat and human CYP450 isoforms and rat serum esterase that metabolized deltamethrin and esfenvalerate were identified. Table 12 gives the V_{max} and K_m kinetic parameters for the metabolism of deltamethrin and esfenvalerate by rat and human recombinant cytochrome P450s.

Rat serum hydrolyzed deltamethrin and esfenvalerate at rates of 15.23 ± 3.24 and 9.97 ± 2.94 $\text{pmol} \cdot \text{min}^{-1} \cdot \text{ml}^{-1}$ of serum, respectively. Neither deltamethrin nor esfenvalerate were hydrolyzed when incubated with human sera, supporting the lack of CE activity in human blood.

6.5 Binding of Substrates to Microsomes and CYPs; Prediction of K_m and V_{max}

In most in vitro microsomal metabolism studies, the concentration of microsomal protein used in incubation media is approximately $1.0 \text{ mg} \cdot \text{ml}^{-1}$, whereas, substrate concentrations range from 1.0 to 100 μM , depending upon their solubilities. In such

Table 12 Kinetic parameters for deltamethrin and esfenvalerate metabolism by rat and human cytochrome P450s

	K_m , μM	V_{\max} , pmol min^{-1} pmol^{-1} P450	V_{\max}/K_m ^a	V_{\max}/K_m ^b
Deltamethrin rat P450s				
CYP2C6	21.6 \pm 9.4	150.0 \pm 36.6	6.9	3.4 \pm 0.3
CYP2C11	31.9 \pm 25.7	205.8 \pm 107.6	6.5	5.2 \pm 0.7
CYP3A2	6.4 \pm 3.8	25.9 \pm 5.8	4.0	2.1 \pm 0.2
Deltamethrin human P450s				
CYP2C8	10.2 \pm 9.5	42.7 \pm 16.6	4.2	1.6 \pm 0.1
CYP2C19	9.0 \pm 5.6	61.6 \pm 17.7	6.8	2.2 \pm 0.5
CYP3A5	–	–	–	4.8 \pm 0.6
Esfenvalerate rat P450s				
CYP2C6	38.2 \pm 26.2	138.2 \pm 72.8	4.1	3.2 \pm 0.3
CYP2C11	33.5 \pm 21.8	219.4 \pm 92.8	6.5	4.4 \pm 0.4
CYP3A2	4.3 \pm 1.8	39.5 \pm 6.1	9.2	2.4 \pm 0.5
Esfenvalerate human P450s				
CYP2C8	19.1 \pm 11.6	59.2 \pm 21.6	3.1	1.6 \pm 0.3
CYP2C9*1	24.3 \pm 5.6	79.8 \pm 6.3	3.3	2.9 \pm 0.2
CYP2C19	4.1 \pm 2.2	64.4 \pm 12.3	15.7	4.4 \pm 0.6
CYP3A5	–	–	–	4.7 \pm 0.7

^a Calculated value using kinetic parameters obtained from nonlinear regression analysis

^b Catalytic efficiency estimated from, the slope of the linear regression analysis of concentration versus velocity plots

Kinetic assays were conducted with concentrations ranging from 0.5- to 25- μM pyrethroid. Data are the $\pm\text{SE}$ ($n = 3$)

Source: Table 1, Godin et al. 2007. Reproduced with permission

studies the concentration of free or unbound substrate is rarely measured. Obach (1997) showed that increases in microsomal protein over one or more substrate concentrations, resulted in a change in free or unbound substrate. These results suggest that the values obtained for K_m should be adjusted for the concentration of free or unbound substrate.

Unbound or free drug is determined by an equilibrium dialysis procedure. Obach (1997) compared the values obtained by incorporating the rates of microsomal binding with those in which this factor was ignored. In most cases clearance (V_{\max}/K_m ratio) was lower when binding was ignored. Austin et al. (2002) published the following equation for clearance:

$$\text{CL} = \frac{\frac{Q \times A \times B \times f_{u_p} \times \text{CL}_{\text{int}}}{f_{u_{\text{inc}}}}}{\left(Q + \frac{A \times B \times f_{u_p} \times \text{CL}_{\text{int}}}{f_{u_{\text{inc}}}} \right)}, \quad (27)$$

where A is a constant representing the mg of microsomes per gram of liver, B is a constant describing the grams of liver per kg of body weight, Q represents liver

blood flow, f_{u_p} is the free fraction of the compound in plasma, and $f_{u_{inc}}$ is the free fraction of the compound in the microsomal incubation.

In (27), a value for $f_{u_{inc}}$ is needed and may be determined using (28)

$$f_{u_{inc}} = \frac{1}{C \times 10^{0.56 \log P/D - 1.41} + 1}, \quad (28)$$

where C is the microsomal protein concentration in mg per ml, $\log P/D$ is the $\log P$ of the molecule if it is a base (basic $pK_a > 7.4$), and $\log P/D$ is the $\log D_{7.4}$ of the molecule if it is neutral or an acid (acidic $pK_a < 7.4$) (Austin et al. 2002; Halifax and Houston 2006). In a microsomal binding study carried out with amitriptyline (CAS no. 50-48-6), binding was discovered to increase with increasing microsomal protein concentration and was drug-concentration independent over the range of concentrations used in vitro (Venkatakrishnan et al. 2000). Binding produces an over estimation of K_m without affecting the metabolic rate at concentrations that saturate the enzyme. Correcting for microsomal binding, by using the free fraction in incubation matrices, improves the prediction of in vivo clearance from in vitro estimates of clearance for drugs that are extensively bound (Obach 1996, 1997, 1999).

Because a majority of the in vitro work is now being carried out with rCYPs, the question is whether we should be concerned about nonspecific binding that occurs in rCYP studies? According to Bolger (Simulations-Plus, Inc.), the range of protein concentrations used in human liver microsome incubations lies between $3.2 \mu\text{g} \cdot \text{ml}^{-1}$ and up to $1.0 \text{mg} \cdot \text{ml}^{-1}$, while the range in rCYPs range from $1.25 \mu\text{g} \cdot \text{ml}^{-1}$ up to $1 \text{mg} \cdot \text{ml}^{-1}$, suggesting that correction may be needed for CYP studies, as well. On the basis of K_m data plots developed by Youdim and Dodia (2010), which permits one to compare the K_m values from rCYPs vs. HLM for product formation and substrate depletion, the correction on K_m was found to be less for rCYPs than for HLMs (Bolger 2010). Youdim and Dodia (2010) recommended correcting K_m by multiplying it by the substrate fraction unbound in microsomes, f_u (microsomes), as determined by equilibrium dialysis. The calculated results for $f_{u_{inc}}$ in (28) may also be used. Metabolism in the liver is then defined by (29):

$$R_{\text{Metabolism}} = \sum_{i=1}^n \frac{V_{\text{max},i} C_{\text{liv}}}{[(K_{m,i} \times f_{u(\text{microsomes})}) + C_{\text{liv}}]}, \quad (29)$$

where $V_{\text{max},i}$ is the maximum velocity constant of the i th metabolic enzyme, $K_{a,i}$ is the corresponding concentration at which half the maximum velocity is reached; f_u (microsomes) is the fraction of the drug unbound in microsomes; and n is the number of enzymes involved in clearing the drug.

To our knowledge, a corrected K_m value has not been utilized in the development of Michaelis–Menten constants for the pyrethroid insecticides.

7 QSAR Models for Predicting Biological Parameters Used in PBPK/PD Models

7.1 Toxicity Models

TOPKAT (Enslein et al. 1998) is a toxicity model (for estimating LD₅₀, etc.) and was among the first QSAR models to be developed for predicting the toxicity of pesticides and other chemicals. Software packages, such as DEREK (LHASA, Leeds, UK), CASE and MULTICASE (Multicase, Cleveland, OH), COMPACT, HazardExpert (Compudrun, Budapest, Hungary), ONCOLOGIC (Logichem, Boyertown, PA), and ACD/Tox Suite (Advance Chemistry Development, Inc. Toronto, Canada), are able to predict the toxicity of substances based on chemical structure. ACD/Tox Suite is the latest software product to be marketed specializing in human models that involve hERG (human endoplasmic reticulum) inhibition, CYP3A4 inhibition, genotoxicity, acute toxicity (rodent LD₅₀), aquatic toxicity, health effects, irritation, and endocrine system disruption.

The European Commission, under the 5th Framework Programme, supported the development of five predictive Demetra QSAR models (e.g., acute toxicity for rainbow trout, water flea, bobwhite quail, and honeybees) against five end points (Porcelli et al. 2007). The models were developed to comply with OECD (Organization for Economic Cooperation and Development) principles for validating QSARs for regulatory use. The models require inputting descriptors and SMILES for pesticides of interest to obtain predicted LD₅₀ values for oral toxicity or other exposure parameters. The software is written in Java™ and can run in any machine that has Java or Java 2 runtime environments. The environmental models may not directly predict pyrethroids toxicity to humans or even laboratory animals, but the approach to developing these models for humans, etc., are similar. The major drawback of the Demetra QSAR models appears to be the need to input values for descriptors/SMILES notation for the pesticide/end point of interest to predict LD₅₀ values in mg kg⁻¹ of body weight. The only requirement should be the end point and name of the pesticide, or at most, the SMILES for that pesticide.

At the present time, no predictive QSAR models were found that describe the neurotoxicity of the pyrethroids insecticides.

7.2 QSAR Models for Predicting the Binding of Pyrethroids to Plasma and Hepatic Proteins

Pyrethroids bind strongly to plasma proteins before being distributed by the blood to the organs for metabolism and elimination. Only the unbound or free pyrethroids contribute to toxicity and are susceptible to metabolic reactions. Pyrethroids that have a high binding constant for a plasma protein show lower toxicity and

Table 13 QikProp 3.0 values^a

Pyrethroid	QPPMDCK (nm s ⁻¹) ^b	QPPCaco-2 (nm cm ⁻¹ s ⁻¹)	QPLog ₁ BBB ^c
1. Allethrin	1,066/1.066E-4	2,033/2.033E-4	-0.433
2. Bifenthrin	10,000/10.00E-4	4,367/4.367E-4	0.259
3. Cyfluthrin	3,670/3.670E-4	1,035/1.035E-4	-0.561
4. Cyhalothrin	4,971/4.971E-4	1,279/1.279E-4	-0.490
5. Cypermethrin	2,601/2.601E-4	1,087/1.087E-4	-0.546
6. Deltamethrin	3,127/3.127E-4	1,632/1.632E-4	-0.384
7. Fenvalerate	1,970/1.970E-4	1,557/1.557E-4	-0.652
8. Fenpropathrin	603/0.603E-4	1,201/1.201E-4	-0.762
9. Fluvalinate	7,700/7.700E-4	1,670/1.607E-4	-0.470
10. Permethrin	10,000/10.000E-4	4,413/4.413E-4	0.125
11. Phenothrin	2,456/2.456E-4	4,402/4.402E-4	-0.184
12. Resmethrin	2,679/2.679E-4	4,767/4.767E-4	-0.143
13. Tefluthrin	10,000/10.000E-4	5,197/5.197E-4	0.759
14. Tetramethrin	355/0.355E-4	737/0.737E-4	-0.833
15. Tralomethrin	9,546/9.546	1,452/1.452E-4	-0.343

^a Calculated by Daniel Chang, USEPA, RTP, NC, with QikProp 3.0

^b Permeability in nanometer/s and cm/s nonactive transport

^c Brain/blood partition coefficient

delayed clearance. Human serum albumin (HSA) is the major constituent in plasma. HSA has two ligand-specific binding sites, site I binds warfarin (CAS no. 81-81-2) and site-II binds diazepam (CAS no. 439-14-5). In addition to these binding sites, the pyrethroids may bind to lipoproteins and to alpha 1-acid glycoproteins (AGP). Several quantitative structure–property (QSPR) or QSAR models have been published (Yamazaki and Kanaoka 2004; Saiakhov et al. 2000; Colmenarejo et al. 2001; Colmenarejo 2003). Yamazaki and Kanaoka used the drug data of Vozeh et al. (1990), which contained the protein-binding percents of 346 drugs; Saiakhov et al. (2000) obtained protein-binding affinity information from Goodman and Gilman’s textbook (Goodman 2001); Colmenarejo et al. (2001) and Colmenarejo (2003) used HSA binding data from high-performance affinity chromatographic studies. QikProp (Schrodinger, LLC) used the data base of Colmenarejo et al. (2001) to develop a $\text{Log}K_{\text{hsa}}$ model for predicting $\text{Log}K_{\text{hsa}}$ values for drugs of interest. The $\text{QPLog}K_{\text{hsa}}$ model was used to determine the $\text{Log}K_{\text{hsa}}$ values for the pyrethroids of interest and their metabolites.

7.3 Intestinal Permeability

QikProp 3.0 (Schrodinger, LL) was used to predict log P Caco-2, log P MDCK values and human oral absorption in percent for the 15 pyrethroids targeted in this review. The values obtained from application of this model are given in Table 13, along with QPLog BBB values.

7.4 Liver CYP450 Hydroxylation Models

QSAR models (Enslein et al. 2007) for predicting microsomal and CYP 3A4 V_{\max} and K_m phase I reactions involving hydroxylation of (1) drug aromatic and (2) alicyclic rings and aliphatic groups were reported by Knaak et al. (2008) in their review of parameters for carbamate models. The manuscript submitted for publication in J Comput Aided Mol Des was returned and the models revised and ultimately were included in Simulations-Plus, “ADMET Predictor,” Sect. 4.14.1 Kinetic Models for Recombinant Human Cytochrome P450 Enzymes 1A2, 2C9, 2C19, 2D6, and 3A4. The numbers of compounds in the respective CYP models were 51, 45, 42, 40, and 68. The data were obtained from the open literature, were carefully screened for appropriate experiment methodology, and were assembled into data bases. Preliminary models were built with structural descriptors from Chemical Computing Group’s MOE™ and Semichems’s CODESSA™. However, the final models exclusively used ADMET Predictor’s 2D descriptors and Artificial Neural Network Ensemble (ANNE) modeling methodology.

The models have been updated several times (Enslein 2010). The current statistics for version 5.5 of ADMET Predictor is as follows:

Isoform	1A2	2C9	2C19	2D6	3A4
Number of compounds	51	53	42	36	68
RMSE (root mean square error) $\log K_m$	0.41	0.35	0.38	0.47	0.49
RMSE (root mean square error) $\log V_{\max}$	0.57	0.71	0.54	0.31	0.62

The Enslein Model in “ADMET Predictor” supplies K_m and V_{\max} values, respectively, in units of μM and $\text{nmol} \cdot \text{min}^{-1} \cdot \text{nmol}^{-1}$ P450. For user convenience, V_{\max} is converted into units of $\text{nmol} \cdot \text{min}^{-1} \text{mg}^{-1}$ microsomal protein (human liver) and into metabolic intrinsic clearance units of $\mu\text{L} \text{min}^{-1} \text{mg}^{-1}$ microsomal protein. The conversion factors were obtained from Inoue et al. (2006). The Enslein Metabolism Module was used to predict K_m and V_{\max} values for the hydroxylation of 15 pyrethroids by CYPs 1A2, 2C9, 2C19, 2D6, and 3A4. The results are given in Tables 14–18.

In studies involving intact microsomes, the in vitro V_{\max} , in $\text{nmol} \cdot \text{min}^{-1} \text{mg}^{-1}$ of microsomal protein is multiplied by mg of microsomal protein g^{-1} of liver and by g of liver kg^{-1} of body weight to obtain the in vivo value. A number of the V_{\max} values were out of the range of the QSAR model. No pyrethroids were used in Enslein’s training sets. Pyrethroid K_m and V_{\max} values may be added to the Enslein model to improve predictability. In the ADMET Predictor, V_{\max} values were expressed in $\text{nmol} \cdot \text{min}^{-1} \cdot \text{nmol}^{-1}$ of rCYP. The values were also available (calculated) in $\text{nmol} \cdot \text{min}^{-1} \text{mg}^{-1}$ of microsomal protein.

The in vitro V_{\max} units for recombinantly expressed systems (rCYPs) for permethrin were converted to in vivo values based on the following equation:

$$Cl_{\text{int}}(L/H) = \left[\sum_{j=1}^n \left(\sum_{i=1}^n \frac{V_{\max}(\text{rhCYP}_j)_i X_j}{K_m(\text{rhCYP}_j)_i} \right) \right] \times \text{MPPGL} \times \text{Liverwt} \quad (30)$$

Table 14 Predicted V_{\max} and K_m values for CYP 1A2^a

Pyrethroid	K_m , μM	V_{\max} , $\text{nmol min}^{-1} \text{nmol}^{-1} \text{P450}$	V_{\max} , $\text{nmol min}^{-1} \text{mg}^{-1} \text{microsomal Protein}$	V_{\max} , $\mu\text{L min}^{-1} \text{mg}^{-1} \text{microsomal Protein}$
Allethrin	38.9	0.0101	0.00144	0.134
Bifenthrin	17.1	0.0689	0.00358	0.209
Cyfluthrin	5.71	0.0200	0.00104	0.182
Cyhalothrin	7.22	0.0327	0.0017	0.235
Cypermethrin	10.30	0.0356	0.00185	0.179
Deltamethrin	7.12	0.0467	0.00243	0.341
Fenvalerate	5.97	0.0115	0.0006	0.100
Fenpropathrin	23.10	0.163	0.00848	0.364
Fluvalinate	4.49	0.00919	0.000478	0.106
Permethrin	42.00	0.0992	0.0052	0.123
Phenothrin	64.10	0.0169	0.00877	0.137
Resmethrin	18.60	0.0124	0.00645	0.347
Tefluthrin	19.30	0.0718	0.00373	0.193
Tetramethrin	8.11E+2	0.0121	0.00632	0.008
Tralomethrin	5.45	0.0122	0.00634	1.164

^a Predicted values, ADMET Predictor version 5.5, Simulations-Plus, Inc. According to ADMET Predictor none of the pyrethroids were substrates of CYP 1A2

Table 15 Predicted V_{\max} and K_m values for CYP 2C19^a

Pyrethroid	K_m , μM	V_{\max} , $\text{nmol min}^{-1} \text{nmol}^{-1} \text{P450}$	V_{\max} , $\text{nmol min}^{-1} \text{mg}^{-1} \text{microsomal Protein}$	V_{\max} , $\mu\text{L min}^{-1} \text{mg}^{-1} \text{microsomal Protein}$
Allethrin	35.70	15.00	0.021	5.874
Bifenthrin	3.60	0.0114	0.0016	0.444
Cyfluthrin	6.98	0.0282	0.000395	0.057
Cyhalothrin	7.14	0.0771	0.000995	0.139
Cypermethrin	4.98	0.0745	0.00104	0.209
Deltamethrin	5.20	0.0746	0.00104	0.201
Fenvalerate	5.32	0.0249	0.000349	0.066
Fenpropathrin	9.45	0.0816	0.00114	0.121
Fluvalinate	9.82	0.027	0.000379	0.039
Permethrin	2.82	0.376	0.00526	1.864
Phenothrin	3.23	0.279	0.00391	1.21
Resmethrin	2.77	0.325	0.00455	1.645
Tefluthrin	22.10	11.20	0.157	7.108
Tetramethrin	4.09	33.90	0.474	116.0
Tralomethrin	6.03	0.729	0.00102	0.169

^a Predicted values, ADMET Predictor, version 5.5, Simulations-Plus, Inc. According to ADMET Predictor six pyrethroids were not substrates for CYP 2C19 (Bifenthrin, Cyhalothrin, Deltamethrin, Fluvalinate, Tefluthrin, and Tralomethrin)

where, $\sum_{j=1}^n$ represents the summation of the number of j CYP Isoforms, $\sum_{i=1}^n$ represents the summation of the number i metabolic pathways, V_{\max} the rate of metabolism in $\text{pmol} \cdot \text{min}^{-1} \cdot \text{pmol}^{-1} \text{rCYP}_j$ and X_j CYP abundance in the population in $\text{pmol CYP}_j \text{mg}^{-1} \text{microsomal protein}$. Cl_{int} is the intrinsic clearance (V_{\max}/K_m) and MPPGL, the amount of microsomal protein per gram of liver.

Table 16 Predicted V_{\max} and K_m values for CYP 2C9^{a/}

Pyrethroid	K_m , μM	V_{\max} , $\text{nmol min}^{-1} \text{nmol}^{-1} \text{P450}$	V_{\max} , $\text{nmol min}^{-1} \text{mg}^{-1}$ microsomal Protein	V_{\max} , $\mu\text{L min}^{-1} \text{mg}^{-1}$ microsomal Protein
Allethrin	11.10	10.10	1.47	132.42
Bifenthrin	3.01	6.42	0.468	155.56
Cyfluthrin	8.44	14.60	1.06	125.86
Cyhalothrin	5.47	5.66	0.413	75.54
Cypermethrin	4.84	5.47	0.399	82.49
Deltamethrin	5.35	5.47	0.399	74.62
Fenvalerate	3.93	5.00	0.365	92.90
Fenpropathrin	6.87	2.49	0.182	26.45
Fluvalinate	7.55	0.524	0.0382	5.06
Permethrin	3.60	4.50	0.329	91.19
Phenothrin	4.54	2.98	0.217	47.95
Resmethrin	3.76	0.567	0.0414	11.02
Tefluthrin	5.55	18.91	1.38	249.12
Tetramethrin	21.60	15.50	1.13	52.35
Tralomethrin	4.58	4.38	0.320	69.91

^a Predicted values, ADMET Predictor, version 5.5, Simulations-Plus, Inc. According to ADMET Predictor only two pyrethroids were substrates for CYP 2C9 (Fenpropathrin and Phenothrin)

Table 17 Predicted V_{\max} and K_m values for CYP 2D6^{a/}

Pyrethroids	K_m , μM	V_{\max} , $\text{nmol min}^{-1} \text{nmol}^{-1} \text{P450}$	V_{\max} , $\text{nmol min}^{-1} \text{mg}^{-1}$ microsomal Protein	V_{\max} , $\mu\text{L min}^{-1} \text{mg}^{-1}$ microsomal Protein
Allethrin	102.0 ^b	107.0	0.858	8.43
Bifenthrin	0.109	0.0328	0.000263	2.40
Cyfluthrin	0.614	0.3881	0.00311	5.06
Cyhalothrin	0.102	0.0331	0.000265	2.60
Cypermethrin	0.629	0.373	0.00298	4.74
Deltamethrin	2.18	11.41	0.0915	41.88
Fenvalerate	0.435	0.156	0.00124	2.86
Fenpropathrin	44.80	0.213	0.00170	0.038
Fluvalinate	0.0531	0.126	0.00101	18.99
Permethrin	0.618	1.02	0.00817	13.21
Phenothrin	41.30	46.90	0.375	9.09
Resmethrin	57.80	58.30	0.466	8.06
Tefluthrin	0.117	0.0556	0.000445	3.82
Tetramethrin	87.30	18.60	0.149	1.17
Tralomethrin	0.541	0.272	0.00218	4.03

^a Predicted values, ADMET Predictor, version 5.5, Simulations-Plus, Inc. According to ADMET Predictor none of the pyrethroids were substrates of CYP 2D6

When individual CYPs act on the pyrethroid insecticides, hydroxylation may occur at more than one position on the aromatic rings and on one or more alkyl groups. The Ensein QSAR model, however, uses V_{\max} and K_m values for the

Table 18 Predicted V_{\max} and K_m values for CYP 3A4^a

Pyrethroid	K_m , μM	V_{\max} , $\text{nmol min}^{-1} \text{nmol}^{-1} \text{P450}$	V_{\max} , $\text{nmol min}^{-1} \text{mg}^{-1}$ microsomal Protein	V_{\max} , $\mu\text{L min}^{-1} \text{mg}^{-1}$ microsomal Protein
Allethrin	43.60	322.60	35.80	820.86
Bifenthrin	7.83	3.66	0.406	51.83
Cyfluthrin	37.20	0.755	0.0838	2.25
Cyhalothrin	30.60	1.05	0.117	3.82
Cypermethrin	41.30	1.14	0.127	3.08
Deltamethrin	41.50	1.21	0.135	3.25
Fenvalerate	23.90	3.07	0.340	14.25
Fenpropathrin	45.70	0.781	0.0867	1.86
Fluvalinate	31.30	0.840	0.0933	2.98
Permethrin	27.70	0.953	0.106	3.82
Phenothrin	17.50	1.22	0.136	7.737
Resmethrin	14.40	0.848	0.0941	6.53
Tefluthrin	33.50	0.484	0.0537	1.603
Tetramethrin	74.80	8.31E+5	0.000922	1.233E+6
Tralomethrin	43.10	0.774	0.0859	1.995

^a Predicted values, ADMET Predictor, version 5.5, Simulations-Plus, Inc. According to ADMET Predictor all of the pyrethroids are substrates of CYP 3A4

hydroxylation of one site on the drugs used in the training set. No pyrethroids were included in the Ensein models. The predicted pyrethroid V_{\max} values represent the hydroxylation of more than one aromatic or alkyl site by the individual CYPs. Total hydroxylation represents the summation of the activity of the individual CYPs.

Rodrigues (1999) described the multiplication of V_{\max} , in terms of $\text{pmol} \cdot \text{min}^{-1} \cdot \text{pmol}^{-1}$ CYP by the mean specific content of the corresponding CYP in native liver microsomes as the “normalized rate” (NR) in $\text{pmol} \cdot \text{min}^{-1} \text{mg}^{-1}$ of microsomal protein. The normalized rate for each CYP is totaled to give total normalized rate (TNR). Each NR may be expressed as a percent of the TNR (% TNR). Foxenberg et al. (2011), using the values obtained from human rCYPs, expressed the total amount of parent OPs (organophosphate pesticides; viz., chlorpyrifos or parathion) metabolized in liver to its oxon or dearylated form (TCPy or PNP), respectively as:

$$\text{RAM} = \frac{[V_{\max A}(C)]}{[K_{mA} + C]} + \frac{[V_{\max B}(C)]}{[K_{mB} + C]} + \frac{[V_{\max C}(C)]}{[K_{mC} + C]} + \frac{[V_{\max D}(C)]}{[K_{mD} + C]} + \frac{[V_{\max E}(C)]}{[K_{mE} + S]} + \frac{[V_{\max F}(C)]}{[K_{mF} + C]}, \quad (31)$$

where RAM is the rate of metabolism in $\text{pmol h}^{-1} \text{kg}^{-1}$ of bwt, CYP A-F content = pmol CYP/mg of microsomal protein; CYP A-F activity = 1A2, 2B6, 2C19, 3A4, 3A5, 3A7 in $\text{pmol} \cdot \text{min}^{-1} \cdot \text{pmol}^{-1}$ of CYP; V_{\max} A-F = CYP A-F content \times CYP A-F activity $\times 60 \text{ min} \times 30.0 \text{ mg}$ of microsomal protein g^{-1} of liver $\times 27 \text{ g}$ liver kg^{-1} of bwt, C = concentration of OP in venous blood in the liver.

According to Barter et al. (2007), Lipscomb et al. (1998), and Wilson et al. (2003) the microsomal content of human liver ranges from 21 to 33 · g⁻¹ liver with reports as high as 53 · g⁻¹ liver. The average adult liver has been reported to be 25.7 g kg⁻¹ of bwt (Brown et al. 1997; Davies and Morris 1993).

Oral bioavailability in vivo is dependent on both permeability and first pass metabolism that may occur in the intestine and liver. The intrinsic clearance per pmol CYP is assumed to be the same in human liver microsomes (HLM) as in intestinal microsomes (Yang et al. 2004), whereas CYP3A abundance represents the total amount of enzyme, 70,000 pmol in the gut (Paine et al. 1997). The abundance of CYP3A in the gut is calculated using (32).

$$\begin{aligned} \text{Individual CYP3A gut abundance} &= \text{Average CYP3A gut abundance} \\ &\times \frac{\text{Individual GSA}}{\text{Average GSA}}, \end{aligned} \quad (32)$$

where GSA is the surface area of the small intestine (ileum, jejunum, and duodenum). The surface areas of each segment of gut are calculated from their length and diameter. To be useful in predicting absorption, the P_{eff} values in Table 13 and the CYP3A activities (V_{max} and K_m , etc.) in the intestinal tract require use of an ACAT or CAT submodel to augment the PBPK/PD model (Simulations-Plus, Inc.).

7.5 Comparison of Predicted vs. Experimental V_{max} and K_m Values

The predicted V_{max} and K_m values for deltamethrin were compared to experimental values published by Godin et al. (2007) in Table 12 (Sect. 6.5), where 2C19 was the major human CYP involved. K_m was expressed in μM and V_{max} in $\text{pmol} \cdot \text{min}^{-1} \cdot \text{pmol}^{-1}$ of CYP. The experimental V_{max} value for 2C19 is equivalent to 56.3 $\mu\text{mol} \cdot \text{h}^{-1} \cdot \text{kg}^{-1}$ of bwt (19 $\text{pmol} \cdot \text{mg}^{-1}$ protein; Godin et al. 2007), while the predicted V_{max} is 0.051 $\mu\text{mol} \cdot \text{h}^{-1} \cdot \text{kg}^{-1}$ of bwt (ADMET Predictor: Table 15, $(1.04\text{E}-3 \times 60 \times 30 \times 27)/1,000$). ADMET Predictor gave a similar human K_m value (5.20 μM) relative to the experimental value shown in Table 12 (9 μM). According to ADMET Predictor (Table 15), deltamethrin is not a CYP 2C19 substrate, but rather is a substrate of CYP3A4 (Table 18), which has a V_{max} of 6.56 $\mu\text{mol} \cdot \text{h}^{-1} \cdot \text{kg}^{-1}$ of bwt, and a K_m of 41.50 μM . The P450 V_{max} value for rat liver microsomes reported by Mirfazaelian et al. (2006) was 76.1 $\mu\text{mol} \cdot \text{h}^{-1} \cdot \text{kg}^{-1}$ of bwt and 74.0 μM for K_m .

In calculating V_{max} , the following in vitro to in vivo extrapolations were used: 30 mg of microsomal protein g⁻¹ of liver, 27 g of liver kg⁻¹ of bwt. These values may be changed and V_{max} recalculated as desired. In this calculation, the 2C19 CYP content in the microsomes was corrected by ADMET Predictor (Inoue et al. 2006).

7.6 Prediction of Liver and Plasma Carboxylesterase Activity

Two studies that addressed the use of *in silico* models for predicting human carboxylesterase (hCES1 and hCES2) activity have been published (Yoon et al. 2003; Vistoli et al. 2010). Yoon et al. examined the hydrolysis of the prodrug CPT-11 ([1,4'-bipiperidine]-1'-carboxylic acid, (4*S*)-4,11-diethyl-3,4,12,14-tetrahydro-4-hydroxy-3,14-dioxo-1*H*-pyrano[3',4':6,7]indolizino[1,2-*b*]quinolin-9-yl ester; CAS no. 1255644-71-3) by carboxylesterases (CE) and CPT-11 analogs to the active metabolite SN-38 (1*H*-pyrano[3',4':6,7]indolizino[1,2-*b*]quinoline-3,14(4*H*,12*H*)-dione, 4,11-diethyl-4,9-dihydroxy-, (4*S*)-; CAS no. 86639-52-3), a topoisomerase I inhibitor. Comparative molecular field analysis and molecular similarity index analysis, along with docking studies were used to predict the biological activity of a derivative of CPT-11, i.e., BP-CPT (1-piperazinecarboxylic acid, 4-(phenylmethyl)-, (4*S*)-4,11-diethyl-3,4,12,14-tetrahydro-4-hydroxy-3,14-dioxo-1*H*-pyrano[3',4':6,7]indolizino[1,2-*b*]quinolin-9-yl ester; CAS no. 97682-40-1) in U373MG glioma cell lines (Yoon et al. 2003). Docking models showed a similar orientation of the SN-38 moiety for both CPT-11 and BP-CPT in the active site of rCE. The rate of hydrolysis of CPT-11 or BP-CPT by CEs to SN-38 appears to be determined by either the proximity or the angle of the carbonyl group of the prodrug to the hydroxyl of the Ser-221. QSAR (3D structures) studies performed on CPT-11 analogs (structures vs. relative activity of rat serum, Tsuji et al. 1991) were evaluated by CoMFA and CoMSIA analyses. Comparative molecular field analysis (CoMFA) is a mathematical expression of the correlation between the chemical structure of a series of compounds and the experimentally determined biological activities of the compounds (Cramer et al. 1988). Comparative molecular similarity index analysis (CoMSIA) is an alternative molecular field analysis method to CoMFA.

Vistoli et al. (2010) studied the docking analysis of known substrates to develop both predictive models and molecular dynamics (MD) simulations to identify the *in situ* behavior of substrates and products. Pyrethroids and their respective carboxylesterase K_m data (Ross et al. 2006) were used as substrates in the training set and in the external test sets for a series of docking experiments. A rich interaction pattern with hCES1 was shared by all the pyrethroid insecticides examined, and explains the marked efficacy with which the esterases hydrolyze the pyrethroids. Molecular dynamics simulations were used to examine the hydrolysis of heroin (CAS no. 561-27-3) to 6-*O*-acetylmorphine and morphine (CAS no. 57-27-2) by hCES1.

Chang et al. (2009) reported the viability of using a consensus 3D QSAR pharmacophore model to predict the stereospecific rat serum carboxylesterase (CEs) hydrolysis rates and half lives for the pyrethroids. Utilizing a stereoselective *in vitro* metabolism dataset from Sprague–Dawley rat serum CES, and 27 Type I and II pyrethroids, a ligand-derived pharmacophore model was developed to filter catalytically “competent” and “incompetent” ligands, that were based on four pharmacophore features (i.e., two aromatic, and two projected hydrogen bond

acceptors). A concurrent pharmacophore model was further enhanced to determine the features that were common within the “incompetent” set of ligands, and these features were used to further discriminate for false positives. By filtering catalytically “competent” ligands (i.e., on the basis of hydrolysis rates $>6 \text{ h}^{-1}$; “fast” hydrolysis), two subsequent QSAR models were developed that demonstrated two distinct chemical descriptor spaces for the two filtered ligand sets. Docking simulations that were based on a homology-modeled rat serum carboxylesterase sequence were also performed. Further analysis via protein–ligand interaction fingerprints (PLIF) showed that catalytically “competent” ligands were dominated by SER (serine) and GLY (glycine) interactions, which were consistent with the deduced projected hydrogen bond acceptor pharmacophore features in the model. Several QSAR models developed for predicting CES-mediated hydrolysis rates were suggestive of these criteria (i.e., pharmacophore features), with an emphasis on terms that were consistent with enzymatic hydrolysis. The best substrate-predicted rates gave higher significance to the carbonyl carbon atom charge, lipophilicity, and molecular dipole moment that were consistent with an enzymatic metabolism mechanism. The 31 selected stereoisomers, along with their catalytic hydrolysis rates (k_{cat}), are presented in Table 19.

The 3D QSAR pharmacophore model selected “very fast” and “very slow” metabolizers, leaving the catalytic hydrolysis rates in the middle group as being questionable. Catalytic rates (k_{cat}) for the pyrethroids that were outside of the training set ($8\text{--}25 \text{ h}^{-1}$) were obtained by extrapolation. Less confidence should be placed on these predicted values. The hydrolysis rate for deltamethrin (1R, cis, α S) fell into the middle group and was not included in Table 19. However, catalytic rates (rat serum carboxylesterases) for two trans deltamethrin (1R,3S, α R; 1S,3R, α R) isomers were included in the table and compared favorably with the rat hydrolase A and B k_{cat} values in Table 11. Cypermethrin (1R, trans, α R), cyfluthrin (1R, trans, α R; 1R, trans, α R), and permethrin (1R, trans; 1S, trans) were fast metabolizers. Among the slow metabolizers were permethrin (1S, cis), cyfluthrin (1S, cis, α S) and cypermethrin (1R, trans, α S).

7.7 Conjugation of Intact Pyrethroids and Aromatic Leaving Groups

Sorich et al. (2006) evaluated the ability of glucuronosyltransferases (UGT) to transfer glucuronic acid to various substrates (drugs with hydroxy groups). ADMET Predictor contains a QSAR model developed by Kurt Enslein that predicts “Yes” or “No” answers for the glucuronidation of various substrates, based on the data provided by Sorich et al. (2006). UGT does not appear to glucuronidate the intact hydroxylated pyrethroids. Enslein’s QSAR model for predicting which drugs may become glucuronidated was used to predict whether the hydroxylated pyrethroids are glucuronidated. Generally, the model responded with a “No” answer.

Table 19 Predicted stereoselective hydrolysis rates (k_{cat}) for rat serum carboxylesterase

Pyrethroid	Stereoisomer (IUPAC)	k_{cat} 1/h
Allethrin	n/a ^a	n/a
Bifenthrin	n/a ^a	n/a
Cyfluthrin	(R)-cyano(4-fluoro-3-phenoxyphenyl)methyl (1R,3S)-3-(2,2-dichloroethenyl)-2,2-dimethylcyclopropanecarboxylate	30
	(R)-cyano(4-fluoro-3-phenoxyphenyl)methyl (1R,3R)-3-(2,2-dichloroethenyl)-2,2-dimethylcyclopropanecarboxylate	4.3
	(R)-cyano(4-fluoro-3-phenoxyphenyl)methyl (1S,3R)-3-(2,2-dichloroethenyl)-2,2-dimethylcyclopropanecarboxylate	15
Cyhalothrin	(R)-cyano(3-phenoxyphenyl)methyl (1R,3S)-3-[(1Z)-2-chloro-3,3,3-trifluoroprop-1-en-1-yl]-2,2-dimethylcyclopropanecarboxylate	62
	(R)-cyano(3-phenoxyphenyl)methyl (1R,3R)-3-[(1Z)-2-chloro-3,3,3-trifluoroprop-1-en-1-yl]-2,2-dimethylcyclopropanecarboxylate	18
	(R)-cyano(3-phenoxyphenyl)methyl (1S,3R)-3-[(1Z)-2-chloro-3,3,3-trifluoroprop-1-en-1-yl]-2,2-dimethylcyclopropanecarboxylate	60
Cypermethrin	(R)-cyano(3-phenoxyphenyl)methyl (1R,3S)-3-(2,2-dichloroethenyl)-2,2-dimethylcyclopropanecarboxylate	15
	(R)-cyano(3-phenoxyphenyl)methyl (1R,3R)-3-(2,2-dichloroethenyl)-2,2-dimethylcyclopropanecarboxylate	3.8
	(R)-cyano(3-phenoxyphenyl)methyl (1S,3R)-3-(2,2-dichloroethenyl)-2,2-dimethylcyclopropanecarboxylate	9
Deltamethrin	(R)-cyano(3-phenoxyphenyl)methyl (1R,3S)-3-(2,2-dibromoethenyl)-2,2-dimethylcyclopropanecarboxylate	18
	(R)-cyano(3-phenoxyphenyl)methyl (1R,3R)-3-(2,2-dibromoethenyl)-2,2-dimethylcyclopropanecarboxylate	6
	(R)-cyano(3-phenoxyphenyl)methyl (1S,3R)-3-(2,2-dibromoethenyl)-2,2-dimethylcyclopropanecarboxylate	11
Fenvalerate	(R)-cyano(3-phenoxyphenyl)methyl (2R)-2-(4-chlorophenyl)-3-methylbutanoate	5.3
	(S)-cyano(3-phenoxyphenyl)methyl (2R)-2-(4-chlorophenyl)-3-methylbutanoate	9.5
	(R)-cyano(3-phenoxyphenyl)methyl (2S)-2-(4-chlorophenyl)-3-methylbutanoate	10
	(S)-cyano(3-phenoxyphenyl)methyl (2S)-2-(4-chlorophenyl)-3-methylbutanoate	6.1
Fenpropathrin	(R)-cyano(3-phenoxyphenyl)methyl 2,2,3,3-tetramethylcyclopropanecarboxylate	2.5
Fluvalinate	(R)-cyano(3-phenoxyphenyl)methyl (2R)-2-[[2-chloro-4-(trifluoromethyl)phenyl]amino]-3-methylbutanoate	36
	(S)-cyano(3-phenoxyphenyl)methyl (2R)-2-[[2-chloro-4-(trifluoromethyl)phenyl]amino]-3-methylbutanoate	6.8
	(R)-cyano(3-phenoxyphenyl)methyl (2S)-2-[[2-chloro-4-(trifluoromethyl)phenyl]amino]-3-methylbutanoate	50
	(S)-cyano(3-phenoxyphenyl)methyl (2S)-2-[[2-chloro-4-(trifluoromethyl)phenyl]amino]-3-methylbutanoate	12
Permethrin	3-phenoxybenzyl (1R,3S)-3-(2,2-dichloroethenyl)-2,2-dimethylcyclopropanecarboxylate	15
	3-phenoxybenzyl (1R,3R)-3-(2,2-dichloroethenyl)-2,2-dimethylcyclopropanecarboxylate	3.4

(continued)

Table 19 (continued)

Pyrethroid	Stereoisomer (IUPAC)	k_{cat} 1/h
	3-phenoxybenzyl (1S,3R)-3-(2,2-dichloroethyl)-2,2-dimethylcyclopropanecarboxylate	9.1
Phenothrin	(3-phenoxyphenyl)methyl (1R,3R)-2,2-dimethyl-3-(2-methylprop-1-en-1-yl)cyclopropane-1-carboxylate	13
	(3-phenoxyphenyl)methyl (1S,3S)-2,2-dimethyl-3-(2-methylprop-1-en-1-yl)cyclopropane-1-carboxylate	7.0
Resmethrin	(5-benzylfuran-3-yl)methyl (1R,3R)-2,2-dimethyl-3-(2-methylprop-1-en-1-yl)cyclopropane-1-carboxylate	6.4
	(5-benzylfuran-3-yl)methyl (1S,3S)-2,2-dimethyl-3-(2-methylprop-1-en-1-yl)cyclopropane-1-carboxylate	5.3
Tralomethrin	(R)-cyano(3-phenoxyphenyl)methyl (1S,3S)-2,2-dimethyl-3-(1,2,2,2-tetrabromoethyl)cyclopropanecarboxylate	82
	(R)-cyano(3-phenoxyphenyl)methyl (1R,3R)-2,2-dimethyl-3-(1,2,2,2-tetrabromoethyl)cyclopropanecarboxylate	67
	(R)-cyano(3-phenoxyphenyl)methyl (1S,3R)-2,2-dimethyl-3-(1,2,2,2-tetrabromoethyl)cyclopropanecarboxylate	64

^a Pharmacophore filter did not select any stereoisomers as a rat serum carboxylesterase-enabled ligand

7.8 Skin Permeation Constants

A QSAR model was developed by Potts and Guy (1992) to predict the permeability of a wide range of structurally different chemicals and was based upon the size of the permeant and its octanol/water partition coefficient. Flynn (1990) compiled data on ~90 compounds for which (33), below, was used to derive K_p values. The compounds ranged in molecular weight from 18 to >750, and in $\log K_{\text{oct}}$ from -3 to +6.

The results obtained by applying (33) (below) indicate that an increase in K_p with increasing K_{oct} is offset by increasing molecular size.

$$\log K_p(\text{cm s}^{-1}) = -6.3 + 0.71 \log K_{\text{oct}} - 0.0061 \text{ MW}. \quad (33)$$

Table 20 provides the computed $\log K_p$ and K_p values for the 15 pyrethroid insecticides we address in this review, by applying (33) and by using the algorithm of Potts and Guy (1995) within QikProp. The K_p values for permethrin and phenothrin (1.967 and 3.724) were at least tenfold larger than those of the other pyrethroids. The $\log K_{\text{oct}}$ values (7.64 and 7.68) appear to be responsible for these large values.

Reifenrath et al. (2011) reported that 2.1% of a $200 \mu\text{g} \cdot \text{cm}^{-2}$ dose of permethrin was absorbed through excised human skin during a 24-h period, in which 0.1% was found in the receptor fluid and 2.0% in the dermis. A dose of $2.25 \mu\text{g} \cdot \text{cm}^{-2}$ resulted in 1.3% percutaneous absorption of permethrin 24 h after 0.23% was found in the receptor fluid and 1.1% in dermis. For the $200 \mu\text{g} \cdot \text{cm}^{-2}$ dose of 0.1% in the receptor fluid, the flux was calculated to be $200 \mu\text{g} \cdot \text{cm}^{-2} \times 0.10$ divided by $24 \text{ h} = 0.833 \mu\text{g} \cdot \text{cm}^{-2} \cdot \text{h}^{-1}$. The K_p was calculated by dividing the flux by the dose in $\mu\text{g} \cdot \text{cm}^{-3}$ to give $4.164 \times 10^{-3} \cdot \text{cm} \cdot \text{h}^{-1}$.

Table 20 Predicted percutaneous K_p ($\text{cm} \cdot \text{h}^{-1}$) for the pyrethroids using Potts and Guy (1992) QSAR equation and the Potts and Guy (1995) equation in QikProp

Pyrethroid	Log K_{oct}	Log K_p ($\text{cm} \cdot \text{h}^{-1}$)		K_p ($\text{cm} \cdot \text{h}^{-1}$)		Flux ($\mu\text{g cm}^{-2} \text{h}^{-1}$)
		P&G ^a 1992	QikProp ^b	P&G ^a 1992	QikProp ^b	
1. Allethrin	4.62	-1.3020	-2.197	0.0499	0.0064	1.53E-2
2. Bifenthrin	7.42	-0.2551	-0.705	0.5558	0.1972	0.024E-2
3. Cyfluthrin	6.42	-0.8346	-1.685	0.1463	0.0206	0.0087E-2
4. Cyhalothrin	6.00	-1.2277	-1.409	0.0592	0.0390	0.00289E-2
5. Cypermethrin	6.41	-0.7320	-1.582	0.1853	0.0262	0.02E-2
6. Deltamethrin	6.20	-1.4234	-1.315	0.0377	0.0484	0.047E-2
7. Fenvalerate	6.55	-0.6545	-0.797	0.2215	0.1595	0.045E-2
8. Fenpropathrin	5.28	-1.1263	-1.597	0.0746	0.0252	0.128E-2
9. Fluvalinate	5.98	-1.5656	-0.748	0.0272	0.1786	0.00287E-2
10. Permethrin	7.64	0.2938	-0.444	1.9671	0.3597	0.47E-2
11. Phenothrin	7.68	0.5710	-0.458	3.7244	0.3483	0.915E-2
12. Resmethrin	6.63	-0.1006	-0.633	0.7932	0.2328	1.318E-2
13. Tefluthrin	5.17	-1.6272	-1.507	0.0236	0.0311	0.032E-2
14. Tetramethrin	4.68	-1.4424	-3.279	0.0361	0.0005	0.149E-2
15. Tralomethrin	7.11	-1.7521	-1.231	0.0177	0.0587	0.00325E-2

^aLog K_p ($\text{cm} \cdot \text{s}^{-1}$) = $-6.3 + 0.71 \times \text{Log } K_{\text{oct}} - 0.0061 \cdot \text{MW}$; value converted to $\text{cm} \cdot \text{h}^{-1}$; equation from Potts and Guy (1992)

^bEquation from Potts and Guy (1995); calculated by QikProp 3.0

^cFlux = $\text{cm} \cdot \text{h}^{-1} \times \mu\text{g mol}^{-1} \times \mu\text{mol} \times \text{dm}^{-3} = \mu\text{g cm}^{-2} \text{h}^{-1}$; equation from QikProp 3.0

The K_p value (1.967 and 0.3597) for permethrin (Table 20) is closer to the flux value (0.833) calculated in the Reifenrath et al. (2011) study, whereas the K_p value (0.004164) from Reifenrath et al. (2011) approaches the flux value (0.0047) from QikProp 3.0 (Schrodinger, LLC). The reason for this appears to result from the \log_{oct} values in (33) and the K_p and solubility estimates used in QikProp.

Bast et al. (1997) calculated a K_p of $2.63 \times 10^{-8} \cdot \text{cm} \cdot \text{h}^{-1}$ for permethrin in a single pass rabbit ear perfusion study. The value (1.967) predicted by the Potts and Guy (1992) equation is 7.5×10^7 greater. However, the results of in vivo rat absorption studies (43–46% over 7–14 days) conducted by Sidon et al. (1988) appear to produce similar results to the high Potts and Guy (1992) K_p value for permethrin. According to Farahmand and Maibach (2009), in vitro estimates may be improved when vehicle effect is considered and studies are carried out under steady-state conditions.

7.9 Tissue:Blood Partition Coefficients: QSAR Models

Knaak et al. (2008) reviewed the nonlinear QSAR equation developed by Zhang (2005) and the QSAR model developed by Liu et al. (2005a) for predicting tissue: blood partition coefficients. To our knowledge, neither the QSAR equations nor models are available in the form of ready-to-use programs for obtaining partition

coefficients for the pyrethroids. QikProp has a program for predicting the brain/blood partition coefficients for orally delivered drugs. The log BBB values for the 15 pyrethroids are given in Table 13.

8 Lipids, Target Proteins, and Ion Channels

8.1 Biomembranes and Ion Channels

The nature of bilayer lipid membranes (biomembranes) are infrequently mentioned in papers dealing with ion channels, even though biomembranes harbor receptors, ion channels (membrane proteins), lipid domains, lipid signals, and scaffolding complexes, which function to maintain cellular growth, metabolism, and homeostasis (Sudhakar et al. 2008). In biomembranes, proteins recognize ester groups and headgroups such as choline, ethanolamine, and serine of the phospholipids and the hydroxyl and amide functions of the sphingomyelins. The 3-dimensional structures of these biomembranes are currently being examined (Kuo 1985; White 1994).

Membrane phospholipids (i.e., phosphatidylcholine (PC), phosphatidylethanolamine (PE), and phosphatidylserine (PS)) play an active role in signal transduction and functional modulation. Proteins embedded in outer cell membranes (ATP-binding cassette ABC transporters; P-glycoprotein, multidrug resistance-associated protein 1, and breast cancer resistance protein) regulate the movement of chloride ions, nutrients, and structurally diverse compounds across cell membranes (Robey et al. 2010). Knaak et al. (1997) reviewed the effects of drinking water and dietary levels of mono-, di-, and tri-ethanolamine in animals. A single large dose of either ethanolamine or diethanolamine produces an increase in the formation of liver phospholipids (choline and noncholine). An LD₅₀ dose (2.3 g kg⁻¹) of diethanolamine in the mouse produced abnormal electron microscopic changes in hepatocyte-mitochondria and in smooth and rough endoplasmic reticulum (ER). Widespread changes in mitochondria and ER suggest that cell membranes may have been damaged. The fatty acid (i.e., oleic, linoleic, linolenic, and arachidonic acid) composition of phospholipids may also be affected by dietary levels of ethanolamine. The specificity of CDP-ethanolamine: 1, 2-diacyl-glycerol ethanolamine phosphotransferase was less sensitive to the chain length of the fatty acid in diacyl-glycerol than it was to their degree of unsaturation.

The following schematic (Fig. 13) depicts the structure of the lipids as they appear in biomembranes (Nikolelis et al. 1991).

The relationship between biomembranes, ion channels, and peripheral proteins needs to be addressed in studies involving the neurotoxicity of pyrethroids. The multiple target systems for pyrethroids that is presented in Table 21 indicate that these lipid soluble insecticides are well distributed in biomembranes and bind to the proteins (i.e., ion channels) associated with them. The extent of this distribution is not well known; however, only 1% of the pyrethroid concentration in nervous tissue

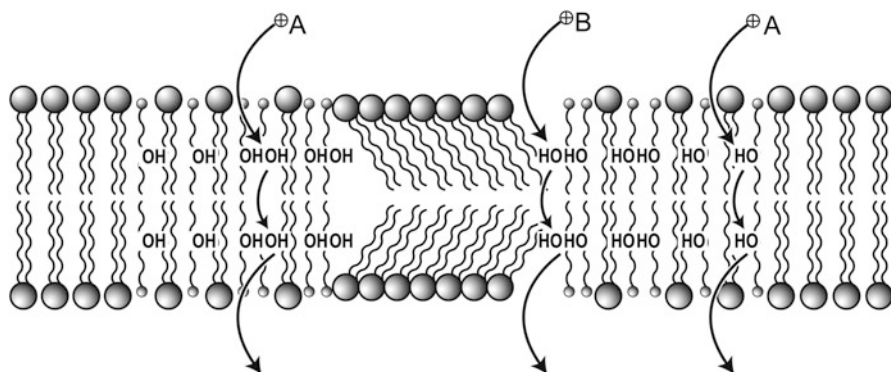


Fig. 13 This schematic is a depiction of the two models that are associated with ion permeation through lipid membranes containing some HSA (10-hydroxystearic acid) (smaller headgroup and one hydroxylated acyl chain). The lipids are represented by larger headgroups and two acyl chains, and are shown to form two zones that are rich in lipid, and which differ in density (phase domains). Conductivity through zone “A” is by electrostatic stabilization of ions occur by hydroxyl moieties that exist in domains that are rich in HSA. Conductivity in zone “B” also involves stabilization of charge by hydroxyl moieties, but it also shows the steric disorder that can exist between domains. This figure is published with permission (Nikolelis et al. 1991)

Table 21 Multiple target systems for the pyrethroids in mammals

Target	Concentrations ^a (M)	Pyrethroids ^b	Reference
Protein phosphorylation	10^{-13}	de, fe, cp, al	Enan and Matsumura (1993)
Voltage-gated sodium channels	10^{-10}	de	Ghiasuddin and Soderlund (1985)
Voltage-gated chloride channels	10^{-10}	de	Ray et al. (1997)
Noradrenaline release	10^{-10}	de	Clark and Brooks (1989)
Membrane depolarization	10^{-8}	de, cp, fe, pe	Eells et al. (1992); Rekling and Theophilidis (1995)
GABA-gated chloride channels	10^{-7}	de, cp	Lawrence et al. (1985)
Nicotinic receptors	10^{-7}	fe	Eldefrawi et al. (1985)
Mitochondrial complex 1	10^{-7}	pe, ch	Gassner et al. (1997)
Apoptosis induction	10^{-7}	de	Wu and Liu (2003)
Voltage-gated calcium channels	10^{-6} – 10^{-7}	al, te	Hagiwara et al. (1988); Hildebrand et al. (2004)
Lymphocyte proliferation	10^{-6}	bi	Diel et al. (1998)
Volume-sensitive anion channels	10^{-5}	bi, te	Culliford et al. (2004)
Calcium ATPase	10^{-5}	pe, cp, es, cf	Kakko et al. (2003); Grosman and Diel (2005)
Intercellular gap junctions	10^{-5}	fe, fc, cp, de	Hemming et al. (1993); Tateno et al. (1993)
Chromosomal damage	10^{-4}	pe	Barrueco et al. (1992)

^aNominal concentrations

^bAbbreviations for pyrethroids: *al* allethrin, *bi* bioallethrin, *cf* cyfluthrin, *ch* cyhalothrin, *cp* cypermethrin, *de* deltamethrin, *es* esbioallethrin, *fc* flucythrinate, *fl* fluvalinate, *fe* fenvalerate, *pe* permethrin, *te* tetramethrin

Table reproduced from Ray and Fry (2006) with permission

is believed to be involved in the modification of ion channel proteins, with the remainder distributed in biomembranes/phospholipids or bound to associated proteins.

According to O'Reilly et al. (2006), the sodium-channel binding cavity is accessible to the lipid bilayer and therefore to lipid-soluble insecticides. The properties of ion channels are measured by recording transmembrane currents using the patch-clamp technique (Horber et al. 1995).

8.2 Patch-Clamp Technique

The patch-clamp technique is an extension of the voltage clamp methodologies. The scope of the technique may be described by Ohm's law:

$$V = IR, \quad (34)$$

where the experimenter controls the voltage (V), records current (I), and the resistance (R) is a variable dependent upon the characteristics of the cell. This is carried out by the use of a single pipette, allowing the application of this technique to cells smaller than the squid giant axon. The patch in patch clamp refers to the patch of cell membrane contained within the polished aperture ($\sim 1 \mu\text{m}$ diameter) of a glass pipette that is placed against the membrane of a single cell. Suction is applied to the pipette to form a high giga-ohm resistance seal. The amplifier controls—"clamps"—the voltage across the cell and measures the current flowing through the ion channels in the cell membrane. Single-type ion channels may be studied using solutions of specific ionic composition. The replacement of K^+ in buffers with Cs^+ allows for Na^+ channels to be studied in the absence of contaminating K^+ current. $\text{IC}_{50\text{S}}$, K_{IS} and K_{DS} (inhibition and dissociation constants) may be measured for voltage-gated channels.

8.3 Voltage Dependence and Kinetics of Activation and Inactivation

The symptoms of pyrethroid poisoning are represented by hyperactivity and are induced primarily by modulation of the sodium channels. Type I and II (without and with cyano groups) pyrethroids cause a multiple action on the gating kinetics (opening and closing of channels by proteins) of the sodium channel. The action is as follows:

1. Activation (opening of channel proteins): voltage is shifted in the hyperpolarizing (change to a more negative potential) direction.
2. Deactivation (closing): voltage relationship is shifted in the hypopolarizing direction (change to a more positive potential).

Table 22 Classification of the pyrethroids into pure Type I, pure Type II, and mixed type based upon FOB, Na⁺, Ca²⁺, and Cl⁻ channel data

Pyrethroid	FOB	Na ⁺ channel	Ca ²⁺ channel	Cl ⁻ channel
Pure Type I				
S-Bioallethrin	I	I	I	I ^a
Cismethrin	NE	I	I	I
Resmethrin	I	NE	NE	NE
Tefluthrin	I	I	I	I
Bifenthrin	I	I-II	I	I
Permethrin	I	I	II	I
Mixed Type I and Type II				
Esfenvalerate	I-II	I-II	II	I
Fenpropathrin	I-II	I-II	I	II
Pure Type II				
β-Cyfluthrin	II	II	II	II
Cypermethrin	II	II	II	II
λ-Cyhalothrin	II	II	II	II ^b
Deltamethrin	II ^c	II	II	II

NE not evaluated

^a Slight increase in open-channel probability not considered significantly

^b Based on the evaluation of λ-cyhalothrin

^c Ignores a slight increase in Ta (Factor 3) at the high dose (Table 3, Figure S4, Breckenridge et al. 2009)

Table from Breckenridge et al. (2009). Published with permission

The pyrethroids cause slow activation (opening) and deactivation (closing) of the sodium channel. Type II pyrethroids increase discharge frequency in sensory neurons by membrane depolarization (change in potential to a more positive value), causing paraesthesia as observed in the arms and hands of workers dermally exposed to these insecticides.

8.4 Atomic Force Microscopy

The atomic force microscope (AFM) is currently used to examine biomembranes and membrane proteins in electrophysiological studies involving the patch-clamp technique (Danker et al. 1997). The structural information of the AFM image may be combined with the functional electrical data (Goksu et al. 2009). Danker et al. (1997) observed three kinds of membrane types, which had different surface morphologies or conducting properties such as the presence of undesired ER.

8.5 Effective Concentrations for Altering Sodium Channels

Ray and Fry (2006) recently published the content of the information presented in Table 22, which is reproduced with permission herein to show that multiple target

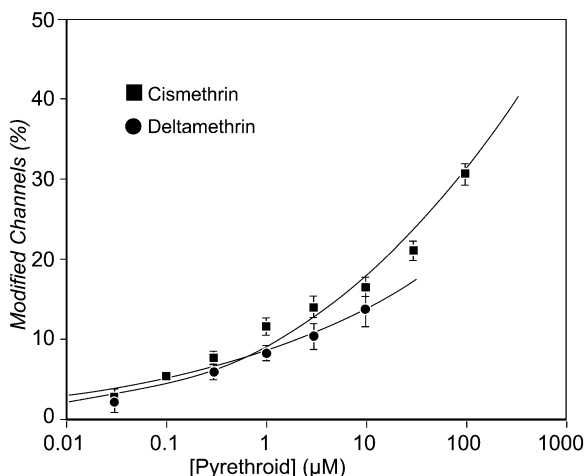


Fig. 14 Concentration-dependent resting modification of $\text{Na}_v1.8$ sodium channels by cismethrin and deltamethrin, obtained by sequential perfusion of oocytes with increasing concentrations of pyrethroid; data points are means of \pm SE of 6 (cismethrin) or 4 (deltamethrin) determinations. This figure is published with permission (Choi and Soderlund 2006)

systems exist for the pyrethroid insecticides. Effective concentrations have ranged from 10^{-4} M down to 10^{-13} M. This is below the concentrations (10–100 μM) used by Choi and Soderlund (2006) to study the time course of $\text{Na}_v1.8$ sodium channel modification by cismethrin, and those used to study the *in vitro* metabolism of the pyrethroids by liver microsomes (up to 100 μM). K_m values for both oxidative and hydrolytic activities exceeded 1 μM , and were generally in the range of 20–75 μM (Godin et al. 2006).

The substrate concentrations (K_{ms} for pyrethroids) agree with the concentrations of other substrates reported in the literature that have low water solubilities. The practice of using solvents to add pyrethroids to incubation media provides a means for saturating lipids in the microsomes and making these substrates available to enzymes associated with the lipids. Information as to whether the pyrethroids are free or bound to tissue proteins is required for use in the PBPK/PD models for determining partition coefficients, or metabolic rates. Binding also influences the results of toxicity studies, because pyrethroid insecticides bind to voltage-sensitive sodium channels and modify their gating kinetics, thereby disrupting nerve function and producing acute neurotoxic effects in both insects and nontarget organisms (Soderlund et al. 2002).

8.6 Sodium Channel Modifications

Figure 14, adapted from Choi and Soderlund (2006), shows that sodium channel modification occurs as a function of pyrethroid concentration.

Such concentrations are in the range of 1–100 μM , as used by Godin et al. (2006) in metabolism studies. The modification was limited at concentrations representing

the solubilities (0.1 μM) in water of these two pyrethroids. The concentrations of these pyrethroids that actually exist near the active sites of the enzymes (CYPs and carboxylesterases) and sodium channels are not known. According to Choi and Soderlund (2006), determining the relative potency of pyrethroids in the assays was complicated by the low aqueous solubility of these compounds, and the complexity of the kinetics by which they partition into the large lipid-rich compartments of the oocyte membrane and yolk. Song and Narahashi (1996) reported a toxicologically meaningful disruption of nerve function that probably occurs at concentrations causing modification of a very small proportion (<1%) of channels.

The percentage of channels modified by the pyrethroids may be calculated using (35) (Tatebayashi and Narahashi 1994):

$$M = (I_{\text{tail}}/(E_{\text{h}} - E_{\text{Na}}))/[I_{\text{Na}}/(E_{\text{t}} - E_{\text{Na}})] \times 100, \quad (35)$$

where I_{tail} is the maximal tail current amplitude, E_{h} is the potential to which the membrane is repolarized, E_{Na} is the reversal potential for sodium current determined from the current-voltage curve, I_{Na} is the amplitude of the peak current during depolarization before pyrethroid exposure, and E_{t} is the potential of step depolarization.

The concentration-response data may be fitted to the Hill equation (Tan et al. 2005):

$$M = \frac{M_{\text{max}}}{(1 + (K_{\text{d}}/[P])^{n_{\text{H}}})}, \quad (36)$$

where $[P]$ represents the concentration of pyrethroid and K_{d} represents the concentration of pyrethroid that produced the half-maximal effect, n_{H} represents the Hill coefficient, and the M_{max} is the maximal percentage of sodium channels modified.

8.7 Mitochondrial Complex in Neurotoxicity

Gassner et al. (1997) studied the effects of permethrin and cyhalothrin on the mitochondrial complex I. Our Fig. 15 was reproduced from this article (with permission) to show that the dose-response curves for permethrin and cyhalothrin on succinate-sustained O_2 consumption of rat liver mitochondria, during state 3 respiration. Half maximum inhibition (50%) occurred at 7.6 μM with permethrin, while 2.4 μM cyhalothrin resulted in 54% inhibition. The concentration is less than the K_{m} values for metabolism.

The most sensitive response (inhibition) appeared to be in the reduction of NADH:duroquinone oxidoreductases activity, wherein half maximal inhibition occurred with 0.73 μM permethrin and 0.57 μM cyhalothrin. These results are shown in Fig. 16. The lipid content of mitochondrial protein was not stated. Duroquinone (CAS no. 527-18-4) is 2,3,5,6-tetramethyl-1,4-benzoquinone (molar solubility = $4.3 \times 10^{-3} \cdot \text{mol} \cdot \text{L}^{-1}$ or 4,300 μM).

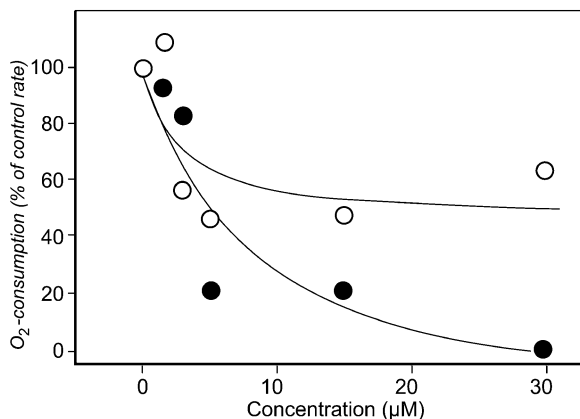


Fig. 15 Dose-response curves are shown for the effects of permethrin (*filled circle*) and cyhalothrin (*open circle*) on succinate-sustained O_2 consumption of rat liver mitochondria during state 3 respiration. Data points are the means of assay duplicates. This figure is published with permission (Gassner et al. 1997)

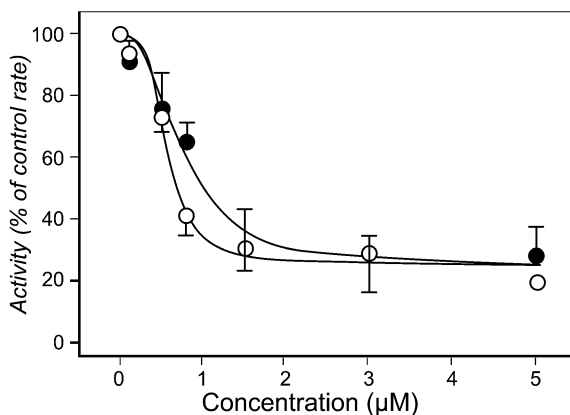


Fig. 16 Dose-response curves are shown for the effects of permethrin (*filled circle*) and cyhalothrin (*open circle*) on rotenone sensitive NADH: duroquinone oxidoreductase of SMP (subfraction of mitochondria protein). The oxidation of NADH was monitored spectrophotometrically. The data are the means \pm SEM of assay triplicates. This figure is published with permission (Gassner et al. 1997)

Mathematical analysis of the inhibition kinetics that occurred with permethrin and cyhalothrin indicated substantial cooperativity. Fitting the data to the equation listed below (37) yielded n -values of 2.4 for permethrin and 3.5 for cyhalothrin, indicating that 3–4 molecules of the two pyrethroids interacted with the mitochondrial complex 1.

$$Y_{[p]} = \frac{Y_{\max}[P]^n}{K' + [P]^n}. \quad (37)$$

Equation (37) is based on the Hill equation. At least 40 subunits of complex 1 are potential targets for binding of the pyrethroids. Model systems have recently been described that use this mode of action for the induction of neurodegenerative diseases (Gassner et al. 1997).

Soderlund et al. (2002) made the following observation: “The diverse toxic actions and pharmacological effects of pyrethroids suggest that simple additivity models based on combined actions at a single target are not appropriate to assess the risks of cumulative exposure to multiple pyrethroids.”

9 Neurotoxicity

The neurotoxicity of the pyrethroids was extensively reviewed by Soderlund et al. (2002), Shafer et al. (2005), Wolansky and Harrill (2008), and Breckenridge et al. (2009). The results of the recent analysis by Breckenridge et al. (2009) support the original hypothesis that pyrethroids exert their toxicological effect through Type I (T-syndrome) (tremor) and Type II (CS syndrome) (choreoathetosis (abnormal body movements)-salivation) syndromes. The CS-syndrome is associated with α -cyano pyrethroids that have slower sodium ion channel kinetics, whereas the T-syndrome is associated with the noncyano pyrethroids that have faster sodium ion channel kinetics. In addition, there are pyrethroids with sodium ion channel properties intermediate between the two extremes (i.e., deltamethrin (α -cyano) and bifenthrin (noncyano)) that tend to show both the T and CS syndrome. Breckenridge et al. (2009) classified the pyrethroids in Table 22 on the basis of acute neurological functional observation battery (FOB) studies (Weiner et al. 2009) and sodium (Choi and Soderlund 2006), calcium- (Symington et al. 2008), and chloride- (Burr and Ray 2004) channel studies.

Factor and multivariate dissimilarity analyses were used to evaluate four independent data sets from the four studies (Weiner et al. 2009; Choi and Soderlund 2006; Symington et al. 2008; Burr and Ray 2004). The analyses (factor and multivariate) by Breckenridge et al. (2009) did not provide useful information for developing the pharmacodynamic portion of a PBPK/PD model. Consequently, the original papers by Weiner et al. (2009), Choi and Soderlund (2006), Symington et al. (2008), and Burr and Ray (2004) were individually examined for useful information.

9.1 Functional Observation Batteries

Weiner et al. (2009) identified the pyrethroids by CAS no. in his FOB studies. Absolute stereochemistry was indicated for deltamethrin, S-Bioallethrin, esfenvalerate, (λ -cyhalothrin), and relative stereochemistry for bifenthrin and tefluthrin. Stereochemistry was not divulged for β -cyfluthrin, cypermethrin, permethrin, resmethrin, fenpropathrin, and the pyrethrins. Dosages, body weights, and time to peak effect provide useful information for setting oral exposure levels (gavage) and comparing peak effect times with predicted tissues concentrations from PBPK/PD models.

9.2 Na^{+1} Ion Channels

Choi and Soderlund (2006) studied the action of pyrethroids on rat $\text{Na}_v1.8$ sodium channels that are expressed in *Xenopus* oocytes. The stereochemistry of single isomers used in the study was identified by stereostructure, common name, and chirality (i.e., RS, *trans*, *cis*). Analytical standards (92.9–99.8% purity) of all compounds, except for cismethrin, were utilized. Before use in this study, cismethrin was purified by preparative high-resolution liquid chromatography (99.8%) by the method of Bloomquist and Soderlund (1988). Compounds were assayed in 0.3% dimethylsulfoxide (DMSO)/97% ND-96 medium (at a final concentration of 100 μM except for deltamethrin, which had a concentration of 10 μM). Data acquisition and analysis were performed using pClamp 8.2 (Axon Instruments, Burlingame, CA) and Origin 7.0 (OriginLab Corp., Northampton, MA). Of the 11 pyrethroids studied, only three compounds other than deltamethrin (cypermethrin, cyfluthrin, and cyhalothrin) exhibited statistically significant useful fractional modifications of the sodium channel.

However, all of the compounds produced clearly detectable tail currents. Tail currents reflect delayed channel deactivation (closing of channel activation gate). The partitioning of lipid-soluble pyrethroids into the lipid-rich compartments of the oocyte membrane and yolk prevented assessment of what the actual concentrations were in the concentration-effect curves. In vivo, pyrethroids bind to plasma proteins making them unavailable to lipids. Determining partition coefficients that involve lipids, and binding measurements that involve active channel protein(s), and also defining tail current decay times, may be useful in building PBPK/PD models.

9.3 Ca^{+2} Ion Channels

Symington et al. (2008) used in vitro techniques to study the influence of 11 pyrethroids on Ca^{2+} influx and glutamate release by rat brain synaptosomes. The low molar concentrations of pyrethroids used in this study were similar to the brain concentrations that were predicted by Mirfazaelian et al. (2006) using a PBPK model. The authors reported the isomeric composition of the commercial pyrethroids (bifenthrin, S-bioallethrin, cismethrin, β -cyfluthrin, λ -cyhalothrin, cypermethrin, deltamethrin, esfenvalerate, fenpropathrin, permethrin, and tefluthrin) used in the study. The Hill equation was used by Symington et al. (2008) to calculate the slope of the Ca^{2+} influx.

9.4 Cl^{-1} Ion Channels

The activity of 14 different pyrethroids (10 μM concentrations) on voltage-gated chloride ion channels was investigated by Burr and Ray (2004). Patch-clamp

techniques were used in their study. The hardware comprised an Axon Instrument Axopatch-1D, with CV4-1/100 Headstage and Axon Digidata 1200 data acquisition digitizing board, routed through a personal computer. The CAS no., isomeric details, and purity of each pyrethroid (bifenthrin, esbiol, bioresmethrin, b-cyfluthrin, cyfluthrin isomer 2, cyfluthrin isomer 4, cyhalothrin, cypermethrin, deltamethrin, esfenvalerate, fenpropathrin, permethrin, resmethrin and tefluthrin) was given. Open-channel probability values were reported. Overall, 3/6 of the Type II pyrethroids, 2/2 of the mixed-type pyrethroids, and 0/3 of the Type I pyrethroids were active at the chloride ion channel. The type of three of the 14 pyrethroids were not disclosed. The results (probability values) were not considered to be useful in the context of PBPK/PD models.

9.5 *Developmental Neurotoxicity*

Shafer et al. (2005) reported that there is no information on age-dependent toxicity for most pyrethroids. Their review summarizes the results of 22 studies performed on the developmental neurotoxicity of pyrethroids (strengths and limitations of studies). Many of the studies suffer from inadequate study design, problematic statistical analysis, use of formulated products (e.g., unknown isomer mixtures), and/or inadequate controls.

Several research needs were pointed out in this study. These included the additional need for information on the potential differences underlying age-dependent sensitivity to the pyrethroids, clarification of changes in behavioral and biochemical endpoints, and linking these end points to voltage-sensitive sodium channels (VSSCs) or other cellular targets. The authors suggest that BBDR (Biologically based Dose-response Models) be developed (Andersen and Dennison 2001) that describe the relationship between different components of the continuum between exposure to, and the adverse effects of, a chemical. A model of this nature was constructed for the developmental neurotoxicity of perchlorate (Jarabek 2002). A PBPK model that adequately describes the relationship between exposure and target tissue dose is also needed.

10 Discussion

The sections on the metabolism and neurotoxicity of the pyrethroids in this review provide a starting point that feeds into the physiological and biochemical parameters that are needed to develop PBPK/PD models for assessing risks to the pyrethroids. The development of such pyrethroid model parameters requires knowledge of their discovery, chemistry, chirality, their isomers, and their chromatographic separation. To this end, Sect. 2 above (viz., Nature of Pyrethroid Insecticides) was developed with a listing of 15 of the most important pyrethroids

available, their isomers, technical products, and aspects of their analytical chemistry. The detailed information on these 15 pyrethroids is presented in Appendices B and C, which shows the double bond of the chrysanthemic acid being in the *Z* position. The gem-dimethyl group on the cyclopropane ring is essential, because those compounds without it are essentially inactive. A side chain on the alcoholic moiety is also necessary. Unsaturation in the side chain of the alcohol may be alkenyl, cycloalkenyl, or aromatic (furyl, benzyl, or phenoxy) and is important to the biological activity of these insecticides.

The absolute stereochemistry of the active isomers (i.e., registered commercial products) is given in Appendix B. Registered products may contain all of the known isomers or only several of the more active isomers. Alpha-cypermethrin, a well-known product used on cotton in Egypt, contains a 50:50 mixture of two *cis* isomers [(1R, 3R, S) and (1S, 3S, R)], whereas deltamethrin contains only one *cis* isomer [(1R, 3R, S)] as the active ingredient. The wording on a label of a product (Bisect L, Loveland Products, Inc., Greeley, CO) containing 7.9% bifenthrin states that the product contains *cis* isomers 97% minimum and *trans* isomers 3% maximum. The absolute configuration of these isomers (*cis* and *trans*) are given in Table B3, Appendix B. Over the last 10 years, the development of chiral columns (HPLC and GC) has made it possible to easily separate the pyrethroid isomers. The lag in the development of analytical methodology and the relative lack of availability of metabolic standards has discouraged many investigators from undertaking pyrethroid studies, in particular metabolism and electrophysiological studies, in which isomers and their metabolic products need to be identified and quantitated.

PBPK models (i.e., GastroPlus, SimulationsPlus, Inc., Lancaster, CA) that are used in the pharmaceutical industry include code for the ACAT models, which describe the passage of a drug through the GI tract (Yu et al. 1996). The CAT models require additional parameters (e.g., length, radius, transit time, and pH) for GI tract, regional effective drug permeability (P_{eff}), solubility, absorption scale factors and metabolic data that are not required by simple gastrointestinal absorption models (i.e., rates of absorption from stomach and GI tract) for use in most pesticide-based PBPK/PD models. An ACAT PBPK/PD model has not been used as yet to describe the absorption of pyrethroids by the GI tract. Pyrethroid solubility data are available, and investigators at the University of Georgia, Athens, are currently developing permeability data involving P-glycoprotein using Caco-2 cells. V_{max} and K_{m} values obtained from work on liver enzymes may be used to simulate metabolism by gut enzymes based on their regional content in the GI tract.

The percutaneous absorption of pyrethroids is described in terms of their permeability to skin (K_{p} , $\text{cm} \cdot \text{h}^{-1}$); such permeability constitutes their rate of movement from the surface of the skin, through the stratum corneum, to the capillary bed. Bast et al. (1997) calculated a K_{p} value of $2.63 \times 10^{-8} \cdot \text{cm} \cdot \text{h}^{-1}$ for permethrin. Moreover, Bast et al. (1997) commented on the high permeability data of Sidon et al. (1988) involving permethrin, which they thought defied interpretation. From the QSAR equation of Potts and Guy (1992) a percutaneous K_{p} ($\text{cm} \cdot \text{h}^{-1}$) for permethrin was predicted to be 1.967. This value is 7.5×10^7 greater than the value reported by Bast et al. (1997). Additional work is needed to determine whether

the high results of Sidon et al. (1988) are inconsistent with the Bast et al. (1997) value. At present the absorption K_{ps} for the pyrethroids appear to be extremely low, based on the rat in vivo studies of Scott and Ramsay (1987) with cypermethrin and in vitro studies with isolated rat and human skin. The in vitro percutaneous studies of Reifenrath et al. (2011), performed on human skin with permethrin, support these observations.

The mechanistic models of Poulin and Theil, Berezhkovskly and Rodgers, Leahy, and Rowland provide non-laboratory approaches for predicting tissue: blood partition coefficients for nonvolatile chemicals, such as the pyrethroids and their metabolites. Although this procedure may not be as precise as the laboratory methods developed by Gargas et al. (1989) for volatile chemicals, or the procedure of Jepson et al. (1992, 1994) for nonvolatiles, the values may be easily calculated and recalculated as PBPK/PD modeling is performed, and later can be compared to values developed in the laboratory. The parameters inputted to the Poulin and Theil and Berezhkovskly partitioning models included a value for F_{up} (% unbound in plasma) for calculating f_{up} and the ratio of f_{up}/f_{ut} , which was used as a multiplier for correcting the lipid partition coefficients. This correction substantially reduced the pyrethroid and pyrethroid metabolite partition coefficients determined for fat, as shown in the tables of Appendix D. The Rodgers, Leahy and Rowland equations for the binding of basic drugs with acidic phospholipids, and the binding of neutral-acidic drugs with albumin, were not used to determine the partition coefficients of the pyrethroids or their metabolites (neutrals and acids), because plasma binding was adequately handled by the Poulin and Theil and Berezhkovskly partitioning and binding models.

The generic structures, technical names, physical and chemical properties, and tissue partition coefficients of the 15 pyrethroids and their metabolites are provided in Tables D1–D15 of Appendix D. Physical property values for modeling were obtained using a 2D model, ACD 12 (Advanced Chemistry Development, Inc., Toronto, Canada). A QSAR 3D model (i.e., QikProp 3.0 (Schrodinger, LL)), used in the development of F_{up} (fraction unbound to plasma protein), indicated that the differences in physical binding properties between isomers were small. Differences, however, exist in chemical properties as noted in metabolism studies reviewed in Sect. 5. Biotransformation and elimination paths for the pyrethroids that are presented in Tables E1–E15 of Appendix E incorporate preliminary metabolic rate data for PBPK/PD model development.

The importance of chirality (*cis*, *trans* isomers, etc.) to the pyrethroids was recognized early by Abernathy and Casida (1973), Casida et al. (1971a), and Casida et al. (1975) as they conducted studies on houseflies, mice, or rats, or esterase and oxidase systems derived from the organisms. Microsomal P450 enzymes oxidize the (+)-*trans*-chrysanthemate moiety at the *trans*-methyl group of the isobutenyl (propenyl) substituent and at one of the gem-dimethyl groups (2-(hydroxymethyl)-2-methyl-cyclopropane), while the (+)-*cis*-isomer is oxidized at either of the isobutenyl methyl groups. Products isomerized at C3 of the cyclopropane moiety are detected only after ester cleavage and oxidation of an isobutenyl methyl group. The alcohols are oxidized at various sites that depend upon whether they possess pentadienyl, allyl,

benzylic methylene, or aromatic substituents. The presence of chloro and trifluoro groups (2-chloro-3,3,3-trifluoro-1-propenyl) on the isobutenyl group of bifenthrin, cyhalothrin and tefluthrin result in the hydroxylation of one of the gem-dimethyls and one or more positions on their alcohols (aromatic, benzylic, etc.).

Hydrolysis of the pyrethroids may occur prior to hydroxylation. For dichloro groups (i.e., cyfluthrin, cypermethrin and permethrin) on the isobutenyl group, hydrolysis of the *trans*-isomers is the major route, and is followed by hydroxylation of one of the gem-dimethyls, the aromatic rings, and hydrolysis of the hydroxylated esters. The *cis*-isomers are not as readily hydrolyzed as the *trans*-isomers and are metabolized mainly by hydroxylation. Metabolism of the dibromo derivative of cypermethrin, deltamethrin, is similar to other pyrethroids (i.e., cyfluthrin, cypermethrin, and permethrin) that possess the dichloro group. Type II pyrethroid compounds containing cyano groups (i.e., cyfluthrin, cypermethrin, deltamethrin, fenvalerate, fenpropathrin, and fluralinate) yield cyanohydrins (benzeneacetonitrile, α -hydroxy-3-phenoxy-) upon hydrolysis, which decompose to an aldehyde, SCN ion, and 2-iminothiazolidine-4-carboxylic acid (ITCA). Chrysanthemic acid or derivatives were not used in the synthesis of fenvalerate and fluralinate. The acids (i.e., benzeneacetic acid, 4-chloro- α -(1-methylethyl) and DL-valine, *N*-[2-chloro-4-(trifluoromethyl) phenyl]-) were liberated from their esters and further oxidized/conjugated prior to elimination. Fenpropathrin is the only pyrethroid that contains 2,2,3,3-tetramethyl cyclopropanecarboxylic acid. The gem-dimethyl is hydroxylated prior to or after hydrolysis of the ester and is oxidized further to a carboxylic acid prior to elimination.

Phenothrin, resmethrin, and tetramethrin are Type I compounds possessing 2,2-dimethyl-3-(2-methyl-1-propen-1-yl)-cyclopropanecarboxylic acid. The gem-dimethyls remain largely untouched except for *cis*-phenothrin, while the (2-methyl-1-propen-1-yl) groups are oxidized to alcohols and ultimately to carboxylic acids. The alcohol moieties are hydroxylated or sulfonated prior to ester hydrolysis. The metabolites of the pyrethroids (i.e., acids and alcohols) are largely conjugated with glucuronic or sulfuric acids prior to being eliminated in urine. No evidence was obtained to indicate that intact hydroxylated esters were conjugated.

PBPK/PD models require metabolic rate constants (V_{\max} and K_m) adequate to describe the hydrolytic and oxidative (hydroxylation) metabolism of the pyrethroids in humans, rats, and other mammals that are used in modeling. Appendices D and E provide physical/chemical descriptions of the pyrethroids, their metabolites or degradation products along with their pathways (i.e., rate of metabolism, RAM, etc.) in rat tissues. Hydrolysis by hepatic microsomal carboxylesterase (CEs) of the parent pyrethroid is generally considered to be the first and most important step in the biotransformation in mammals. Ross et al. (2006) determined the rate of metabolism of several Type I (i.e., bioresmethrin > *trans*-permethrin > *cis*-permethrin) and Type II (i.e., deltamethrin > alpha-cypermethrin) pyrethroids by using rabbit rCEs to measure rates of product formation (acid and alcohol leaving groups). Metabolic rate constants for these pyrethroids were also examined for human hCE-1, hCE-2, and two pure rat CE (hydrolase A and B). Protein expression of hCE-1 was determined in human liver microsomes using anti-hCE-1. Ross et al. (2006) concluded that hepatic

microsomes from rats, mice, and humans were similarly active in hydrolyzing the pyrethroids studied. No information was provided concerning the activity of the CEs in rat or human sera against the pyrethroids, or their action on hydroxylated pyrethroid esters. Crow et al. (2007) extended the work of Ross et al. (2006) to include the expression and hydrolytic activity of CEs present in the cytosol and various other rat and human tissues, including rat and human intestinal microsomes and serum. The hydrolysis products detected after HPLC analysis included the parent acids and alcohols of bioresmethrin, deltamethrin, and *trans*-permethrin. Human serum was found to lack pyrethroid hydrolytic activity. Variable amounts of hCE-1 protein were observed to exist in cytosolic samples, in contrast to the nonvariable levels found in human microsomes. Chang et al. (2009) developed k_{cat} values for the hydrolysis of pyrethroids by rat serum carboxylesterase, using a consensus 3D QSAR pharmacophore model. These values have not yet been used in any published PBPK/PD model.

Using the parent compound depletion method, pyrethroid metabolic rate constants (i.e., V_{max} and K_m , k_{cat} , etc.) for hydroxylation by cytochrome P450 enzymes or hydrolysis by carboxylesterases were developed by Scollon et al. (2009). The sources of the enzymes were rat and human microsomes. The pyrethroids they studied included bifenthrin, S-bioallethrin, bioresmethrin, β -cyfluthrin, cypermethrin, *cis*-permethrin, and *trans*-permethrin. The depletion method considers multiple hydroxylations as a single biotransformation at sites on either the acid or alcohol moieties, or on a combination of both. The metabolic pathways (Tables D1–D15 and E1–E15 of Appendices D and E, respectively) require V_{max} , K_m , and k_{cat} values for the individual hydroxylated and hydrolyzed products. It is interesting that only bioresmethrin and cypermethrin per se were found to actually be hydrolyzed.

Supersomes from BD Biosciences containing rat (i.e., CYP1A1, 1A2, 2A1, 2B1, 2C6, 2C11, 2C13, 2D1, 2D2, 3A1, and 3A2) or human CYPs (i.e., 1A1, 1A2, 2B6, 2CD8, 2C9*1, 2C9*2, 2C9*3, and 3A4) were individually used to obtain the percentage of each pyrethroid (0.5 μM) metabolized by 10 pmol of P450, during a 10-min incubation period. The results are interesting, but to be useful in PBPK/PD models, rate constants ($\text{pmol} \cdot \text{min}^{-1} \cdot \text{pmol}^{-1}$ of CYP), CYP content ($\text{pmol} \cdot \text{mg}^{-1}$ of microsomal protein), and mg of microsomal protein g^{-1} of liver are needed to make in vitro to in vivo extrapolations.

According to Anand et al. (2006), CYP450-catalyzed metabolism of deltamethrin in the rat exceeds that by either plasma or liver carboxylesterases. The velocity of the reaction was expressed in nmol deltamethrin disappearance $\text{h}^{-1} \text{g}^{-1}$ liver or plasma. This information was used to construct a PBPK/PD model in the adult male rat (Mirfazaelian et al. 2006). Godin et al. (2006) examined species differences between rat and human liver microsomal carboxylesterases. A significant species difference was noted in the in vitro biotransformation of deltamethrin, due in part to differences in the rate of hydrolysis by human liver microsomes. Godin et al. (2007) identified the rat and human CYP450 isoforms, and rat serum esterases that metabolize deltamethrin and esfenvalerate. Differences in the rates of hepatic oxidative metabolism were related to expression levels (abundance) of the individual P450 isoforms rather than their specific activity.

Godin et al. (2006) recognized that the rat may not be a good model for understanding the metabolism of pyrethroids in humans. Their conclusions on this point were based only on hydrolysis and oxidation of the parent pyrethroid (i.e., deltamethrin), rather than on the full metabolic pathways of the pyrethroids as outlined in Appendices D and E and in the context of a PBPK/PD modeling. We do agree, however, that a rat PBPK/PD model per se may not be suitable for extrapolating the results to humans, because of differences in biochemical (i.e., enzymes, their activities, specific content, etc.) and physiological parameters between the species. There is still disagreement as to the microsomal content of liver ($\text{mg} \cdot \text{g}^{-1}$ of liver) and the content of the individual CYPs per mg of microsomal protein in humans (Barter et al. 2007; Brown et al. 1997; Davies and Morris 1993; Houston 1994; Iwatsubo et al. 1997; Lipscomb et al. 1998; Wilson et al. 2003).

The tables in Appendix E were developed to provide modelers with complete information on the rat metabolic pathway for each of the pyrethroid insecticides. The tables in Appendix D are designed to provide the tissue:blood partition coefficients for the parent pyrethroids and their metabolites. Some metabolic rates may not exist for either rat or human metabolic pathways, and hence, modelers may have to zero out this parameter in the PBPK/PD models they work with. In any case, the importance of each metabolic pathway needs to be determined from the enzymes that exist in tissues, their rate constants (i.e., V_{max} and K_m), and the amount or content of each enzyme present. If in vitro enzyme work is to be performed, good analytical methods and analytical samples for each metabolite are essential.

Despite the fact that over 6,000 biological equations have been developed, there are still no QSAR models that relate chemical structure to neurotoxicity (Hansch et al. 1995). Models that relate structure to effects (i.e., Enslein et al. 1998; Klopman and Rosenkranz 1995; Porcelli et al. 2007) have focused on broad-based toxic end points such as carcinogenesis, mutagenesis, irritation, teratogenesis, and cholinesterase inhibition. Researchers and others need neurotoxicity models that address ion channels, or another end point closely related to the toxicity of the pyrethroids, such as the results of functional observation batteries (FOB). QSAR models that provide LD_{50} values, such as TOPKAT, are useful to modelers for selecting dosages to use in PBPK/PD models. QuikProp (3D model) and the kinetic models for recombinant human cytochrome P450 enzymes 1A2, 2C9, 2C19, 2D6, and 3A4 in SimulationsPlus Inc.'s "ADMET Predictor" appear to be the only models commercially available for predicting MDCK, Caco-2, log BBB, or the individual CYP V_{max} and K_m values for use in PBPK/PD models. To our knowledge, the previously mentioned parameters are not being used in pyrethroid PBPK/PD models. The addition of rCYP V_{max} and K_m data from recent studies performed on the pyrethroids (Enslein 2010) may offer improvements over the predicted values obtained using ADMET Predictor 5.5.

Literature K_m values, derived from liver microsomal studies, are rarely adjusted for the fraction of unbound pyrethroid remaining in the microsomes. According to Youdim et al. (2008), the use of equilibrium dialysis to generate accurate

protein-binding measurements ($f_{u,mic}$, unbound drug in microsomes) is especially important for highly bound drugs. F_{up} (unbound pyrethroids in plasma) value measurements reported in this review that are used to calculate partition coefficients provide evidence that the pyrethroids are highly bound to plasma proteins. The F_{up} and $F_{u,mic}$ values published by Youdim et al. (2008) provided data for 11 drugs that show $F_{u,mic}$ values to be larger (unbound drug in microsomes greater than unbound drug in plasma) than F_{up} values. By definition, F_{up} values represent only protein binding and not a combination of protein binding and lipid partitioning (f_{up}). Youdim and Dodia (2010) used the product-formation approach to determine V_{max} and K_m values; they then multiplied the K_m by the $F_{u,mic}$ values to obtain the unbound K_m -value. If we multiply the F_{up} value (0.02422) for bifenthrin by its K_m value ($\sim 5.42 \mu\text{M}$), the new K_m is 0.131 and V_{max}/K_m ratio increases from 0.118 to 4.885. The $F_{u,mic}$ value for bifenthrin is probably larger than the F_{up} value. However, the example using the calculated F_{up} value certainly supports the work of Youdim et al. (2008) and Youdim and Dodia (2010) for obtaining values for $F_{u,mic}$ and using them to correct the K_m .

To our knowledge equilibrium dialysis has not been used to measure unbound bifenthrin or that of any other pyrethroids studied, in microsomes. Wang et al. (2010) reported that the FDA (Food and Drug Administration) considers stereoisomers to be distinct chemical entities, if they are biologically distinguishable. For example, racemic amlodipine (CAS no. 88150-42-9) is active in the treatment of hypertension, but also causes peripheral edema, while S-amlodipine (CAS no. 103129-82-4), administered at half the dose, is as effective as the racemic mixture, but produces negligible edema. Similar examples of activity, inactivity, and toxicity linked to target or off target-effects probably also occur with the pyrethroids. However, the inability to separate, identify, and carefully study the individual isomers has prevented researchers from definitively studying their toxicity, especially to undertake work on their inhibition or activation of ion-channel gating proteins.

The development of human CYP-based QSAR models by Enslein (ADMET Predictor 5.5, SimulationsPlus, Inc.) for predicting drug-hydroxylation rate constants (i.e., V_{max} and K_m) now provides pharmacologists and toxicologists with QSAR models for obtaining rate constants while working on PBPK/PD models. We believe this is an important step in securing a place for QSAR in toxicology and PBPK/PD model development. It is probable that these predictive QSAR models will be updated as new V_{max} and K_m data become available. Plans are currently being made to add new rate constants from the kinetic studies mentioned in this review.

Studies on the in vivo distribution and fate of pyrethroids in membranes are needed to better understand how these insecticides partition into lipids, bind to channel proteins and ultimately produce neurotoxicity by affecting how ions move through nerve membranes. Since 1962, many voltage-gated channel studies that have utilized intracellular microelectrodes and patch-clamping techniques have been performed. Patch-clamping has proved to be an essential tool for studying the electrochemical properties of membranes and their protein components. New

technologies, such as nanofabricated scanning electrochemical microscopy and atomic force microscopy (SECM-AFM), may be capable of recording signals across individual ion channels while providing real-time structural information (Goksu et al. 2009).

Currently, combining AFM with the nuclear patch clamp is useful in disclosing the structural correlates of nuclear patch-clamp currents. The finding that different nuclear envelope membrane configurations may occur at the tip of the patch pipette could help to explain conflicting results. To our knowledge, patch-clamped membranes exposed to the pyrethroids have not been examined by AFM to obtain structural data, in conjunction with functional electrical data. Waxman et al. (2004) reported at least nine different genes that encode distinct voltage-gated Na^+ channels ($\text{Na}_v1.1$ – $\text{Na}_v1.9$), and all share a common structure, although different amino acid sequences, voltage-dependencies, and kinetics exist for them. $\text{Na}_v1.1$, $\text{Na}_v1.2$, $\text{Na}_v1.3$, and $\text{Na}_v1.6$ channels are found in the nervous system, $\text{Na}_v1.7$, $\text{Na}_v1.8$, and $\text{Na}_v1.9$ channels are expressed within the dorsal root ganglion and trigeminal ganglion neurons. $\text{Na}_v1.4$ and $\text{Na}_v1.5$ channels are found within somatic and cardiac muscle, respectively. In most unmyelinated axons, ion channels are distributed uniformly along the axon to facilitate stable propagation of action potentials. Several models (i.e., stochastic Hodgkin-Huxley and compartments models) are used to simulate nerve impulse (action potential) propagation (Zeng and Tang 2009).

Na^+ channel dysfunctions present themselves under various clinical conditions (i.e., ischemia, drug use, electrolyte imbalance) and may cause life-threatening arrhythmias (Tan et al. 2003). Some aspects of cardiovascular research may be useful in exploring the combined or separate effects of drug and/or pyrethroid-based pharmacological Na^+ channel blockage. So far pyrethroid neurotoxicity is based largely on acute neurotoxicity and on ion channel studies, with few if any whole animal or organ pharmacological studies having been performed. Tatebayashi and Narahashi (1994) and Tan et al. (2005) suggested using the maximal tail current amplitude as a means of estimating the percentage of channels modified by the pyrethroids.

11 Recommendations

On the basis of this pyrethroid parameter review a number of data gaps became obvious. We recommend the following work be performed to improve the scientific value of QSAR and PBPK/PD models:

1. Synthesize analytical standards for hydroxylated pyrethroids (enantiomer pairs) and develop chromatographic methods for separating and identifying them.
2. Develop in vitro metabolic rate constants (V_{max} and K_m) for the CYP-catalyzed hydroxylation of parent pyrethroids (i.e., active pyrethroid isomers, enantiomer pairs), and the carboxylesterase-catalyzed hydrolysis of parent and hydroxylated

pyrethroids. Species-specific metabolic and stereoisomer-specific constants for pyrethroids, particularly for human models are needed to support risk-assessment efforts.

3. In vitro metabolic rate constants (i.e., V_{\max} , $\text{nmol} \cdot \text{min}^{-1} \cdot \text{nmol}^{-1}$ P450) should be converted to in vivo values ($\mu\text{mol} \cdot \text{h}^{-1} \cdot \text{kg}^{-1} \cdot \text{bwt}$, Inoue et al. 2006) and be examined for their validity in model runs.
4. Plasma protein binding should be accounted for in the development of tissue: blood partition coefficients; and microsomal and CYP protein binding in the development of metabolic rate constants. Plasma protein binding was accounted for in the development of tissue: blood partition coefficients in Appendix D (Berezhkovskly 2004a; Poulin and Thiele 2000). K_m values may need to be adjusted for any nonspecific microsomal or CYP binding that occurs during kinetic measurements (Austin et al. 2002).
5. Diffusion-limited tissue parameters should be considered and developed (Mirfazaelian et al. 2006).
6. The recovery of low to high percentages of oral dosages in the stomach, small and large intestine suggests that additional compartment and parameters (Caco-2-cell permeation constants, enterocytic metabolism, and enterohepatic circulation) may be needed to adequately describe gut absorption.
7. In vitro ion channel electrophysiological studies are the major studies being performed now and in the past with the pyrethroids. The authors of these studies have not determined the distribution/concentration or fate of the pyrethroids (single isomers) in biomembranes that surround the ion channels being evaluated. Estimates indicate that only 1% of the applied pyrethroids are bound to proteins in the ion channels, with the remaining pyrethroids distributed or bound to other proteins. The structure of the “patch” used in pClamp studies needs to be reexamined using Atomic Force Microscopy to ensure biological consistency across ion channel preparations. Tail current measurements have been suggested as a measure of the % of modified channels. These measurements, although suggested by a number of investigators, have not been used in PBPK/PD models to describe the pharmacodynamics of pyrethroids in nerve tissue, although they should be. The toxicological relationship between the results of the functional observation batteries (FOB) and the in vitro electrophysiological studies needs to be further examined.

12 Summary

In this review we have examined the status of parameters required by pyrethroid QSAR–PBPK/PD models for assessing health risks. In lieu of the chemical, biological, biochemical, and toxicological information developed on the pyrethroids since 1968, the finding of suitable parameters for QSAR and PBPK/PD model development was a monumental task. The most useful information obtained came from rat toxicokinetic studies (i.e., absorption, distribution, and

excretion), metabolism studies with ^{14}C -cyclopropane- and alcohol-labeled pyrethroids, the use of known chiral isomers in the metabolism studies and their relation to commercial products. In this review we identify the individual chiral isomers that have been used in published studies and the chiral HPLC columns available for separating them. Chiral HPLC columns are necessary for isomer identification and for developing kinetic values (V_{\max} and K_m) for pyrethroid hydroxylation. Early investigators synthesized analytical standards for key pyrethroid metabolites, and these were used to confirm the identity of urinary metabolites, by using TLC. These analytical standards no longer exist, and must be resynthesized if further studies on the kinetics of the metabolism of pyrethroids are to be undertaken.

In an attempt to circumvent the availability of analytical standards, several CYP450 studies were carried out using the substrate depletion method. This approach does not provide information on the products formed downstream, and may be of limited use in developing human environmental exposure PBPK/PD models that require extensive urinary metabolite data. Hydrolytic standards (i.e., alcohols and acids) were available to investigators who studied the carboxylesterase-catalyzed hydrolysis of several pyrethroid insecticides. The data generated in these studies are suitable for use in developing human exposure PBPK/PD models.

Tissue:blood partition coefficients were developed for the parent pyrethroids and their metabolites, by using a published mechanistic model introduced by Poulin and Thiele (2002a; b) and $\log D_{\text{pH } 7.4}$ values. The estimated coefficients, especially those of adipose tissue, were too high and had to be corrected by using a procedure in which the proportion of parent or metabolite residues that are unbound to plasma albumin is considered, as described in the GastroPlus model (SimulationsPlus, Inc., Lancaster, CA). The literature suggested that K_m values be adjusted by multiplying K_m by the substrate (decimal amount) that is unbound to microsomal or CYP protein. Mirfazaelian et al. (2006) used flow- and diffusion-limited compartments in their deltamethrin model. The addition of permeability areas (PA) having diffusion limits, such as the fat and slowly perfused compartments, enabled the investigators to bring model predictions in line with *in vivo* data.

There appears to be large differences in the manner and rate of absorption of the pyrethroids from the gastrointestinal tract, implying that GI advanced compartmental transit models (ACAT) need to be included in PBPK models. This is especially true of the absorption of an oral dose of tefluthrin in male rats, in which 3.0–6.9%, 41.3–46.3%, and 5.2–15.5% of the dose is eliminated in urine, feces, and bile, respectively (0–48 h after administration). Several percutaneous studies with the pyrethroids strongly support the belief that these insecticides are not readily absorbed, but remain on the surface of the skin until they are washed off. In one particular study (Sidon et al. 1988) the high levels of permethrin absorption through the forehead skin (24–28%) of the monkey was reported over a 7- to 14-days period. Wester et al. (1994) reported an absorption of 1.9% of pyrethrin that had been applied to the forearm of human volunteers over a 7-days period.

QSAR models capable of predicting the binding of the pyrethroids to plasma and hepatic proteins were developed by Yamazaki and Kanaoka (2004), Saiakhov

et al. (2000), Colmenarejo et al. (2001), and Colmenarejo (2003). QikProp (Schrodinger, LLC) was used to obtain F_{up} values for calculating partition coefficients and for calculating permeation constants (Caco-2, MDCK, and log BBB). ADMET Predictor (SimulationsPlus Inc.) provided V_{max} and K_m values for the hydroxylation of drugs/pyrethroids by human liver recombinant cytochrome P450 enzymes making the values available for possible use in PBPK/PD models. The Caco-2 permeability constants and CYP3A4 V_{max} and K_m values are needed in PBPK/PD models with GI ACAT sub models. Modeling work by Chang et al. (2009) produced rate constants (k_{cat}) for the hydrolysis of pyrethroids by rat serum carboxylesterases. The skin permeation model of Potts and Guy (1992) was used to predict K_p values for the dermal absorption of the 15 pyrethroids.

The electrophysiological studies by Narahashi (1971) and others (Breckenridge et al. 2009; Shafer et al. 2005; Soderlund et al. 2002; Wolansky and Harrill 2008) demonstrated that the mode of action of pyrethroids on nerves is to interfere with the changes in sodium and potassium ion currents. The pyrethroids, being highly lipid soluble, are bound or distributed in lipid bilayers of the nerve cell membrane and exert their action on sodium channel proteins. The rising phase of the action potential is caused by sodium influx (sodium activation), while the falling phase is caused by sodium activation being turned off, and an increase in potassium efflux (potassium activation). The action of allethrin and other pyrethroids is caused by an inhibition or block of the normal currents. An equation by Tatebayashi and Narahashi (1994) that describes the action of pyrethroids on sodium channels was found in the literature. This equation, or some variation of it, may be suitable for use in the PD portion of pyrethroid PBPK models.

Acknowledgments Our thanks are extended to Prof. Herbert N. Nigg, University of Florida, and Prof. James R. Olson, The State University of New York at Buffalo, for reviewing the manuscript of this article and making helpful suggestions that improve its quality. We also thank SRA International, Las Vegas, NV, for their skilled work in preparing this manuscript for publication and Dr. Robert Fraczkiwicz, Simulations-plus, Lancaster, California, for calculating the Predicted V_{max} and K_m values for the CYP450s using ADMET Predictor.

The work on this review was funded by the US EPA through General Services Administration Contract GS-35F-43570, tasks EP0THO00393 and EP11HO00301 with General Dynamics Information Technology (GDIT), Henderson, NV. Although this work was reviewed by EPA and approved for publication, it may not necessarily reflect official Agency policy, nor does it represent the official views of GDIT. Mention of trade names or commercial products does not constitute endorsement or recommendation for use.

References

- Abernathy CO, Casida JE (1973) Pyrethroid insecticides: esterase cleavage in relation to selective toxicity. *Science* 179:1235–1236
- Ackermann P, Bourgeois F, Drabek J (1980) The optical isomers of alpha-cyano-3-phenoxybenzyl 3-1,2-dibromo-2,2-dichloroethyl-2,2-dimethylcyclopropanecarboxylate and their insecticidal activities. *J Pestic Sci* 11:169–179
- Agoram B, Woltosz WS, Bolger MB (2001) Predicting the impact of physiological and biochemical processes on oral drug bioavailability. *Adv Drug Deliver Rev* 50:S41–S67

- Allen S, Leah A (1990) Lambda-cyhalothrin: acute oral toxicity study in the rat. Zeneca Agricultural Products Laboratory No. CTL/P/3209:AR4840, Wilmington, DE.
- Anadon A, Martinez-Larranaga MR, Fernandez-Cruz ML, Diaz MJ, Fernandez MC, Martinez MA (1996) Toxicokinetics of deltamethrin and its 4'-OH-metabolite in the rat. *Toxicol Appl Pharmacol* 141:8–16
- Anand SS, Bruckner JV, Haines WT, Muralidhara S, Fisher JW, Padilla S (2006) Characterization of deltamethrin metabolism by rat plasma and liver microsomes. *Toxicol Appl Pharmacol* 212:156–166
- Andersen ME, Dennison JE (2001) Mode of action and tissue dosimetry in current and future risk assessments. *Sci Total Environ* 274(1–3):3–14
- Angerer J, Ritter A (1997) Determination of metabolites of pyrethroids in human urine using solid-phase extraction and gas chromatography-mass spectrometry. *J Chromatogr* 695:217–226
- Artursson P, Palm K, Luthan K (1996) Caco-2 monolayers in experimental and theoretical predictions of drug transport. *Adv Drug Deliv Rev* 22:67–84
- Audegond L, Collas E, Glomot R (1981a) RU 25474 (tralomethrin) single administration study by oral route in the rat. Study No. RU-4BE-81.240/A, Roussel-Uclaf, Paris.
- Audegond L, Collas E, Glomot R (1981b) RU 25474 (tralomethrin) single administration study by oral route in the rat. Study No. 81240 DS/84/A, Roussel-Uclaf, Paris.
- Austin RP, Barton P, Cockroft SL, Wenlock MC, Riley RJ (2002) The influence of nonspecific microsomal binding on apparent intrinsic clearance, and its prediction from physicochemical properties. *Drug Metab Dispos* 30:1497–1503
- Baker H, Kligman AM (1967) Measurement of transepidermal water loss by electrical hygrometry. *Arch Dermatol* 96:441–452
- Barbero AM, Frasch HF (2009) Pig and guinea pig skin as surrogates for human in vitro penetration studies: a quantitative review. *Toxicol In Vitro* 23:1–13
- Barrueco D, Herrera A, Caballo C, Delapena E (1992) Cytogenic effects of permethrin in cultured human-lymphocytes. *Mutagenesis* 7:433–437
- Barter ZE, Bayliss MK, Beaune PH, Boobis AR, Carlile DJ, Edwards RJ, Houston JB, Lake BG, Lipscomb JC, Pelkonen OR, Tucker GT, Rostami-Hodjegan A (2007) Scaling factors for the extrapolation of in vivo metabolic drug clearance from in vitro data: reaching a consensus on values of human microsomal protein and hepatocellularity per gram of liver. *Curr Drug Metab* 8:33–45
- Bast GE, Taeschner D, Kampffmeyer HG (1997) Permethrin absorption not detected in single-pass perfused rabbit ear, and absorption with oxidation of 3-phenoxybenzyl alcohol. *Arch Toxicol* 71:179–186
- Baynes RE, Halling KB, Riviere JE (1997) The influence of Diethyl-m-toluamide (DEET) on the percutaneous absorption of permethrin and carbaryl. *Toxicol Appl Pharmacol* 144:332–339
- Berenson GS, Burch GE (1951) Studies of diffusion through dead human skin. *Am J Trop Med Hyg* 31:842–853
- Berezhkovskly LM (2004a) Determination of volume of distribution at steady state with complete consideration of the kinetics of protein and tissue binding in linear. *J Pharm Sci* 93:364–364
- Berezhkovskly LM (2004b) Volume of distribution at steady state for a linear pharmacokinetic system with peripheral elimination. *J Pharm Sci* 93:1628–1640
- Berezhkovskly LM (2007) The connection between the steady state (V_{ss}) and Terminal (V_{β}) volumes of distribution in linear pharmacokinetics and the general proof that $V_{\beta} \geq V_{ss}$. *J Pharm Sci* 96:1638–1650
- Bilsback MM, Parker CM, Wimberly HC (1984) Comparative oral toxicity of technical MO70616 and technical SD 42775 in rats. Study No. WRC-RIR 357. Corporation Study No. NCT584.01, Shell Development Company, Houston, TX.
- Blancato JN, Knaak JB, Power F (2000) Use of PBPK models for assessing absorbed dose and ChE inhibition from aggregate exposure of infants and children to organophosphorous insecticides. Presented at 10th Annual Meeting of the International Society of Exposure Analysis, Monterey, CA (Abstract 3F-09o)

- Bloomquist JR, Soderlund DM (1988) Pyrethroid insecticides and DDT modify alkaloid-dependent sodium channel activation and its enhancement by sea anemone toxin. *Mol Pharmacol* 33:543–550
- Boatman RJ, Knaak JB (2001) Ethers of ethylene glycol and derivatives. In: Bingham E, Cohnsson B, Powell CH (eds) *Patty's toxicology* (5th ed). Wiley, NY, NY
- Bolger MB (2010) Simulations-Plus, Inc., Lancaster, CA. Memo to Kurt Enslein, Enslein Research, Rochester, NY.
- Breckenridge CB, Holden L, Sturgess N, Weiner M, Sheets L, Sargent D, Soderlund DM, Choi J-S, Symington S, Clark JM, Burr S, Ray D (2009) Evidence for a separate mechanism of toxicity for the Type I and the Type II pyrethroid insecticides. *Neurotoxicology* 30(Suppl 1):S17–S31
- Bronaugh RL, Stewart RF, Congdon ER (1982) Methods for in vitro percutaneous absorption studies II. Animal models for human skin. *Toxicol Appl Pharmacol* 62:481–488
- Bronaugh RL, Stewart RF, Simon M (1986) Methods for in vitro percutaneous absorption studies. VII: use of excised human skin. *J Pharm Sci* 75:1094–1097
- Brown RP, Delp MD, Lindstedt SL, Rhomberg LR, Beliles RP (1997) Physiological parameter values for physiologically based pharmacokinetic models. *Toxicol Ind Health* 13:407–484
- Burr SA, Ray DE (2004) Structure-activity and interaction effects of 14 different pyrethroids on voltage-gated chloride ion channels. *Toxicol Sci* 77:341–346
- Cahn RS, Ingold CK, Prelog V (1966) Specification of chirality. *Angew Chem Int Ed Engl* 5:385–415
- Casida JE, Kimmel EC, Elliott M, Janes NF (1971a) Oxidative metabolism of pyrethrins in mammals. *Nature* 230:326–327
- Casida JE, Kimmel ED, Elliott M, Janes NF (1971b) Oxidative metabolism of pyrethrins in mammals. *Pyrethrum Post* 11:58–59
- Casida JE, Ueda K, Gaughan LC, Jao LT, Soderlund DM (1975) Structure-biodegradability relationships in pyrethroid insecticides. *Arch Environ Contam Toxicol* 3:491–500
- Cayley GR, Simpson BW (1986) Separation of pyrethroid enantiomers by chiral high-performance liquid chromatography. *J Chromatogr A* 356:123–134
- Chamberlain K, Matsuo N, Kaneko H, Khambay BPS (1998) Pyrethroids. In: *Chirality in agrochemicals*. Wiley, New York
- Chang JH, Benet LZ (2005) Glucuronidation and the transport of the glucuronide metabolites in LLC-PK1 cells. *Mol Pharmacol* 2:428–434
- Chang SK, Brooks JB, Monteiriviere NA, Riviere JE (1995) Enhancing or blocking effect of fenvalerate on the subsequent percutaneous absorption of pesticides in vitro. *Pestic Biochem Physiol* 51:214–219
- Chang DT, Goldsmith M-R, Tornero-Velez L-J, Ulrich E, Lindstrom AB, Dary CC (2009) A novel application of QSAR and PH4 models for the elucidation of the stereoselective hydrolysis rates of pyrethroids by rat serum carboxylesterase. Society of Environmental Toxicology and Chemistry, New Orleans, LA, November 2009 meeting.
- Chemical Abstracts Service (2002) Chemical abstracts 2002 index guide, appendix IV, naming and indexing of chemical substances for chemical abstracts, E. Stereochemistry and stereoparents (paragraphs 202–212). Chemical Abstracts Service, Columbus, Ohio.
- Choi J-S, Soderlund DM (2006) Structure-activity relationships for the action of 11 pyrethroid insecticides on rat Nav1.8 sodium channels expressed in *Xenopus* oocytes. *Toxicol Appl Pharmacol* 211:233–244
- Clark JM, Brooks MW (1989) Role of ion channels and intraterminal calcium homeostasis in the action of deltamethrin at presynaptic nerve terminals. *Biochem Pharmacol* 38:2233–2245
- Class TJ, Ando T, Casida JE (1990) Pyrethroid metabolism: microsomal oxidase metabolites of (S)-bioallethrin and the six natural pyrethrins. *J Agric Food Chem* 38:529–537
- Cole LM, Ruzo LO, Wood EJ, Casida JE (1982) Pyrethroid metabolism: comparative fate in rats of tralomeethrin, tralocyrthrin, deltamethrin, and (1R, alphaS)-*cis*-cypermethrin. *J Agric Food Chem* 30:631–636
- Colmenarejo G (2003) In silico prediction of drug-binding strengths to human serum albumin. *Med Res Rev* 23:275–301

- Colmenarejo G, Alvarez-Pedraglio A, Lavandera J (2001) Cheminformatic models to predict binding affinities to human serum albumin. *J Med Chem* 44:4370–4378
- Cramer RD, Patterson DE, Bunce JD (1988) Comparative molecular field analysis (CoMFA). 1. Effect of shape on binding of steroids to carrier proteins. *J Am Chem Soc* 110:5959–5967
- Crane AL, Browner RW, Knaak JB, Bonner MR, Fenske RA, Farahat FM, Anger WK, Lein PJ, Olson JR (2011) Inhibition of acetylcholinesterase (AChE) and butyrylcholinesterase (BChE) in human blood following in vitro and in vivo exposure to chlorpyrifos. Abstract No. 1243, 49th Annual Meeting and ToxExpo, Salt Lake City, Utah, March 7–11.
- Crawford MJ, Hutson DH (1977) The metabolism of the pyrethroid insecticide (\pm)- α -cyano-3-phenoxybenzyl 2, 2, 3, 3-tetramethylcyclopropanecarboxylate, WL 41706, in the rat. *Pestic Sci* 8:579–599
- Crawford MJ, Croucher A, Hutson DH (1981a) Metabolism of *cis*- and *trans*-cypermethrin in rats. Balance and tissue retention study. *J Agric Food Chem* 29:130–135
- Crawford MJ, Croucher A, Hutson DH (1981b) The metabolism of the pyrethroid insecticide cypermethrin in rats: excreted metabolites. *Pestic Sci* 12:399–411
- Crow JA, Borazjani A, Potter PM, Ross MK (2007) Hydrolysis of pyrethroids by human and rat tissues: examination of intestinal, liver and serum carboxylesterases. *Toxicol Appl Pharmacol* 221:1–12
- Culliford SJ, Borg JJ, O'Brien MJ, Kozlowski RZ (2004) Differential effects of pyrethroids on volume-sensitive anion and organic osmolyte pathways. *Clin Exp Pharmacol Physiol* 31:134–144
- Danker T, Mazzanti M, Tonini R, Rakowska A, Oberleithner H (1997) Using the atomic force microscopy to investigate patch-clamped nuclear membrane. *Cell Biol Int* 21:747–757
- Davies B, Morris T (1993) Physiological parameters in laboratory animals and humans. *Pharm Res (NY)* 10:1093–1095
- Delie F, Rubas W (1997) A human colonic cell line sharing similarities with enterocytes as a model to examine oral absorption: advantages and limitations of the Caco-2 model. *Crit Rev Ther Drug Carrier Syst* 14:221–286
- L'Hoste J (ed) (1982) Deltamethrin monograph. Roussel-Uclaf, Paris
- Diel F, Detscher M, Schock B, Ennis M (1998) In vitro effects of the pyrethroid S-bioallethrin on lymphocytes and basophils from atopic and nonatopic subjects. *Allergy* 53:1052–1059
- Eadsforth CV, Baldwin MK (1983) Human dose-excretion studies with pyrethroid insecticide, cypermethrin. *Xenobiotica* 13:67–72
- Eadsforth CV, Bragt PC, Sittert NJ (1988) Human dose-excretion studies with pyrethroid insecticides: cypermethrin and alpha cypermethrin: relevance for biological monitoring. *Xenobiotica* 18:603–614
- EC-HCPDG (2002) European Commission, Health & Consumer Protection Directorate-General, Directorate E1: Plant Health. Beta-Cyfluthrin, Review Report # 6841/VI/97-final, 12-2-2002.
- Eells JT, Bandettini PA, Holman PA, Propp JM (1992) Pyrethroid insecticide-induced alterations in mammalian synaptic membrane-potential. *J Pharmacol Exp Ther* 262:1173–1181
- Eldefrawi ME, Sherby SM, Abalis IM, Eldefrawi AT (1985) Interactions of pyrethroid and cyclodiene insecticides with nicotinic acetylcholine and GABA receptors. *Neurotoxicology* 6:47–62
- Elflein L, Berger-Preiss E, Preiss A, Elend M, Levsen K, Wunsch G (2003) Human biomonitoring of pyrethroid insecticides used indoors: determination of the metabolites E-*cis/trans*-chrysanthemum dicarboxylic acid in human urine by gas chromatography-mass spectrometry with negative chemical ionizations. *J Chromatogr B* 795:195–207
- Elliott M (1989) The pyrethroids: early discovery, recent advances and the future. *Pestic Sci* 27:337–351
- Elliott M, Janes NF (1978) Synthetic pyrethroids: a new class of insecticide. *Chem Soc Rev* 7:473–505
- Elliott M, Farnham AW, Janes NF, Needham PH, Pearson BC (1967) 5-Benzyl-3-furylmethyl chrysanthemate a new potent insecticide. *Nature (London)* 213:493–494
- Elliott M, Janes NF, Kimmel EC, Casida JE (1972) Metabolic fate of pyrethrin I, pyrethrin II, and allethrin administered orally to rats. *J Agric Food Chem* 20:300–313

- Elliott M, Farnham AW, Janes NF, Needhan DH, Pulman DA (1974) Synthetic insecticides with a new order of activity. *Nature (London)* 248:710–711
- Elliott M, Janes NF, Pulman DA, Gaughan LC, Unai T, Casida JE (1976) Radiosynthesis and metabolism in rats of the 1R-isomers of the insecticide permethrin. *J Agric Food Chem* 24:270–276
- Elliott M, Janes NF, Potter C (1978) The future of pyrethroids in insect control. *Ann Rev Entomol* 23:443–469
- Ellison CA, Knaak JB, McDougall R, Lein PJ, Farahat FM, Anger WK, Olson JR (2011) Construction and validation of a human PBPK/PD model for dermal chlorpyrifos exposure utilizing human biomarker data. Abstract No. 2106, 50th Annual Meeting and ToxExpos, Washington, DC, March 6–10.
- Enan E, Matsumura F (1993) Activation of phosphoinositide protein-kinase-c pathway in rat-brain tissue by pyrethroids. *Biochem Pharmacol* 45:703–710
- Enslein K (2010) ADMET predictor. Simulations-Plus, Lancaster, CA
- Enslein K, Gombar VK, Shapiro D, Blake BW (1998) Prediction of rat oral LD₅₀ values of chemicals by QSAR equations. TOPKAT Health Designs, Rochester, NY
- Enslein K, Knaak JB, Van Nostrand K, Susa R, Koestler D (2007) CYP3A4 hydroxylation kinetics: QSAR models with application to PBPK modeling. *J Comput Aided Mol Des*. An internal document-Enslein Research, Inc., Rochester, NY. (submitted).
- Farahat FM, Ellison CA, Bonner MR, McGarrigle BP, Crane AL, Fenske RA, Lasarev MR, Rohlman DS, Anger WK, Lein PJ, Olson JR (2011) Biomarkers of chlorpyrifos exposure and effect in Egyptian cotton field workers. *Environ Health Perspect* 119:801–816
- Farahmand S, Maibach HI (2009) Estimating skin permeability from physicochemical characteristics of drugs: a comparison between conventional models and an in vivo-based approach. *Int J Pharm* 375:41–47
- Faraoni M, Messina A, Polcaro CM, Aturki Z, Sinibaldi M (2004) Chiral separation of pesticides by coupled-column liquid chromatography application to the stereoselective degradation of fenvalerate in soil. *J Liq Chromatogr Rel Technol* 27:995–1012
- Feldmann RJ, Maibach HI (1974) Percutaneous penetration of some pesticides and herbicides in man. *Toxicol Appl Pharmacol* 28:126–132
- Fisher JB, Debray PH, Robinson J (1983) In: *Plant Protection for Human Welfare*, Proc 10th Internat Congr Plant Prot Vol 1, BCPC, Croydon, UK, 1983, pp 452–459. FMC, U.S. Patent 4,262,921 (1981)
- Fleischer R (1877) Untersuchgen uber das resporptions-vermogen der menschlichen haut. Erlangen 1877. Habilitationsschrift p 81.
- Flynn GL (1990) Physicochemical determinants of skin absorption. In: Gerrity TR, Henry CJ (eds) *Principles of route-to-route extrapolation for risk assessment*. Elsevier, New York, pp 93–127
- Foxenberg RJ, Knaak JB, McGarrigle BP, Kostyniak PJ, Olson JR (2007) Human hepatic cytochrome P450-specific metabolism of parathion and chlorpyrifos. *Drug Metab Dispos* 35:189–193
- Foxenberg RJ, Ellison CA, Knaak JB, Ma C, Olson JR (2011) Cytochrome P450-specific human PBPK/PD models for the organophosphorus pesticides: chlorpyrifos and parathion. *Toxicology* 285:57–66
- Freeman C (1982) Acute oral toxicity study in rats: FMC 54800. Study No. A83-859, FMC Corporation, Philadelphia PA.
- Freeman C (1987) Acute oral toxicity study-FMC 45806 technical: Study No. A87-2282, FMC Corporation, Philadelphia, PA.
- Freeman C (1989) Acute oral toxicity of FMC 56701 technical in rats. Study No. A89-2914, FMC Corporation, Philadelphia, PA.
- Fujikawa M, Nakao K, Shimizu R, Akamatsu M (2007) QSAR study on permeability of hydrophobic compounds with artificial membranes. *Bioorg Med Chem* 15:3756–3767
- Fujimoto K, Itaya N, Okuno Y, Kadota T, Yamaguchi T (1973) A new insecticidal pyrethroid ester. *Agric Biol Chem* 37:2681–2682

- Furnax R, Audegond L (1985a) Bioallethrin (synthetic) acute oral toxicity in rat. Study No. 84324/5635/5637, Roussel-Uclaf, Paris.
- Furnax R, Audegond L (1985b) RU 16121 acute oral toxicity in rat. Study No. 84327/5640/5641, Roussel-Uclaf, Paris.
- Gabriel D (1992) Acute oral toxicity study in rats. Study No. 92-7529A, Pyrethrin Joint Venture Chemical Specialties Manufacturing Association, Washington, DC.
- Gao R, Zhu L, Chen Z (1998) Separation of pyrethroid enantiomers of fenpropathrin and fluvalinate by chiral high performance liquid chromatography. *Nongyao (Pesticides)* 37(9):22–24
- Gargas ML, Burgess RJ, Voisard DE, Cason GH, Andersen ME (1989) Partition coefficients of low-molecular-weight volatile chemicals in various liquids and tissues. *Toxicol Appl Pharmacol* 98:87–99
- Gassner B, Wuthrich A, Scholtysik G, Solioz M (1997) The pyrethroids permethrin and cyhalothrin are potent inhibitors of the mitochondrial complex I. *J Pharmacol Exp Ther* 281:855–860
- GastroPlus Users Manual (2008) version 6.0, Simulations-Plus, Inc., Lancaster, CA
- Gaughan LC, Unai T, Casida JE (1977) Permethrin metabolism in rats. *J Agric Food Chem* 25:9–17
- Geinoz S, Guy RH, Testa B, Carrupt PA (2004) Quantitative structure-permeation relationships (QSPeRs) to predict skin permeation: a critical evaluation. *Pharm Res* 21:83–92
- Ghiasuddin SM, Soderlund DM (1985) Pyrethroid insecticides potent, stereospecific enhancers of mouse brain sodium channel activation. *Pestic Biochem Physiol* 24:200–206
- Girelli AM, Messina A, Sinibaldi M (2002) A study on the separation of synthetic pyrethroid stereoisomers by HPLC. *Ann Chim* 92:417–424
- Glomot R (1979) RU 25474, active material: acute oral toxicity study in the rat. American Hoechst Corporation Study No. RU-4BE-79818-19/A.
- Godin SJ, Scollon EJ, Hughes MF, Potter PM, DeVito MJ, Ross MK (2006) Species differences in the in vitro metabolism of deltamethrin and esfenvalerate: differential oxidative and hydrolytic metabolism by humans and rats. *Drug Metab Dispos* 34:1764–1771
- Godin SJ, Crow JA, Scollon EJ, Hughes MF, DeVito MJ, Ross MK (2007) Identification of rat and human cytochrome P450 isoforms and a rat serum esterase that metabolize the pyrethroid insecticides Deltamethrin and Esfenvalerate. *Drug Metab Dispos* 35:1664–1671
- Godin SJ, DeVito MJ, Hughes MF, Ross DG, Scollon EJ, Starr JM, Setzer RW, Conolly RB, Tornero-Velez R (2010) Physiologically based pharmacokinetic modeling of deltamethrin: development of a rat and human diffusion-limited model. *Toxicol Sci* 115:330–343
- Goksu EI, Vanegas JM, Blanchette CD, Lin W-C, Longo ML (2009) AFM for structure and dynamics of biomembranes. *Biochem Biophys Acta* 1788:254–266
- Goodman LS (2001) Goodman & Gilman's the pharmacological basis of therapeutics, 10th edn. McGraw-Hill, New York
- Gray AJ, Soderlund DM (1985) Mammalian toxicology of pyrethroids. In: Hutson DH, Roberts TR (eds) *Insecticides*. Wiley, New York, pp 193–248
- Grosman N, Diel F (2005) Influence of pyrethroids and piperonyl butoxide on the Ca^{+2} -ATPase activity. *Int J Immunopharmacol* 5:263–270
- Guengerich FP, Martin MV (1998) Purification of cytochromes P450. Rat and human hepatic forms. *Methods Mol Biol* 107:35–53
- Guy RH, Hadgraft J, Bucks DA (1987) Transdermal drug delivery and cutaneous metabolism. *Xenobiotica* 17:325–343
- Hagiwara N, Irisawa H, Kameyama M (1988) Contribution of two types of calcium currents to the pacemaker potentials of rabbit sino-atrial node cells. *J Physiol* 395:233–253
- Hallifax D, Houston JB (2006) Binding of drugs to hepatic microsomes: comment and assessment of current prediction methodology with recommendation for improvement. *Drug Metab Dispos* 34:724–726
- Hamman I, Fuchs R (1981) Baythroid[®], a new insecticide. *Pflanzenschutz-Nachrichten Bayer* 34:121–151

- Hansch C, Hoekman D, Leo A, Zhang L, Li P (1995) The expanding role of quantitative structure-activity relationships (QSAR) in toxicology. *Toxicol Lett* 79:45–43
- Hardt J, Angerer J (2003) Biological monitoring of workers after the application of insecticidal pyrethroids. *Int Arch Occup Environ Health* 76:492–498
- Harrison SM, Barry BW, Dugard PH (1984) Effects of freezing on human-skin permeability. *J Pharm Pharmacol* 36:261–262
- Heimann KG (1987) FCR 1272 (c.n. cyfluthrin): Study for acute oral toxicity to rats (formulation acetone and peanut oil). Bayer Corporation Agricultural Division Report No. 106805.
- Hemming H, Flodstrom S, Warngard L (1993) Enhancement of altered hepatic foci in rat-liver and inhibition of intercellular communication in-vitro by the pyrethroid insecticides fenvalerate, flucythrinate and cypermethrin. *Carcinogenesis* 14:2531–2535
- Henrick CA (1977) Zoecon Corp. (patent for fluvalinate development).
- Henrick CA, Garcia BA, Staal GB, Cerf DC, Anderson RJ, Gill K, Chinn HR, Labovitz JN, Leippe MM, Woo SL, Carney RL, Gordon DC, Kohn GK (1980) 2-Anilino-3-methylbutyrate and 2-(isoindolin-2-yl)-3-methylbutyrate, two novel groups of synthetic pyrethroid esters not containing a cyclopropane ring. *Pestic Sci* 11(2):224–241
- Hildebrand ME, McRory JE, Snutch TP, Stea A (2004) Mammalian voltage-gated calcium channels are potently blocked by the pyrethroid insecticide allethrin. *J Pharmacol Exp Ther* 308:805–813
- Hood SR, Shah G, Jones P (1998) Ch 24, Expression of cytochromes P450 in a Baculovirus system. In: Phillips IR, Shepard EA (eds) *Methods in molecular biology: CYP protocols*. Humana, Totowa, NJ, pp 203–218
- Horber JKH, Mosbacher J, Haberle W, Ruppertsberg JP, Sakmann B (1995) A look at membrane patches with a scanning force microscope. *Biophys J* 68:1687–1693
- Hosokawa M, Maki T, Satoh T (1987) Multiplicity and regulation of hepatic microsomal carboxylesterases in rats. *Mol Pharmacol* 31:579–584
- Hosokawa M, Maki T, Satoh T (1990) Characterization of molecular species of liver microsomal carboxylesterases of several animal species and humans. *Arch Biophys* 277:219–227
- Hotchkiss SAM, Miller JM, Caldwell J (1992) Percutaneous absorption of benzyl acetate through rat skin in vitro. 2. Effect of vehicle and occlusion. *Food Chem Toxicol* 30:145–153
- Houston JB (1994) Utility of in vitro drug metabolism data in predicting in vivo metabolic clearance. *Biochem Pharmacol* 47:1469–1479
- Huang T, Kuang C, Zhou J, Gou D (1991) Chiral separation of water soluble. BETA-Lactam Enantiomers on BETA-Cyclodextrin bonded stationary phase. *Fenxi Huaxue* 16:687–689
- Huckle KR, Chipman JK, Hutson DH, Milibum P (1981a) Metabolism of 3-phenoxybenzoic acid and the enterohepato-renal disposition of its metabolites in the rat. *Drug Metab Dispos* 9:360–368
- Huckle KR, Hutson DH, Millburn P (1981b) Species differences in the metabolism of 3-phenoxybenzoic acid. *Drug Metab Dispos* 9:352–359
- Huckle KR, Hutson DH, Millburn P (1984) Metabolism of 3-phenoxybenzoic acid in isolated rat hepatocytes and renal tubule fragments. *Drug Metab Dispos* 12:264–265
- Huff RK (1978) Halogenated esters of cyclopropane acids, their preparation, composition and use as pesticides. *Eur Pat* 0010879 ICI.
- Hutson DH, Logan CJ (1986) The metabolic fate in rats of the pyrethroid insecticide WL85871, a mixture of two isomers of cypermethrin. *Pestic Sci* 17:548–558
- IARC (1991) Occupational exposures in insecticide application and some pesticides. IARC, Lyon
- Inoue S, Howgate EM, Rowland-Yeo K, Shimada T, Yamazaki H, Tucker GT, Rostami-Hodjegan A (2006) Prediction of in vivo drug clearance from in vitro data. II: Potential inter-ethnic differences. *Xenobiotica* 36:499–513
- Irvine JD, Takahashi L, Lockhart K, Cheong J, Tolan JW, Selick HE, Grove JR (1999) MDCK (Madin-Darby Canine Kidney) cells: a tool for membrane permeability screening. *J Pharm Sci* 88:28–33
- Iwatsubo T, Hirota N, Ooie T, Suzuki H, Chiba K, Ishizaki T, Green CE, Tyson CA, Sugiyama Y (1997) Prediction of in vivo drug metabolism in the human liver from in vitro metabolism data. *Pharmacol Ther* 73:147–171

- Izumi T, Kaneko H, Matsuo M, Miyamoto J (1984) Comparative metabolism of the six stereoisomers of phenothrin in rats and mice. *J Pestic Sci* 9:259–267
- Jarabek A (2002) External Review Draft NCEA-1-0503, Office of Research and Development. US Environmental Protection Agency, Washington, DC
- Jepson GW, Hoover DK, Black RK, McCafferty JD, Mahle DA, Gearhart JM (1992) Partition coefficient determination for nonvolatile and intermediate volatility chemicals in biological tissues. *Toxicology* 12:262
- Jepson GW, Hoover DK, Black RK, McCafferty JD, Mahle DA, Gearhart JM (1994) A partition coefficient determination methods for non-volatile chemicals in biological issues. *Fundam Appl Toxicol* 22:519–524
- Johnson PL (2007) Synthesis of (S)-cyano (3-phenoxyphenyl) methyl (1R, 3R)-3-[(1Z)-2-chloro-3, 3, 3-trifluoro-1-propenyl]-2, 2-dimethylcyclopropanecarboxylate-1-¹⁴C. *J Label Compd Radiopharm* 50:47–53
- Jutsum AR, Gordon RF, Ruscoe CNE (1986) In: Proc. 1986 Brit Crop Prot Conf Pests and Diseases, BCPC, Croydon, pp 97–106.
- Kakko I, Toimela T, Tahti H (2003) The synaptosomal membrane bound ATPase as a target for the neurotoxic effects of pyrethroids, permethrin and cypermethrin. *Chemosphere* 51:475–480
- Kaneko H (2010) Chapter 76, Pyrethroid chemistry and metabolism. In: Krieger R (ed) Hayes' handbook of pesticide toxicology, 3rd edn. Academic, San Diego, CA
- Kaneko H, Miyamoto J (2001) Pyrethroid chemistry and metabolism, chapter 58. In: Krieger R (ed) Hayes handbook of pesticide toxicology, 2nd edn. Academic, San Diego, CA
- Kaneko H, Ohkawa H, Miyamoto J (1981a) Adsorption and metabolism of dermally applied phenothrin in rats. *Nippon Noyaku Gakkaishi* 6:169–182
- Kaneko H, Ohkawa H, Miyamoto J (1981b) Comparative metabolism of fenvalerate and the [2S, α S]-isomer in rats and mice. *Nippon Noyaku Gakkaishi* 6:317–326
- Kaneko H, Ohkawa H, Miyamoto J (1981c) Metabolism of tetramethrin isomers in rats. *Nippon Noyaku Gakkaishi* 6:425–435
- Kaneko H, Matsuo M, Miyamoto J (1984) Comparative metabolism of stereoisomers of cyphenothrin and phenothrin isomers in rats. *Nippon Noyaku Gakkaishi* 9:237–247
- Kaneko H, Shiba K, Yoshitake A, Miyamoto J (1987) Metabolism of fenpropathrin (S-3206) in rats. *Nippon Noyaku Gakkaishi* 12:385–395
- Kansy M, Senner F, Gubernator K (1998) Physicochemical high throughput screening: parallel artificial membrane permeation assay in the description of passive absorption processes. *J Med Chem* 41(7):1007–1010
- Kato T, Ueda K, Fujimoto K (1965) New insecticidally active chrysanthemate. *Agric Biol Chem* 28:914–915
- Katsuda Y (1975) Sumitomo Chemical Co, LTD. (patent for fluvalinate development).
- Katsuda Y (1999) Development of and future prospects for pyrethroid chemistry. *Pestic Sci* 55:775–782
- Khambay BPS (2002) Pyrethroid insecticides. Royal Society of Chemistry (UK). *Pestic Outlook* 49–54.
- Killeen CJ (1975) Acute oral toxicity study in rats with FMC 33297. FMC Corp, Philadelphia, PA
- Klopman G, Rosenkranz HS (1995) Toxicity estimation by chemical substructure analysis: the TOX II program. *Toxicol Lett* 79:145–155
- Knaak JB, Iwata Y, Maddy KT (1989) The worker hazard posed by reentry into pesticide-treated foliage: development of safe reentry times, with emphasis on chlordiophos and carbosulfan, Ch 24. In: Paustenbach D (ed) *The risk assessment of environmental hazards: a textbook of case studies*. Wiley, New York, pp 797–842
- Knaak JB, Wagner B, Boutchyard H Jr, Smith LW, Jones T, Wang RH (1993) Computerization of toxicological data by government agencies, chemical, and information industries, Ch 19. In: Jolley RL, Wang RGM (eds) *Effective and safe waste management; interfacing sciences and engineering with monitoring and risk analysis*. Lewis, Boca Raton, FL, pp 227–264

- Knaak JB, Leung H-W, Stott WT, Busch J, Bilsky J (1997) Toxicology of mono-, di-, and triethanolamine. *Rev Environ Contam Toxicol* 149:1–86
- Knaak JB, Dary C, Patterson GT, Blancato J (2002) The worker hazard posed by reentry into pesticide-treated foliage: reassessment of reentry levels/intervals using foliar residue transfer-percutaneous absorption PBPK/PD models, with emphasis on isofenphos and parathion. In: Paustenbach D (ed) *Human and ecological risk assessment: theory and practice*. Wiley, New York, pp 673–731
- Knaak JB, Dary CC, Power F, Thompson CB, Blancato JN (2004) Physicochemical and biological data for the development of predictive organophosphorus pesticides QSARs and PBPK/PD models for human risk assessment. *Crit Rev Toxicol* 34:143–207
- Knaak JB, Dary CC, Okino MS, Power FW, Zhang X, Thompson CB, Tornero-Velez R, Blancato JN (2008) Parameters for carbamate pesticide QSAR and PBPK/PD models for human risk assessment. *Rev Environ Contam Toxicol* 193:53–212
- Kuo JK (1985) *Phospholipids and cellular regulation*. CRC, Boca Raton, FL
- Kurihara N, Miyamoto J, Paulson GD, Zeeh B, Skidmore MW, Hollingsworth RM, Kuiper HA (1997a) Chirality in synthetic agrochemicals: bioactivity and safety considerations. *Pure Appl Chem* 69:1335–1348
- Kurihara N, Miyamoto J, Paulson GD, Zeeh B, Skidmore MW, Hollingsworth RM, Kipper HA (1997b) Chirality in synthetic agrochemicals: bioactivity and safety consideration. *Pure Appl Chem* 69:2007–2026
- Kutter JP, Class TJ (1992) Diastereoselective and enantioselective chromatography of the pyrethroid insecticides allethrin and cypermethrin. *Chromatographia* 33:103–112
- LaForge FB, Haller HL (1936) Constituents of pyrethrum flowers. VI. The structure of pyrethrolone. *J Am Chem Soc* 58:1777–1780
- LaForge FB, Soloway SB (1947) Structure of dihydrocinerolone. *J Am Chem Soc* 69:186
- Lau YY, Wu C-Y, Okochi H, Benet LZ (2003) Ex situ inhibition of hepatic uptake and efflux significantly changes metabolism: hepatic enzyme-transporter interplay. *J Pharmacol Exp Ther* 308:1040–1045
- Lawrence LJ, Gee KW, Yamamura HI (1985) Interactions of pyrethroid insecticides with chloride ionophore-associated binding sites. *Neurotoxicology* 6:87–98
- Lee W, Kim B-H (1998) Liquid chromatographic resolution of pyrethroic acids and their esters on chiral stationary phases. *J High Resol Chromatogr* 21:189–192
- Leng G, Leng A, Kuhn K-H, Lewalter J, Pauluhn J (1997) Human dose-excretion studies with the pyrethroid insecticide cyfluthrin: urinary metabolite profile following inhalation. *Xenobiotica* 27:1273–1293
- Li Z-Y, Zhang Z-C, Zhou Q-L, Wang Q-M, Gao R-Y, Wang Q-S (2003) Stereo and enantioselective determination of pesticides in soil by using achiral and chiral liquid chromatography in combination with matrix solid-phase dispersion. *J AOAC Int* 86(3):521–528
- Li Z-Y, Zhang Z-C, Zhang L, Leng L (2006) Chiral separation of pyrethroids pesticides and fenvaleric acid. *Fenxi Shiyanshi (Chin J Anal Lab)* 25(11):11–14
- Li Z, Zhang Z, Zhang L, Leng L (2009) Isomer- and enantioselective degradation and chiral stability of fenpropathrin and fenvalerate in soils. *Chemosphere* 76:509–516
- Liang R, Fei Y-J, Prasad PD, Ramamoorthy S, Han H, Yang-Feng TL, Hediger MA, Ganapathy V, Leibach FH (1995) Human intestinal H⁺/peptide cotransporter: cloning, functional expression, and chromosomal localization. *J Biol Chem* 270:6456–6463
- Lin JH, Yamazaki M (2003) Role of P-glycoprotein in pharmacokinetics: clinical implications. *Clin Pharmacokinet* 42:59–98
- Lipscomb JC, Fisher JW, Confer PD, Byczkowski JZ (1998) In vitro to in vivo extrapolation for trichloroethylene metabolism in humans. *Toxicol Appl Pharmacol* 152:376–387
- Liu HX, Yao XJ, Zhang RS, Liu MC, Hu ZD, Fan BT (2005a) Prediction of the tissue/blood partition coefficients of organic compounds based on the molecular structure using least-squares support vector machines. *J Comput Aided Mol Des* 19:499–508

- Liu W, Gan J, Schlenk D, Jury WA (2005b) Enantioselectivity in environmental safety of current chiral insecticides. *Proc Natl Acad Sci USA* 102(3):701–706
- Liu W, Gan JJ, Qin S (2005c) Separation and aquatic toxicity of enantiomers of synthetic pyrethroid insecticides. *Chirality* 17:S127–S133
- Liu W, Gan J, Lee S, Werner I (2005d) Isomer selectivity in aquatic toxicity and biodegradation of bifenthrin and permethrin. *Environ Toxicol Chem* 24(8):1861–1866
- Lu AYH, West SB (1980) Multiplicity of mammalian microsomal cytochrome P450. *Pharmacol Rev* 31:277–291
- Maibach HI, Feldmann RJ, Milby TH, Serat WF (1971) Regional variation in percutaneous penetration in man. *Arch Environ Health* 23:208–211
- Mancini F, Fiori J, Bertucci C, Cavrini V, Bragieri M, Zanotti MC, Liverani A, Borzatta V, Andrisano V (2004) Stereoselective determination of allethrin by two-dimensional achiral/chiral liquid chromatography with ultraviolet/circular dichroism detection. *J Chromatogr A* 1046:67–73
- Martel J (1976) Roussel UCLAF (patent, tralomethrin development).
- Matsuo T, Itaya N, Mizutani T, Ohno N, Fujimoto K, Okuno Y, Yoshioka H (1976) 3-phenoxy-a-cyanobenzyl esters, the most potent synthetic pyrethroids. *Agric Biol Chem* 40:247–249
- Mattie DR, Bates GD, Jepson GW, Fisher JW, McDougal JN (1994) Determination of skin: air partition coefficients for volatile chemicals: experimental method and applications. *Toxicol Appl Pharmacol* 22:51–57
- McGregor DB (1999) Permethrin Joint Meeting, FAO Panel of Experts on Pesticide Residues in Food and the Environment, and WHO Core Assessment Group, Rome.
- Meylan WM, Howard PH (1994a) Upgrade of PCGEMS water solubility estimation method (draft). US Environmental Protection Agency, Office of Pollution Prevention and Toxics, Washington, DC
- Meylan WM, Howard PH (1994b) Validation of water solubility estimation methods using log K_{ow} for application in PCGEMS & EPI. Final report, U.S. Environmental Protection Agency, Office of Pollution Prevention and Toxics, Washington, DC.
- Mirfazaelian A, Kim K-B, Anand SS, Kim HJ, Tornero-Velez R, Bruckner JV, Fisher JW (2006) Development of a physiologically based pharmacokinetic model for deltamethrin in the adult male Sprague-Dawley rat. *Toxicol Sci* 93:432–442
- Miyamoto J (1976) Degradation, metabolism and toxicity of synthetic pyrethroids. *Environ Health Perspect* 14:15–28
- Miyamoto J, Nishida T, Ueda K (1971) Metabolic fate of resmethrin, 5-benzyl-3-furylmethyl *dl-trans* chrysanthemate in the rat. *Pestic Biochem Physiol* 1:293–306
- Miyamoto J, Suzuki T, Nakae C (1974) Metabolism of phenothrin (3-phenoxybenzyl *d-trans*-chrysanthemumate) in mammals. *Pestic Biochem Physiol* 4:438–450
- Moss GP, Derden JC, Patel H, Cronin MT (2002) Quantitative structure-permeability relationships (QSPRs) for percutaneous absorption. *Toxicol In Vitro* 16:299–317
- Mugeng J, Soderlund DM (1982) Liquid chromatographic determination and resolution of the enantiomers of the acid moieties of pyrethroid insecticides as their (-)-1-(1-phenyl)ethylamide derivatives. *J Chromatogr A* 248(1):143–149
- Myer JR (1989) Acute oral toxicity study of deltamethrin in rats. Hoechst-Roussel Agri-Vet Company Study No. 327-122.
- Nakamura Y, Sugihara K, Sone T, Isobe M, Ohta S, Kitamura S (2007) The in vitro metabolism of a pyrethroid insecticide, permethrin, and its hydrolysis products in rats. *Toxicology* 235:176–184
- Narahashi T (1971) Mode of action of pyrethroids. *Bull World Health Organ* 44:337–345
- Nardini M, Dijkstra BW (1999) α/β Hydrolase fold enzymes: the family keeps growing. *Curr Opin Struct Biol* 9:732–737
- Naumann K (1998) Research into fluorinated pyrethroid alcohols-an episode in the history of pyrethroid discovery. *Pestic Sci* 52:3–20

- Nicoli S, Santi P (2007) Suitability of excised rabbit ear skin – fresh and frozen – for evaluation Transdermal permeation of estradiol. *Drug Deliv* 14:195–199
- Nigg HN, Knaak JB (2000) Blood cholinesterases as human biomarkers of organophosphorus pesticide exposure. *Rev Environ Contam Toxicol* 163:29–112
- Nikolelis DP, Brennan JD, Brown S, McGibbon G, Krull UJ (1991) Ion permeability through bilayer lipid membranes for biosensor development: control by chemical modification of interfacial regions between phase domains. *Analyst* 116:1221–1226
- Nishizawa Y (1971) Development of new synthetic pyrethroids. *Bull World Health Organ* 44:325–336
- Nong A, Tan Y-M, Krolski ME, Wang J, Lunchick C, Conolly RB, Clewell HJ III (2008) Bayesian calibration of a physiologically-based pharmacokinetic/pharmacodynamic model of carbaryl cholinesterase inhibition. *J Toxicol Environ Health A* 71:1363–1381
- O'Reilly AO, Khanbay BPS, Williamson MS, Field LM, Wallace BS, Davies TGE (2006) Modeling insecticide-binding sites in the voltage-gated sodium channel. *Biochem J* 396:255–263
- Obach RS (1996) The importance of nonspecific binding in in vitro matrices, its impact on enzyme kinetic studies of drug metabolism and implications for in vitro-in vivo correlations. *Drug Metab Dispos* 24:1047–1049
- Obach RS (1997) Nonspecific binding to microsomes: impact on scale-up of in vitro intrinsic clearance to hepatic clearance as assessed through examination of warfarin, imipramine, and propranolol. *Drug Metab Dispos* 25:1359–1369
- Obach RS (1999) The prediction of human clearance of twenty-nine drugs from hepatic microsomal intrinsic clearance data: an examination of the in vitro half-life approach and nonspecific binding to microsomes. *Drug Metab Dispos* 27:1350–1359
- Ohkawa H, Kaneko H, Tsuji H, Miyamoto J (1979) Metabolism of fenvalerate (Sumicidin) in rats. *J Pestic Sci (J Nippon Noyaku Gakkaishi)* 4:143–155
- Ohno N, Fujimoto K, Okuno Y, Mizutani T, Hirano M, Yoshioka H (1974) A new class of pyrethroidal insecticides: α -substituted phenylacetic acid esters. *Agric Biol Chem* 38:881–883
- Oi N (2005) Development of practical chiral stationary phases for chromatography and their applications. *Chromatography* 26(1):1–5
- Oi N, Horiba M, Kitahara H (1981) Gas chromatographic separation of optical isomers of chrysanthemic acid on an optically active stationary phase. *Agric Biol Chem* 45(6):1509–1510
- Oi N, Kitahara H, Kira R (1990) Enantiomer separation of pyrethroid insecticides by high-performance liquid chromatography with chiral stationary phases. *J Chromatogr A* 515:441–450
- Oi N, Kitahara H, Aoki F, Kisu N (1995) Direct separation of carboxylic acid enantiomers by high-performance liquid chromatography with amide and urea derivatives bonded to silica gel as chiral stationary phases. *J Chromatogr A* 689(2):195–201
- Oi N, Kitahara H, Matsushita Y, Kisu N (1996) Enantiomer separation by gas and high-performance liquid chromatography with tripeptide derivatives as chiral stationary phases. *J Chromatogr A* 722(1–2):229–232
- Omura T, Sato (1964) The carbon monoxide-binding pigment of liver microsomes. I. Evidence for its hemoprotein nature. *J Biol Chem* 239:2370–2378
- Paine MF, Khalighi M, Fisher JM, Shen DD, Kunze KOL, Cl M, Perkins JD, Thummel KE (1997) Characterization of interintestinal and intrainestinal variations in human CYP3A-dependent metabolism. *J Pharmacol Exp Ther* 283:1552–1562
- Papadopoulou-Mourkidou E (1985) Direct analysis of fenvalerate isomers by liquid chromatography. Application to formulation and residue analysis of fenvalerate. *Chromatographia* 20(6):376–378
- Payne MP, Kenny LC (2002) Comparison of models for the estimation of biological partition coefficients. *J Toxicol Environ Health A* 65:897–931
- PMRA (Canada Pest Management Regulatory Agency) (2005) Report PRDD#2005-02 (imiprothrin), www.pmr-arla.gc.ca/english/pdf/prdd/prdd2005-02-e.pdf, Aug 8 2005.

- Plummer EL, Cardis AB, Martinez AJ, Van Saun WA, Palmere RM, Pincus DS, Stewart RR (1983) Pyrethroid insecticides derived from substituted biphenyl-3-methods. *Pestic Sci* 14:560–570
- Porcelli C, Roncaglioni A, Chana A, Boriani E, Benfenati A (2007) A protocol for quantitative structure, activity relationship (QSAR) for regulatory purposes: the example of DEMETRA. In *Environmental fate and ecological effects of pesticides*, symposium pesticide chemistry, 13th, Placenza, Italy, Sept. 3–6, 2007, pp 669–674.
- Potts RO, Guy RH (1992) Predicting skin permeability. *Pharm Res* 9:663–669
- Potts RO, Guy RH (1995) A predictive algorithm for skin permeability: the effects of molecular size and hydrogen bond activity. *Pharm Res* 12:1628–1633
- Poulin P, Theil F-P (2000) A priori prediction of tissue: plasma partition coefficients of drugs to facilitate the use of physiologically-based pharmacokinetic models in drug discovery. *J Pharm Sci* 89:16–35
- Poulin P, Theil F-P (2002a) Prediction of pharmacokinetics prior to in vivo studies. I. Mechanism-based prediction of volume of distribution. *J Pharm Sci* 91:129–156
- Poulin P, Theil F-P (2002b) Prediction of pharmacokinetics prior to in vivo studies. II. Generic physiologically-based pharmacokinetic models of drug disposition. *J Pharm Sci* 91:1358–1370
- Prout M, Howard E (1985b) PP993: excretion and tissue distribution of a single oral dose (10 mg/kg) in the rat. Syngenta unpublished report, no. CTL/P/1256, UK.
- Prout M, Howard E, Soames A (1985a) PP993: Absorption, excretion and tissue distribution of a single oral dose (1 mg/kg) in the rat. Syngenta unpublished report, no. CTL/P/1064, UK.
- Prout M, Gibson N, Howard E (1986) PP993: Biotransformation in the rat. Syngenta unpublished report, no. CTL/P/1295, UK.
- Casida JE (ed) (1973) *Pyrethrum: the natural insecticide*. Academic, New York
- Quistad GB, Staiger LE, Jamieson GC, Schooley DA (1983) Fluvalinate metabolism by rats. *J Agric Food Chem* 31:589–596
- Rand G (1983) Acute oral toxicity-cypermethrin technical. FMC Corporation Study No. A82-727.
- Rao RN, Shankaraiah B, Sunder MS (2004) Separation and determination of diastereomers of γ -Cyhalothrin by normal phase-liquid chromatography using a CN column. *Anal Sci* 20: 1745–1748
- Ray DE, Fry JR (2006) A reassessment of the neurotoxicity of pyrethroids insecticides. *Pharmacol Ther* 111:174–193
- Ray DE, Sutharsan S, Forshaw PJ (1997) Actions of pyrethroid insecticides on voltage-gated chloride channels in neuroblastoma cells. *Neurotoxicology* 18:755–760
- Reifenrath WG, Kamppainen BW (1991) Skin storage conditions. In: Bronaugh R, Maibach H (eds) *In vitro percutaneous absorption: principles, fundamentals and applications*. CRC, Boca Raton, pp 115–125
- Reifenrath WG, Ross JH, Driver JH (2011) Experimental methods for determining permethrin dermal absorption. Submitted for review and publication. *J Toxicol Environ Health A* 74: 325–335.
- Rekling JC, Theophilidis GN (1995) Effects of the pyrethroid insecticide, deltamethrin, on respiratory modulated hypoglossal moto-neurons in a brain stem slice from newborn mice. *Neurosci Lett* 198:189–192
- Riddles PW, Richards LJ, Bowles MR, Pond SM (1991) Cloning and analysis of a cDNA encoding a human liver carboxylesterase. *Gene (Amst)* 108:389–392
- Riviere JE, Monteiro-Riviere NA (1991) The isolated perfused porcine skin flap as an in vitro model for percutaneous absorption and cutaneous toxicology. *Crit Rev Toxicol* 21:329–344
- Riviere JE, Bowman KF, Monteiro-Riviere NA, Dix LP, Carver MP (1986) The isolated perfused porcine skin flap (IPPSF). I. A novel in vitro model for percutaneous absorption and cutaneous toxicology studies. *Fund Appl Toxicol* 7:444–453
- Robey RW, Lin B, Qui J, Chan LL, Bates SE (2010) Rapid detection of ABC transporter interaction: potential utility in pharmacology. *J Pharmacol Toxicol Methods* 63:217–222

- Rodgers T, Rowland M (2006) Physiologically based pharmacokinetic modelling 2: predicting the tissue distribution of acids, very weak bases, neutral and zwitterions. *J Pharm Sci* 95: 1238–1257
- Rodgers T, Rowland M (2007) Mechanistic approaches to volume of distribution predictions: understanding the processes. *Pharm Res* 24:918–933
- Rodgers T, Leahy D, Rowland M (2005) Physiologically based pharmacokinetic modeling 1: predicting the tissue distribution of moderate-to-strong bases. *J Pharm Sci* 94:1259–1276
- Rodgers T, Leahy D, Rowland M (2007) (ERRATA) Physiologically based pharmacokinetic modeling 1: predicting the tissue distribution of moderate to strong bases. *J Pharm Sci* 96:1259–1276, *J Pharm Sci* 96: 3151–3152
- Rodrigues AD (1999) Integrated cytochrome P450 reaction phenotyping: attempting to bridge the gap between cDNA-expressed cytochrome P450 and native human liver microsomes. *Biochem Pharmacol* 57:465–480
- Ross MK, Borazjani A, Edwards CC, Potter PM (2006) Hydrolytic metabolism of pyrethroids by human and other mammalian carboxylesterases. *Biochem Pharmacol* 71:657–669
- Ruzo LO, Casida JE (1977) Metabolism and toxicology of pyrethroids with dihalovinyl substituents. *Environ Health Perspect* 21:285–292
- Ruzo LO, Casida JE (1981) Pyrethroid photochemistry: (S)- α -cyano-3-phenoxybenzyl *cis*-(1R,3R,1'R or S)-3-(1',2'-dibromo-2',2'-dihaloethyl)-2,2-dimethylcyclopropanecarboxylates. *J Agric Food Chem* 29:702–706
- Ruzo LO, Unai T, Casida JE (1978) Decamethrin metabolism in rats. *J Agric Food Chem* 26:918–925
- Ruzo LO, Engel JL, Casida JE (1979) Decamethrin metabolites from oxidative, hydrolytic, and conjugative reactions in mice. *J Agric Food Chem* 27:725–731
- Saiaikhov RD, Stefan LR, Klopman G (2000) Multiple computer-automated structure evaluation model of the plasma protein binding affinity of diverse drugs. *Perspect Drug Discov Des* 19:133–155
- Sanchez FG, Diaz AN, Pareja AG (1996) Enantiomeric resolution of pyrethroids by high-performance liquid chromatography with diode-laser polarimetric detection. *J Chromatogr A* 754:97–102
- Satoh T, Hosokawa M (1998) The mammalian carboxylesterases: from molecules to functions. *Annu Rev Pharmacol Toxicol* 38:257–288
- Satoh T, Hosokawa M (2010) Carboxylesterases: structure, function and polymorphism in mammals. *J Pestic Sci* 35:218–228
- Scheuplein RJ, Blank IH (1971) Permeability of the skin. *Physiol Rev* 51:702–747
- Schwenkenbecker A (1904) Das absorptions verniogen der haut. *Arch Anat Physiol* 121–165.
- Schwer H, Langmann T, Daig R, Becker A, Aslanidis C, Schmitz G (1997) Molecular cloning and characterization of a novel putative carboxylesterase, present in human intestine and liver. *Biochem Biophys Res Commun* 233:117–120
- Scollon EJ, Starr JM, Godin SJ, DeVitro MJ, Hughes MF (2009) In vitro metabolism of pyrethroid pesticides by rat and human hepatic microsomes and cytochrome P450 isoforms. *DMD* 37:221–228
- Scott RC, Ramsay JD (1987) Comparison of the in vivo and in vitro percutaneous absorption of a lipophilic molecule (cypermethrin, a pyrethroid insecticide). *J Invest Dermatol* 89:142–146
- Serat WF (1973) Calculation of a safe reentry time into an orchard treated with a pesticide chemical which produces a measurable physiological response. *Arch Environ Contam Toxicol* 1:170–181
- Serat WF, Bailey JB (1974) Estimating the relative toxicologic potential of each pesticide in mixture of residues on foliage. *Bull Environ Contam Toxicol* 12:682–686
- Serat WF, Mengle DC, Anderson HP, Kahn E (1975) On the estimation of worker entry intervals into pesticide treated fields with and without the exposure of human subjects. *Bull Environ Contam Toxicol* 13:506–512
- Shafer TJ, Meyer DA, Crofton KM (2005) Developmental neurotoxicity of pyrethroid insecticides: critical review and future research needs. *Environ Health Perspect* 113:123–135

- Sidon EW, Moody RP, Franklin CA (1988) Percutaneous absorption of *cis*- and *trans*-permethrin in rhesus monkeys and rats: Anatomic site and interspecies variation. *J Toxicol Environ Health A* 23:207–216
- Smith PA, Thompson MJ, Edwards JW (2002) Estimating occupational exposure to the pyrethroid termiticide bifenthrin by measuring metabolites in urine. *J Chromatogr B* 778:113–120
- Soderlund DM, Clark JM, Sheets LP, Mullin LS, Piccirillo VJ, Sargent D, Stevens JT, Weiner ML (2002) Mechanisms of pyrethroid neurotoxicity: implications for cumulative risk assessment. *Toxicology* 171:3–59
- Song J-H, Narahashi T (1996) Modulation of sodium channels of rat cerebellar Purkinje neurons by the pyrethroid tetramethrin. *J Pharmacol Exp Ther* 277:445–453
- Sorich MJ, McKinnon RA, Miners JO, Smith PA (2006) The importance of local chemical structure for chemical metabolism by human uridine 5'-diphosphate-glucosyltransferase. *J Chem Inf Model* 46:2692–2697
- Southwood J (1985a) PP321: Acute oral toxicity studies. Zeneca Agricultural Products Laboratory Project No. CTL/P/1102, Wilmington, DE.
- Southwood J (1985b) PP993: Acute oral toxicity, acute intraperitoneal toxicity, and acute dermal toxicity studies. Zeneca Agricultural Products Laboratory Project No. CTL/P/986, Wilmington, DE.
- Staiger LE, Quistad GB (1984) Metabolism of [benzyl-U-ring-¹⁴C] fluralinate by rats. *J Agric Food Chem* 32:1130–1133
- Stevens RH, O'Neill CA, Warhurst A, Carlson GL, Rowland M, Warhurst G (2001) Kinetic profiling of P-glycoprotein-mediated drug efflux in rat and human intestinal epithelia. *J Pharmacol Exp Ther* 296:584–591
- Stok JE, Huang H, Jones PD, Wheelock CE, Morisseau C, Hammock BD (2004) Identification, expression, and purification of a pyrethroid-hydrolyzing carboxylesterase from mouse liver microsomes. *J Biol Chem* 279:29863–29869
- Sudhahar CG, Haney RM, Xue Y, Stahelin RV (2008) Cellular membranes and lipid-binding domains as attractive targets for drug development. *Curr Drug Targets* 9:603–613
- Suzuki T, Miyamoto J (1974) Metabolism of tetramethrin in houseflies and rats in vitro. *Pestic Biochem Physiol* 4:86–97
- Suzuki T, Ohno N, Miyamoto J (1976) New metabolites of (+)-*cis*-fenothrin, 3 phenoxybenzyl (+)-*cis*-chrysanthemumate, in rats. *J Pestic Sci* 1:151–152
- Symington SB, Frisbie RK, Clark JM (2008) Characterization of 11 commercial pyrethroids on the functional attributes of rat brain synaptosomes. *Pestic Biochem Physiol* 92:61–69
- Tamai I, Takanaga H, Maeda H, Sai Y, Ogihara T, Higashida H, Tsuji A (1995) Participation of a proton-cotransporter, MCT1, in the intestinal transport of monocarboxylic acid. *Biochem Biophys Res Commun* 214:482–489
- Tan HL, Bezzina CR, Smits JPP, Verkerk AO, Wilde AAM (2003) Genetic control of sodium channel function. *Cardiovasc Res* 57:961–973
- Tan J, Liu Z, Wang R, Huang ZY, Chen AC, Gurevitz M, Dong K (2005) Identification of amino acid residues in the insect sodium channel critical for pyrethroid binding. *Mol Pharmacol* 67:513–522
- Tan X, Hou S, Wang M (2007) Enantioselective and diastereoselective separation of synthetic pyrethroid insecticides on a novel chiral stationary phase by high-performance liquid chromatography. *Chirality* 19:574–580
- Tatebayashi H, Narahashi T (1994) Differential mechanism of action of the pyrethroid tetramethrin on tetrodotoxin-sensitive and tetrodotoxin-resistant sodium channels. *J Pharmacol Exp Ther* 270:595–603
- Tateno C, Ito S, Tanaka M, Yoshitake A (1993) Effects of pyrethroid insecticides on gap junctional intercellular communications in Balb/c3T3 cells by dye-transfer assay. *Cell Biol Toxicol* 9:215–221
- Timchalk C, Nolan RJ, Mendrala AL, Dittenber DA, Brzak KA, Mattsson JL (2002) A physiologically-based pharmacokinetic and pharmacodynamic (PBPK/PD) model for the organophosphate insecticide chlorpyrifos in rats and humans. *Toxicol Sci* 66:34–53

- Tomigahara Y, Mori M, Shiba K, Isobe N, Kaneko H, Nakatsuka I, Yamada H (1994a) Metabolism of tetramethrin isomers in rat. I. Identification of a sulfonic acid type of conjugate and reduced metabolites. *Xenobiotica* 24:473–484
- Tomigahara Y, Mori M, Shiba K, Isobe N, Kaneko H, Nakatsuka I, Yamada H (1994b) Metabolism of tetramethrin isomers in rat. II. Identification and quantification of metabolites. *Xenobiotica* 24:1205–1214
- Tomigahara Y, Shiba K, Isobe N, Kaneko H, Nakatsuka I, Yamada H (1994c) Identification of two new types of S-linked conjugates of EtoC in rat. *Xenobiotica* 24:839–852
- Tomigahara Y, Onogi M, Miki M, Yanagi K, Shiba K, Kaneko H, Nakatsuka I, Yamada H (1996) Metabolism of tetramethrin isomers in rat. III. Stereochemistry of reduced metabolites. *Xenobiotica* 26:201–210
- Tomigahara Y, Onogi M, Saito K, Kaneko H, Nakatsuka I, Yamane S (1997) Metabolism of tetramethrin in rat. IV. Tissues responsible for formation of reduced and hydrated metabolites. *Xenobiotica* 27(9):961–971
- Tornero-Velez R, Mirfazaelian A, Kim KB, Anand SS, Kim HJ, Haines WT, Bruckner JV, Fisher JW (2010) Evaluation of deltamethrin kinetics and dosimetry in the maturing rat using PBPK model. *Toxicol Appl Pharmacol* 244:208–217
- Tsuji T, Kaneda N, Kado K, Yokokura T, Yoshimoto T, Tsuru D (1991) CPT-11 converting enzyme from rat serum: purification and some properties. *J Pharmacobiodyn* 14:341–349
- Tubic M, Wagner D, Spahn-Langguth H, Bolger MB, Langguth P (2006) In silico modeling of non-linear drug absorption for the P-gp substrate Talinolol and of consequences for the resulting pharmacodynamic effect. *Pharm Res* 23:1712–1720
- Tullman RH (1987) Data Evaluation Report No. 005731. U.S. Environmental Protection Agency, Washington, DC
- Ueda K, Gaughan LC, Casida JE (1975) Metabolism of (+)-*trans*- and (+)-*cis*-Resmethrin in rats. *J Agric Food Chem* 23:106–115
- Ueda K, Cornwell MM, Gottesman MM, Pastan I, Roninson IB, Ling V, Riordan JR (1986) The *mdr1* gene, responsible for multidrug-resistance, codes for P-glycoprotein. *Biochem Biophys Res Commun* 141:956–962
- Ulrich E, Sey YM, Harrison RA, DeVito MJ (2008) LC/MS method for the analysis of permethrin enantiomers in biological matrices. 20th International Symposium on Chirality, Geneva, Switzerland, July 6–9, 2008.
- Unai T, Casida JE (1977) Synthesis of isomeric 3-(2,2-Dichlorovinyl)-2-hydroxymethyl-2-methylcyclopropanecarboxylic acids and other permethrin metabolites. *J Agric Food Chem* 25:979–987
- Valverde A, Aguilera A, Rodriguez M, Boulaid M (2001) What are we determining using gas chromatographic multiresidue methods: tralomethrin or deltamethrin? *J Chromatogr A* 943 (1):101–111
- Van der Rhee HJ, Farquhar JA, Vermeulen NP (1989) Efficacy and transdermal absorption of permethrin in scabies patients. *Acta Derm Venerol* 69:170–173
- Varsho BJ (1996) Acute oral toxicity study of deltamethrin in albino rats. AgrEvo USA Company Study No. WIL-274001.
- Venkatakrishnan K, Von Moltke LL, Obach RS, Greenblatt DJ (2000) Microsomal binding of amitriptyline: effect on estimation of enzyme kinetic parameters in vitro. *J Pharmacol Exp Ther* 293:343–350
- Vistoli G, Pedretti A, Mazzolari A, Testa B (2010) In silico prediction of human carboxylesterase-1 (hCES1) metabolism combining docking analysis and MD simulations. *Bioorg Med Chem* 18:320–329
- Vozeh S, Taeschner W, Wenk M (1990) Pharmacokinetic drug data. In: *Clinical pharmacokinetics drug data handbook*. ADIS, Auckland, NZ. pp 1–38.
- Wadkins RM, Hyatt JL, Wei X, Yoon KJP, Wierdl M, Edwards CC, Morton CL, Obenauer JC, Damodaran K, Beroza P, Danks MK, Potter PM (2005) Identification and characterization of

- novel benzyl (diphenylethane-1,2-dione) analogues as inhibitors of mammalian carboxylesterases. *J Med Chem* 48:2906–2915
- Wang P, Zhou Z, Jiang S, Yang L (2004) Chiral resolution of cypermethrin on cellulose-tris(3,5-dimethylphenyl-carbamate) chiral stationary phase. *Chromatographia* 59:625–629
- Wang Q, Qiu J, Zhu W, Jia G, Li J, Bi C, Zhou Z (2006) Stereoselective degradation kinetics of theta-cypermethrin in rats. *Environ Sci Technol* 40:721–726
- Wang M, Wang Q, Hong C, Slecza B, D'Arienzo C, Josephs J, Ye X-Y, Robl J, Gordon D, Rodrigues D, Harper T (2010) Prediction of in vivo enantiomeric compositions by modeling in vitro metabolic profiles. *J Pharm Sci* 99:3234–3245
- Waxman SG, Craner MJ, Black JA (2004) Na⁺ channel expression along axons in multiple sclerosis and its models. *Trends Pharmacol Sci* 25:584–591
- Weiner ML, Nemeč M, Sheets L, Sargent D, Breckenridge (2009) Comparative functional observational battery study of twelve commercial pyrethroid insecticides in male rats following oral exposure. *Neurotoxicology* 30S:S1–S16
- Wester RC, Maibach HI (1977) In: Drill VA, Lazar P (eds) *Cutaneous toxicology*. Academic, New York, p 111
- Wester RC, Maibach HI (1993) Animal models for percutaneous absorption. In: Wang RGM, Knaak JB, Maibach HI (eds) *Health risk assessment: dermal and inhalation exposure and absorption of toxicants*. CRC, Boca Raton, FL
- Wester RC, Noonan PK (1980) Relevance of animal-moles for percutaneous-absorption. *Int J Pharm* 7:99–110
- Wester RC, Bucks DAW, Maibach HI (1994) Human in vivo percutaneous absorption of pyrethrin and piperonyl butoxide. *Food Chem Toxicol* 32:51–53
- Wheelock CE, Wheelock AM, Zhang R, Stok JE, Morisseau C, Le Valley SE (2003) Evaluation of alpha-cyanoesters as fluorescent substrates for examining interindividual variation in general and pyrethroid-selective esterases in human liver microsomes. *Anal Biochem* 315:208–222
- Wheelock CR, Miller JL, Miller MJ, Phillips BM, Huntley SA, Gee SJ, Tjeerdem RS, Hammock BD (2006) Use of carboxylesterase activity to remove pyrethroid-associated toxicity to *Ceriodaphnia dubia* and *Hyalella azteca* toxicity in identification evaluations. *Environ Toxicol Chem* 25:973–984
- White S (1994) *Protein membrane structure*. Oxford University Press, Oxford
- White INH, Verschoyle RD, Moradian MH, Barnes JM (1976) The relationship between brain levels of cismethrin and bioresmethrin in female rats and neurotoxic effects. *Pestic Biochem Physiol* 6:491–500
- WHO (2005a) WHO Specifications and evaluations for public health pesticides, Deltamethrin, (S)-a-cyano-3-phenoxybenzyl (1R,3R)-3-(2,2-dibromovinyl)-2,2-dimethylcyclopropane carboxylate. WHO, Genève.
- WHO (2005b) The WHO Recommended Classification of Pesticides by Hazard. Guidelines to Classification 2004, International Programme on Chemical Safety. WHO/PCS/01.5, Genève, http://www.who.int/ipcs/publications/pesticides_hazard/en/.
- WHO (World Health Organization) (1965) Evaluation of the toxicity of pesticide residues in food: dimethrin. FAO meeting report PL/1965/10/1. Food and Agriculture Organization (United Nations) www.inchem.org/documents/jmpr/jmpmono/v065pr21.htm
- Williams RL, Bernard CE, Krieger RI (2003) Human exposure to indoor residential cyfluthrin residues during a structured activity program. *J Expo Anal Environ Epidemiol* 13:112–119
- Wilson ZE, Rostami-Hodjegan A, Burn JL, Tooley A, Boyle J, Ellis SW, Tucker GT (2003) Inter-individual variability in levels of human microsomal protein and hepatocellularity per gram of liver. *Br J Clin Pharmacol* 56:433–440
- Wolansky MJ, Harrill JA (2008) Neurobehavioral toxicology of pyrethroid insecticides in adult animals: a critical review. *Neurotoxicol Teratol* 30:55–78
- Woollen BH, Marsh JR, Laird WJD, Lesser JE (1992) The metabolism of cypermethrin in man: differences in urinary profiles following oral and dermal administration. *Xenobiotica* 22:983–991

- Wu A, Liu Y (2003) Prolonged expression of c-Fos and c-Jun in the cerebral cortex of rats after deltamethrin treatment. *Brain Res Mol Brain Res* 110:147–151
- Xu C, Wang J, Liu W, Sheng GD, Tu Y, Ma Y (2007) Separation and aquatic toxicity of enantiomers of the pyrethroid insecticide Lambda-Cyhalothrin. *Environ Toxicol Chem* 27:174–181
- Yamamoto I, Elliot M, Casida JE (1971) Metabolic fate of pyrethrin I, pyrethrin II, and allethrin. *Bull World Health Organ* 44:347–348
- Yamazaki K, Kanaoka M (2004) Computational prediction of the plasma protein-binding percent of diverse pharmaceutical compounds. *J Pharm Sci* 93:1480–1494
- Yang J, Tucker GT, Rostami-Hodjegan A (2004a) Cytochrome P450 3A expression and activity in the human small intestine. *Clin Pharmacol Ther* 76:931
- Yang G-S, Vazquez PP, Frenich AG, Vidal JLM, Aboul-Enein HY (2004b) Separation on CHIRALCEL OD-R with methanol/water, and acetonitrile/water mobile phases. *J Liq Chromatogr Rel Technol* 27(10):1507–1521
- Yoon KJ-P, Krull EJ, Morton CL, Borrmann WG, Lee RE, Potter PM, Danks MK (2003) Activation of a camptothecin prodrug by specific carboxylesterases as predicted by quantitative structure-activity relationship and molecular docking studies. *Mol Cancer Ther* 2:1171–1181
- Youdim K, Dodia R (2010) Comparison between recombinant P450s and human liver microsomes in the determination of cytochrome P450 Michaelis–Menten constants. *Xenobiotica* 40:235–244
- Youdim KA, Zayed A, Dickins M, Phipps A, Griffiths M, Darekar A, Hyland R, Fahmi O, Hurst S, Plowchalk DR, Cook J, Guo F, Obach RS (2008) Application of CYP3a4 in vitro data to predict clinical drug-drug interactions: predictions of compounds as objects of interaction. *Br J Clin Pharmacol* 65:680–692
- Yu LX, Lipka E, Crison JR, Amidon GL (1996) Transport approaches to the biopharmaceutical design of oral drug delivery systems: prediction of intestinal absorption. *Adv Drug Del Rev* 19:359–376
- Zeng S, Tang Y (2009) Effect of clustered ion channels along an unmyelinated axon. *Physical Rev E* 80:1–9
- Zhang H (2005) A new approach for the tissue–blood partition coefficients of neutral and ionized compounds. *J Chem Inf Model* 45:121–127
- Zhang X, Tsang AM, Okino MS, Power FW, Knaak JB, Harrison LS, Dary CC (2007) A physiologically-based pharmacokinetic/pharmacodynamic (PBPK/PD) model for carbofuran in Sprague-Dawley rats using the Exposure Related Dose Estimating Model (ERDEM). *Toxicol Sci* 100:345–359
- Zhe X, Wenwei X, Hua H, Lirui P, Xu X (2008) Direct chiral resolution and its application to the determination of the pesticide tetramethrin in soil by high-performance liquid chromatography using polysaccharide-type chiral stationary phase. *J Chromatogr Sci* 46:783–786

Appendix A: Nomenclature

Table A1 Acronyms and abbreviations

ABC/ABCT	ABC transporter-ATP-binding cassette
ACAT	Advanced CAT
ACD	Advance Chemistry Development
AChE	Acetylcholinesterase
ACSL	Advanced Continuous Simulation Language
ADH	Human alcohol dehydrogenase
ADME	Absorption, distribution, metabolism and elimination
ADMET	Adsorption, distribution, metabolism, elimination and toxicity
AFM	Atomic force microscope
AGP	Alpha-1-acid glycoproteins
ALDH	Aldehyde dehydrogenases
ANNE	Artificial neural network ensemble
ASF	Absorption scale factor
ATPase	Adenosinetriphosphotase
BBB	Blood brain barrier
BF	BF acid (CAS no. 24313-22-2)
BBDR	Biologically based dose-response
BuChE	Butyrylcholinesterase
bwt	Body weight
CA	Chrysanthemic acid
CaE/CE	Carboxylesterase
CALEPA	California Environmental Protection Agency
CAS	Chemical Abstracts Service
CAT	Compartmental absorption and transit
CDMB	1,2-Ethanedione, 1-(2-chlorophenyl)-2-(3,4-dimethoxyphenyl)
CEs	Rat CEs (CaEs) belong to two classes, hydrolase A and B
CES1/CES2	hCE-1 and hCE-2 belong to these two classes of human carboxylesterases
CIPAC	Collaborative International Pesticide Analytical Council
CL _{int}	Intrinsic clearance

(continued)

Table A1 (continued)

CNP	-Silanized silica gel HPLC column
CPCA	<i>trans</i> -Chrysanthemic acid (CAS no. 10453-89-1)
CSP	Chiral specific
CYP/CYP450	Cytochrome P450
DCCA	3-(2-Dichlorovinyl)-2,2-dimethylcyclopropane carboxylic acid
DEET	Diethyl-m-toluamide (CAS no. 134-62-3)
DP	Dustable powder
EC	Emulsifiable concentrate
EC ₅₀	Concentration producing half-maximal flux
EHC	Enterohepatic circulation
EPA	Environmental Protection Agency, U.S.
ER	Endoplasmic reticulum
ERDEM	Exposure Related Dose Estimating Model See web site: http://www.epa.gov/heads/products/erdem/erdem.html
ES	Electrospray
ESF	Gut enzyme distribution factors
FAO	Food and Agriculture Organization, WHO
FDA	Food and Drug Administration
FID	Flame ionization detector
FOB	Functional observation batteries
FPBA	4-Fluoro-3-phenoxybenzoic acid (CAS no. 77279-89-1)
GC	Gas chromatography
GDIT	General Dynamics Information Technology
GI	Gastrointestinal
GLC	Gas liquid chromatography
GLY	Glycine, amino acid
GSA	Gut surface area
HB	Hydrogen bonding
hCE-1/hCE-2	Human liver isozymes
hERG	Human endoplasmic reticulum
His	Histidine
HLM	Human liver microsomes
HPI	HPI (CAS no. 1444-94-6)
HPLC	High performance liquid chromatography
HSA	Human serum albumen
ID	Inner diameter
ITCA	2-Iminothiazolidine-4-carboxylic acid
IUPAC	International Union of Pure and Applied Chemistry
LC	Liquid chromatography
LD ₅₀	Lethal dose for 50% of the population
MCT	Monocarboxylic transporter
MBP	2-MBP alcohol, [1'-biphenyl]-3-methanol, 2-methyl
MD	Molecular dynamics
MDCK	Madin-Darby canine kidney
MFO	Mixed function oxidase
MPPGL	Amount of microsomal protein per gram of liver
MS	Mass spectrometry
NADPH	Nicotinamide adenine dinucleotide phosphate
NADH	Nicotinamide adenine dinucleotide

(continued)

Table A1 (continued)

NCEA	National Center for Environmental Assessment
NR	Normalized rate
OECD	Organization for Economic Cooperation and Development
OP	Organophosphorus
OMPA	Tetraisopropylpyrophosphoramidate (CAS no. 513-00-8)
OPP	Office of Pesticide Programs (U.S. EPA, Washington, DC)
P450	See CYP450
PA	Permeability areas
PAMPA	Parallel artificial membrane permeation assay
PB acid	PB acid (benzoic acid, 3-phenoxy)
PB ald	Benzaldehyde, 3-phenoxy
PBPK/PD	Physiologically based pharmacokinetic/pharmacodynamic
PC	Phosphatidylcholine
PD	Pharmacodynamics
PE	Phosphatidylethanolamine
PEG	Polyethylene glycol
PepT1	Peptide transporter
Pgp	P-glycoprotein
PLIF	Protein ligand interaction fingerprints
PNP	p-Nitrophenol
PS	Phosphatidylserine
QSAR	Quantitative structure-activity relationship
QSPR	Quantitative structure-property relationship
RAM	Rate of metabolism
rCEs	Recombinant carboxylesterases
rCYP	Recombinant cytochrome P450
RfD	Reference dose
RLM	Rat liver microsomes
RMSE	Root-mean-square error
RP	Reverse phase
RPF	Relative potency factor
SECM	Scanning electrochemical microscopy
SER	Serine, amino acid
SFC	Supercritical fluid chromatography
SMILES	Simplified Molecular Input Line Entry System
TC	Total cholesterol
TCPy	Trichloropyridinol
TEPP	Diphosphoric acid, P, P, P', P'-tetraethyl ester, CAS no. 107-49-3
TFP	TFP acid (CAS no. 74609-46-4)
THAM	THAM (CAS no. 81951-65-7)
TLC	Thin layer chromatography
TMPA	2,2,3,3-Tetramethylcyclopropanecarboxylic acid
TNR	Total normalized rate
TOPKAT	Toxicity Prediction by Komputer Assisted Technology
TPI	TPI 3,4,5,6-tetrahydrophthalimide (CAS no. 4720-86-9)
UDP	Uridine diphosphate
UGT	UDP-glucuronosyltransferase
UL	Ultra low volume liquid

(continued)

Table A1 (continued)

UV	Ultraviolet
VSSCs	Voltage-sensitive sodium channels
WHO	World Health Organization
WP	Wettable powder

Table A2 Chemical and mathematical expressions

Expression	Description
$[P]$	Concentration of pyrethroid
$[S]$	Substrate concentration
A	Surface area
C	Concentration
Cl_{int}	Intrinsic clearance
D	Diffusion coefficient
$D_{o:w}$ (pH 7.4)	Distribution between octanol and buffer at pH 7.4
$D^*_{vo:w}$ (pH 7.4)	Distribution between vegetable oil and buffer at pH 7.4
E	Enzyme
E_0	Initial enzyme
E_h	Potential to which membrane is repolarized
E_{Na}	Reverse potential for sodium current
$ESF_{(i,j)}$	Scale factor for maximum transport rate for transporter i in compartment j
E_t	Potential of step polarization
F_a	Association constant of basic compound with acidic phospholipids
F_c	Fraction of drug with positive charge in plasma
$f_{u,inc}$	Free fraction of compound in microsomal incubation
$f_{u,mic}$	Free fraction of compound in microsomes
$F_{u,mic}$	Unbound drug in microsomes
$f_{u,p}$	Unbound drug in plasma
f_{up}	Drug fraction unbound in plasma (represents binding and partitioning)
F_{up}	Unbound drug in plasma (represents only protein binding)
f_{ut}	Drug fraction unbound to protein in tissue
f_{ue}	Drug fraction unbound in the enterocytes
F_{ut}	Unbound drug in tissue
IC_{50S}	Concentrations producing 50% inhibition
I_{Na}	Amplitude of peak current during repolarization
I_{tail}	Maximal tail current amplitude
J	Net flux
J_{max}	Maximum flux (permeability)
J_s	Steady state flux
K	K_m , substrate concentration that results in half maximum velocity
K_a	Association constant of basic compound with acidic phospholipids
k_{cat}	Hydrolysis rate constant, h^{-1}
K_d	Concentration of pyrethroid
K_{dj}	Equilibrium dissociation constant for protein concentration P_j
K_{DS}	Dissociation constants
K_{hsa}	Binding constant for human serum albumin
K_{is}	Inhibition constants
K_m	Substrate concentration that results in half maximum velocity

(continued)

Table A2 (continued)

Expression	Description
K_{ms}	Substrate concentrations that result in half maximum velocity
K_{oct}	Octanol: water partition coefficient
K_{ow}	Octanol: water partition coefficient
K_p	Skin permeation constant; partition coefficient
K_{pu}	Unbound partition coefficient
k_s	Series of rate constants
l	Thickness
$\text{Log } D$	Distribution coefficient for partially dissociated compounds
$\text{Log } D_{(pH\ 7.4)}$	$\text{Log } D$ calculated with pH of 7.4
$\text{Log } K_{oct}$	Log of octanol: water partition coefficient
$\text{Log } P$	Log of octanol: water partition coefficient, neutral compounds
M	Modified channels by pyrethroids
M_{max}	Maximal percentage of sodium channels modified
MW	Molecular weight (g mol^{-1})
Na_v	Voltage gated sodium channel
n_H	Hill coefficient
o	Octanol
P	Partition coefficient and concentration of pyrethroid
P_{app}	Apparent permeability
PC	Partition constant
$PC_{b:adipose}$	Blood: adipose tissue partition coefficient
$PC_{b:liver}$	Blood: liver partition coefficient
PC_t	Tissue: blood partition coefficient
$PC_{t:b}$	Tissue: blood partition coefficient
$PC_{t:b-adipose}$	Adipose tissue: blood partition coefficient
$PC_{t:b-liver}$	Partition coefficient liver: blood
P_{eff}	Effective permeability
ph	Phospholipids
pH	Hydrogen ion concentration
pI	Isoionic point
P_j	Partition coefficient for tissue j, also protein concentration
P-gp	P-glycoprotein
pK_a	Acid-base ionization constant
$P_{o:w}$ (pH 7.4)	n-Octanol: buffer partition coefficient, nonionized species at pH 7.4
$P_{t:b}$	Tissue: blood partition coefficient
$P_{t:p}$	Tissue: plasma partition coefficient
$P_{t:p\ adipose}$	Partition coefficient between adipose tissue and plasma
$P_{t:p\ nonadipose}$	Partition coefficient between nonadipose tissue and plasma
$Q_{l-b\ plasma}$	Flow rate, liver blood plasma
Q	Volumetric flow rate
$QPLogK_{hsa}$	Prediction of binding to human serum albumin
r^2	Coefficient of determination
RA_t	Ratio of albumin or lipoprotein concentration found in tissue
R	Resistance (electrical), rate (catalytic)
R_f	Recovered fraction
SF	Scale factor

(continued)

Table A2 (continued)

Expression	Description
t	Tissue
V	Fractional tissue volume content
V_{\max}	Half maximum velocity
V_{nt}	Fractional volume of neutral nonpolar lipids in tissue
V_{phlt}	Fractional volume of phoslipids in tissue
W	Water
WS	Water solubility (g L^{-1})

Appendix B: Pyrethroids, Pyrethroids Isomers and Technical Products

Table B1 Allethrin, individual isomers

Stereo-isomer code	Chiral configuration			OR ^a	1C/3C <i>cis/trans</i>	Enantiomer pair	CAS no.
	1C	3C	α C				
A	R	R	R	(–)–	<i>trans</i> –	I	61009-26-5 abs
B	R	R	S	(–)–	<i>trans</i> –	II	28434-00-6 abs
C	R	S	R	(+)–	<i>cis</i> –	III	61009-23-2 abs
D	R	S	S	(+)–	<i>cis</i> –	IV	61046-09-1 abs
E	S	R	R	(–)–	<i>cis</i> –	IV	61009-25-4 abs
F	S	R	S	(–)–	<i>cis</i> –	III	61009-24-3 abs
G	S	S	R	(+)–	<i>trans</i> –	II	23453-09-0 abs
H	S	S	S	(+)–	<i>trans</i> –	I	61009-27-6 abs

See Table 2 (2.1) for generic structure and technical name of allethrin.

^aOR = Optical rotation

Table B2 Allethrin, technical products and mixtures

Name, synonym	CAS no.	Isomers – Composition	EPA PC code
Allethrin	584-79-2	A,B,C,D — 18. 0% ea	004-001, liquid
–		E,F,G,H — 4.5% ea	004-002, solid
Pynamin forte	231937-89-6 abs	A, B — 36% ea	004-005
d-Allethrin		C, D — 9% ea	
D- <i>cis-trans</i> -allethrin			
Allethrin (ISO)			
Bioallethrin	260359-57-7 abs	A, B — \geq 46% ea	004-003
D- <i>trans</i> -allethrin	(584-79-2)	C, D — $<$ 2% ea	
Bioallethrin (BSI)			
Esbiol	28434-00-6 abs	A — 5%	004-004
S-bioallethrin		B — $>$ 90%	
Allethrin (ISO)		C, D — $<$ 2% ea	

(continued)

Table B2 (continued)

Name, synonym	CAS no.	Isomers – Composition	EPA PC code
Esbiothrin	260359-57-7 abs	A — 21%	004-007
Allethrin (ISO)		B — 72%	
–		C, D — <2% ea	
dl- <i>trans</i> -Allethrin	61009-27-6 abs	H — 100%	

Table B3 Bifenthrin, individual isomers

Stereo-isomer code	Chiral configuration*			1C/3C <i>cis/trans</i>	Enantiomer pair	CAS no.
	1C	3C	OR ^a			
A	R	R	(+)–	<i>cis</i> -	I	439680-76-9 abs
B	R	S	(–)–	<i>trans</i> -	II	552880-52-1 abs
C	S	R	(+)–	<i>trans</i> -	II	207347-00-0 abs
D	S	S	(–)–	<i>cis</i> -	I	439680-77-0 abs

See Table 2 (2.2) for generic structure and technical name of bifenthrin.

* All stereoisomers of interest have a Z configuration about the double bond

^aOR = Optical rotation

Table B4 Bifenthrin, technical products and mixtures

Name	CAS no.	Isomers – Composition	EPA PC code
Bifenthrin	82657-04-3 rel	A + D – > 97%	128-825
		<i>trans</i> isomer	128-825

Table B5 Cyfluthrin, individual isomers

Stereo-isomer code	Chiral configuration			OR ^a	1C/3C <i>cis/trans</i>	Enantiomer pair	CAS no.
	1C	3C	α C				
A	R	R	R	(–)–	<i>cis</i> -	I	85649-12-3 abs
B	R	R	S	(+)–	<i>cis</i> -	II	85649-15-6 abs
C	R	S	R	(–)–	<i>trans</i> -	III	85649-16-7 abs
D	R	S	S	(+)–	<i>trans</i> -	IV	85649-19-0 abs
E	S	R	R	(–)–	<i>trans</i> -	IV	85649-18-9 abs
F	S	R	S	(+)–	<i>trans</i> -	III	85649-17-8 abs
G	S	S	R	(–)–	<i>cis</i> -	II	85649-14-5 abs
H	S	S	S	(+)–	<i>cis</i> -	I	85649-13-4 abs

See Table 2 (2.3) for generic structure and technical name of cyfluthrin.

^aOR = Optical rotation

Table B6 Cyfluthrin, technical products and mixtures

Name	CAS no.	Isomers – Composition	EPA PC code
Cyfluthrin	68359-37-5	A,B,C,D,E,F,G,H	128-831
Beta-cyfluthrin	68359-37-5	A + H — < 2%	118-831
–		B + G — 30 to 40%	
–		C + F — < 3%	
–		D + E — 57 to 67%	

Table B7 Cyhalothrin, individual isomers

Stereo-isomer code	Chiral configuration*			OR ^a	1C/3C <i>cis/trans</i>	Enantiomer pair	CAS no.
	1C	3C	α C				
A	R	R	R		<i>cis</i> -	I	76703-63-4 abs
B	R	R	S	(-)-	<i>cis</i> -	II	76703-62-3 abs
C	R	S	R		<i>trans</i> -	III	76703-67-8 abs
D	R	S	S		<i>trans</i> -	IV	76703-66-7 abs
E	S	R	R		<i>trans</i> -	IV	76703-69-0 abs
F	S	R	S		<i>trans</i> -	III	76703-68-9 abs
G	S	S	R	(+)	<i>cis</i> -	II	76703-65-6 abs
H	S	S	S		<i>cis</i> -	I	76703-64-5 abs

See Table 2 (2.4) for generic structure and technical name of cyhalothrin.

SciFinder Scholar indicates that "B" is a (+)-*cis* isomer

* The configuration about the double bond is always Z in commercial products

^aOR = Optical rotation

Table B8 Cyhalothrin, technical products and mixtures

Name	CAS no.	Isomers – Composition	EPA PC code
Cyhalothrin	68085-85-8	(A,H):(B,G) – 60:40	128-867
Lambda Cyhalothrin	91465-08-6 rel	B + G – 50:50	128-897
Gamma Cyhalothrin	76703-62-3	B – >80%	128-807

Table B9 Cypermethrin, individual isomers

Stereo-isomer code	Chiral configuration*			OR ^a	1C/3C <i>cis/trans</i>	Enantiomer pair	CAS no.
	1C	3C	C				
A	R	R	R	(-)-	<i>cis</i> -	I	65731-83-1 abs
B	R	R	S	(+)-	<i>cis</i> -	II	65731-84-2 abs
.C	R	S	R	(-)-	<i>trans</i> -	III	66841-24-5 abs
D	R	S	S	(+)-	<i>trans</i> -	IV	65732-07-2 abs
.E	S	R	R	(-)-	<i>trans</i> -	IV	83860-31-5 abs
F	S	R	S	(+)-	<i>trans</i> -	III	66841-24-5 abs
G	S	S	R	(-)-	<i>cis</i> -	II	72204-44-5 abs
H	S	S	S	(+)-	<i>cis</i> -	I	72204-43-4 abs

See Table 2 (2.5) for generic structure and technical name of cypermethrin.

* The configuration about the double bond is always Z in commercial products

^aOR = Optical rotation

Table B10 Cypermethrin, technical products and mixtures

Name	CAS no.	Isomers – Composition	EPA PC code
Cypermethrin	52315-07-8	A,B,C,D,E,F,G,H	109-704
Alpha-cypermethrin	67375-30-8 rel	B,G – 50:50	209-600
Beta-cypermethrin	65731-84-2 abs	(B+G):(D+E) – 40:60	109-702
Theta-cypermethrin	71697-59-1 rel	D,E – 50:50	
Zeta-cypermethrin	52315-07-8	B,D,F,H – 24% ea	129-064
S-cypermethrin		A,C,E,G – 1% ea	

Table B11 Deltamethrin, individual isomers

Stereo-isomer code	Chiral configuration			OR ^a	1C/3C <i>cis/trans</i>	Enantiomer pair	CAS no.
	1C	3C	α C				
A	R	R	R		<i>cis</i> -	I	55700-99-7 abs
B	R	R	S	(+)-	<i>cis</i> -	II	52918-63-5 abs
C	R	S	R		<i>trans</i> -	III	64363-97-9 abs
D	R	S	S		<i>trans</i> -	IV	64363-96-8 abs
E	S	R	R		<i>trans</i> -	IV	NA
F	S	R	S		<i>trans</i> -	III	64364-03-0 abs
G	S	S	R	(-)-	<i>cis</i> -	II	80845-12-1 abs
H	S	S	S		<i>cis</i> -	I	64364-02-9 abs

See Table 2 (2.6) for generic structure and technical name of deltamethrin.

^aOR = Optical rotation

Table B12 Deltamethrin, technical products and mixtures

Name	CAS no.	Isomers – Composition	EPA PC code
Deltamethrin	52918-63-5	B ^a – >97%	097-805

^aSee Table B11

Table B13 Esfenvalerate/fenvalerate, individual isomers

Stereo-isomer code	Chiral configuration		OR ^a	Enantiomer pair	CAS no.
	α C	1C			
A	R	R	(+)-	I	67614-33-9 abs
B	R	S	(+)-	II	67614-32-8 abs
C	S	R	(-)-	II	66267-77-4 abs
D	S	S	(-)-	I	66230-04-4 abs

The OR for A is inferred from the OR for D. Cyano group is attached to the 1C carbon atom

See Table 2 (2.7) for generic structure and technical name of fenvalerate.

^aOR = Optical rotation

Table B14 Esfenvalerate/fenvalerate, technical products and mixtures

Name	CAS no.	Isomers – Composition	EPA PC code
Esfenvalerate	66230-04-4	D – 84%	109-303
–		B – 8%	
–		C – 7%	
–		A – 1%	
Fenvalerate	51630-58-1	A, D – 23% ea	109-301
Pydrin		B, C – 27% ea	

Table B15 Fenpropathrin, individual isomers

Stereo-isomer code	Chiral configuration		CAS no.
	α C	OR ^a	
A	R	(–)–	67890-36-4 abs
B	S	(+)–	67890-415-9 abs

See Table 2 (2.8) for generic structure and technical name of fenpropathrin.

The rotation for A is inferred from the rotation for B

^aOR = Optical rotation

Table B16 Fenpropathrin, technical products and mixtures

Name	CAS no.	Isomers – Composition	EPA PC code
Fenpropathrin	39515-41-8	A + B ^a – 50:50	127-901

^a See Table B15

Table B17 (tau-)Fluvalinate, individual isomers

Stereo-isomer code	Chiral configuration		Enantiomer pair	CAS no.
	2C	α C		
A	R	R	I	76821-52-8 abs
B	R	S	II	76821-53-9 abs
C	S	R	II	76821-59-5 abs
D	S	S	I	76821-60-8 abs

2C is at the 2 position of valine; cyano group is attached to the α C or methyl carbon

See Table 2 (2.9) for generic structure and technical name of fluvalinate.

Table B18 (tau-)Fluvalinate, technical products and mixtures

Name	CAS no.	Isomers – Composition	EPA PC code
Fluvalinate	69409-94-5	A, B, C, D – 25% ea	109-302
tau-Fluvalinate	102851-06-9 abs	A + B – 50:50	109-302

Table B19 Permethrin, individual isomers

Stereo-isomer code	Chiral configuration			1C/3C <i>cis/trans</i>	Enantiomer pair	CAS no.
	1C	3C	OR ^a			
A	R	R	(+)–	<i>cis</i> -	I	54774-45-7 abs
B	R	S	(+)–	<i>trans</i> -	II	51877-74-8 abs
C	S	R	(–)–	<i>trans</i> -	II	54774-47-9 abs
D	S	S	(–)–	<i>cis</i> -	I	54774-46-8 abs

See Table 2 (2.10) for generic structure and technical name of permethrin.

^aOR = Optical rotation

Table B20 Permethrin, technical products and mixtures

Name	CAS no.	Isomers – Composition	EPA PC code
Permethrin	52645-53-1	(A, D):(B, C) – 40:60	109-701
<i>cis</i> -Permethrin	61949-76-6 rel	A or D	209-500
<i>trans</i> -Permethrin	61949-77-7 rel	B or C	
Biopermethrin	51877-74-8 abs	B	

Table B21 Phenothrin, individual isomers

Stereo-isomer code	Chiral configuration		OR ^a	1C/3C <i>cis/trans</i>	Enantiomer pair	CAS no.
	1C	3C				
A	R	R	(–)–	<i>trans</i> -	I	26046-85-5 abs
B	R	S	(+)–	<i>cis</i> -	II	51186-88-0 abs
C	S	R	(–)–	<i>cis</i> -	II	51134-88-4 abs
D	S	S	(+)–	<i>trans</i> -	I	66036-31-5 abs

See Table 2 (2.11) for generic structure of phenothrin and technical name.

^aOR = Optical rotation

Table B22 Phenothrin, technical products and mixtures

Name	CAS no.	Isomers – Composition	EPA PC code
Phenothrin	26002-80-2	A, B, C, D – nominal 25%	069-005
<i>cis</i> -Phenothrin	74430-92-5 rel	B or C	
<i>trans</i> -Phenothrin	74430-94-7 rel	A or D	
Sumithrin	26046-85-5 abs	(A:B) – 80:20	069-005
<i>d</i> -phenothrin	51186-88-0 abs		

(A) is the most insecticidally active isomer

Table B23 Resmethrin, individual isomers

Stereo-isomer code	Chiral configuration		OR	1C/3C <i>cis/trans</i>	Enantiomer pair	CAS no.
	1C	3C				
A	R	R	(+)–	<i>trans</i> -	I	28434-01-7 abs
B	R	S	(+)–	<i>cis</i> -	II	35764-59-1 abs
C	S	R	(–)–	<i>cis</i> -	II	10453-56-2 rel
D	S	S	(–)–	<i>trans</i> -	I	33911-28-3 abs

OR = Optical rotation

See Table 2 (2.12) for generic structure of resmethrin and technical name.

Table B24 Resmethrin, technical products and mixtures

Name	CAS no.	Isomers – Composition	EPA PC code
Resmethrin	10453-86-8	A, B, C, D – 40:10:10:40	097-801
<i>cis</i> -Resmethrin	10453-56-2 rel	B or C	097-804
<i>trans</i> -Resmethrin	10453-55-1 rel	A or D	097-802
Bioresmethrin	28434-01-7	A ^a – >90 %	097-802
Cismethrin	35764-59-1	B ^a	097-804

^aSee Table B23

Table B25 Tefluthrin, individual isomers

Stereo-isomer code	Chiral configuration*		1C/3C <i>cis/trans</i>	Enantiomer pair	CAS no.
	1C	3C			
A	R	R	<i>cis</i> -	I	79538-32-2 rel
B	R	S	<i>trans</i> -	II	79538-33-3 rel
C	S	R	<i>trans</i> -	II	79538-33-3 rel
D	S	S	<i>cis</i> -	I	79538-32-2 rel

See Table 2 (2.13) for generic structure and technical name of tefluthrin.

* Only Z configurations for the double bond are produced in commercial products

Table B26 Tefluthrin, technical products and mixtures

Name	CAS no.	Isomers – Composition	EPA PC code
Tefluthrin	79538-32-2 rel	A or D – 50:50	128-912

Tefluthrin was developed by ICI as PP993 and ICIA0993. It is based on the same Z-*cis*-acid as used for lambda cyhalothrin and the product as sold, now by Syngenta, is racemic, i.e. it has equal amounts of the isomers A + D in the table. Isomer A is the main active component

Table B27 Tetramethrin, individual isomers

Stereo-isomer code	Chiral configuration		1C/3C <i>cis/trans</i>	Enantiomer pair	CAS no.
	1C	3C			
A	R	R	<i>trans</i> -	I	1166-46-7 abs
B	R	S	<i>cis</i> -	II	51348-90-4 abs
C	S	R	<i>cis</i> -	II	NA
D	S	S	<i>trans</i> -	I	NA

See Table 2 (2.14) for generic structure and technical name of tetramethrin.

Table B28 Tetramethrin, technical products and mixtures

Name	CAS no.	Isomers – Composition	EPA PC code
Tetramethrin	7696-12-0 rel	A:B:C:D – 4:1:1:4	069-003

Table B29 Tralomethrin, individual isomers

Stereo-isomer code	Chiral configuration				1C/3C <i>cis/trans</i>	Enantiomer pair	CAS no.
	1C	3C	α C	C-Br			
A	R	R	R	R	<i>trans</i> -	I	NA
B	R	R	R	S	<i>trans</i> -	II	NA
C	R	R	S	R	<i>trans</i> -	III	68198-89-0 abs
D	R	R	S	S	<i>trans</i> -	IV	68198-90-3 abs
E	R	S	R	R	<i>cis</i> -	V	78184-93-7 abs
F	R	S	R	S	<i>cis</i> -	VI	78184-94-8 abs
G	R	S	S	R	<i>cis</i> -	VII	66818-66-4 abs
H	R	S	S	S	<i>cis</i> -	VIII	66841-22-3-abs

(continued)

Table B29 (continued)

Stereo-isomer code	Chiral configuration				1C/3C <i>cis/trans</i>	Enantiomer pair	CAS no.
	1C	3C	α C	C-Br			
I	S	R	R	R	<i>cis</i> -	VIII	NA
J	S	R	R	S	<i>cis</i> -	VII	NA
K	S	R	S	R	<i>cis</i> -	VI	NA
L	S	R	S	S	<i>cis</i> -	V	NA
M	S	S	R	R	<i>trans</i> -	IV	NA
N	S	S	R	S	<i>trans</i> -	III	NA
O	S	S	S	R	<i>trans</i> -	II	NA
P	S	S	S	S	<i>trans</i> -	I	207347-23-7 abs

Cyano group is attached to the methyl position (α C)

See Table 2 (2.15) for generic structure and technical name of tralomethrin.

Table B30 Tralomethrin, technical products and mixtures

Name	CAS no.	Isomers – Composition	EPA PC code
Tralomethrin	66841-25-6	G + H	121-501

Table B31 Chrysanthemic acid, individual isomers (allethrin, phenothrin and resmethrin)

Stereo-isomer code	Chiral configuration			1C/3C <i>cis/trans</i>	Enantiomer pair	CAS no.
	1C	3C	OR ^a			
A	R	R	(+)–	<i>trans</i> -	I	4638-92-0 abs
B	R	S	(+)–	<i>cis</i> -	II	26771-11-9 abs
C	S	R	(–)–	<i>cis</i> -	II	26771-06-2 abs
D	S	S	(–)–	<i>trans</i> -	I	2259-14-5 abs

See Table 3 (3.1) for generic structure and technical name of chrysanthemic acid

^aOR = Optical rotation

Table B32 Chrysanthemum dicarboxylic acid, individual isomers

Stereo-isomer code	Chiral configuration			1C/3C <i>cis/trans</i>	Enantiomer pair	CAS no.
	1C	3C	OR			
A	R	R	(+)–	<i>trans</i> - (E)	I	72120-98-0 abs
B	R	S	(+)–	<i>cis</i> -	II	NA
C	S	R	(–)–	<i>cis</i> -	II	NA
D	S	S	(–)–	<i>trans</i> - (E)	I	33383-55-0 abs

See Table 3 (3.2) for generic structure and technical name of chrysanthemum dicarboxylic acid

OR = Optical rotation

NA = Not available

Table B33 Permethrinic acid, individual isomers

Stereo-isomer code	Chiral configuration		OR	1C/3C <i>cis/trans</i>	Enantiomer pair	CAS no.
	1C	3C				
A	R	R	(+)–	<i>cis</i> -	I	55667-40-8 abs
B	R	S	(+)–	<i>trans</i> -	II	55701-03-6 abs
C	S	R	(–)–	<i>trans</i> -	II	55701-09-2 abs
D	S	S	(–)–	<i>cis</i> -	I	55701-08-1 abs

OR = Optical rotation

See Table 3 (3.3) for generic structure and technical name of permethrinic acid

Table B34 Esfenvaleric acid/fenvaleric acid, individual isomers

Stereo-isomer code	Chiral configuration		OR ^a	Enantiomer pair	CAS no.
	α C				
A	R		(–)–	I	63640-09-5
B	S		(+)–	I	55332-38-2

See Table 3 (3.4) for generic structure and technical name of esfenvaleric/fenvaleric acid

^aOR = Optical rotation**Table B35** Decamethrinic acid, individual isomers

Stereo-isomer code	Chiral configuration		OR ^a	1C/3C <i>cis/trans</i>	Enantiomer pair	CAS no.
	1C	3C				
A	R	R	(+)–	<i>cis</i> -	I	53179-78-5 abs
B	R	S	(+)–	<i>trans</i> -	II	61914-48-5 abs
C	S	R	(–)–	<i>trans</i> -	II	74560-76-2 abs
D	S	S	(–)–	<i>cis</i> -	I	72691-18-0 abs

See Table 3 (3.5) for generic structure and technical name of decamethrinic acid

^aOR = Optical rotation

Appendix C: Chromatographic Separation of Pyrethroids and Their Isomers

Table C1 Separation of allethrin isomers (by HPLC, chiral or achiral columns)

Chiral column	Isomers/ enantiomer pairs/ diastereoisomer pairs	Separation conditions	Results
100 mm × 4.6 mm ID silica HPLC column (Chromolith, Merck), followed by 250 mm × 4.6 mm ID, CHIRALCEL OJ HPLC column (Chiral Technologies, Inc., West Chester, PA) ^a	A thru H <i>trans</i> - and <i>cis</i> - isomers separated independently	n-Hexane: <i>tert</i> -butylmethyl ether (96.4:4) v/v, Flow rate 1 ml min ⁻¹ followed by either <i>trans</i> -separation: Mobile phase: n-hexane/ <i>tert</i> -butylmethyl ether (90:10) v/v, Flow rate: 1 ml min ⁻¹ . or <i>cis</i> -separation: Mobile phase: n-hexane/isopropanol (99.3:0.7) v/v, Flow rate: 0.5 ml min ⁻¹	All eight stereoisomers were separated using two procedures
250 mm × 4.6 mm ID (RP-CSP-) silica gel modified with β-cyclodextrin; Cyclobond 1, 5 μm, HPLC column (Astec, Whippany, NJ, USA) ^b	A and H B and G	Mobile phase: acetonitrile/water (22:78) v/v Flow rate: 1 ml min ⁻¹	<i>trans</i> - isomers B, G, A, H were separated in the order above
250 mm × 4 mm ID, Sumichiral OA-4600 HPLC column (Sumika Chemical Analysis Service, Osaka, Japan) ^{c,d}	A thru H	Mobile phase: hexane/1,2-dichloroethane/ethanol (500:30:0.15) v/v/v; Flow rate: 1 ml min ⁻¹	Separation of all 8 stereoisomers

^a Mancini et al. (2004)

^b Kutter and Class (1992)

^c Oi et al. (1990)

^d Oi (2005)

Table C2 Separation of *cis*-Bifenthrin by HPLC and GLC, chiral column

Chiral column	Isomers/ enantiomer pairs/ diastereoisomer pairs	Separation conditions	Results
30 m × 0.25 mm, β-cyclodextrin-coated BGB-172 GC column, (BGB Analytik, Adliswil, Switzerland) ^{a, b}	Isomers: A and D	Helium, Flow rate: 1.5 ml min ⁻¹ . Initial temperature 180°C for 2 min., +1°C min ⁻¹ to 225°C, after 60 min., +5°C min ⁻¹ to 230°C, hold at 230°C.	Isomer A followed by D; at 54.3 and 55.5 min.
250 mm × 4.6 mm ID, Sumichiral OA-2500-1 HPLC column, (R)- N-(3,5-dinitrobenzoyl)- 1-naphthylglycine bonded to 3- aminopropylsilanized silica (Sumika Chemical Analysis Service, Osaka, Japan) ^c	Isomers: A and D	Hexane/1,2-dichloroethane (500:1) v/v, Flow rate: 1 ml min ⁻¹	Isomer A followed by D; at 10.57 and 11.25 min.
250 mm × 4 mm ID, Chirasphere 5 μm particle size HPLC column (Merck, Darmstadt, Germany) ^d	Isomers A, B, C, and D	Hexane/ethanol (99.5:0.5) v/v, Flow rate: 1 ml min ⁻¹	Isomers separated in the order C, B, A, and D

^a Liu W et al. (2005a) (Z)-(1RS)-*cis*-bifenthrin purchased from Chem Service, West Chester, PA. (1R-*cis*)-bifenthrin (97.2%) provided by FMC

^b Liu W et al. (2005c)

^c Liu W et al. (2005b)

^d Sanchez et al. (1996)

Table C3 Separation of cyfluthrin by GLC, chiral and achiral columns

Chiral/achiral columns	Isomers/enantiomer pairs/diastereoisomer pairs	Separation conditions	Results
250 mm × 4 mm ID, Chirex 00G-3019-DO HPLC column (Phenomenex, Torrance, CA) ^a (two columns used, amino acids or carboxylic acids covalently bonded to α-aminopropyl silica)	Isomers: A, B, C, D, E, F, G and H	Mobile phase hexane/1,2- dichloroethane/ ethanol (500:30:0.15) v/v/v	All isomers separated in the order A, H, G, B, C, F, E, D
CHIRALCEL OD HPLC column (Daicel Chemical Industries Ltd., Osaka, Japan) ^b	β-Cyfluthrin Isomers: B, G – II and D, E – IV	n-hexane/2- propanol (100 + 2, v/v) mobile phase.	All 4 isomers were baseline separated. Order <i>cis</i> -/ <i>cis</i> -/ <i>trans</i> -/ <i>trans</i> -

(continued)

Table C3 (continued)

Chiral/achiral columns	Isomers/enantiomer pairs/diastereoisomer pairs	Separation conditions	Results
250 mm × 4.6 mm ID, - CNP-silanized silica gel (5 μm) HPLC column (LabService, Milan, Italy)	Isomers: A, B, C, D, E, F, G, and H	n-Hexane/2-propanol (99.9:0.1) v/v	Enantiomer pairs I (A,H), II (B,G), III (C,F), and IV (D,E)
followed by:			
150 mm × 4.6 mm ID, CHIRALCEL OD-H, HPLC column (Daicel, Tokyo, Japan)		n-Hexane/2-propanol (99.5:0.5) v/v	Isomers A, G, H, B, E, D in that order.
or:			
Pirkle-type CSP (DNBPG) HPLC column, (Aldrich-Chimica, Milan, Italy) ^c		n-Hexane/2-propanol (99.9:0.1) v/v	Isomers C and F, in that order

^a Liu et al. (2005b)^b Li et al. (2003)^c Faraoni et al. (2004)**Table C4** Separation of cyhalothrin and lambda cyhalothrin by a CN achiral HPLC column

Chiral/achiral column	Isomers/enantiomer pairs/diastereoisomer pairs	Separation conditions	Results
250 mm × 4.6 mm ID, particle size 5 μm, Normal phase Nucleosil Sherisorb CN HPLC column (Shimadzu, Kyoto, Japan) ^a	Isomers: I (A + H), II (B + G). (in practice λ-Cyhalothrin is produced as enantiomer pairs I and II. Pair I has a low concentration.)	Mobile phase: n-hexane/tetrahydrofuran/2-propanol (99:0.9:0.1) v/v/v. Flow rate: 1.2 ml min ⁻¹ , T = 28°C	Separated B, G, A, and H isomers. II separated prior to I, B prior to G, and H prior to A
250 mm × 4.6 mm ID, cellulose tris(3,5-dimethylphenyl carbamate) CSP (CHIRALCEL OD-R, from Daicel Chemical Industries Ltd., Tokyo, Japan) ^b	Isomers B and G, enantiomer pair II, (λ-Cyhalothrin)	Mobile phase: Acetonitrile/water (70:30) v/v. Flow rate: 0.5 ml min ⁻¹ , diode array detector	Separated isomers B and G

^a Rao et al. (2004)^b Yang et al. (2004)

Table C5 Separation of cypermethrin isomers on chiral HPLC column

Chiral/achiral column	Isomers/enantiomer pairs/diastereoisomer pairs	Separation conditions	Results
250 mm × 4 mm ID, optically pure amino acids or carboxylic acids bonded to α -aminopropyl silica. Chirex 00G-3019-OD HPLC column (Phenomenex, Torrance CA) (two columns used) ^a	Isomers: A, B, C, D, E, F, G and H	Liu et al. Mobile phase: hexane/1,2-dichloroethane/ethanol (500:30:0.15) v/v/v	Separated A, H, G, B, C, F, E and D in order. <i>cis</i> - isomers before <i>trans</i> - isomers
CHIRALCEL OD HPLC column (Daicel Chemical Industries Ltd., Osaka, Japan) ^b	β -cypermethrin Isomers: B, G – II D, E – IV	Mobile phase: n-hexane/2-propanol (100 + 2) v/v	All 4 isomers were baseline separated. Order <i>cis</i> /trans/ <i>cis</i> /trans
250 mm × 4.6 mm ID, CDMPC-CSP HPLC column ^c	Theta-cypermethrin: Isomers D and E	Mobile phase: hexane/2-propanol (99:1) v/v, Flow rate: 0.8 ml min ⁻¹	Isomer E followed by D
250 mm × 4.6 mm ID, cellulose-tris(3,5-dimethylphenyl-carbamate) coated on α -aminopropyl silica ^d	Alpha-cypermethrin (B,G) Theta-cypermethrin (D,E) Beta-cypermethrin (B,G,D,E) Cypermethrin (A thru H)	n-hexane:2-propanol, flow rate 1 ml min ⁻¹ Alpha-C... and Theta-C... 10% 2-propanol Beta-C... and Cypermethrin, 1% 2-propanol	Alpha-C... both isomers separated Theta-C... both isomers separated Beta-C... All 4 isomers separated Cypermethrin, 7 of 8 isomers separated

^a Liu et al. (2005b)^b Li et al. (2003)^c Wang et al. (2006)^d Wang et al. (2004)**Table C6** Separation of deltamethrin isomers on chiral HPLC column

Chiral/achiral column	Isomers/enantiomer pairs/diastereoisomer pairs	Separation conditions	Results
250 mm × 4.6 mm ID, Spherisorb 5 μ m CN packing (Phase Separations, Deeside, UK) ^a	Isomers A, B	Mobile phase: hexane/propan-2-ol (99.9:0.1) v/v, Flow rate: 2 ml min ⁻¹	Isomer B was separated from isomer A
250 mm × 2 mm ID, CHIRALPAK AD HPLC column (GROM, Herrenberg-Kayh, Germany) ^b	Isomers B, G	Ethanol/water, (85:15) v/v. Flow rate: 0.3 ml min ⁻¹	Isomer B was separated from its enantiomer G

^a Cayley and Simpson (1986)^b Yang et al. (2004)

Table C7 Separation of fenvalerate by HPLC, chiral column

Chiral column	Isomers/enantiomer pairs/diastereoisomer pairs	Separation conditions	Results
250 mm × 4.6 mm ID, CSP HPLC column (Venusil XBP-NH3 and DIPEA in THF) ^a	Isomers: A, B, C and D	n-hexane/1,2-chloroethane/2-propanol (97.45:2.5:0.05) v/v/v, Flow rate: 1 ml min ⁻¹	Isomers C, B, A, and D were baseline separated in the order indicated
CHIRALCEL OD HPLC column (Daicel Chemical Industries Ltd., Osaka, Japan) ^b	fenvalerate Isomers: A, B, C and D	Mobile phase: n-hexane/2-propanol (100 + 6) v/v, Flow rate: 1 ml min ⁻¹	All 4 isomers were baseline separated
250 mm × 4.6 mm ID, 5 μm silica bonded to (R)-N-3,4-dinitrobenzoylphenylglycine Bakerbond HPLC column (J. T. Baker Co.) ^c	Isomers: A, B, C and D	Mobile phase: hexane/2-propanol (99.9:0.1) v/v. Flow rate: 1 ml min ⁻¹ Analysis in milk used: Mobile phase: methanol/2-propanol/hexane (0.1:0.3:99.6) v/v/v. flow rate: 1 ml min ⁻¹	Separated all 4 isomers
Pirkle type 1-A chiral HPLC column ^d	Isomers: A, B, C, and D	Hexane/2-propanol (100:0.1) v/v	Isomers B, C, D and A were separated in the order indicated

^aTan et al. (2007)^bLi et al. (2003)^cPapadopoulou-Mourkidou (1985)^dHuang et al. (1991)**Table C8** Separation of fenprothrin by HPLC, chiral column

Chiral column	Isomers/enantiomer pairs/diastereoisomer pairs	Separation conditions	Results
250 mm × 4.6 mm ID, CSP HPLC Column (Venusil XBP-NH3 and DIPEA in THF) ^a	Isomers: A and B	n-hexane/1,2-dichloromethane/2-propanol (96.8:3.0:0.2) v/v/v. Flow rate 1 ml min ⁻¹	Isomers A and B were baseline separated in the order indicated
250 mm × 4.6 mm ID, CHIRALCEL OD-R (Daicel Chemical Industries, Tokyo, Japan) ^b	Isomers: A and B	Mobile phase: ethanol/water (85:15) v/v. Flow rate: 0.3 ml min ⁻¹	Isomers A and B were baseline separated

^aTan et al. (2007)^bYang et al. (2004)

Table C9 Separation of fluvalinate by HPLC, chiral column

Chiral column	Isomers/enantiomer pairs/diastereoisomer pairs	Separation conditions	Results
250 mm × 4.6 mm ID, Pirkle type Sumichiral OA-4700, HPLC column (Sumika Chemical Analysis Services, Osaka, Japan) ^a	Enantiomers: (A + D), I and (B + C), II	Mobile phase: ether/isopropanol/dichloroethane (97.96:2.00:0.04) v/v/v, Flow rate: 1 ml min ⁻¹	Two enantiomer pairs were baseline separated. (A and D) and (B and C)
250 mm × 2 mm ID, CHIRALCEL OJ HPLC column, (GROM, Herrenberg-Kayh, Germany) ^b	Tau-fluvalinate: isomers A and B	Mobile phase: ethanol/n-hexane (10:90) v/v. Flow rate: 0.3 mL min ⁻¹	Isomers A and B were separated

^a Gao et al. (1998)^b Yang et al. (2004)**Table C10** Separation of permethrin by HPLC, chiral column

Chiral column	Isomers/enantiomer pairs/diastereoisomer pairs	Separation conditions	Results
250 mm × 4.6 mm ID, Sumichiral OA-25000-1 HPLC column (Sumika Chemical Analysis Service (Osaka, Japan) ^a	Isomers: A, B, C, and D	Mobile phase: n-hexane/1,2-dichloromethane (500:1) v/v	Isomers A, D, B and C were baseline separated in the order indicated
CHIRALCEL OJ HPLC column ^b	Isomers: A, B, C, and D	Mobile phase: hexane/ethanol (98:2.0) v/v. Flow rate: 1.5 ml min ⁻¹	Isomers D, A, B and C were baseline separated in the order indicated

^a Liu et al. (2005b)^b Ulrich et al. (2008)**Table C11** Separation of phenothrin by HPLC, chiral column

Chiral column	Isomers/enantiomer pairs/diastereoisomer pairs	Separation conditions	Results
250 mm × 4 mm ID, CHIRALCEL OD-H HPLC column, (Daicel, Tokyo, Japan) ^a	Isomers A and B	Mobile phase: n-hexane/2-propanol (99:1) v/v, Flow rate: 0.7 ml min ⁻¹	Separated isomers A and B

(continued)

Table C11 (continued)

Chiral column	Isomers/enantiomer pairs/diastereoisomer pairs	Separation conditions	Results
Covalently bonded Pirkle type I-A HPLC column ^b	Isomers A, B, C and D	Mobile phase: n-hexane:2-propanol (99.975:0.025) v/v, Flow rate: 1 ml min ⁻¹	Isomers B, C, A, and D were separated in the order indicated
250 mm × 4 mm ID, Sumichiral OA-2500I HPLC column, (Sumika Chemical Analysis Services, Osaka Japan) ^c	Isomers A, B, C, and D	Mobile phase: hexane/1,2-dichloroethane, (500:1) v/v, Flow rate: 1 ml min ⁻¹	All isomers separated

^a Girelli et al. (2002)^b Cayley and Simpson (1986)^c Oi et al. (1990)**Table C12** Separation of resmethrin by HPLC, chiral column

Chiral column	Isomers/enantiomer pairs/diastereoisomer pairs	Separation conditions	Results
250 mm × 4 mm ID, CHIRALCEL OD-H HPLC column, (Daicel, Tokyo, Japan) ^a	Isomers: A, B, C, and D	Mobile phase: n-hexane/2-propanol (99:1) v/v, Flow rate: 0.7 ml min ⁻¹	Separated all 4 isomers
250 mm × 4.6 mm ID, Pirkle type 1-A HPLC column (Phase Separations, Deeside, UK) ^b	Isomers: A, B, C, and D	Mobile phase: hexane/propen-2-ol (99.975:0.025) v/v, flow rate: 1 ml min ⁻¹	All 4 isomers in the order B, C, A, D
250 mm × 4 mm ID, Sumichiral OA-2500I HPLC column (Sumika Chemical Analysis Services, Osaka, Japan) ^c	Isomers A, B, C, and D	Mobile phase: hexane/1,2-dichloroethane, (500:1) v/v. Flow rate: 1 ml min ⁻¹	All 4 isomers separated

^a Girelli et al. (2002)^b Cayley and Simpson (1986)^c Oi et al. (1990)**Table C13** Tefluthrin

No chromatographic data.

Table C14 Separation of tetramethrin by HPLC, chiral column

Chiral column	Isomers/enantiomer pairs/diastereoisomer pairs	Separation conditions	Results
150 mm × 4.6 mm ID, CHIRALPAK AD-H HPLC column CSP, 5 μm silica-gel coated with amylose tris 3,5-dimethylphenyl-carbamate (Daicel Chemical Industries, Japan) ^a	Isomers A, B, C, D	Mobile phase: n-hexane/ethanol/2-propanol (99:0.9:0.1) v/v/v, Flow rate = 1 ml min ⁻¹ , Temp. = 35°C	Baseline separation of the 4 isomers of tetramethrin within 20 min. in the order B, D, A, C

^a Zhe et al. (2008)**Table C15** Separation of tralomethrin by HPLC, chiral column

Chiral column	Isomers/enantiomer pairs/diastereoisomer pairs	Separation conditions	Results
Li ChroCART 125-4 Superspher 100 RP-18 HPLC column (Hewlett-Packard, Palo Alto, CA, USA) ^a	Isomers: G and H	Isocratic elution with acetonitrile – (50 mM ammonium formate in water-acetonitrile, 95:5, acidified with formic acid, pH 3.5) (80:20). Flow rate: 1 ml min ⁻¹	Separated tralomethrin isomers into two peaks

^a Valverde et al. (2001)**Table C16** Separation of chrysanthemic acid by HPLC, chiral column

Chiral column	Isomers/enantiomer pairs/diastereoisomer pairs	Separation conditions	Results
CHIRALCEL OD and OF, and brush type Whelk-O 1 ^a	Isomers: A, B, C and D	Not indicated in abstract	Base-line separation
Glass capillary (60 m × 0.25 mm I.D.) coated with OA-300 ^b	Isomers: A, B, C, and D	Carrier gas, He at 0.57 ml min ⁻¹	Base-line separation of amide derivative, order B, C, A, D
Fused silica capillary (25 m × 0.25 I.D.) coated with CSP-2 ^{c,d}	Isomers: A, B, C, and D	Carrier gas, He at 0.8 ml min ⁻¹	Base-line separation in the order C, B, A, D
(0.25 m × 4.6 mm I.D.) stationary phase CSP-10 ^{d,e}	Isomers: A, B, C, and D	0.1 M ammonium acetate/tetrahydrofuran (60:40). Flow rate 1.0 ml min ⁻¹	Base-line separation in the order D, A, C, B

^a Lee and Kim (1998)^b Oi et al. (1981)^c Oi et al. (1996)^d Oi (2005)^e Oi et al. (1995)

Table C17 Separation of chrysanthemum dicarboxylic acid by HPLC, chiral column

Chiral column	Isomers/enantiomer pairs/ diastereoisomer pairs	Separation conditions	Results
GC (column not indicated) ^a	<i>E-cis/trans</i> CDCA Acid esterified with 1,1,1,3,3,3-hexafluoroisopropanol	Not indicated	Separated into two peaks

^a Elflein et al. (2003)**Table C18** Separation of permethrinic acid by HPLC, chiral column (permethrin, cypermethrin, cyfluthrin)

Chiral column	Isomers/enantiomer pairs/diastereoisomer pairs	Separation conditions	Results
5% phenyl methylpolysiloxane GC column (CP-SIL-8 CB capillary column) ^a	Isomers: <i>cis</i> - and <i>trans</i> - Cl ₂ CA (two chemicals)	Column: 60 m × 0.25 mm I.D., 0.25 μm film thickness	Methyl esters of <i>cis</i> - and <i>trans</i> - Cl ₂ CA baseline separated in less than 20 min. with <i>cis</i> - isomer followed by <i>trans</i> - isomer

^a Angerer and Ritter (1997)**Table C19** Separation of fenvaleric acid by HPLC, chiral column

Chiral column	Isomers/enantiomer pairs/diastereoisomer pairs	Separation conditions	Results
β-DEX-120 chiral GC column ^a	Isomers: (R) and (S) Fenvaleric acid	Conditions not indicated in abstract	Methyl esters were baseline separated
HPLC silica column ^b	Isomers: (R) and (S) Fenvaleric acid	Eluted with 25% ether-hexane	Baseline separated as amides of (-)-1-(1-phenyl)ethylamine

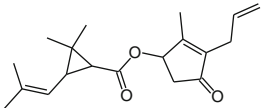
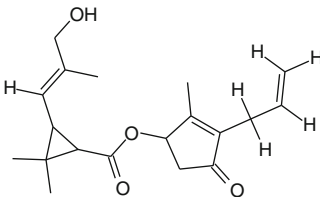
^a Li et al. (2006)^b Mugereng and Soderlund (1982)**Table C20** Separation of decamethrinic acid by HPLC, chiral column

Chiral column	Isomers/enantiomer pairs/diastereoisomer pairs	Separation conditions	Results
5% phenyl methylpolysiloxane GC column (CP-SIL-8 CB capillary column) ^a	Isomer: Br ₂ CL (stereochemistry not indicated)	Column: 60 m × 0.25 mm I.D., 0.25 μm film thickness	Methyl ester of Br ₂ CL separated from esters of <i>cis</i> - and <i>trans</i> - Cl ₂ CA

^a Angerer and Ritter (1997)

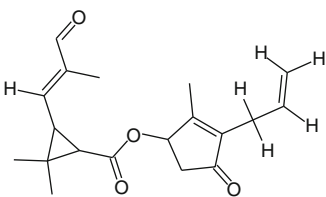
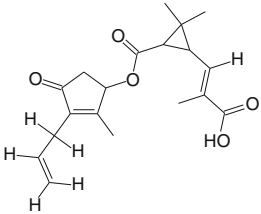
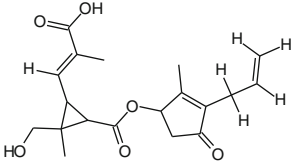
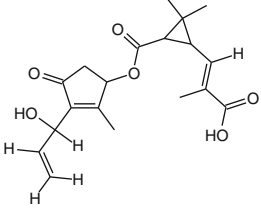
Appendix D: Chemical Structures, Physical Parameters, and Tissue: Partition Coefficients of Parent Pyrethroids and Metabolites

Table D1 Chemical structure, physical and chemical properties, and tissue partition coefficients for Allethrin and resulting metabolites

No. ^a	Chemical structure ^b	Pesticide metabolism and physical and chemical properties ^{c, d}	Partition coefficients ^e			
			Tissue	Rat	Human	
1.	Allethrin Cyclopropanecarboxylic, 2,2-dimethyl-3-(-2-methyl-1-propenyl-1-yl)-, 2-methyl-4-oxo-3-(2-propen-1-yl)-2-cyclopenten-1-yl ester					
		CAS no.	584-79-2	Fat	66.4	31.8
		MW, g/mol	302.41	Brain	7.39	8.98
		Exp Kow @ pH 7.4	NA	Rapid	4.62	2.18
		Log <i>D</i> @ pH 7.4	4.62	Kidney	5.48	3.38
		Log <i>P</i>	4.62	Liver	6.02	5.60
		pKa	NA	Slow	3.34	3.43
		<i>K</i> _p , cm/h ^f	0.0498	Skin	7.71	4.20
		Log <i>K</i> _p ^g	-1.302			
		WS, g/L (1.42E-3)	9.96E-3			
2.	Allethrin alcohol Cyclopropanecarboxylic acid, 3-[3-hydroxy-2-methyl-1-propen-1-yl]-2,2-dimethyl-, 2-methyl-4-oxo-3-(2-propen-1-yl)-2-cyclopenten-1-yl ester					
		CAS no.	23512-04-1	Fat	22.1	18.1
		MW, g/mol	318.41	Brain	11.6	8.64
		Exp Kow @ pH 7.4	NA	Rapid	3.81	2.18
		Log <i>D</i> @ pH 7.4	2.92	Kidney	4.50	3.32
		Log <i>P</i>	2.92	Liver	4.90	5.42
		pKa, MA	14.83	Slow	2.81	3.37
		WS, g/L (3.23E-2)	0.12	Skin	6.20	4.09

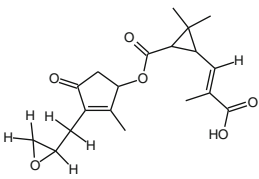
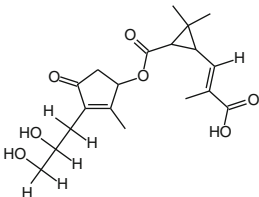
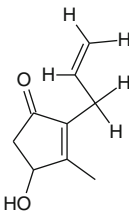
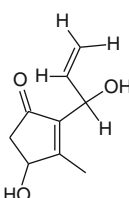
(continued)

Table D1 (continued)

No. ^a	Chemical structure ^b	Pesticide metabolism and physical and chemical properties ^{c, d}	Partition coefficients ^e		
			Tissue	Rat	Human
3	Allethrin aldehyde Cyclopropanecarboxylic acid, 2,2-dimethyl-3-[2-methyl-3-oxo-1-propen-1-yl]-, 2-methyl-4-oxo-3-(2-propen-1-yl)-2-cyclopenten-1-yl ester				
		CAS no.	23512-05-2	Fat	34.5 25.9
		MW, g/mol	316.39	Brain	13.3 9.27
		Exp Kow @ pH 7.4	NA	Rapid	4.31 2.30
		Log <i>D</i> @ pH 7.4	3.16	Kidney	5.09 3.53
		Log <i>P</i>	3.16	Liver	5.57 5.80
		pKa	NA	Slow	3.15 3.58
		WS, g/L (2.07E-2)	3.87E-2	Skin	7.08 4.36
4	Allethrin acid Cyclopropanecarboxylic acid, 3-[2-carboxy-1-propen-1-yl]-2,2-dimethyl-, 2-methyl-4-oxo-3-(2-propen-1-yl)-2-cyclopenten-1-yl ester				
		CAS no.	124915-69-1	Fat	0.21 0.24
		MW, g/mol	332.39	Brain	0.92 0.97
		Exp Kow @ pH 7.4	NA	Rapid	0.73 0.72
		Log <i>D</i> @ pH 7.4	0.69	Kidney	0.75 0.78
		Log <i>P</i>	3.08	Liver	0.70 0.83
		pKa, MA	4.99	Slow	0.69 0.76
		WS, g/L (2.15)	4.42	Skin	0.68 0.75
5	Allethrin hydroxymethyl acid Cyclopropanecarboxylic acid, 3-[2-carboxy-1-propen-1-yl]-2-(hydroxymethyl)-2-methyl-2-methyl-4-oxo-3-(2-propen-1-yl)-2-cyclopenten-1-yl ester				
		CAS no.	36912-77-3	Fat	0.12 0.17
		MW, g/mol	348.39	Brain	0.83 0.84
		Exp Kow @ pH 7.4	NA	Rapid	0.77 0.77
		Log <i>D</i> @ pH 7.4	-0.73	Kidney	0.78 0.80
		Log <i>P</i>	1.66	Liver	0.72 0.79
		pKa	4.99	Slow	0.75 0.77
		WS, g/L (28.15)	46.96	Skin	0.66 0.74
6	Allethrin hydroxy acid Cyclopropanecarboxylic acid, 3-[2-carboxy-1-propen-1-yl]-2,2-dimethyl-, 3-(1-hydroxy-2-propen-1-yl)-2-methyl-4-oxo-2-cyclopenten-1-yl ester				
		CAS no.	31338-06-4	Fat	0.09 0.13
		MW, g/mol	348.39	Brain	0.75 0.75
		Exp Kow @ pH 7.4	NA	Rapid	0.71 0.71
		Log <i>D</i> @ pH 7.4	-0.73	Kidney	0.71 0.73
		Log <i>P</i>	1.66	Liver	0.65 0.71
		pKa, MA	4.99	Slow	0.69 0.71
		WS, g/L (28.72)	42.36	Skin	0.60 0.67

(continued)

Table D1 (continued)

No. ^a	Chemical structure ^b	Pesticide metabolism and physical and chemical properties ^{c, d}	Partition coefficients ^e		
			Tissue	Rat	Human
7	Allethrin epoxide acid Cyclopropanecarboxylic acid, 3-[2-carboxy-1-propen-1-yl]-2,2-dimethyl-, 2-methyl-3-(oxiranylmethyl)-4-oxo-2-cyclopenten-1-yl ester				
		CAS no.	NA	Fat	0.13 0.18
		MW, g/mol	348.39	Brain	0.85 0.87
		Exp Kow @ pH 7.4	NA	Rapid	0.79 0.79
		Log <i>D</i> @ pH 7.4	-0.16	Kidney	0.80 0.82
		Log <i>P</i>	2.23	Liver	0.73 0.81
		pKa, MA	4.99	Slow	0.76 0.79
		WS, g/L (9.18)	4.34	Skin	0.68 0.76
8	Allethrin dihydroxy acid Cyclopropanecarboxylic acid, 3-[2-carboxy-1-propen-1-yl]-2,2-dimethyl-, 3-(2,3-dihydroxypropyl)-2-methyl-4-oxo-2-cyclopenten-1-yl ester				
		CAS no.	31338-05-3	Fat	0.12 0.18
		MW, g/mol	366.41	Brain	0.86 0.87
		Exp Kow @ pH 7.4	NA	Rapid	0.82 0.82
		Log <i>D</i> @ pH 7.4	-0.81	Kidney	0.82 0.85
		Log <i>P</i>	1.58	Liver	0.76 0.82
		pKa, MA	4.99	Slow	0.79 0.82
		WS, g/L (25.70)	38.45	Skin	0.69 0.78
	Hydrolysis products of esters: alcohol leaving groups, metabolites and conjugates				
9-1	Allethrolone + CCPCA 2-cyclopenten-1-one, 4-hydroxy-3-methyl-2-(2-propen-1-yl)-				
		CAS no.	29605-88-7	Fat	0.12 0.18
		MW, g/mol	152.19	Brain	0.87 0.87
		Exp Kow @ pH 7.4	NA	Rapid	0.83 0.83
		Log <i>D</i> @ pH 7.4	0.29	Kidney	0.83 0.85
		Log <i>P</i>	0.29	Liver	0.76 0.83
		pKa, MA	12.94	Slow	0.80 0.82
		WS, g/L (42.99)	15.87	Skin	0.70 0.78
10-2	Met B, hydrolysis product of allethrin hydroxy acid + Hydroxymethyl CCPCA 2-cyclopenten-1-one, 4-hydroxy-2-(1-hydroxy-2-propen-1-yl)-3-methyl-				
		CAS no.	NA	Fat	0.14 0.20
		MW, g/mol	168.19	Brain	0.92 0.93
		Exp Kow @ pH 7.4	NA	Rapid	0.85 0.85
		Log <i>D</i> @ pH 7.4	-0.26	Kidney	0.86 0.88
		Log <i>P</i>	-0.26	Liver	0.79 0.87
		pKa, A	12.72	Slow	0.82 0.85
		WS, g/L (107.45)	25.54	Skin	0.73 0.81

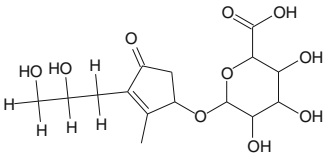
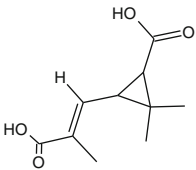
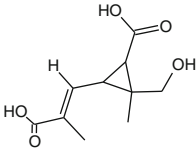
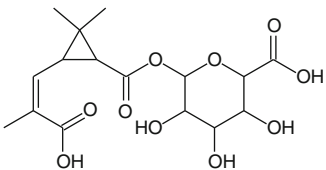
(continued)

Table D1 (continued)

No. ^a	Chemical structure ^b	Pesticide metabolism and physical and chemical properties ^{c, d}		Partition coefficients ^e			
				Tissue	Rat	Human	
11-3	Met A, hydrolysis product of allethrin dihydroxy acid + CCPCA 2-cyclopenten-1-one, 2-(2,3-dihydroxypropyl)-4-hydroxy-3-methyl-		CAS no.	NA	Fat	0.13	0.20
			MW, g/mol	186.21	Brain	0.92	0.93
			Exp Kow @ pH 7.4	NA	Rapid	0.88	0.88
			Log <i>D</i> @ pH 7.4	-1.24	Kidney	0.88	0.91
			Log <i>P</i>	-1.24	Liver	0.81	0.88
			p <i>K</i> _a , A	4.5	Slow	0.85	0.87
			WS, g/L (602.9)	43.53	Skin	0.74	0.83
12-4	Allethrolone glucuronic acid 2-cyclopenten-1-one, 4-(hexopyranuronosyloxy)-3-methyl-2-(2-propen-1-yl)-		CAS no.	NA	Fat	0.14	0.21
			MW, g/mol	328.31	Brain	0.94	0.95
			Exp Kow @ pH 7.4	NA	Rapid	0.90	0.90
			Log <i>D</i> @ pH 7.4	-3.4	Kidney	0.91	0.93
			Log <i>P</i>	0.31	Liver	0.83	0.90
			p <i>K</i> _a , MA	2.79	Slow	0.87	0.90
			WS, g/L (7,059.0)	1,000.0	Skin	0.76	0.85
13-5	Allethrolone sulfate 2-cyclopenten-1-one, 3-methyl-2-(2-propen-1-yl)-4-(sulfooxy)-		CAS no.	NA	Fat	0.13	0.20
			MW, g/mol	232.25	Brain	0.92	0.92
			Exp Kow @ pH 7.4	NA	Rapid	0.88	0.88
			Log <i>D</i> @ pH 7.4	-3.23	Kidney	0.88	0.91
			Log <i>P</i>	0.27	Liver	0.81	0.88
			p <i>K</i> _a , MA	-4.05	Slow	0.85	0.87
			WS, g/L (17,614.0)	1,000.0	Skin	0.74	0.83
14-6	Met B glucuronic acid 2-cyclopenten-1-one, 4-(hexopyranuronosyl)-2-(1-hydroxy-2-propen-1-yl)-3-methyl-		CAS no.	NA	Fat	0.14	0.21
			MW, g/mol	344.31	Brain	0.95	0.96
			Exp Kow @ pH 7.4	NA	Rapid	0.91	0.91
			Log <i>D</i> @ pH 7.4	-3.91	Kidney	0.91	0.94
			Log <i>P</i>	-0.19	Liver	0.84	0.91
			p <i>K</i> _a , MA	2.79	Slow	0.88	0.90
			WS, g/L (15,474.0)	1,000.0	Skin	0.77	0.86

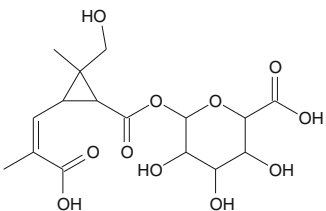
(continued)

Table D1 (continued)

No. ^a	Chemical structure ^b	Pesticide metabolism and physical and chemical properties ^{c, d}		Partition coefficients ^e		
				Tissue	Rat	Human
15-7	Met A glucuronic acid					
	2-(2,3-dihydroxypropyl)-4-(hexopyranuronosyloxy)-3-methyl-2-cyclopenten-1-one,					
		CAS no.	NA	Fat	0.14	0.21
		MW, g/mol	362.33	Brain	0.96	0.97
		Exp Kow @ pH 7.4	NA	Rapid	0.92	0.92
		Log <i>D</i> @ pH 7.4	-4.93	Kidney	0.92	0.95
		Log <i>P</i>	-1.22	Liver	0.85	0.92
		p <i>K</i> _a , MA	2.79	Slow	0.89	0.91
		WS, g/L (89,727.0)	1,000.0	Skin	0.78	0.87
	Hydrolysis products: Acid leaving groups and conjugates					
	Products for allethrin, phenothrin, resmethrin and tetramethrin					
16-1	(cis, trans) chrysanthemic dicarboxylic acid (CCPCA)					
	Cyclopropanecarboxylic acid, 3-[2-carboxy-1-propen-1-yl]-2,2-dimethyl-					
		CAS no.	497-95-0	Fat	0.12	0.19
		MW, g/mol	198.22	Brain	0.89	0.90
		Exp Kow @ pH 7.4	NA	Rapid	0.85	0.85
		Log <i>D</i> @ pH 7.4	-3.83	Kidney	0.86	0.88
		Log <i>P</i>	0.70	Liver	0.79	0.85
		p <i>K</i> _a , MA	4.64	Slow	0.83	0.85
		WS, g/L (86,060.0)	1,000.0	Skin	0.72	0.81
17-2	(cis, trans)-2-carboxy (cis, trans)-2-OH methyl (cis, trans)-chrysanthemic acid (2-OH Me CCPCA)					
	Cyclopropanecarboxylic acid, 3-[2-carboxy-1-propen-1-yl]-2-(hydroxymethyl)-2-methyl-					
		CAS no.	NA	Fat	0.13	0.20
		MW, g/mol	214.22	Brain	0.93	0.93
		Exp Kow @ pH 7.4	NA	Rapid	0.89	0.89
		Log <i>D</i> @ pH 7.4	-5.18	Kidney	0.89	0.92
		Log <i>P</i>	-0.6	Liver	0.82	0.89
		p <i>K</i> _a , MA	4.36	Slow	0.86	0.88
		WS, g/L (1E+06)	1,000.0	Skin	0.75	0.84
18-3	(cis, trans) CCPCA glucuronic acid					
	Hexopyranuronic acid, 1-O-[[3-[(1 <i>Z</i>)-2-carboxy-1-propen-1-yl]-2,2-dimethylcyclopropyl]carbonyl]-					
		CAS no.	NA	Fat	0.13	0.21
		MW, g/mol	374.34	Brain	0.94	0.95
		Exp Kow @ pH 7.4	NA	Rapid	0.90	0.90
		Log <i>D</i> @ pH 7.4	-3.99	Kidney	0.90	0.93
		Log <i>P</i>	0.74	Liver	0.83	0.90
		p <i>K</i> _a , MA	2.68	Slow	0.87	0.90
		WS, g/L (11,960.0)	1,000.0	Skin	0.76	0.85

(continued)

Table D1 (continued)

No. ^a	Chemical structure ^b	Pesticide metabolism and physical and chemical properties ^{c, d}	Partition coefficients ^e		
			Tissue	Rat	Human
19-4	(cis, trans) 2-hydroxymethyl (cis, trans) CCPCA glucuronic acid Hexopyranuronic acid, 1-O-[[3-[(1Z)-2-carboxy-1-propen-1-yl]-2-(hydroxymethyl)-2-methylcyclopropyl]carbonyl]-				
		CAS no.	NA	Fat	0.14 0.21
		MW, g/mol	390.34	Brain	0.95 0.96
		Exp Kow @ pH 7.4	NA	Rapid	0.91 0.92
		Log <i>D</i> @ pH 7.4	-5.41	Kidney	0.92 0.94
		Log <i>P</i>	-0.68	Liver	0.84 0.91
		pKa, MA	2.68	Slow	0.89 0.91
		WS, g/L (156,038.0)	1,000.0	Skin	0.77 0.86

^a Parent chemical or metabolite number for cross-reference to Table E1 ([Appendix E](#), Allethrin)

^b Metabolism source, Kaneko and Miyamoto (2001) and Kaneko (2010). CAS names are used from ACD/Names, version 12.0 (Advanced Chemistry Development, Toronto, Ontario, Canada)

^c NA = Not Available. WS (g/L) was obtained using the Syracuse Equation in Accord 6 for Excel (http://www.accelrys.com/products/accord/accordproducts/acc_4excel.html) and Log *D*_{pH7.4} above. Values in (...) after WS were calculated using ACD's Log *D* Solubility Suite, version 12.0 (<http://www.acdlabs.com/products/>)

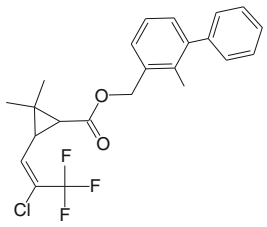
^d For pKa, A = acidic, MA = more acidic, MB = more basic

^e Tissue: blood partition coefficients

^f *K*_p, Table 20, Potts and Guy (1992)

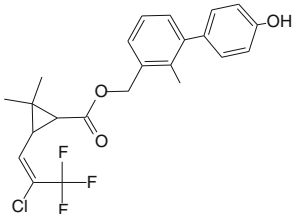
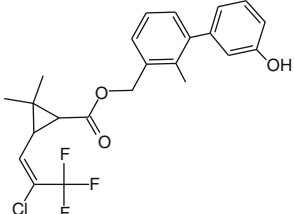
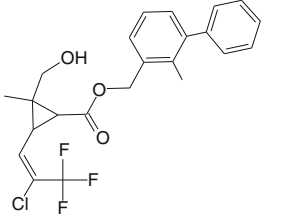
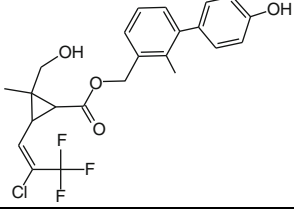
^g Log *K*_p, Table 20, Potts and Guy (1992)

Table D2 Chemical structure, physical and chemical properties, and tissue partition coefficients for bifenthrin and resulting metabolites

No. ^a	Chemical structure ^b	Pesticide metabolism and physical and chemical properties ^{c, d}	Partition coefficients ^e		
			Tissue	Rat	Human
1	Bifenthrin Cyclopropanecarboxylic acid, 3-[2-chloro-3,3,3-trifluoro-1-propen-yl]-2,2-dimethyl-(2-methyl[1,1'-biphenyl]-3-yl)methyl ester				
		CAS no.	99267-18-2	Fat	67.4 31.2
		MW, g/mol	442.87	Brain	14.5 8.94
		Exp Kow @ pH 7.4	NA	Rapid	4.62 2.17
		Log <i>D</i> @ pH 7.4	7.31	Kidney	5.48 3.36
		Log <i>P</i>	7.31	Liver	6.02 5.57
		pKa ^f	NA	Slow	3.34 3.42
		<i>K</i> _p , cm/h ^g	NA	Skin	7.71 4.18
		Log <i>K</i> _p	NA		
		WS, g/L (9.45E-7)	7.61E-5		

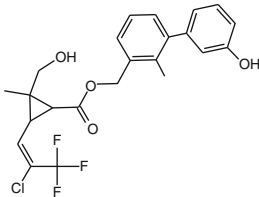
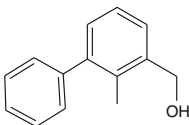
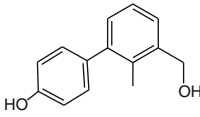
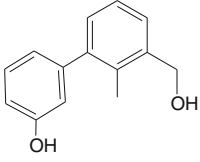
(continued)

Table D2 (continued)

No. ^a	Chemical structure ^b	Pesticide metabolism and physical and chemical properties ^{c, d}	Partition coefficients ^e		
			Tissue	Rat	Human
2	<p>4'-OH bifenthrin</p> <p>Cyclopropanecarboxylic acid, 3-[2-chloro-3,3,3-trifluoro-1-propen-1-yl]-2,2-dimethyl-, (4'-hydroxy-2-methyl[1,1'-biphenyl]-3-yl)methyl ester</p> 	<p>CAS no. 115404-73-4</p> <p>MW, g/mol 438.87</p> <p>Exp Kow @ pH 7.4 NA</p> <p>Log <i>D</i> @ pH 7.4 6.67</p> <p>Log <i>P</i> 6.67</p> <p>p<i>K</i>_a, MA 9.73</p> <p>WS, g/L (3.53E-6) 1.91E-4</p>	<p>Fat 67.5</p> <p>Brain 14.5</p> <p>Kidney 5.48</p> <p>Liver 6.02</p> <p>Skin 7.71</p>	<p>31.3</p> <p>8.94</p> <p>2.17</p> <p>3.36</p> <p>5.57</p> <p>4.18</p>	
3	<p>3'-OH bifenthrin</p> <p>Cyclopropanecarboxylic acid, 3-[2-chloro-3,3,3-trifluoro-1-propen-1-yl] 2,2-dimethyl-, (3'-hydroxy-2-methyl[1,1'-biphenyl]-3-yl)methyl ester</p> 	<p>CAS no. NA</p> <p>MW, g/mol 438.87</p> <p>Exp Kow @ pH 7.4 NA</p> <p>Log <i>D</i> @ pH 7.4 6.69</p> <p>Log <i>P</i> 6.69</p> <p>p<i>K</i>_a, MA 9.7</p> <p>WS, g/L (3.39E-6) 1.88E-4</p>	<p>Fat 67.5</p> <p>Brain 14.5</p> <p>Kidney 5.48</p> <p>Liver 6.02</p> <p>Skin 7.71</p>	<p>31.3</p> <p>8.94</p> <p>2.17</p> <p>3.36</p> <p>5.57</p> <p>4.18</p>	
4	<p>2-OH methyl bifenthrin</p> <p>Cyclopropanecarboxylic acid, 3-[2-chloro-3,3,3-trifluoro-1-yl]-2-(hydroxymethyl)-2-methyl-, (2-methyl[1,1'-biphenyl]-3-yl)methyl ester</p> 	<p>CAS no. NA</p> <p>MW, g/mol 438.87</p> <p>Exp Kow @ pH 7.4 NA</p> <p>Log <i>D</i> @ pH 7.4 5.89</p> <p>Log <i>P</i> 5.89</p> <p>p<i>K</i>_a, MA 15.1</p> <p>WS, g/L (1.63E-5) 7.31E-4</p>	<p>Fat 68.1</p> <p>Brain 14.5</p> <p>Kidney 5.48</p> <p>Liver 6.02</p> <p>Skin 7.71</p>	<p>31.6</p> <p>8.94</p> <p>2.17</p> <p>3.36</p> <p>5.58</p> <p>4.18</p>	
5	<p>4'-OH, 2-OH methyl bifenthrin</p> <p>Cyclopropanecarboxylic acid, 3-[2-chloro-3,3,3-trifluoro-1-propen-1-yl]-2-(hydroxymethyl)-2-methyl-, (2-methyl[1,1'-biphenyl]-3-yl)methyl ester</p> 	<p>CAS no. NA</p> <p>MW, g/mol 454.87</p> <p>Exp Kow @ pH 7.4 NA</p> <p>Log <i>D</i> @ pH 7.4 5.25</p> <p>Log <i>P</i> 5.25</p> <p>p<i>K</i>_a, MA 9.73</p> <p>WS, g/L (4.56E-5) 1.84E-3</p>	<p>Fat 70.8</p> <p>Brain 14.5</p> <p>Kidney 5.48</p> <p>Liver 6.02</p> <p>Skin 7.71</p>	<p>33.0</p> <p>8.95</p> <p>2.17</p> <p>3.37</p> <p>5.58</p> <p>4.18</p>	

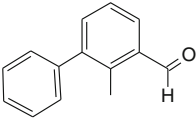
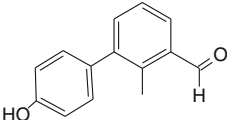
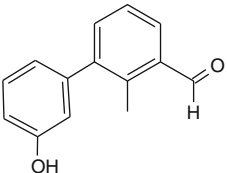
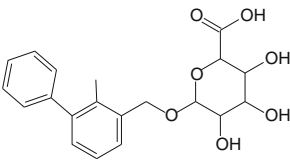
(continued)

Table D2 (continued)

No. ^a	Chemical structure ^b	Pesticide metabolism and physical and chemical properties ^{c, d}		Partition coefficients ^e		
				Tissue	Rat	Human
6	3'-OH, 2-OH methyl bifenthrin Cyclopropanecarboxylic acid, 3-[2-chloro-3,3,3-trifluoro-1-propen-1-yl]-2-(hydroxymethyl)-2-methyl-, (3'-hydroxy-2-methyl[1,1'-biphenyl]-3-yl)methyl ester 	CAS no.	NA	Fat	70.7	33.0
		MW, g/mol	454.87	Brain	14.5	8.95
		Exp Kow @ pH 7.4	NA	Rapid	4.62	2.17
		Log <i>D</i> @ pH 7.4	5.27	Kidney	5.48	3.37
		Log <i>P</i>	5.27	Liver	6.02	5.58
		p <i>K</i> _a , MA	9.7	Slow	3.34	3.42
		WS, g/L (4.38E-5)	1.80E-3	Skin	7.71	4.18
	Hydrolysis Products: Alcohol leaving groups, metabolites and conjugates					
7-1	2-MBP alcohol [1,1'-biphenyl]-3-methanol, 2-methyl 	CAS no.	76350-90-8	Fat	75.7	50.5
		MW, g/mol	198.26	Brain	14.0	9.25
		Exp Kow @ pH 7.4	NA	Rapid	4.48	2.27
		Log <i>D</i> @ pH 7.4	3.43	Kidney	5.31	3.50
		Log <i>P</i>	3.43	Liver	5.82	5.78
		p <i>K</i> _a , MA	14.28	Slow	3.26	3.56
		WS, g/L (5.26E-2)	0.51	Skin	7.43	4.34
8-2	4'-OH, 2-MBP alcohol [1,1'-biphenyl]-3-methanol, 4'-hydroxy-2-methyl 	CAS no.	115340-46-0	Fat	29.1	24.7
		MW, g/mol	214.26	Brain	11.2	8.73
		Exp Kow @ pH 7.4	NA	Rapid	3.73	2.23
		Log <i>D</i> @ pH 7.4	2.79	Kidney	4.38	3.38
		Log <i>P</i>	2.79	Liver	4.77	5.50
		p <i>K</i> _a , MA	9.75	Slow	2.76	3.43
		WS, g/L (1.53E-1)	0.8	Skin	6.02	4.15
9-3	3'-OH, 2-MBP alcohol [1,1'-biphenyl]-3-methanol, 3'-hydroxy-2-methyl 	CAS no.	NA	Fat	30.6	25.8
		MW, g/mol	214.26	Brain	11.4	8.80
		Exp Kow @ pH 7.4	NA	Rapid	3.77	2.25
		Log <i>D</i> @ pH 7.4	2.81	Kidney	4.44	3.41
		Log <i>P</i>	2.81	Liver	4.83	5.53
		p <i>K</i> _a , MA	9.71	Slow	2.79	3.45
		WS, g/L (1.47E-1)	0.79	Skin	6.10	4.17

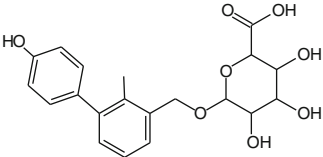
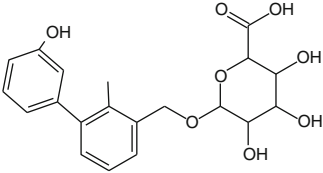
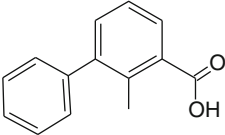
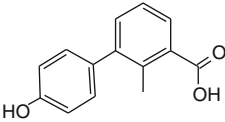
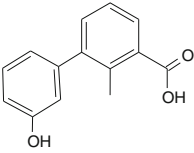
(continued)

Table D2 (continued)

No. ^a	Chemical structure ^b	Pesticide metabolism and physical and chemical properties ^{c, d}	Partition coefficients ^e		
			Tissue	Rat	Human
10-4	2-MBP aldehyde [1,1'-biphenyl]-3-carboxaldehyde, 2-methyl-				
		CAS no.	89951-60-0	Fat	99.5 57.8
		MW, g/mol	195.24	Brain	14.4 9.17
		Exp Kow @ pH 7.4	NA	Rapid	4.59 2.24
		Log <i>D</i> @ pH 7.4	3.75	Kidney	5.44 3.46
		Log <i>P</i>	3.75	Liver	5.97 5.73
		pKa, MA	NA	Slow	3.33 3.52
		WS, g/L (2.90E-2)	3.01E-2	Skin	7.63 4.29
11-5	4'-OH, 2-MBP aldehyde [1,1'-biphenyl]-3-carboxaldehyde, 4'-hydroxy-2-methyl-				
		CAS no.	NA	Fat	52.6 40.3
		MW, g/mol	212.24	Brain	13.1 9.24
		Exp Kow @ pH 7.4	NA	Rapid	4.25 2.30
		Log <i>D</i> @ pH 7.4	3.11	Kidney	5.02 3.53
		Log <i>P</i>	3.11	Liver	5.49 5.79
		pKa, MA	9.68	Slow	6.26 3.58
		WS, g/L (8.35E-2)	7.98E-2	Skin	3.11 4.35
12-6	3'-OH, 2-MBP aldehyde [1,1'-biphenyl]-3-carboxaldehyde, 3'-hydroxy-2-methyl-				
		CAS no.	NA	Fat	39.1 31.6
		MW, g/mol	212.24	Brain	12.2 9.04
		Exp Kow @ pH 7.4	NA	Rapid	4.02 2.28
		Log <i>D</i> @ pH 7.4	2.95	Kidney	4.73 3.47
		Log <i>P</i>	2.95	Liver	5.17 5.67
		pKa, MA	9.67	Slow	2.95 3.52
		WS, g/L (11.44E-2)	9.12E-2	Skin	6.55 4.27
13-7	2-MBP alcohol glucuronic acid Hexopyranosiduronic acid, (2-methyl[1,1'-biphenyl]-3-yl)methyl				
		CAS no.	NA	Fat	0.13 0.19
		MW, g/mol	374.38	Brain	0.89 0.89
		Exp Kow @ pH 7.4	NA	Rapid	0.83 0.83
		Log <i>D</i> @ pH 7.4	-0.55	Kidney	0.84 0.86
		Log <i>P</i>	3.16	Liver	0.77 0.84
		pKa	NA	Slow	0.81 0.83
		WS, g/L (12.98)	1,000.0	Skin	0.71 0.79
14-8	4'-OH, 2-MBP alcohol glucuronic acid Hexopyranosiduronic acid, (4'-hydroxy-2-methyl[1,1'-biphenyl]-3-yl)methyl				
		CAS no.	NA	Fat	0.12 0.19
		MW, g/mol	390.38	Brain	0.90 0.90
		Exp Kow @ pH 7.4	NA	Rapid	0.85 0.85
		Log <i>D</i> @ pH 7.4	-1.19	Kidney	0.86 0.88
		Log <i>P</i>	2.52	Liver	0.79 0.85

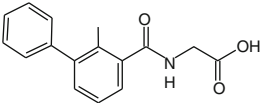
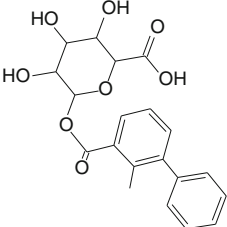
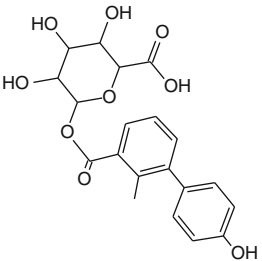
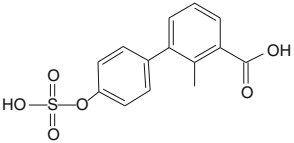
(continued)

Table D2 (continued)

No. ^a	Chemical structure ^b	Pesticide metabolism and physical and chemical properties ^{c, d}		Partition coefficients ^e		
				Tissue	Rat	Human
		pKa, MA	2.8	Slow	0.83	0.85
		WS, g/L (36.46E-2)	1,000.0	Skin	0.72	0.81
15-9	3'-OH, 2-MBP alcohol glucuronic acid Hexopyranosiduronic acid, (3'-hydroxy-2-methyl[1,1'-biphenyl]-3-yl)methyl	CAS no.	NA	Fat	0.12	0.19
		MW, g/mol	390.38	Brain	0.90	0.90
		Exp Kow @ pH 7.4	NA	Rapid	0.85	0.85
		Log D @ pH 7.4	-1.17	Kidney	0.86	0.88
		Log P	2.54	Liver	0.79	0.85
		pKa, MA	2.8	Slow	0.83	0.85
		WS, g/L (35.05)	1,000.0	Skin	0.72	0.81
16-10	2-MBP acid [1,1'-biphenyl]-3-carboxylic acid	CAS no.	115363-11-6	Fat	0.31	0.35
		MW, g/mol	212.24	Brain	1.07	1.14
		Exp Kow @ pH 7.4	NA	Rapid	0.80	0.78
		Log D @ pH 7.4	0.85	Kidney	0.82	0.86
		Log P	3.85	Liver	0.78	0.94
		pKa, MA	3.89	Slow	0.75	0.84
		WS, g/L (7.11)	69.9	Skin	0.76	0.84
17-11	4'-OH, 2-MBP acid [1,1-biphenyl]-3-carboxylic acid, 4'-hydroxy-2-methyl-	CAS no.	NA	Fat	0.15	0.19
		MW, g/mol	228.24	Brain	0.87	0.89
		Exp Kow @ pH 7.4	NA	Rapid	0.79	0.77
		Log D @ pH 7.4	0.21	Kidney	0.78	0.81
		Log P	3.21	Liver	0.73	0.81
		pKa, MA	3.91	Slow	0.75	0.78
		WS, g/L (20.58)	185.81	Skin	0.68	0.75
18-12	3'-OH, 2-MBP acid [1,1'-biphenyl]-3-carboxylic acid, 3'-hydroxy-2-methyl-	CAS no.	NA	Fat	0.15	0.20
		MW, g/mol	228.24	Brain	0.87	0.90
		Exp Kow @ pH 7.4	NA	Rapid	0.78	0.77
		Log D @ pH 7.4	0.22	Kidney	0.79	0.81
		Log P	3.23	Liver	0.73	0.81
		pKa, MA	3.87	Slow	0.75	0.78
		WS, g/L (20.18)	184.8	Skin	0.68	0.76

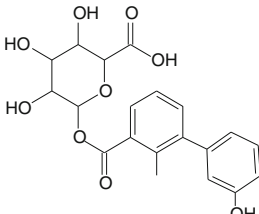
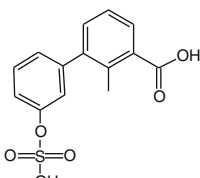
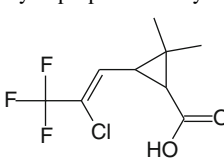
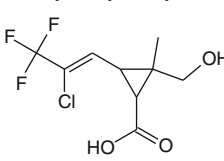
(continued)

Table D2 (continued)

No. ^a	Chemical structure ^b	Pesticide metabolism and physical and chemical properties ^{c, d}	Partition coefficients ^e		
			Tissue	Rat	Human
19-13	2-MBP acid glycine Glycine, N-[(2-methyl[1,1'-biphenyl]-3-yl)carbonyl]- 	CAS no. NA MW, g/mol 269.3 Exp Kow @ pH 7.4 NA Log <i>D</i> @ pH 7.4 -0.33 Log <i>P</i> 3.26 pKa, MA 3.63 WS, g/L (35.28) 808.0	Fat 0.09 Brain 0.74 Rapid 0.70 Kidney 0.70 Liver 0.64 Slow 0.67 Skin 0.59	0.13 0.75 0.70 0.72 0.71 0.70 0.66	
20-14	2-MBP acid glucuronide Hexopyranuronic acid, 1-O-[(2-methyl[1,1'-biphenyl]-3-yl)carbonyl]- 	CAS no. NA MW, g/mol 388.37 Exp Kow @ pH 7.4 NA Log <i>D</i> @ pH 7.4 -0.85 Log <i>P</i> 2.87 pKa, MA 2.67 WS, g/L (19.22) 830.74	Fat 0.12 Brain 0.88 Rapid 0.83 Kidney 0.84 Liver 0.77 Slow 0.80 Skin 0.70	0.18 0.88 0.83 0.86 0.83 0.72 0.68	
21-15	4'-OH, 2-MBP acid glucuronide Hexopyranuronic acid, 1-O-[(4'-hydroxy-2-methyl[1,1'-biphenyl]-3-yl)carbonyl]- 	CAS no. NA MW, g/mol 404.37 Exp Kow @ pH 7.4 NA Log <i>D</i> @ pH 7.4 -1.49 Log <i>P</i> 2.23 pKa, A 9.65 WS, g/L (53.90) 1,000.0	Fat 0.12 Brain 0.89 Rapid 0.85 Kidney 0.85 Liver 0.78 Slow 0.82 Skin 0.72	0.19 0.90 0.85 0.88 0.85 0.85 0.80	
22-16	4'-OH, 2-MBP acid sulfate [1,1'-biphenyl]-3-carboxylic acid, 2-methyl-4'-(sulfoxy)- 	CAS no. NA MW, g/mol 308.31 Exp Kow @ pH 7.4 NA Log <i>D</i> @ pH 7.4 -1.94 Log <i>P</i> 2.55 pKa, MA -3.98 WS, g/L (498.0) 1,000.0	Fat 0.12 Brain 0.90 Rapid 0.85 Kidney 0.86 Liver 0.79 Slow 0.83 Skin 0.72	0.19 0.90 0.86 0.88 0.85 0.85 0.81	

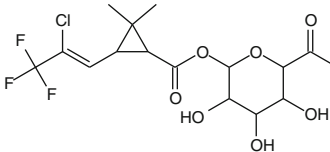
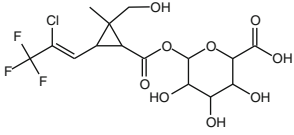
(continued)

Table D2 (continued)

No. ^a	Chemical structure ^b	Pesticide metabolism and physical and chemical properties ^{c, d}	Partition coefficients ^e		
			Tissue	Rat	Human
23-17	3'-OH, 2-MBP acid glucuronide				
	Hexopyranuronic acid, 1-O-[(3'-hydroxy-2-methyl[1,1'-biphenyl]-3-yl)carbonyl]-				
		CAS no.	NA	Fat	0.12 0.19
		MW, g/mol	404.37	Brain	0.90 0.90
		Exp Kow @ pH 7.4	NA	Rapid	0.85 0.85
		Log <i>D</i> @ pH 7.4	-1.47	Kidney	0.85 0.88
		Log <i>P</i>	2.25	Liver	0.78 0.85
		pKa, A	9.64	Slow	0.82 0.84
		WS, g/L (51.80)	1,000	Skin	0.72 0.80
24-18	3'-OH, 2-MBP acid sulfate				
	[1,1-biphenyl]-3-carboxylic acid, 2-methyl-3'-(sulfoxy)-				
		CAS no.	NA	Fat	0.12 0.19
		MW, g/mol	308.31	Brain	0.90 0.90
		Exp Kow @ pH 7.4	NA	Rapid	0.85 0.86
		Log <i>D</i> @ pH 7.4	-2.08	Kidney	0.86 0.88
		Log <i>P</i>	2.24	Liver	0.80 0.85
		pKa, MA	-4.01	Slow	0.83 0.85
		WS, g/L (655.9)	1,000.0	Skin	0.72 0.81
	Hydrolysis products: Acid leaving groups, metabolites and conjugates				
25-1	TFP acid				
	Cyclopropanecarboxylic acid, 3-[2-chloro-3,3,3-trifluoro-1-propen-1-yl]-2,2-dimethyl				
		CAS no.	74609-46-4	Fat	0.09 0.14
		MW, g/mol	242.62	Brain	0.77 0.77
		Exp Kow @ pH 7.4	NA	Rapid	0.73 0.74
		Log <i>D</i> @ pH 7.4	-1.35	Kidney	0.74 0.76
		Log <i>P</i>	1.78	Liver	0.68 0.73
		pKa, MA	4.15	Slow	0.71 0.73
		WS, g/L (875.9)	1,000.0	Skin	0.62 0.69
26-2	2-OH methyl TFP acid (cis and trans configuration)				
	Cyclopropanecarboxylic acid, 3-[2-chloro-3,3,3-trifluoro-1-propenyl-1-yl]-2-(hydroxymethyl)-2-methyl-				
		CAS no.	107900-83-4	Fat	0.11 0.17
		MW, g/mol	258.62	Brain	0.86 0.86
		Exp Kow @ pH 7.4	NA	Rapid	0.82 0.82
		Log <i>D</i> @ pH 7.4	-2.78	Kidney	0.75 0.85
		Log <i>P</i>	0.48	Liver	0.83 0.82
		pKa, MA	3.87	Slow	0.79 0.81
		WS, g/L (13,590.4)	1,000.0	Skin	0.70 0.77

(continued)

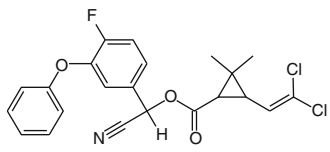
Table D2 (continued)

No. ^a	Chemical structure ^b	Pesticide metabolism and physical and chemical properties ^{c, d}	Partition coefficients ^e				
			Tissue	Rat	Human		
27-3	TFP acid glucuronide Hexopyranuronic acid, 1-O-[[3-[2-chloro-3,3,3-trifluoro-1-propen-1-yl]-2,2-dimethylcyclopropyl]carbonyl]-		CAS no.	120851-78-7	Fat	0.12	0.19
		MW, g/mol	418.75	Brain	0.89	0.89	
		Exp Kow @ pH 7.4	NA	Rapid	0.85	0.85	
		Log <i>D</i> @ pH 7.4	-1.89	Kidney	0.85	0.87	
		Log <i>P</i>	1.83	Liver	0.78	0.85	
		p <i>K</i> _a , MA	2.68	Slow	0.82	0.84	
		WS, g/L (96.27)	1,000.0	Skin	0.71	0.80	
28-4	2-OH methyl TFP acid glucuronide Hexopyranuronic acid, 1-O-[[3-[2-chloro-3,3,3-trifluoro-1-propen-1-yl]-2-(hydroxymethyl)-2-methylcyclopropyl]carbonyl]-		CAS no.	NA	Fat	0.13	0.20
		MW, g/mol	434.75	Brain	0.93	0.93	
		Exp Kow @ pH 7.4	NA	Rapid	0.88	0.88	
		Log <i>D</i> @ pH 7.4	-3.31	Kidney	0.88	0.91	
		Log <i>P</i>	0.41	Liver	0.81	0.88	
		p <i>K</i> _a , MA	2.68	Slow	0.86	0.88	
		WS, g/L (1,247.3)	1,000.0	Skin	0.74	0.83	

^a Parent chemical or metabolite number for cross-reference to Table E2 ([Appendix E](#), Bifenthrin)

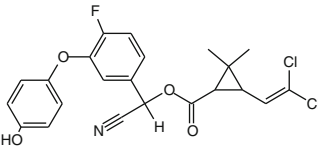
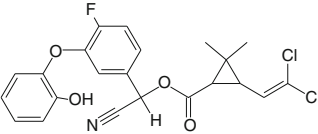
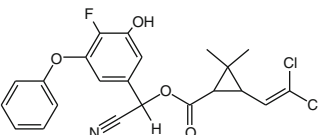
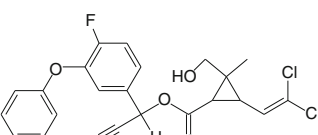

^{b-g} Metabolism source, Kaneko and Miyamoto (2001) and Kaneko (2010). See footnotes in Table D1 ([Appendix D](#))

Table D3 Chemical structure, physical and chemical properties, and tissue partition coefficients for cyfluthrin and resulting metabolites

No. ^a	Chemical structure ^b	Pesticide metabolism and physical and chemical properties ^{c, d}	Partition coefficients ^e				
			Tissue	Rat	Human		
1	Cyfluthrin Cyclopropanecarboxylic acid, 3-(2,2-dichloroethenyl)-2,2-dimethyl-, cyano(4-fluoro-3-phenoxyphenyl)methyl ester		CAS no.	68359-37-5	Fat	67.59	31.31
		MW, g/mol	434.29	Brain	14.52	8.94	
		Exp Kow @ pH 7.4	NA	Rapid	4.62	2.17	
		Log <i>D</i> @ pH 7.4	6.42	Kidney	5.48	3.36	
		Log <i>P</i>	6.42	Liver	6.02	5.57	
		p <i>K</i> _a	NA	Slow	3.34	3.42	
		<i>K</i> _p , cm/h ^f	0.146	Skin	7.71	4.18	
		Log <i>K</i> _p ^g	-0.835				
		WS, g/L (6.15E-6)	1.68E-5				

(continued)

Table D3 (continued)

No. ^a	Chemical structure ^b	Pesticide metabolism and physical and chemical properties ^{c, d}	Partition coefficients ^e				
			Tissue	Rat	Human		
2	4'-OH cyfluthrin Cyclopropanecarboxylic acid, 3-(2,2-dichloroethenyl)-2,2-dimethyl-,cyano[4-fluoro-3-(4-hydroxyphenoxy)phenyl]methyl ester		CAS no. MW, g/mol Exp Kow @ pH 7.4 Log <i>D</i> @ pH 7.4 Log <i>P</i> p <i>K</i> _a , MA WS, g/L (2.31E-5)	NA 450.29 NA 5.63 5.63 9.73 4.77E-5	Fat Brain Rapid Kidney Liver Slow Skin	68.83 14.52 4.62 5.48 6.02 3.34 7.71	31.96 2.75 0.67 1.04 1.72 1.05 1.29
3	2'-OH cyfluthrin Cyclopropanecarboxylic acid, 3-(2,2-dichloroethenyl)-2,2-dimethyl-,cyano[4-fluoro-3-(2-hydroxyphenoxy)phenyl]methyl ester		CAS no. MW, g/mol Exp Kow @ pH 7.4 Log <i>D</i> @ pH 7.4 Log <i>P</i> p <i>K</i> _a , MA WS, g/L (1.75E-5)	NA 450.29 NA 5.77 5.78 8.91 4.33E-5	Fat Brain Rapid Kidney Liver Slow Skin	68.42 14.52 4.62 5.48 6.02 3.34 7.71	31.74 2.73 0.66 1.03 1.55 1.04 1.28
4	5-OH cyfluthrin Cyclopropanecarboxylic acid, 3-(2,2-dichloroethenyl)-2,2-dimethyl-,cyano (4-fluoro-3-hydroxy-5-phenoxyphenyl)methyl ester		CAS no. MW, g/mol Exp Kow @ pH 7.4 Log <i>D</i> @ pH 7.4 Log <i>P</i> p <i>K</i> _a , MA WS, g/L (1.75E-5)	NA 450.29 NA 5.77 6.14 7.26 7.35E-5	Fat Brain Rapid Kidney Liver Slow Skin	68.41 14.52 4.62 5.48 6.02 3.34 7.71	31.74 8.94 2.17 3.37 5.58 3.42 4.18
5	2-OH methyl cyfluthrin Cyclopropanecarboxylic acid, 3-(2,2-dichloroethenyl)-2-(hydroxymethyl)-2-methyl-,cyano(4-fluoro-3-phenoxyphenyl) methyl ester		CAS no. MW, g/mol Exp Kow @ pH 7.4 Log <i>D</i> @ pH 7.4 Log <i>P</i> p <i>K</i> _a , MA WS, g/L (8.13E-5)	NA 450.29 NA 4.99 4.99 15.1 1.61E-4	Fat Brain Rapid Kidney Liver Slow Skin	73.93 14.52 4.61 5.48 6.02 3.34 7.71	34.71 8.96 2.17 3.37 5.59 3.42 3.81
6	4'-OH, 2-OH methyl cyfluthrin Cyclopropanecarboxylic acid, 3-(2,2-dichloroethenyl)-2-(hydroxymethyl)-2-methyl-,cyano[4-fluoro-3-(4-hydroxyphenoxy)phenyl]methyl ester		CAS no. MW, g/mol	NA 466.29	Fat Brain	90.08 14.48	45.62 9.04

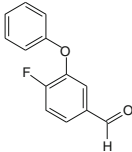
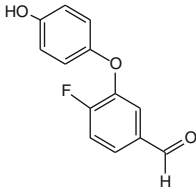
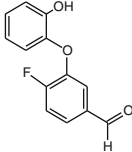
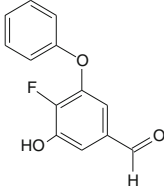
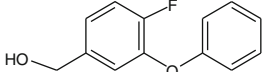
(continued)

Table D3 (continued)

No. ^a	Chemical structure ^b	Pesticide metabolism and physical and chemical properties ^{c, d}		Partition coefficients ^e		
				Tissue	Rat	Human
		Exp Kow @ pH 7.4	NA	Rapid	4.61	2.20
		Log <i>D</i> @ pH 7.4	4.21	Kidney	5.47	3.40
		Log <i>P</i>	4.21	Liver	6.01	5.63
		p <i>K</i> _a , MA	9.73	Slow	3.34	3.46
		WS, g/L (2.98E-4)	4.58E-4	Skin	7.69	4.22
	Hydrolysis products: Alcohol leaving group, metabolites and conjugates					
7-1	Cyanohydrin of 4'-fluoro PB aldehyde					
	Benzeneacetonitrile, 4-fluoro- α -hydroxy-3-phenoxy-					
		CAS no.	76783-44-3	Fat	19.06	16.91
		MW, g/mol	243.23	Brain	9.50	8.04
		Exp Kow @ pH 7.4	NA	Rapid	3.25	2.13
		Log <i>D</i> @ pH 7.4	2.57	Kidney	3.80	3.18
		Log <i>P</i>	2.57	Liver	4.11	5.09
		p <i>K</i> _a , MA	10.08	Slow	2.44	3.21
		WS, g/L (1.65E-1)	6.07E-2	Skin	5.14	3.86
8-2	Cyanohydrin of 4'-OH, 4'-fluoro PB aldehyde					
	Benzeneacetonitrile, 4-fluoro- α -hydroxy-3-(4-hydroxyphenoxy)-					
		CAS no.	NA	Fat	3.11	2.98
		MW, g/mol	259.23	Brain	3.45	3.71
		Exp Kow @ pH 7.4	NA	Rapid	1.53	1.33
		Log <i>D</i> @ pH 7.4	1.78	Kidney	1.70	1.77
		Log <i>P</i>	1.78	Liver	1.75	2.51
		p <i>K</i> _a , MA	9.74	Slow	1.27	1.76
		WS, g/L (6.34E-1)	0.18	Skin	2.02	2.00
9-3	Cyanohydrin of 2'-OH, 4'-fluoro-PB aldehyde					
	Benzeneacetonitrile, 4-fluoro- α -hydroxy-3-(2-hydroxyphenoxy)-					
		CAS no.	NA	Fat	4.38	4.15
		MW, g/mol	259.23	Brain	4.26	4.46
		Exp Kow @ pH 7.4	NA	Rapid	1.77	1.48
		Log <i>D</i> @ pH 7.4	1.92	Kidney	1.98	2.02
		Log <i>P</i>	1.93	Liver	2.07	2.96
		p <i>K</i> _a , MA	8.93	Slow	1.43	2.02
		WS, g/L (4.82E-1)	0.16	Skin	2.44	2.32
10-4	Cyanohydrin of 5-OH, 4'-fluoro-PB aldehyde					
	Benzeneacetonitrile, 4-fluoro- α ,3-dihydroxy-5-phenoxy-					
		CAS no.	NA	Fat	5.47	5.16
		MW, g/mol	259.23	Brain	4.87	5.00
		Exp Kow @ pH 7.4	NA	Rapid	1.94	1.58
		Log <i>D</i> @ pH 7.4	2.01	Kidney	2.20	2.20
		Log <i>P</i>	2.29	Liver	2.31	3.28
		p <i>K</i> _a , MA	7.45	Slow	1.55	2.20
		WS, g/L (4.04E-1)	0.22	Skin	2.75	2.56

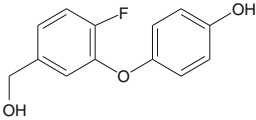
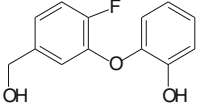
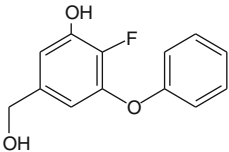
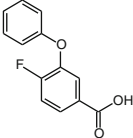
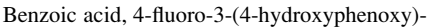
(continued)

Table D3 (continued)

No. ^a	Chemical structure ^b	Pesticide metabolism and physical and chemical properties ^{c, d}	Partition coefficients ^e		
			Tissue	Rat	Human
11-5	4-fluoro-PB aldehyde Benzaldehyde, 4-fluoro-3-phenoxy-	 CAS no. 68359-57-9 MW, g/mol 216.21 Exp Kow @ pH 7.4 NA Log <i>D</i> @ pH 7.4 3.16 Log <i>P</i> 3.16 pKa NA WS, g/L (7.21E-2) 1.12E-2	Fat	60.93	45.75
			Brain	13.35	9.32
			Rapid	4.33	2.31
			Kidney	5.12	3.55
			Liver	5.60	5.84
			Slow	3.17	3.60
			Skin	7.13	4.39
12-6	4'-OH, 4-fluoro-PB aldehyde Benzaldehyde, 4-fluoro-3-(4-hydroxyphenoxy)-	 CAS no. NA MW, g/mol 232.21 Exp Kow @ pH 7.4 NA Log <i>D</i> @ pH 7.4 2.37 Log <i>P</i> 2.37 pKa, MA 9.97 WS, g/L (2.80E-1) 3.32E-2	Fat	12.03	10.97
			Brain	7.68	7.02
			Rapid	2.73	1.94
			Kidney	3.16	2.84
			Liver	3.39	4.48
			Slow	2.09	2.87
			Skin	4.20	3.42
13-7	2'-OH, 4-fluoro-PB aldehyde Benzaldehyde, 4-fluoro-3-(2-hydroxyphenoxy)-	 CAS no. NA MW, g/mol 232.21 Exp Kow @ pH 7.4 NA Log <i>D</i> @ pH 7.4 2.51 Log <i>P</i> 2.52 pKa, MA 8.93 WS, g/L (2.13E-1) 3.01E-2	Fat	16.71	14.97
			Brain	8.97	7.77
			Rapid	3.10	2.08
			Kidney	3.61	3.09
			Liver	3.90	4.93
			Slow	2.34	3.12
			Skin	4.87	3.75
14-8	5-OH, 4-fluoro-PB aldehyde Benzaldehyde, 4-fluoro-3-hydroxy-5-phenoxy- (or 4-fluoro-3-phenoxy-5-hydroxy)	 CAS no. NA MW, g/mol 232.21 Exp Kow @ pH 7.4 NA Log <i>D</i> @ pH 7.4 2.78 Log <i>P</i> 3.12 pKa, MA 7.32 WS, g/L (1.25E-1) 3.92E-2	Fat	30.84	26.21
			Brain	11.29	8.83
			Rapid	3.76	2.26
			Kidney	4.41	3.43
			Liver	4.81	5.56
			Slow	2.79	3.47
			Skin	6.07	4.20
15-9	4-fluoro PB alcohol Benzenemethanol, 4-fluoro-3-phenoxy-	 CAS no. 68359-53-5 MW, g/mol 218.22 Exp Kow @ pH 7.4 NA Log <i>D</i> @ pH 7.4 3.2 Log <i>P</i> 3.2	Fat	64.90	47.94
			Brain	13.49	9.33
			Rapid	4.37	2.31
			Kidney	5.16	3.55
			Liver	5.66	5.84

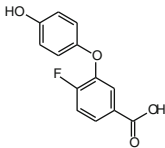
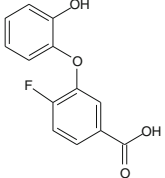
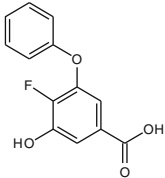
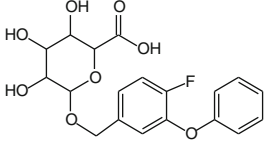
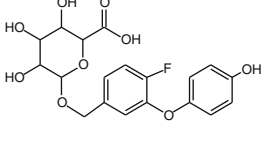
(continued)

Table D3 (continued)

No. ^a	Chemical structure ^b	Pesticide metabolism and physical and chemical properties ^{c, d}		Partition coefficients ^e		
				Tissue	Rat	Human
		pKa, MA	13.94	Slow	3.19	3.61
		WS, g/L (6.51E-2)	8.26E-2	Skin	7.20	4.39
16-10	4'-OH, 4-fluoro-PB alcohol					
	Benzenemethanol, 4-fluoro-3-(4-hydroxyphenoxy)-					
		CAS no.	NA	Fat	13.43	12.19
		MW, g/mol	234.22	Brain	8.08	7.27
		Exp Kow @ pH 7.4	NA	Rapid	2.85	1.99
		Log <i>D</i> @ pH 7.4	2.41	Kidney	3.31	2.93
		Log <i>P</i>	2.42	Liver	3.56	4.64
		pKa, MA	9.80	Slow	2.17	2.96
		WS, g/L (2.53E-1)	0.25	Skin	4.41	3.54
17-11	2'-OH, 4-fluoro-PB alcohol					
	Benzenemethanol, 4-fluoro-3-(2-hydroxyphenoxy)-					
		CAS no.	NA	Fat	19.01	16.90
		MW, g/mol	234.22	Brain	9.46	8.03
		Exp Kow @ pH 7.4	NA	Rapid	3.24	2.13
		Log <i>D</i> @ pH 7.4	2.56	Kidney	3.78	3.18
		Log <i>P</i>	2.57	Liver	4.10	5.09
		pKa, MA	9.01	Slow	2.44	3.21
		WS, g/L (1.88E-1)	0.22	Skin	5.12	3.86
18-12	5-OH, 4-fluoro-Pb alcohol					
	Benzenemethanol, 4-fluoro-3-hydroxy-5-phenoxy (or 3-phenoxy-4-fluoro-5-hydroxy)					
		CAS no.	NA	Fat	24.81	21.56
		MW, g/mol	234.22	Brain	10.49	8.51
		Exp Kow @ pH 7.4	NA	Rapid	3.54	2.21
		Log <i>D</i> @ pH 7.4	2.68	Kidney	4.14	3.33
		Log <i>P</i>	2.81	Liver	4.50	5.37
		pKa, MA	7.82	Slow	2.64	3.37
		WS, g/L (1.49E-1)	0.24	Skin	5.66	4.06
19-13	4-fluoro PB acid					
	Benzoic acid, 4-fluoro-3-phenoxy-					
		CAS no.	77279-89-1	Fat	0.38	0.41
		MW, g/mol	232.21	Brain	1.15	1.24
		Exp Kow @ pH 7.4	NA	Rapid	0.85	0.83
		Log <i>D</i> @ pH 7.4	0.89	Kidney	0.88	0.92
		Log <i>P</i>	3.88	Liver	0.83	1.02
		pKa, MA	3.89	Slow	0.79	0.89
		WS, g/L (5.14)	15.32	Skin	0.82	0.90
20-14	4'-OH, 4-fluoro-PB acid					
	Benzoic acid, 4-fluoro-3-(4-hydroxyphenoxy)-					
		CAS no.	205433-70-1	Fat	0.15	0.20
		MW, g/mol	248.21	Brain	0.89	0.91
		Exp Kow @ pH 7.4	NA	Rapid	0.80	0.80

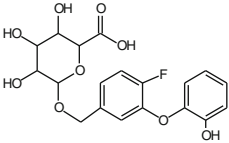
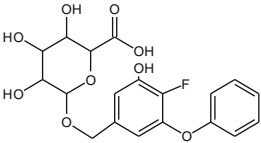
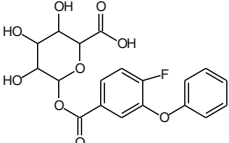
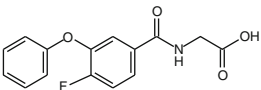
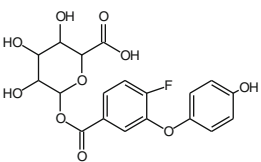
(continued)

Table D3 (continued)

No. ^a	Chemical structure ^b	Pesticide metabolism and physical and chemical properties ^{c, d}		Partition coefficients ^e		
				Tissue	Rat	Human
		Log <i>D</i> @ pH 7.4	0.1	Kidney	0.81	0.84
		Log <i>P</i>	3.09	Liver	0.75	0.83
		p <i>K</i> _a , MA	3.94	Slow	0.77	0.81
		WS, g/L (19.90)	44.81	Skin	0.69	0.84
21-15	2'-OH, 4-fluoro-PB acid Benzoic acid, 4-fluoro-3-(2-hydroxyphenoxy)-	CAS no.	NA	Fat	0.16	0.22
		MW, g/mol	248.21	Brain	0.91	0.93
		Exp Kow @ pH 7.4	NA	Rapid	0.81	0.81
		Log <i>D</i> @ pH 7.4	0.23	Kidney	0.82	0.85
		Log <i>P</i>	3.24	Liver	0.76	0.85
		p <i>K</i> _a , MA	3.9	Slow	0.78	0.82
		WS, g/L (15.40)	41.77	Skin	0.71	0.79
22-16	5-OH, 4-fluoro-PB acid Benzoic acid, 4-fluoro-3-hydroxy-5-phenoxy-	CAS no.	NA	Fat	0.26	0.31
		MW, g/mol	248.21	Brain	1.03	1.08
		Exp Kow @ pH 7.4	NA	Rapid	0.84	0.83
		Log <i>D</i> @ pH 7.4	0.60	Kidney	0.86	0.90
		Log <i>P</i>	3.71	Liver	0.81	0.94
		p <i>K</i> _a , MA	3.77	Slow	0.80	0.87
		WS, g/L (7.44)	35.46	Skin	0.77	0.85
23-17	4-fluoro-PB alcohol glucuronic acid Hexopyranosiduronic acid, (4-fluoro-3-phenoxyphenyl)methyl	CAS no.	NA	Fat	0.12	0.19
		MW, g/mol	394.35	Brain	0.89	0.90
		Exp Kow @ pH 7.4	NA	Rapid	0.85	0.85
		Log <i>D</i> @ pH 7.4	-1.43	Kidney	0.86	0.88
		Log <i>P</i>	2.28	Liver	0.79	0.85
		p <i>K</i> _a , MA	2.81	Slow	0.83	0.85
		WS, g/L (55.2)	551.39	Skin	0.72	0.80
24-18	4'-OH, 4-fluoro-PB alcohol glucuronic acid Hexopyranosiduronic acid, [4-fluoro-3-(4-hydroxyphenoxy)phenyl]methyl	CAS no.	NA	fat	0.13	0.20
		MW, g/mol	410.35	brain	0.91	0.92
		Exp Kow @ pH 7.4	NA	rapid	0.87	0.87
		Log <i>D</i> @ pH 7.4	-2.22	kidney	0.87	0.90
		Log <i>P</i>	1.50	liver	0.80	0.87
		p <i>K</i> _a , MA	2.81	slow	0.84	0.87
		WS, g/L (207.8)	1,000.0	skin	0.74	0.91
25-19	2'-OH, 4-fluoro-PB alcohol glucuronic acid β-D-Glucopyranosiduronic acid, [4-fluoro-3-(2-hydroxyphenoxy)phenyl]methyl	CAS no.	NA	fat	0.13	0.19
		MW, g/mol	410.35	brain	0.91	0.91

(continued)

Table D3 (continued)

No. ^a	Chemical structure ^b	Pesticide metabolism and physical and chemical properties ^{c, d}	Partition coefficients ^e		
			Tissue	Rat	Human
		Exp Kow @ pH 7.4 NA	rapid	0.87	0.87
		Log <i>D</i> @ pH 7.4 -2.08	kidney	0.87	0.89
		Log <i>P</i> 1.65	liver	0.80	0.87
		p <i>K</i> _a , MA 2.81	slow	0.84	0.86
		WS, g/L (157.8) 1,000.0	skin	0.73	0.82
26-20	5-OH, 4-fluoro PB alcohol glucuronic acid Hexopyranosiduronic acid, (4-fluoro-3-hydroxy-5-phenoxyphenyl)methyl	CAS no. NA	fat	0.13	0.20
		MW, g/mol 410.35	brain	0.91	0.92
		Exp Kow @ pH 7.4 NA	rapid	0.87	0.87
		Log <i>D</i> @ pH 7.4 -1.93	kidney	0.88	0.90
		Log <i>P</i> 1.92	liver	0.80	0.87
		p <i>K</i> _a , MA 2.80	slow	0.84	0.87
		WS, g/L (115.2) 1,000.0	skin	0.73	0.82
27-21	4-fluoro-PB acid glucuronic acid Hexopyranuronic acid, 1-(4-fluoro-3-phenoxybenzoate)	CAS no. 674773-71-8	Fat	0.12	0.19
		MW, g/mol 408.33	Brain	0.90	0.91
		Exp Kow @ pH 7.4 NA	Rapid	0.86	0.86
		Log <i>D</i> @ pH 7.4 -1.19	Kidney	0.86	0.89
		Log <i>P</i> 2.54	Liver	0.79	0.86
		p <i>K</i> _a , MA 2.65	Slow	0.83	0.85
		WS, g/L (28.20) 236.92	Skin	0.72	0.81
28-22	4-fluoro PB acid glycine Glycine, N-(4-fluoro-3-phenoxybenzoyl)-	CAS no. 674773-69-4	Fat	0.09	0.14
		MW, g/mol 289.26	Brain	0.77	0.78
		Exp Kow @ pH 7.4 NA	Rapid	0.73	0.73
		Log <i>D</i> @ pH 7.4 -1.07	Kidney	0.74	0.76
		Log <i>P</i> 2.55	Liver	0.68	0.74
		p <i>K</i> _a , MA 3.13	Slow	0.71	0.73
		WS, g/L (116.0) 347.26	Skin	0.62	0.69
29-23	4'-OH, 4-fluoro-PB acid glucuronide Hexopyranuronic acid, 1-[4-fluoro-3-(4-hydroxyphenoxy)benzoate]	CAS no. NA	Fat	0.13	0.19
		MW, g/mol 424.33	Brain	0.91	0.91
		Exp Kow @ pH 7.4 NA	Rapid	0.87	0.87
		Log <i>D</i> @ pH 7.4 -1.98	Kidney	0.87	0.90
		Log <i>P</i> 1.75	Liver	0.80	0.87
		p <i>K</i> _a , A 9.73	Slow	0.84	0.86
		WS, g/L (106.0) 665.99	Skin	0.73	0.82

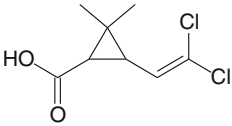
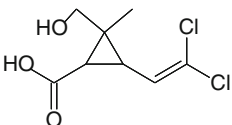
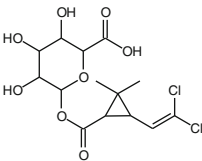
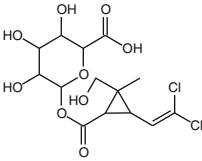
(continued)

Table D3 (continued)

No. ^a	Chemical structure ^b	Pesticide metabolism and physical and chemical properties ^{c, d}		Partition coefficients ^e			
				Tissue	Rat	Human	
30-24	2'-OH, 4-fluoro-PB acid glucuronide Hexopyranuronic acid, 1-[4-fluoro-3-(2-hydroxyphenoxy)benzoate]		CAS no.	NA	fat	0.13	0.20
			MW, g/mol	434.33	brain	0.91	0.92
			Exp Kow @ pH 7.4	NA	rapid	0.87	0.87
			Log <i>D</i> @ pH 7.4	-1.84	kidney	0.87	0.90
			Log <i>P</i>	1.9	liver	0.80	0.87
			pKa, MA	2.65	slow	0.84	0.87
			WS, g/L (80.5)	602.27	skin	0.73	0.82
31-25	4'-OH, 4-fluoro-PB acid sulfate Benzoic acid, 4-fluoro-3-[4-(sulfooxy)phenoxy]-		CAS no.	NA	Fat	0.13	0.20
			MW, g/mol	323.27	Brain	0.92	0.92
			Exp Kow @ pH 7.4	NA	Rapid	0.87	0.87
			Log <i>D</i> @ pH 7.4	-1.82	Kidney	0.88	0.90
			Log <i>P</i>	2.68	Liver	0.81	0.87
			pKa, A	3.91	Slow	0.85	0.87
			WS, g/L (320.9)	1,000.0	Skin	0.74	0.82
31-26	2'-OH, 4-fluoro-PB acid sulfate Benzoic acid, 4-fluoro-3-[2-(sulfooxy)phenoxy]-		CAS no.	NA	Fat	0.13	0.20
			MW, g/mol	328.27	Brain	0.92	0.92
			Exp Kow @ pH 7.4	NA	Rapid	0.87	0.87
			Log <i>D</i> @ pH 7.4	-2.21	Kidney	0.88	0.90
			Log <i>P</i>	2.29	Liver	0.81	0.87
			pKa, A	3.92	Slow	0.85	0.87
			WS, g/L (645.0)	1,000.0	Skin	0.74	0.83
32-27	5-OH, 4-fluoro-PB acid glucuronide Hexopyranuronic acid, 1-(4-fluoro-3-hydroxy-5-phenoxybenzoate)		CAS no.	NA	fat	0.13	0.20
			MW, g/mol	424.33	brain	0.92	0.92
			Exp Kow @ pH 7.4	NA	rapid	0.88	0.88
			Log <i>D</i> @ pH 7.4	-1.88	kidney	0.88	0.90
			Log <i>P</i>	2.24	liver	0.81	0.88
			pKa, MA	2.65	slow	0.85	0.87
			WS, g/L (87.1)	1,000.0	skin	0.74	0.83
33-28	5-OH, 4-fluoro-PB acid sulfate Benzoic acid, 4-fluoro-3-phenoxy-5-(sulfooxy)-		CAS no.	NA	fat	0.13	0.20
			MW, g/mol	328.27	brain	0.92	0.92
			Exp Kow @ pH 7.4	NA	rapid	0.87	0.87
			Log <i>D</i> @ pH 7.4	-1.86	kidney	0.88	0.90
			Log <i>P</i>	2.64	liver	0.81	0.87
			pKa, MA	-5.36	slow	0.85	0.87
			WS, g/L (324.2)	1,000.0	skin	0.74	0.82
Hydrolysis products: Acid Leaving groups, metabolites and conjugates							
Products for cyfluthrin, cypermethrin and permethrin							

(continued)

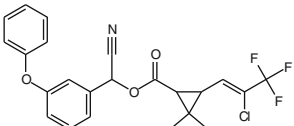
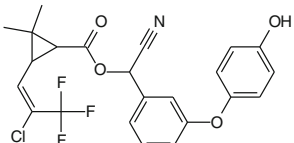
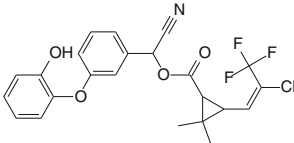
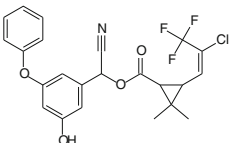
Table D3 (continued)

No. ^a	Chemical structure ^b	Pesticide metabolism and physical and chemical properties ^{c, d}	Partition coefficients ^e			
			Tissue	Rat	Human	
34-1	Permethrinic acid (DCCA) Cyclopropanecarboxylic acid, 3-(2,2-dichloroethenyl)-2,2-dimethyl-					
		CAS no.	55701-05-8	fat	0.16	0.22
		MW, g/mol	209.07	brain	0.97	0.98
		Exp Kow @ pH 7.4	NA	rapid	0.90	0.90
		Log <i>D</i> @ pH 7.4	-0.22	kidney	0.91	0.93
		Log <i>P</i>	2.24	liver	0.83	0.92
		p <i>K</i> _a , MA	4.92	slow	0.87	0.90
		WS, g/L (60.6)	225.4	skin	0.77	0.86
35-2	2-OH Methyl permethrinic acid (2OHMeDCCA) Cyclopropanecarboxylic acid, 3-(2,2-dichloroethenyl)-2-(hydroxymethyl)-2-methyl-					
		CAS no.	64162-73-8	fat	0.13	0.20
		MW, g/mol	225.07	brain	0.93	0.94
		Exp Kow @ pH 7.4	NA	rapid	0.89	0.89
		Log <i>D</i> @ pH 7.4	-1.74	kidney	0.89	0.92
		Log <i>P</i>	0.94	liver	0.82	0.89
		p <i>K</i> _a , MA	4.56	slow	0.86	0.89
		WS, g/L (990.0)	1,000.0	skin	0.75	0.84
36-3	DCCA glucuronic acid Hexopyranuronic acid, 1-O-[[3-(2,2-dichloroethenyl)-2,2-dimethylcyclopropyl]carbonyl]-					
		CAS no.	80446-46-4	fat	0.13	0.20
		MW, g/mol	385.19	brain	0.93	0.94
		Exp Kow @ pH 7.4	NA	rapid	0.89	0.89
		Log <i>D</i> @ pH 7.4	-1.48	kidney	0.89	0.92
		Log <i>P</i>	2.24	liver	0.82	0.89
		p <i>K</i> _a , MA	2.68	slow	0.86	0.89
		WS, g/L (69.4)	1,000.0	skin	0.75	0.84
37-4	2-OH methyl DCCA glucuronic acid Hexopyranuronic acid, 1-O-[[3-(2,2-dichloroethenyl)-2-(hydroxymethyl)-2-methylcyclopropyl]carbonyl]-					
		CAS no.	61183-31-1	fat	0.13	0.20
		MW, g/mol	401.19	brain	0.93	0.94
		Exp Kow @ pH 7.4	NA	rapid	0.89	0.89
		Log <i>D</i> @ pH 7.4	-2.9	kidney	0.89	0.92
		Log <i>P</i>	0.82	liver	0.82	0.89
		p <i>K</i> _a , MA	2.68	slow	0.86	0.88
		WS, g/L (902.2)	1,000.0	skin	0.75	0.84

^a Parent chemical or metabolite number for cross-reference to Table E3 (Appendix E, Cyfluthrin)

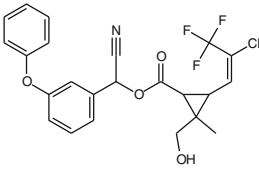
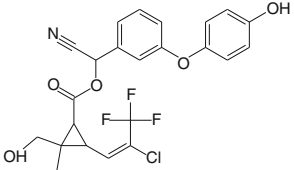
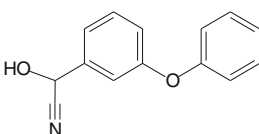
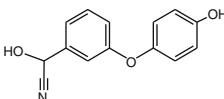
^{b-g} Metabolism source, Kaneko and Miyamoto (2001) and Kaneko (2010). See footnotes in Table D1 (Appendix D)

Table D4 Chemical structure, physical and chemical properties, and tissue partition coefficients for cyhalothrin and resulting metabolites

No. ^a	Chemical structure ^b	Pesticide metabolism and physical and chemical properties ^{c, d}	Partition coefficients ^e			
			Tissue	Rat	Human	
1	Cyhalothrin Cyclopropanecarboxylic acid, 3-[2-chloro-3,3,3-trifluoro-1-propen-yl]-2,2-dimethyl-, cyano(3-hydroxy-5-phenoxyphenyl)methyl ester					
		CAS no.	68085-85-8	Fat	67.96	31.51
		MW, g/mol	449.85	Brain	14.52	8.94
		Exp Kow @ pH 7.4	NA	Rapid	4.62	2.17
		Log D @ pH 7.4	6.0	Kidney	5.48	3.36
		Log P	6.0	Liver	6.02	5.57
		pKa	NA	Slow	3.34	3.42
		K _p , cm/h ^f	0.0591	Skin	7.71	4.18
		Log K _p ^g	-1.228			
		WS, g/L (1.12E-5)	5.56E-5			
2	4'-OH cyhalothrin Cyclopropanecarboxylic acid, 3-[2-chloro-3,3,3-trifluoro-1-propen-1-yl]-2,2-dimethyl-, cyano[3-(4-hydroxyphenoxy)phenyl]methyl ester					
		CAS no.	96495-13-5	Fat	71.03	31.15
		MW, g/mol	465.85	Brain	14.52	8.95
		Exp Kow @ pH 7.4	NA	Rapid	4.62	2.17
		Log D @ pH 7.4	5.21	Kidney	5.48	3.37
		Log P	5.21	Liver	6.02	5.58
		pKa, MA	9.97	Slow	3.34	3.42
		WS, g/L (4.20E-5)	1.57E-4	Skin	7.71	4.18
3	2'-OH cyhalothrin Cyclopropanecarboxylic acid, 3-[2-chloro-3,3,3-trifluoro-1-propen-1-yl] 2,2-dimethyl-, cyano[3-(2-hydroxyphenoxy)phenyl]methyl ester					
		CAS no.	NA	Fat	70.08	32.63
		MW, g/mol	465.85	Brain	14.52	8.95
		Exp Kow @ pH 7.4	NA	Rapid	4.62	2.17
		Log D @ pH 7.4	5.35	Kidney	5.48	3.37
		Log P	5.35	Liver	6.02	5.58
		pKa, MA	9.22	Slow	3.34	3.42
		WS, g/L (3.19E-5)	1.41E-4	Skin	7.71	4.18
4	5-OH cyhalothrin Cyclopropanecarboxylic acid, 3-[2-chloro-3,3,3-trifluoro-1-propen-1-yl] 2,2-dimethyl-, cyano(3-hydroxy-5-phenoxyphenyl)methyl ester					
		CAS no.	NA	Fat	69.15	32.13
		MW, g/mol	465.85	Brain	14.52	8.95
		Exp Kow @ pH 7.4	NA	Rapid	4.62	2.17
		Log D @ pH 7.4	5.54	Kidney	5.48	3.37
		Log P	5.57	Liver	6.02	5.58
		pKa, MA	8.52	Slow	3.34	3.42
		WS, g/L (2.20E-5)	2.29E-5	Skin	7.71	4.18

(continued)

Table D4 (continued)

No. ^a	Chemical structure ^b	Pesticide metabolism and physical and chemical properties ^{c, d}	Partition coefficients ^c			
			Tissue	Rat	Human	
5	2-OH methyl cyhalothrin Cyclopropanecarboxylic acid, 3-[2-chloro-3,3,3-trifluoro-1-propen-yl]-2-(hydroxymethyl)-2-methyl-, cyano(3-phenoxyphenyl)methyl ester					
		CAS no.	NA	Fat	79.56	38.25
		MW, g/mol	465.85	Brain	14.51	8.98
		Exp Kow @ pH 7.4	NA	Rapid	4.62	2.18
		Log <i>D</i> @ pH 7.4	4.58	Kidney	5.48	3.38
		Log <i>P</i>	4.58	Liver	6.02	5.60
		pKa, MA	15.1	Slow	3.34	3.43
		WS, g/L (1.45E-4)	5.33E-4	Skin	7.70	4.20
6	4'-OH, 2-OH methyl cyhalothrin Cyclopropanecarboxylic acid, 3-[2-chloro-3,3,3-trifluoro-1-propen-yl]-2-(hydroxymethyl)-2-methyl-, cyano[3-(4-hydroxyphenoxy)phenyl]methyl ester					
		CAS no.	NA	Fat	77.47	44.29
		MW, g/mol	481.85	Brain	14.27	9.09
		Exp Kow @ pH 7.4	NA	Rapid	4.56	2.22
		Log <i>D</i> @ pH 7.4	3.79	Kidney	5.40	3.43
		Log <i>P</i>	3.79	Liver	5.93	5.67
		pKa, MA	9.97	Slow	3.31	3.48
		WS, g/L (5.42E-4)	1.51E-3	Skin	7.58	4.25
	Hydrolysis products: Alcohol Leaving groups, metabolites and conjugates					
	Products for cypermethrin, deltamethrin, fenvalerate, fenpropathrin, fluvalinate and tralomethrin					
7-1	Cyanohydrin of PB aldehyde Benzeneacetonitrile, α -hydroxy-3-phenoxy-					
		CAS no.	39515-47-4	Fat	19.11	16.98
		MW, g/mol	225.24	Brain	9.47	8.04
		Exp Kow @ pH 7.4	NA	Rapid	3.25	2.13
		Log <i>D</i> @ pH 7.4	2.56	Kidney	3.79	3.18
		Log <i>P</i>	2.56	Liver	4.10	5.10
		pKa, MA	10.33	Slow	2.44	3.22
		WS, g/L (2.10E-1)	0.16	Skin	7.38	3.87
8-2	Cyanohydrin of 4'-OH PB aldehyde Benzeneacetonitrile, α -hydroxy-3-(4-hydroxyphenoxy)-					
		CAS no.	82186-81-0	Fat	3.11	2.98
		MW, g/mol	241.24	Brain	3.44	3.70
		Exp Kow @ pH 7.4	NA	Rapid	1.54	1.34
		Log <i>D</i> @ pH 7.4	1.77	Kidney	1.70	1.77
		Log <i>P</i>	1.78	Liver	1.75	2.51
		pKa, MA	10.0	Slow	1.27	1.76
		WS, g/L (8.14E-4)	0.48	Skin	2.02	2.00
9-3	Cyanohydrin of 2'-OH PB aldehyde Benzeneacetonitrile, α -hydroxy-3-(2-hydroxyphenoxy)-					
		CAS no.	NA	Fat	7.16	6.70
		MW, g/mol	241.24	Brain	5.67	5.66

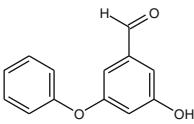
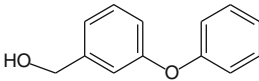
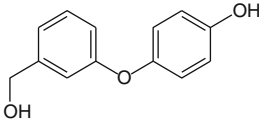
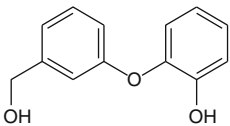
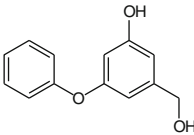
(continued)

Table D4 (continued)

No. ^a	Chemical structure ^b	Pesticide metabolism and physical and chemical properties ^{c, d}		Partition coefficients ^c		
				Tissue	Rat	Human
		Exp Kow @ pH 7.4	NA	Rapid	2.17	1.71
		Log <i>D</i> @ pH 7.4	2.11	Kidney	2.48	2.42
		Log <i>P</i>	2.13	Liver	2.63	3.69
		pKa, MA	8.71	Slow	1.72	2.43
		WS, g/L (4.17E-1)	0.38	Skin	3.17	2.85
10-4	Cyanohydrin of 5-OH PB aldehyde Benzeneacetonitrile, α,3-dihydroxy-5-phenoxy-					
		CAS no.	NA	Fat	4.49	4.25
		MW, g/mol	241.24	Brain	4.30	4.51
		Exp Kow @ pH 7.4	NA	Rapid	1.78	1.49
		Log <i>D</i> @ pH 7.4	1.92	Kidney	2.00	2.04
		Log <i>P</i>	1.93	Liver	2.09	2.99
		pKa, MA	9.26	Slow	1.44	2.04
		WS, g/L (6.06E-1)	0.43	Skin	2.46	2.35
11-5	PB aldehyde Benzaldehyde, 3-phenoxy-					
		CAS no.	39515-51-0	Fat	84.70	57.83
		MW, g/mol	198.22	Brain	13.98	9.34
		Exp Kow @ pH 7.4	NA	Rapid	4.50	2.30
		Log <i>D</i> @ pH 7.4	3.38	Kidney	5.33	3.54
		Log <i>P</i>	3.38	Liver	5.84	5.84
		pKa	NA	Slow	3.28	3.59
		WS, g/L (5.80E-2)	2.47E-2	Skin	7.45	4.38
12-6	4'-OH PB aldehyde Benzaldehyde, 3-(4-hydroxyphenoxy)-					
		CAS no.	NA	Fat	20.64	18.25
		MW, g/mol	214.22	Brain	9.76	8.19
		Exp Kow @ pH 7.4	NA	Rapid	3.33	2.16
		Log <i>D</i> @ pH 7.4	2.59	Kidney	3.89	3.23
		Log <i>P</i>	2.59	Liver	4.21	5.19
		pKa, MA	9.97	Slow	2.50	3.27
		WS, g/L (2.27E-1)	7.38E-2	Skin	5.28	3.93
13-7	2'-OH PB aldehyde Benzaldehyde, 3-(2-hydroxyphenoxy)-					
		CAS no.	NA	Fat	28.81	24.72
		MW, g/mol	214.22	Brain	11.02	8.75
		Exp Kow @ pH 7.4	NA	Rapid	3.69	2.25
		Log <i>D</i> @ pH 7.4	2.74	Kidney	4.33	3.40
		Log <i>P</i>	2.74	Liver	4.71	5.51
		pKa, MA	9.22	Slow	2.74	3.45
		WS, g/L (1.69E-1)	6.60E-2	Skin	5.93	4.16
14-8	5-OH PB aldehyde Benzaldehyde, 3-hydroxy-5-phenoxy- (or Benzaldehyde, 5-hydroxy-3-phenoxy-)					
		CAS no.	79897-38-4	Fat	64.40	48.37

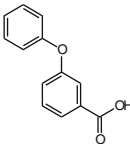
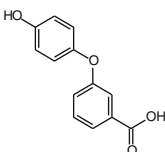
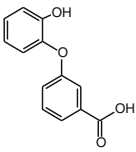
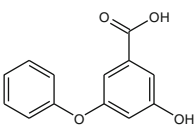
(continued)

Table D4 (continued)

No. ^a	Chemical structure ^b	Pesticide metabolism and physical and chemical properties ^{c, d}		Partition coefficients ^e		
				Tissue	Rat	Human
		MW, g/mol	214.22	Brain	13.42	9.37
		Exp Kow @ pH 7.4	NA	Rapid	4.35	2.33
		Log <i>D</i> @ pH 7.4	3.16	Kidney	5.14	3.57
		Log <i>P</i>	3.19	Liver	5.63	5.87
		pKa, MA	9.22	Slow	3.18	3.62
		WS, g/L (7.39E-2)	4.80E-2	Skin	7.16	4.41
15-9	PB alcohol Benzenemethanol, 3-phenoxy-					
		CAS no.	13826-35-2	Fat	80.91	54.99
		MW, g/mol	200.2	Brain	13.96	9.31
		Exp Kow @ pH 7.4	NA	Rapid	4.49	2.29
		Log <i>D</i> @ pH 7.4	3.39	Kidney	5.31	3.53
		Log <i>P</i>	3.39	Liver	5.83	5.82
		pKa, MA	14.19	Slow	3.27	3.58
		WS, g/L (5.56E-2)	0.19	Skin	7.43	4.37
16-10	4'-OH PB alcohol Benzenemethanol, 3-(4-hydroxyphenoxy)-					
		CAS no.	63987-19-9	Fat	21.47	18.95
		MW, g/mol	216.2	Brain	9.89	8.27
		Exp Kow @ pH 7.4	NA	Rapid	3.70	2.18
		Log <i>D</i> @ pH 7.4	2.60	Kidney	3.94	3.26
		Log <i>P</i>	2.60	Liver	4.27	5.23
		pKa, MA	10.07	Slow	2.52	3.29
		WS, g/L (2.17E-1)	0.56	Skin	5.35	3.96
17-11	2'-OH PB alcohol Benzenemethanol, 3-(2-hydroxyphenoxy)-					
		CAS no.	63987-17-7	Fat	29.94	25.63
		MW, g/mol	216.2	Brain	11.14	8.80
		Exp Kow @ pH 7.4	NA	Rapid	3.72	2.26
		Log <i>D</i> @ pH 7.4	2.75	Kidney	4.39	3.42
		Log <i>P</i>	2.75	Liver	4.75	5.55
		pKa, MA	9.35	Slow	2.76	3.47
		WS, g/L (1.62E-1)	0.50	Skin	5.99	4.19
18-12	5-OH PB alcohol Benzenemethanol, 3-hydroxy-5-phenoxy- (or Benzenemethanol, 5-hydroxy-3-phenoxy-)					
		CAS no.	NA	Fat	35.50	29.79
		MW, g/mol	216.2	Brain	11.73	9.01
		Exp Kow @ pH 7.4	NA	Rapid	3.89	2.30
		Log <i>D</i> @ pH 7.4	2.83	Kidney	4.57	3.49
		Log <i>P</i>	2.84	Liver	4.98	5.67
		pKa, MA	9.08	Slow	2.87	3.53
		WS, g/L (1.38E-1)	0.47	Skin	6.29	4.28

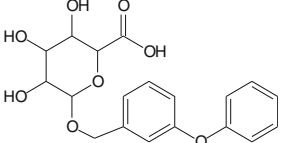
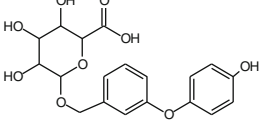
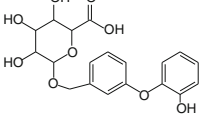
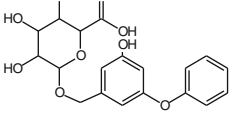
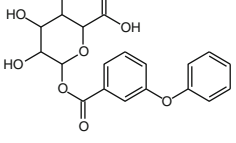
(continued)

Table D4 (continued)

No. ^a	Chemical structure ^b	Pesticide metabolism and physical and chemical properties ^{c, d}		Partition coefficients ^c			
				Tissue	Rat	Human	
19-13	PB acid Benzoic acid, 3-phenoxy-		CAS no.	3739-38-6	Fat	0.26	0.31
			MW, g/mol	214.2	Brain	1.02	0.89
			Exp Kow @ pH 7.4	NA	Rapid	0.82	0.67
			Log <i>D</i> @ pH 7.4	0.67	Kidney	0.84	0.72
			Log <i>P</i>	3.65	Liver	0.79	0.77
			pKa, MA	3.95	Slow	0.77	0.70
			WS, g/L (9.89)	47.45	Skin	0.75	0.69
20-14	4'-OH PB acid Benzoic acid, 3-(4-hydroxyphenoxy)-		CAS no.	35065-12-4	Fat	0.13	0.187
			MW, g/mol	230.2	Brain	0.87	0.77
			Exp Kow @ pH 7.4	NA	Rapid	0.80	0.70
			Log <i>D</i> @ pH 7.4	-0.11	Kidney	0.81	0.73
			Log <i>P</i>	2.86	Liver	0.75	0.72
			pKa, MA	4.0	Slow	0.78	0.70
			WS, g/L (37.67)	139.28	Skin	0.69	0.67
21-15	2'-OH PB acid Benzoic acid, 3-(2-hydroxyphenoxy)-		CAS no.	35101-26-9	Fat	0.14	0.19
			MW, g/mol	230.2	Brain	0.88	0.78
			Exp Kow @ pH 7.4	NA	Rapid	0.81	0.70
			Log <i>D</i> @ pH 7.4	1.86E-2	Kidney	0.81	0.73
			Log <i>P</i>	3.01	Liver	0.75	0.72
			pKa, MA	3.96	Slow	0.78	0.71
			WS, g/L (29.25)	129.33	Skin	0.79	0.68
22-16	5-OH PB acid Benzoic acid, 3-hydroxy-5-phenoxy- (or Benzoic acid, 5-hydroxy-3-phenoxy-)		CAS no.	63987-26-8	Fat	0.17	0.23
			MW, g/mol	230.2	Brain	0.93	0.84
			Exp Kow @ pH 7.4	NA	Rapid	0.82	0.71
			Log <i>D</i> @ pH 7.4	0.27	Kidney	0.83	0.75
			Log <i>P</i>	3.32	Liver	0.77	0.76
			pKa, MA	3.83	Slow	0.79	0.73
			WS, g/L (17.85)	113.11	Skin	0.72	0.70
23-17	PB alcohol glucuronic acid Hexopyranosiduronic acid, (3-phenoxyphenyl)methyl		CAS no.	65658-93-7	Fat	0.13	0.19
			MW, g/mol	376.36	Brain	0.90	0.91

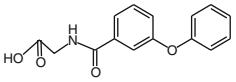
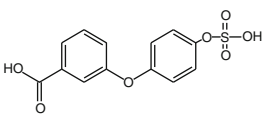
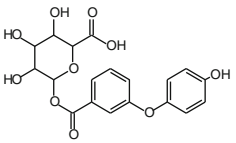
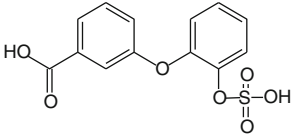
(continued)

Table D4 (continued)

No. ^a	Chemical structure ^b	Pesticide metabolism and physical and chemical properties ^{c, d}		Partition coefficients ^c		
				Tissue	Rat	Human
		Exp Kow @ pH 7.4	NA	Rapid	0.86	0.86
		Log <i>D</i> @ pH 7.4	-1.24	Kidney	0.86	0.89
		Log <i>P</i>	2.47	Liver	0.79	0.86
		pKa, MA	2.81	Slow	0.83	0.85
		WS, g/L (697.9)	1,000.0	Skin	0.72	0.81
24-18	4'-OH PB alcohol glucuronic acid Hexopyranosiduronic acid, [3-(4-hydroxyphenoxy)phenyl]methyl	CAS no.	NA	Fat	0.13	0.20
		MW, g/mol	392.36	Brain	0.92	0.92
		Exp Kow @ pH 7.4	NA	Rapid	0.87	0.87
		Log <i>D</i> @ pH 7.4	-2.03	Kidney	0.88	0.90
		Log <i>P</i>	1.68	Liver	0.81	0.87
		pKa, MA	2.81	Slow	0.85	0.87
		WS, g/L (184.9)	1,000.0	Skin	0.74	0.82
25-19	2'-OH PB alcohol glucuronic acid Hexopyranosiduronic acid, [3-(2-hydroxyphenoxy)phenyl]methyl	CAS no.	NA	Fat	0.13	0.20
		MW, g/mol	392.36	Brain	0.92	0.92
		Exp Kow @ pH 7.4	NA	Rapid	0.87	0.87
		Log <i>D</i> @ pH 7.4	-1.88	Kidney	0.88	0.90
		Log <i>P</i>	1.83	Liver	0.81	0.87
		pKa, MA	2.81	Slow	0.85	0.87
		WS, g/L (137.6)	1,000.0	Skin	0.74	0.82
26-20	5-OH PB alcohol glucuronic acid Hexopyranosiduronic acid, (3-hydroxy-5-phenoxyphenyl)methyl	CAS no.	NA	Fat	0.13	0.20
		MW, g/mol	392.36	Brain	0.92	0.92
		Exp Kow @ pH 7.4	NA	Rapid	0.87	0.87
		Log <i>D</i> @ pH 7.4	-1.77	Kidney	0.88	0.90
		Log <i>P</i>	1.95	Liver	0.81	0.87
		pKa, MA	2.81	Slow	0.85	0.87
		WS, g/L (110.8)	1,000.0	Skin	0.74	0.83
27-21	PB acid glucuronide β-D-Glucopyranuronic acid, 1-(3-phenoxybenzoate)	CAS no.	57991-35-2	Fat	0.12	0.19
		MW, g/mol	390.3	Brain	0.90	0.90
		Exp Kow @ pH 7.4	NA	Rapid	0.86	0.86
		Log <i>D</i> @ pH 7.4	-1.34	Kidney	0.86	0.88
		Log <i>P</i>	2.38	Liver	0.79	0.86
		pKa, MA	2.66	Slow	0.83	0.85
		WS, g/L (48.99)	729.57	Skin	0.72	0.81

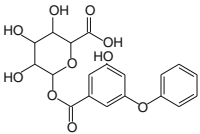
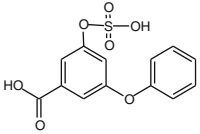
(continued)

Table D4 (continued)

No. ^a	Chemical structure ^b	Pesticide metabolism and physical and chemical properties ^{c, d}	Partition coefficients ^c		
			Tissue	Rat	Human
28-22	PB acid glycine Glycine, N-(3-phenoxybenzoyl)- 	CAS no. 57991-36-3 MW, g/mol 271.3 Exp Kow @ pH 7.4 NA Log <i>D</i> @ pH 7.4 -0.96 Log <i>P</i> 2.55 pKa, MA 3.61 WS, g/L (118.68) 706.70	Fat Brain Rapid Kidney Liver Slow Skin	0.10 0.79 0.75 0.75 0.69 0.72 0.63	0.15 0.79 0.75 0.77 0.75 0.74 0.71
29-23	4'-OH PB acid sulfate Benzoic acid, 3-[4-(sulfoxy)phenoxy]- 	CAS no. 58218-91-0 MW, g/mol 310.3 Exp Kow @ pH 7.4 NA Log <i>D</i> @ pH 7.4 -2.05 Log <i>P</i> 2.45 pKa, A 3.97 WS, g/L (602.0) 1,000.0	Fat Brain Rapid Kidney Liver Slow Skin	0.13 0.92 0.88 0.88 0.81 0.85 0.74	0.20 0.88 0.84 0.86 0.84 0.83 0.79
30-24	4'-OH PB acid glucuronide β-D-Glucopyranuronic acid, 1-[3-(4-hydroxyphenoxy)benzoate] 	CAS no. 66856-01-7 MW, g/mol 406.34 Exp Kow @ pH 7.4 NA Log <i>D</i> @ pH 7.4 -2.13 Log <i>P</i> 1.6 pKa, A 9.93 WS, g/L (184.4) 1,000.0	Fat Brain Rapid Kidney Liver Slow Skin	0.13 0.91 0.87 0.87 0.80 0.84 0.86	0.20 0.87 0.83 0.85 0.82 0.82 0.78
31-25	2'-OH PB acid sulfate Benzoic acid, 3-[2-(sulfoxy)phenoxy]- 	CAS no. 61183-26-4 MW, g/mol 310.3 Exp Kow @ pH 7.4 NA Log <i>D</i> @ pH 7.4 -2.44 Log <i>P</i> 2.06 pKa, A 3.98 WS, g/L (1,296.6) 1,000.0	Fat Brain Rapid Kidney Liver Slow Skin	0.13 0.92 0.87 0.88 0.81 0.85 0.74	0.20 0.88 0.83 0.86 0.83 0.83 0.79

(continued)

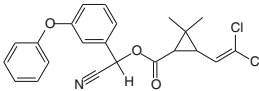
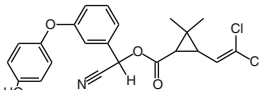
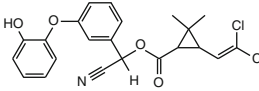
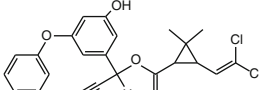
Table D4 (continued)

No. ^a	Chemical structure ^b	Pesticide metabolism and physical and chemical properties ^{c, d}	Partition coefficients ^c			
			Tissue	Rat	Human	
32-26	5-OH PB acid glucuronide Hexopyranuronic acid, 1-(3-hydroxy-5-phenoxybenzoate) or 1-(5-hydroxy-3-phenoxybenzoate)					
		CAS no.	80405-64-7	Fat	0.13	0.20
		MW, g/mol	406.34	Brain	0.92	0.92
		Exp Kow @ pH 7.4	NA	Rapid	0.87	0.87
		Log <i>D</i> @ pH 7.4	-1.83	Kidney	0.88	0.90
		Log <i>P</i>	1.93	Liver	0.80	0.87
		p <i>K</i> _a , A	8.38	Slow	0.84	0.87
		WS, g/L (102.2)	1,000.0	Skin	0.74	0.82
33-27	5-OH PB acid sulfate Benzoic acid, 3-phenoxy-5-(sulfoxy)-					
		CAS no.	NA	Fat	0.13	0.20
		MW, g/mol	310.28	Brain	0.92	0.88
		Exp Kow @ pH 7.4	NA	Rapid	0.88	0.83
		Log <i>D</i> @ pH 7.4	-1.96	Kidney	0.88	0.86
		Log <i>P</i>	2.54	Liver	0.81	0.83
		p <i>K</i> _a , MA	-4.72	Slow	0.85	0.83
		WS, g/L (504.4)	1,000.0	Skin	0.74	0.79
	Hydrolysis products: Acid leaving groups, metabolites and conjugates					
	Products for bifenthrin, cyhalothrin and tefluthrin					
34-1	TFP acid Cyclopropanecarboxylic acid, 3-[2-chloro-3,3,3-trifluoro-1-propen-1-yl]-2,2-dimethyl- CAS no. 74609-46-4					
35-2	2-OH methyl TFP acid Cyclopropanecarboxylic acid, 3-[2-chloro-3,3,3-trifluoro-1-propen-1-yl]-2-(hydroxymethyl)-2-methyl- CAS no. 107900-83-4					
36-3	TFP acid glucuronide Hexopyranuronic acid, 1-O-[[3-[2-chloro-3,3,3-trifluoro-1-propen-1-yl]-2,2-dimethylcyclopropyl]carbonyl]- CAS no. 120851-78-7					
37-4	2-OH methyl TFP acid glucuronide Hexopyranuronic acid, 1-O-[[3-[2-chloro-3,3,3-trifluoro-1-propen-1-yl]-2-(hydroxymethyl)-2-methylcyclopropyl]carbonyl]- CAS no. NA					

^a Parent chemical or metabolite number for cross-reference to Table E4 (Appendix E, Cyhalothrin)

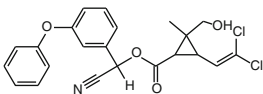
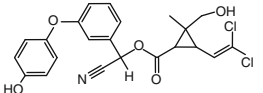
^{b-g} Metabolism source, Kaneko and Miyamoto (2001) and Kaneko (2010). See footnotes in Table D1 (Appendix D)

Table D5 Chemical structure, physical and chemical properties, and tissue partition coefficients for cypermethrin and resulting metabolites

No. ^a	Chemical structure ^b	Pesticide metabolism and physical and chemical properties ^{c, d}	Partition coefficients ^c		
			Tissue	Rat	Human
1	Cypermethrin Cyclopropanecarboxylic acid, (1 <i>RS</i>)-cis-trans-3-(2,2-dichloroethenyl)-2,2-dimethyl-, (1 <i>RS</i>)- α -cyano(3-phenoxyphenyl)methyl ester-		CAS no. 52315-07-8 MW, g/mol 416.3 Exp Kow @ pH 7.4 NA Log <i>D</i> @ pH 7.4 6.41 Log <i>P</i> 6.41 p <i>K</i> _a NA <i>K</i> _p , cm/h ^f 0.185 Log <i>K</i> _p ^g -0.732 WS, g/L (8.14E-6) 4.56E-5	Fat 66.70 Brain 14.50 Rapid 4.60 Kidney 5.50 Liver 6.11 Slow 3.33 Skin 7.70	31.11 7.94 1.92 2.99 4.95 3.03 3.71
2	4'-OH cypermethrin Cyclopropanecarboxylic acid, 3-(2,2-dichloroethenyl)-2,2-dimethyl-, cyano[3-(4-hydroxyphenoxy)phenyl]methyl ester-		CAS no. 64691-63-0 MW, g/mol 432.3 Exp Kow @ pH 7.4 NA Log <i>D</i> @ pH 7.4 5.62 Log <i>P</i> 5.62 p <i>K</i> _a , MA 9.97 WS, g/L (3.06E-5) 1.30E-4	Fat 68.88 Brain 14.52 Rapid 4.62 Kidney 5.48 Liver 6.02 Slow 3.34 Skin 7.71	31.98 8.95 2.17 3.37 5.58 3.42 4.18
3	2'-OH cypermethrin Cyclopropanecarboxylic acid, 3-(2,2-dichloroethenyl)-2,2-dimethyl-, cyano[3-(2-hydroxyphenoxy)phenyl]methyl ester-		CAS no. 122565-02-0 MW, g/mol 432.3 Exp Kow @ pH 7.4 NA Log <i>D</i> @ pH 7.4 5.77 Log <i>P</i> 5.77 p <i>K</i> _a , MA 9.22 WS, g/L (2.28E-5) 1.16E-4	Fat 68.42 Brain 14.52 Rapid 4.62 Kidney 5.48 Liver 6.02 Slow 3.34 Skin 7.71	31.74 8.94 2.17 3.37 5.58 3.42 4.18
4	5-OH cypermethrin Cyclopropanecarboxylic acid, 3-(2,2-dichloroethenyl)-2,2-dimethyl-, cyano (3-hydroxy-5-phenoxyphenyl)methyl ester-		CAS no. 69321-07-9 MW, g/mol 432.3 Exp Kow @ pH 7.4 NA Log <i>D</i> @ pH 7.4 5.95 Log <i>P</i> 5.98 p <i>K</i> _a , MA 8.52 WS, g/L (1.59E-5) 1.03E-4	Fat 68.05 Brain 14.52 Rapid 4.62 Kidney 5.48 Liver 6.02 Slow 3.34 Skin 7.71	31.55 8.94 2.17 3.36 5.58 3.42 4.18

(continued)

Table D5 (continued)

No. ^a	Chemical structure ^b	Pesticide metabolism and physical and chemical properties ^{c, d}	Partition coefficients ^e			
			Tissue	Rat	Human	
5	2-OH methyl cypermethrin Cyclopropanecarboxylic acid, 3-(2,2-dichloroethenyl)-2-(hydroxymethyl)-2-methyl-, cyano(3-phenoxyphenyl)methyl ester					
		CAS no.	69321-08-0	Fat	73.67	34.58
		MW, g/mol	432.3	Brain	14.52	8.96
		Exp Kow @ pH 7.4	NA	Rapid	4.62	2.17
		Log <i>D</i> @ pH 7.4	4.99	Kidney	5.48	3.37
		Log <i>P</i>	4.99	Liver	6.02	5.59
		p <i>K</i> _a , MA	15.1	Slow	3.34	3.42
		WS, g/L (1.05E-4)	4.39E-4	Skin	7.71	4.18
6	4'-OH, 2-OH methyl cypermethrin Cyclopropanecarboxylic acid, 3-(2,2-dichloroethenyl)-2-(hydroxymethyl)-2-methyl-, Cyanol[3-(4-hydroxyphenoxy)phenyl]methyl ester					
		CAS no.	112066-68-9	Fat	19.55	15.42
		MW, g/mol	448.3	Brain	9.55	7.88
		Exp Kow @ pH 7.4	NA	Rapid	3.04	1.92
		Log <i>D</i> @ pH 7.4	4.2	Kidney	3.62	2.97
		Log <i>P</i>	4.2	Liver	4.04	4.92
		p <i>K</i> _a , MA	9.97	Slow	2.20	3.02
		WS, g/L (3.95E-4)	1.25E-3	Skin	5.08	3.68
	Hydrolysis of parent esters: Alcohol Leaving group, metabolites and conjugates See Cyhalothrin					
7-1	Cyanohydrin of PB aldehyde Benzeneacetonitrile, α-hydroxy-3-phenoxy- CAS no. 39515-47-4					
8-2	Cyanohydrin of 4'-OH PB aldehyde Benzeneacetonitrile, α-hydroxy-3-(4-hydroxyphenoxy)- CAS no. 82186-81-0					
9-3	Cyanohydrin of 2'-OH PB aldehyde Benzeneacetonitrile, α-hydroxy-3-(2-hydroxyphenoxy)- CAS no. NA					
10-4	Cyanohydrin of 5-OH PB aldehyde Benzeneacetonitrile, α,3-dihydroxy-5-phenoxy- CAS no. NA					
11-5	PB aldehyde Benzaldehyde, 3-phenoxy- CAS no. 39515-51-0					
12-6	4'-OH PB aldehyde Benzaldehyde, 3-(4-hydroxyphenoxy)- CAS no. NA					
13-7	2'-OH PB aldehyde Benzaldehyde, 3-(2-hydroxyphenoxy)- CAS no. NA					
14-8	5-OH PB aldehyde 3-hydroxy-5-phenoxybenzaldehyde CAS no. 79897-38-4					
15-9	PB alcohol Benzenemethanol, 3-phenoxy- CAS no. 13826-35-2					
16-10	4'-OH PB alcohol Benzenemethanol, 3-(4-hydroxyphenoxy)- CAS no. 63987-19-9					

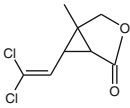
(continued)

Table D5 (continued)

No. ^a	Chemical structure ^b	Pesticide metabolism and physical and chemical properties ^{c, d}	Partition coefficients ^e		
			Tissue	Rat	Human
17-11	2'-OH PB alcohol Benzenemethanol, 3-(2-hydroxyphenoxy)- CAS no. 63987-17-7				
18-12	5-OH PB alcohol 3-(hydroxymethyl)-5-phenoxyphenol CAS no. NA				
19-13	PB acid Benzoic acid, 3-phenoxy- CAS no. 3739-38-6				
20-14	4'-OH PB acid Benzoic acid, 3-(4-hydroxyphenoxy)- CAS no. 35065-12-4				
21-15	2'-OH PB acid Benzoic acid, 3-(2-hydroxyphenoxy)- CAS no. 35101-26-9				
22-16	5-OH PB acid 3-hydroxy-5-phenoxybenzoic acid- CAS no. 63987-26-8				
23-17	PB alcohol glucuronic acid Hexopyranosiduronic acid, (3-phenoxyphenyl)methyl CAS no. 65658-93-7				
24-18	4'-OH PB alcohol glucuronic acid Hexopyranosiduronic acid, [3-(4-hydroxyphenoxy)phenyl]methyl CAS no. NA				
25-19	2'-OH PB alcohol glucuronic acid Hexopyranosiduronic acid, [3-(2-hydroxyphenoxy)phenyl]methyl CAS no. NA				
26-20	5-OH PB alcohol glucuronic acid Hexopyranosiduronic acid, (3-hydroxy-5-phenoxyphenyl)methyl CAS no. NA				
27-21	PB acid glucuronide β-D-Glucopyranuronic acid, 1-(3-phenoxybenzoate) CAS no. 57991-35-2				
28-22	PB acid glycine Glycine, N-(3-phenoxybenzoyl)- CAS no. 57991-36-3				
29-23	4'-OH PB acid glucuronide β-D-Glucopyranuronic acid, 1-[3-(4-hydroxyphenoxy)benzoate] CAS no. 66856-01-7				
30-24	5-OH PB acid glucuronide Hexopyranuronic acid, 1-(3-hydroxy-5-phenoxybenzoate) CAS no. 80405-64-7				
31-25	4'-OH PB acid sulfate Benzoic acid, 3-[4-(sulfooxy) phenoxy]- CAS no. 58218-91-0				
32-26	2'-OH PB acid sulfate Benzoic acid, 3-[2-(sulfooxy)phenoxy]- CAS no. 61183-26-4 Hydrolysis of Parent esters: Acid Leaving groups, metabolites and conjugates See Cyfluthrin				
33-1	Cis/trans-Permethrinic acid (DCCA) Cyclopropanecarboxylic acid, 3-(2,2-dichloroethenyl)-2,2-dimethyl- CAS no. 55701-05-8				
34-2	2-OH Methyl Permethrinic acid (DCCA) Cyclopropanecarboxylic acid, 3-(2,2-dichloroethenyl)-2-(hydroxymethyl)-2-methyl- CAS no. 64162-73-8				
35-3	DCCA glucuronic acid Hexopyranuronic acid, 1-O-[[3-(2,2-dichloroethenyl)-2,2-dimethylcyclopropyl]carbonyl]- CAS no. 80446-46-4				
36-4	2-OH methyl DCCA glucuronic acid Hexopyranuronic acid, 1-O-[[3-(2,2-dichloroethenyl)-2-(hydroxymethyl)-2-methylcyclopropyl]carbonyl]- CAS no. 61183-31-1				

(continued)

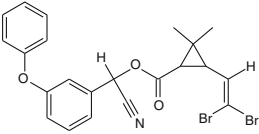
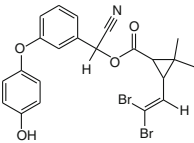
Table D5 (continued)

No. ^a	Chemical structure ^b	Pesticide metabolism and physical and chemical properties ^{c, d}	Partition coefficients ^e			
			Tissue	Rat	Human	
37-5	(Cis)-2-OH methyl-(cis, trans)-DCCA lactone 3-oxabicyclo[3.1.0] hexano-2-one, 6-(2,2-dichloroethenyl)-5-methyl-					
		CAS no.	NA	Fat	1.15	1.18
		MW, g/mol	207.05	Brain	1.97	2.20
		Exp Kow @ pH 7.4	NA	Rapid	1.23	1.17
		Log <i>D</i> @ pH 7.4	1.21	Kidney	1.29	1.37
		Log <i>P</i>	1.21	Liver	1.26	1.65
		p <i>K</i> _a , MA	NA	Slow	1.10	1.34
		WS, g/L (3.73)	0.56	Skin	1.31	1.40

^a Parent chemical or metabolite number for cross-reference to Table E5 ([Appendix E](#), Cypermethrin)

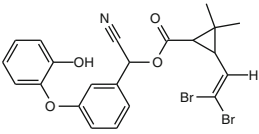
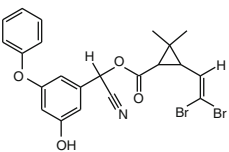
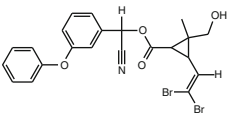
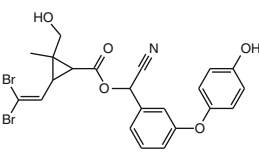
^{b-g} Metabolism source, Kaneko and Miyamoto (2001) and Kaneko (2010). See footnotes in Table D1 ([Appendix D](#))

Table D6 Chemical structure, physical and chemical properties, and tissue partition coefficients for deltamethrin and resulting metabolites

No. ^a	Chemical structure ^b	Pesticide metabolite and physical and chemical properties ^{c, d}	Partition coefficient ^e			
			Tissue	Rat	Human	
1	Cis-Deltamethrin (1R, 3R, α S) Cyclopropanecarboxylic acid, 3-(2,2-dibromoethenyl)-2,2-dimethyl-, cyano(3-phenoxyphenyl)methyl ester-					
		CAS no. (Stereo)	52918-63-5	Fat	67.74	31.39
		MW, g/mol	505.2	Brain	14.52	8.94
		Exp Kow @ pH 7.4	NA	Rapid	4.62	2.17
		Log <i>D</i> @ pH 7.4	6.2	Kidney	5.48	3.36
		Log <i>P</i>	6.2	Liver	6.02	5.57
		p <i>K</i> _a	NA	Slow	3.34	3.42
		<i>K</i> _p , cm/h ^f	0.037	Skin	7.71	4.18
		Log <i>K</i> _p ^g	-1.423			
		WS, g/L (3.36E-6)	6.77E-5			
2	4'-OH Deltamethrin Cyclopropanecarboxylic acid, 3-(2,2-dibromoethenyl)-2,2-dimethyl-, cyano[3-(4-hydroxyphenoxy)phenyl]methyl ester					
		CAS no.	66855-89-8	Fat	70.25	32.71
		MW, g/mol	521.2	Brain	14.52	8.95
		Exp Kow @ pH 7.4	NA	Rapid	4.62	2.17
		Log <i>D</i> @ pH 7.4	5.34	Kidney	5.48	3.37
		Log <i>P</i>	5.34	Liver	6.02	5.58
		p <i>K</i> _a , MA	9.97	Slow	3.34	3.42
		WS, g/L (1.44E-5)	0.000162	Skin	7.71	4.18

(continued)

Table D6 (continued)

No. ^a	Chemical structure ^b	Pesticide metabolite and physical and chemical properties ^{c, d}	Partition coefficient ^e		
			Tissue	Rat	Human
3	2'-OH Deltamethrin Cyclopropanecarboxylic acid, 3-(2,2-dibromoethenyl)-2,2-dimethyl-, cyano[3-(2-hydroxyphenoxy)phenyl]methyl ester				
		CAS no. 66855-88-7	Fat	70.96	33.10
		MW, g/mol 521.2	Brain	14.52	8.95
		Exp Kow @ pH 7.4 NA	Rapid	4.62	2.17
		Log <i>D</i> @ pH 7.4 5.24	Kidney	5.48	3.37
		Log <i>P</i> 5.25	Liver	6.02	5.58
		p <i>K</i> _a , MA 9.22	Slow	3.34	3.42
		WS, g/L (1.75E-5) 0.000177	Skin	7.71	4.15
4	5-OH Deltamethrin Cyclopropanecarboxylic acid, 3-(2,2-dibromoethenyl)-2,2-dimethyl-, cyano(3-hydroxy-5-phenoxyphenyl)methyl ester				
		CAS no. 66855-90-1	Fat	70.33	32.76
		MW, g/mol 521.2	Brain	14.52	8.95
		Exp Kow @ pH 7.4 NA	Rapid	4.62	2.17
		Log <i>D</i> @ pH 7.4 5.6	Kidney	5.48	3.37
		Log <i>P</i> 5.6	Liver	6.02	5.58
		p <i>K</i> _a , MA 8.52	Slow	3.34	3.42
		WS, g/L (8.59E-6) 0.000136	Skin	7.71	4.18
5	2-OH methyl deltamethrin Cyclopropanecarboxylic acid, 3-(2,2-dibromoethenyl)-2-(hydroxymethyl)-2-methyl-, cyano(3-phenoxyphenyl)methyl ester				
		CAS no. NA	Fat	76.54	36.38
		MW, g/mol, 521.2 521.2	Brain	14.52	8.96
		Exp Kow @ pH 7.4 NA	Rapid	4.62	2.17
		Log <i>D</i> @ pH 7.4 5.0	Kidney	5.48	3.37
		Log <i>P</i> 5.0	Liver	6.02	5.59
		p <i>K</i> _a , MA 15.1	Slow	3.34	3.42
		WS, g/L (2.80E-5) 6.48E-4	Skin	7.71	4.18
6	4'-OH, 2-OH methyl deltamethrin Cyclopropanecarboxylic acid, 3-(2,2-dibromoethenyl)-2-(hydroxymethyl)-2-methyl-, cyano[3-(4-hydroxyphenoxy)phenyl]methyl ester				
		CAS no. NA	Fat	75.06	40.73
		MW, g/mol 537.2	Brain	14.46	9.02
		Exp Kow @ pH 7.4 NA	Rapid	4.60	2.19
		Log <i>D</i> @ pH 7.4 4.21	Kidney	5.46	3.40
		Log <i>P</i> 4.21	Liver	6.00	5.63
		p <i>K</i> _a , MA 9.97	Slow	3.36	3.45
		WS, g/L (1.05E-4) 1.83E-3	Skin	7.68	4.21
	Hydrolysis Products: Alcohol Leaving group, metabolites and conjugates				
	Same as cyhalothrin, cypermethrin				

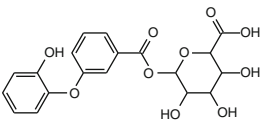
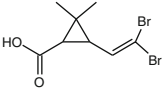
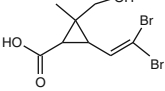
(continued)

Table D6 (continued)

No. ^a	Chemical structure ^b	Pesticide metabolite and physical and chemical properties ^{c, d}	Partition coefficient ^e		
			Tissue	Rat	Human
7-1	Cyanohydrin of PB aldehyde	Benzeneacetonitrile, α -hydroxy-3-phenoxy- CAS no. 39515-47-4			
8-2	Cyanohydrin of 4'-OH PB aldehyde	Benzeneacetonitrile, α -hydroxy-3-(4-hydroxyphenoxy)- CAS no. 82186-81-0			
9-3	Cyanohydrin of 2'-OH PB aldehyde	Benzeneacetonitrile, α -hydroxy-3-(2-hydroxyphenoxy)- CAS no. NA			
10-4	Cyanohydrin of 5-OH PB aldehyde	Benzeneacetonitrile, α ,3-dihydroxy-5-phenoxy- CAS no. NA			
11-5	PB aldehyde	Benzaldehyde, 3-phenoxy- CAS no. 39515-51-0			
12-6	4'-OH PB aldehyde	Benzaldehyde, 3-(4-hydroxyphenoxy)- CAS no. NA			
13-7	2'-OH PB aldehyde	Benzaldehyde, 3-(2-hydroxyphenoxy)- CAS no. NA			
14-8	5-OH PB aldehyde	3-hydroxy-5-phenoxybenzaldehyde CAS no. 79897-38-4			
15-9	PB alcohol	Benzenemethanol, 3-phenoxy- CAS no. 13826-35-2			
16-10	4'-OH PB alcohol	Benzenemethanol, 3-(4-hydroxyphenoxy)- CAS no. 63987-19-9			
17-11	2'-OH PB alcohol	Benzenemethanol, 3-(2-hydroxyphenoxy)- CAS no. 63987-17-7			
18-12	5-OH PB alcohol	3-(hydroxymethyl)-5-phenoxyphenol CAS no. NA			
19-13	PB acid	Benzoic acid, 3-phenoxy- CAS no. 3739-38-6			
20-14	4'-OH PB acid	Benzoic acid, 3-(4-hydroxyphenoxy)- CAS no. 35065-12-4			
21-15	2'-OH PB acid	Benzoic acid, 3-(2-hydroxyphenoxy)- CAS no. 35101-26-9			
22-16	5-OH PB acid	3-hydroxy-5-phenoxybenzoic acid- CAS no. NA			
23-17	PB alcohol glucuronic acid	Hexopyranosiduronic acid, (3-phenoxyphenyl)methyl CAS no. 65658-93-7			
24-18	4'-OH PB alcohol glucuronic acid	Hexopyranosiduronic acid, [3-(4-hydroxyphenoxy)phenyl]methyl CAS no. NA			
25-19	2'-OH PB alcohol glucuronic acid	Hexopyranosiduronic acid, [3-(2-hydroxyphenoxy)phenyl]methyl CAS no. NA			
26-20	5-OH PB alcohol glucuronic acid	Hexopyranosiduronic acid, (3-hydroxy-5-phenoxyphenyl)methyl CAS no. NA			
27-21	PB acid glucuronide	β -D-Glucopyranuronic acid, 1-(3-phenoxybenzoate) CAS no. 57991-35-2			
28-22	PB acid glycine	Glycine, N-(3-phenoxybenzoyl)- CAS no. 57991-36-3			

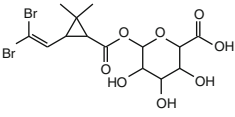
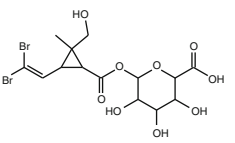
(continued)

Table D6 (continued)

No. ^a	Chemical structure ^b	Pesticide metabolite and physical and chemical properties ^{c, d}	Partition coefficient ^e			
			Tissue	Rat	Human	
29-23	4'-OH PB acid glucuronide					
	β-D-Glucopyranuronic acid, 1-[3-(4-hydroxyphenoxy)benzoate] CAS no. 66856-01-7					
30-24	5-OH PB acid glucuronide					
	Hexopyranuronic acid, 1-(3-hydroxy-5-phenoxybenzoate) CAS no. 80405-64-7					
31-25	4'-OH PB acid sulfate					
	Benzoic acid, 3-[4-(sulfoxy)phenoxy]- CAS no. 58218-91-0					
32-26	2'-OH PB acid sulfate					
	Benzoic acid, 3-[2-(sulfoxy)phenoxy]- CAS no. 61183-26-4					
33-27	2'-OH PB acid glucuronide					
	Hexopyranuronic acid, 1-[3-(2-hydroxyphenoxy)benzoate]					
		CAS no.	NA	Fat	0.14	0.22
		MW, g/mol	406.34	Brain	0.98	0.99
		Exp Kow @ pH 7.4	NA	Rapid	0.94	0.94
		Log <i>D</i> @ pH 7.4	-1.98	Kidney	0.94	0.97
		Log <i>P</i>	1.75	Liver	0.86	0.94
		p <i>K</i> a, A,	2.66	Slow	0.91	0.93
		WS, g/L (137.3)	1,000.0	Skin	0.79	0.88
34-28	5-OH PB acid sulfate					
	Benzoic acid, 3-[5-(sulfoxy)phenoxy] CAS no. NA					
	Hydrolysis Products, Acid Leaving groups, metabolites and conjugates					
35-29	(cis)-decamethrinic acid (Dibromo-CPCA)					
	Cyclopropanecarboxylic acid, 3-(2,2-dibromoethyl)-2,2-dimethyl					
		CAS no.	59952-39-5	Fat	0.10	0.15
		MW, g/mol	297.97	Brain	0.80	0.81
		Exp Kow @ pH 7.4	NA	Rapid	0.76	0.76
		Log <i>D</i> @ pH 7.4	-0.84	Kidney	0.76	0.79
		Log <i>P</i>	2.25	Liver	0.70	0.76
		p <i>K</i> a, MA	4.2	Slow	0.74	0.76
		WS, (g/L) (65.8)	1,000.0	Skin	0.64	0.72
36-2	(cis, trans)-hydroxymethyl-(cis) decamethrinic acid (Hydroxymethyl Dibromo-CPCA)					
	Cyclopropanecarboxylic acid, 3-(2,2-dibromoethyl)-2-(hydroxymethyl)-2-methyl-					
		CAS no.	82079-71-8	Fat	0.12	0.18
		MW, g/mol	313.97	Brain	0.87	0.88
		Exp Kow @ pH 7.4	NA	Rapid	0.83	0.83
		Log <i>D</i> @ pH 7.4	-2.31	Kidney	0.84	0.86
		Log <i>P</i>	0.96	Liver	0.77	0.83
		p <i>K</i> a, MA	3.84	Slow	0.81	0.83
		WS (g/L) (954.8)	1,000.0	Skin	0.70	0.79

(continued)

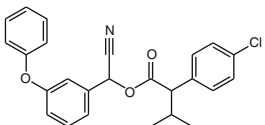
Table D6 (continued)

No. ^a	Chemical structure ^b	Pesticide metabolite and physical and chemical properties ^{c, d}	Partition coefficient ^e			
			Tissue	Rat	Human	
37-3	(cis)-dibromo-CPCA glucuronic acid Hexopyranuronic acid, 1-O-[[3-(2,2-dibromoethenyl)-2,2-dimethylcyclopropyl]carbonyl]-					
		CAS no.	82079-70-7	Fat	0.12	0.19
		MW, g/mol	474.1	Brain	0.90	0.90
		Exp Kow @ pH 7.4	NA	Rapid	0.86	0.86
		Log <i>D</i> @ pH 7.4	-1.47	Kidney	0.86	0.89
		Log <i>P</i>	2.25	Liver	0.79	0.86
		pKa, MA	2.68	Slow	0.83	0.85
		WS (g/L) (18.17)	1,000.0	Skin	0.72	0.81
38-4	(cis, trans)-2-OH Me (cis)-Dibromo-CPCA glucuronic acid Hexopyranuronic acid, 1-O-[[3-(2,2-dibromoethenyl)-2-(hydroxymethyl)-2-methylcyclopropyl]carbonyl]-					
		CAS no.	66856-00-6	Fat	0.13	0.20
		MW, g/mol	490.1	Brain	0.93	0.94
		Exp Kow @ pH 7.4	NA	Rapid	0.89	0.89
		Log <i>D</i> @ pH 7.4	-2.89	Kidney	0.89	0.92
		Log <i>P</i>	0.83	Liver	0.82	0.89
		pKa, MA	2.68	Slow	0.86	0.88
		WS (g/L) (243.4)	1,000.0	Skin	0.75	0.84

^a Parent chemical or metabolite number for cross-reference to Table E6 (Appendix E, Deltamethrin)

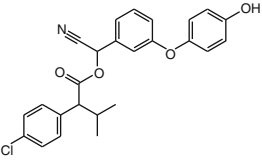
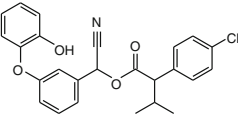
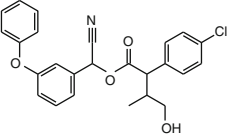
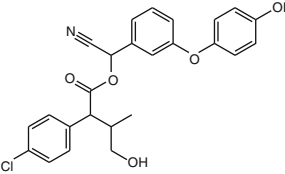
^{b-g} Metabolism source, Kaneko and Miyamoto (2001) and Kaneko (2010). See footnotes in Table D1 (Appendix D)

Table D7 Chemical structure, physical and chemical properties, and tissue partition coefficients for fenvalerate and resulting metabolites

No. ^a	Chemical structure ^b	Pesticide metabolism and physical and chemical properties ^{c, d}	Partition coefficients ^e			
			Tissue	Rat	Human	
1	Fenvalerate Benzeneacetic acid, 4-chloro-a-(1-methylethyl)-, cyano(3-phenoxyphenyl)methyl ester					
		CAS no.	51630-58-1	Fat	67.53	31.28
		MW, g/mol	419.9	Brain	14.52	8.94
		Exp Kow @ pH 7.4	NA	Rapid	4.62	2.17
		Log <i>D</i> @ pH 7.4	6.55	Kidney	5.48	3.36
		Log <i>P</i>	6.55	Liver	6.02	5.57
		pKa	NA	Slow	3.34	3.42
		<i>K_p</i> , cm/h ^f	0.221	Skin	7.71	4.18
		Log <i>K_p</i> ^g	-0.655			
		WS, g/L (5.87E-6)	2.51E-5			

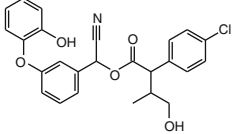
(continued)

Table D7 (continued)

No. ^a	Chemical structure ^b	Pesticide metabolism and physical and chemical properties ^{c, d}		Partition coefficients ^c			
				Tissue	Rat	Human	
2	4'-OH fenvalerate Benzenoacetic acid, 4-chloro-a-(1-methylethyl)-, cyano [3-(4-hydroxyphenoxy)phenyl] methyl ester		CAS no.	NA	Fat	68.43	31.75
		MW, g/mol	435.9	Brain	14.52	8.94	
		Exp Kow @ pH 7.4	NA	Rapid	4.62	2.17	
		Log <i>D</i> @ pH 7.4	5.76	Kidney	5.48	3.37	
		Log <i>P</i>	5.76	Liver	6.02	5.58	
		pKa, MA	9.97	Slow	3.34	3.42	
		WS, g/L (2.20E-5)	7.11E-5	Skin	7.71	4.18	
3	2'-OH fenvalerate Benzenoacetic acid, 4-chloro-a-(1-methylethyl)-, cyano [3-(2-hydroxyphenoxy)phenyl] methyl ester		CAS no.	NA	Fat	68.13	31.59
		MW, g/mol	435.9	Brain	14.52	8.94	
		Exp Kow @ pH 7.4	NA	Rapid	4.62	2.17	
		Log <i>D</i> @ pH 7.4	5.91	Kidney	5.48	3.36	
		Log <i>P</i>	5.91	Liver	6.02	5.58	
		pKa, MA	9.22	Slow	3.34	3.42	
		WS, g/L (1.64E-5)	6.3E-5	Skin	7.71	4.18	
4	2-OH methyl fenvalerate Benzenoacetic acid, 4-chloro-a-(2-hydroxy-1-methylethyl)-, cyano(3-phenoxyphenyl) methyl ester		CAS no.	NA	Fat	74.10	34.82
		MW, g/mol	435.9	Brain	14.52	8.96	
		Exp Kow @ pH 7.4	NA	Rapid	4.62	2.17	
		Log <i>D</i> @ pH 7.4	4.96	Kidney	5.48	3.37	
		Log <i>P</i>	4.96	Liver	6.02	5.59	
		pKa, MA	14.68	Slow	3.34	3.42	
		WS, g/L (1.06E-4)	2.71E-4	Skin	7.71	4.18	
5	4'-OH, 2-OH methyl fenvalerate Benzenoacetic acid, 4-chloro-a-(2-hydroxy-1-methylethyl)-, cyano[3-(4-hydroxyphenoxy)phenyl] methyl ester		CAS no.	NA	Fat	87.87	44.77
		MW, g/mol	451.9	Brain	14.47	9.04	
		Exp Kow @ pH 7.4	NA	Rapid	4.61	2.20	
		Log <i>D</i> @ pH 7.4	4.18	Kidney	5.47	3.40	
		Log <i>P</i>	4.18	Liver	6.01	5.64	
		pKa, MA	9.96	Slow	3.34	3.46	
		WS, g/L (3.90 E-4)	7.68E-4	Skin	7.69	4.22	
6	2'-OH, 2-OH methyl fenvalerate Benzenoacetic acid, 4-chloro-a-(2-hydroxy-1-methylethyl)-, cyano[3-(2-hydroxyphenoxy)phenyl]methyl ester		CAS no.	NA	Fat	86.58	42.98
			MW, g/mol	451.9	Brain	14.49	9.02

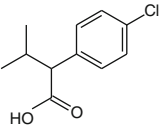
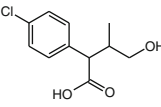
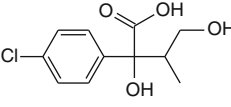
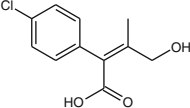
(continued)

Table D7 (continued)

No. ^a	Chemical structure ^b	Pesticide metabolism and physical and chemical properties ^{c, d}		Partition coefficients ^e		
				Tissue	Rat	Human
		Exp Kow @ pH 7.4	NA	Rapid	4.61	2.19
		Log <i>D</i> @ pH 7.4	4.32	Kidney	5.48	3.40
		Log <i>P</i>	4.33	Liver	6.02	5.62
		p <i>K</i> _a , MA	9.22	Slow	3.34	3.45
		WS, g/L (2.96E-4)	6.86E-4	Skin	7.70	4.21
	Hydrolysis products: Alcohol Leaving groups, metabolites and conjugates					
	See Cyhalothrin for data					
7-1	Cyanohydrin of PB aldehyde	Benzeneacetonitrile, α -hydroxy-3-phenoxy- CAS no. 39515-47-4				
8-2	Cyanohydrin of 4'-OH PB aldehyde	Benzeneacetonitrile, α -hydroxy-3-(4-hydroxyphenoxy)- CAS no. 82186-81-0				
9-3	Cyanohydrin of 2'-OH PB aldehyde	Benzeneacetonitrile, α -hydroxy-3-(2-hydroxyphenoxy)- CAS no. NA				
10-4	PB aldehyde	Benzaldehyde, 3-phenoxy- CAS no. 39515-51-0				
11-5	4'-OH PB aldehyde	Benzaldehyde, 3-(4-hydroxyphenoxy)- CAS no. NA				
12-6	2'-OH PB aldehyde	Benzaldehyde, 3-(2-hydroxyphenoxy)- CAS no. NA				
13-7	PB alcohol	Benzenemethanol, 3-phenoxy- CAS no. 13826-35-2				
14-8	4'-OH PB alcohol	Benzenemethanol, 3-(4-hydroxyphenoxy)- CAS no. 63987-19-9				
15-9	2'-OH PB alcohol	Benzenemethanol, 3-(2-hydroxyphenoxy)- CAS no. 63987-17-7				
16-10	PB acid	Benzoic acid, 3-phenoxy- CAS no. 3739-38-6				
17-11	4'-OH PB acid	Benzoic acid, 3-(4-hydroxyphenoxy)- CAS no. 35065-12-4				
18-12	2'-OH PB acid	Benzoic acid, 3-(2-hydroxyphenoxy)- CAS no. 35101-26-9				
19-13	PB alcohol glucuronic acid	Hexopyranosiduronic acid, (3-phenoxyphenyl)methyl CAS no. 65658-93-7				
20-14	4'-OH PB alcohol glucuronic acid	Hexopyranosiduronic acid, [3-(4-hydroxyphenoxy)phenyl]methyl CAS no. NA				
21-15	2'-OH PB alcohol glucuronic acid	Hexopyranosiduronic acid, [3-(2-hydroxyphenoxy)phenyl]methyl CAS no. NA				
22-16	PB acid glucuronide	β -D-Glucopyranuronic acid, 1-(3-phenoxybenzoate) CAS no. 57991-35-2				
23-17	PB acid glycine	Glycine, N-(3-phenoxybenzoyl)- CAS no. 57991-36-3				
24-18	4'-OH PB acid glucuronide	β -D-Glucopyranuronic acid, 1-[3-(4-hydroxyphenoxy)benzoate] CAS no. 66856-01-7				
25-19	4'-OH PB acid sulfate	Benzoic acid, 3-[4-(sulfooxy)phenoxy]- CAS no. 58218-91-0				

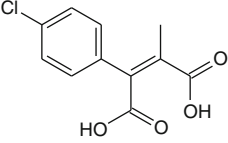
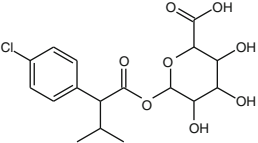
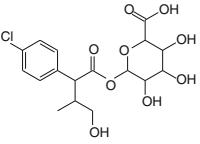
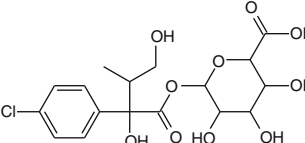
(continued)

Table D7 (continued)

No. ^a	Chemical structure ^b	Pesticide metabolism and physical and chemical properties ^{c, d}	Partition coefficients ^c		
			Tissue	Rat	Human
26-20	2'-OH PB acid glucuronide Hexopyranuronic acid, 1-[3-(2-hydroxyphenoxy)benzoate] CAS No .NA				
27-21	2'-OH PB acid sulfate Benzoic acid, 3-[2-(sulfoxy)phenoxy]- CAS no. 61183-26-4 Hydrolysis Products: Acid leaving groups, metabolites and conjugates				
28-1	Fenvaleric acid (CPIA, chlorophenyl isovaleric acid) Benzeneacetic acid, 4-chloro- α -(1-methylethyl)-, 	CAS no. 2012-74-0 MW, g/mol 212.67 Exp Kow @ pH 7.4 NA Log <i>D</i> @ pH 7.4 0.18 Log <i>P</i> 3.33 pKa, MA 4.13 WS, g/L (26.4) 215.68	Fat 0.14 Brain 0.85 Rapid 0.76 Kidney 0.77 Liver 0.71 Slow 0.73 Skin 0.66	0.18 0.87 0.75 0.79 0.79 0.76 0.73	
29-2	2-OH Fenvaleric acid (2-OH-CPIA) Benzeneacetic acid, 4-chloro- α -(2-hydroxy-1-methylethyl)-, 	CAS no. 72041-47-5 MW, g/mol 228.67 Exp Kow @ pH 7.4 NA Log <i>D</i> @ pH 7.4 -1.46 Log <i>P</i> 1.82 pKa, MA 3.96 WS, g/L (546.2) 1,000.0	Fat 0.11 Brain 0.86 Rapid 0.82 Kidney 0.82 Liver 0.76 Slow 0.79 Skin 0.69	0.17 0.86 0.82 0.86 0.82 0.81 0.77	
30-3	α -OH, 2-OH methyl Fenvaleric acid (α -OH, 2-OH methyl-CPIA) Benzeneacetic acid, 4-chloro- α -hydroxy- α -(2-hydroxy-1-methylethyl)-, 	CAS no. 72041-48-6 MW, g/mol 244.67 Exp Kow @ pH 7.4 NA Log <i>D</i> @ pH 7.4 -2.15 Log <i>P</i> 1.56 pKa, MA 2.99 WS, g/L (11,735.7) 1,000.0	Fat 0.12 Brain 0.89 Rapid 0.85 Kidney 0.85 Liver 0.78 Slow 0.82 Skin 0.71	0.19 0.89 0.85 0.88 0.85 0.84 0.80	
31-4	2-OH methyl Fenvaleric acid (2-OH methyl CPIA) Benzeneacetic acid, 4-chloro- α -(2-hydroxy-1-methylethylidene)-, 	CAS no. 72041-49-7 MW, g/mol 226.66 Exp Kow @ pH 7.4 NA Log <i>D</i> @ pH 7.4 -1.76 Log <i>P</i> 1.61 pKa, MA 3.91 WS, g/L (1,010.0) 1,000.0	Fat 0.11 Brain 0.85 Rapid 0.81 Kidney 0.82 Liver 0.75 Slow 0.79 Skin 0.68	0.17 0.86 0.81 0.84 0.81 0.81 0.77	

(continued)

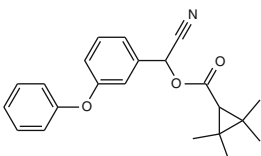
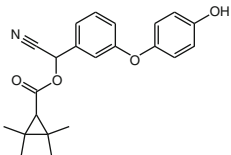
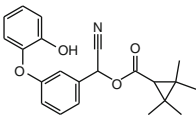
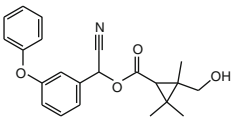
Table D7 (continued)

No. ^a	Chemical structure ^b	Pesticide metabolism and physical and chemical properties ^{c, d}		Partition coefficients ^c		
				Tissue	Rat	Human
32-5	CPdIB acid (chlorophenyl butenedioic acid) 2-butenedioic acid, 2-(4-chlorophenyl)-3-methyl-, 	CAS no.	NA	Fat	0.12	0.19
		MW, g/mol	240.64	Brain	0.89	0.90
		Exp Kow @ pH 7.4	NA	Rapid	0.85	0.85
		Log <i>D</i> @ pH 7.4	-3.46	Kidney	0.85	0.88
		Log <i>P</i>	1.29	Liver	0.78	0.85
		p <i>K</i> _a , MA	3.05	Slow	0.82	0.85
		WS, g/L (24,007.0)	1,000.0	Skin	0.72	0.80
33-6	CPIA glucuronic acid Hexopyranuronic acid, 1-[2-(4-chlorophenyl)-3-methylbutanoate] 	CAS no.	NA	Fat	0.12	0.19
		MW, g/mol	388.8	Brain	0.89	0.90
		Exp Kow @ pH 7.4	NA	Rapid	0.85	0.85
		Log <i>D</i> @ pH 7.4	-1.24	Kidney	0.85	0.88
		Log <i>P</i>	2.48	Liver	0.78	0.85
		p <i>K</i> _a , MA	2.67	Slow	0.82	0.85
		WS, g/L (41.1)	1,000.0	Skin	0.72	0.80
34-7	4-OH methyl CPIA glucuronic acid Hexopyranuronic acid, 1-[2-(4-chlorophenyl)-4-hydroxy-3-methylbutanoate] 	CAS no.	NA	Fat	0.13	0.20
		MW, g/mol	404.8	Brain	0.93	0.93
		Exp Kow @ pH 7.4	NA	Rapid	0.88	0.89
		Log <i>D</i> @ pH 7.4	-2.83	Kidney	0.89	0.91
		Log <i>P</i>	0.9	Liver	0.82	0.88
		p <i>K</i> _a , MA	2.67	Slow	0.86	0.88
		WS, g/L (746.6)	1,000.0	Skin	0.75	0.83
35-8	2, 4-diOH CPIA glucuronic acid Hexopyranuronic acid, 1-[2-(4-chlorophenyl)2,4-dihydroxy-3-methylbutanoate] 	CAS no.	NA	Fat	0.13	0.21
		MW, g/mol	420.8	Brain	0.94	0.94
		Exp Kow @ pH 7.4	NA	Rapid	0.89	0.89
		Log <i>D</i> @ pH 7.4	-3.23	Kidney	0.90	0.92
		Log <i>P</i>	0.49	Liver	0.82	0.89
		p <i>K</i> _a , MA	2.67	Slow	0.86	0.89
		WS, g/L (1,303.0)	1,000.0	Skin	0.75	0.84

^a Parent chemical or metabolite number for cross-reference to Table E7 (Appendix E, Fenvalerate)

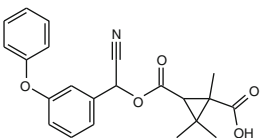
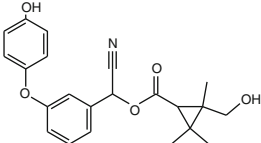
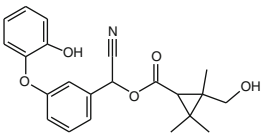
^{b-g} Metabolism source, Kaneko and Miyamoto (2001) and Kaneko (2010). See footnotes in Table D1 (Appendix D)

Table D8 Chemical structure, physical and chemical properties, and tissue partition coefficients for Fenpropathrin and resulting metabolites

No. ^a	Chemical structure ^b	Pesticide metabolism and physical and chemical properties ^{c, d}	Partition coefficients ^e		
			Tissue	Rat	Human
1	Fenpropathrin Cyclopropanecarboxylic acid, 2,2,3,3-tetramethyl-, cyano(3-phenoxyphenyl)methyl ester		CAS no. 39515-41-8 MW, g/mol 349.42 Exp Kow @ pH 7.4 NA Log <i>D</i> @ pH 7.4 5.28 Log <i>P</i> 5.28 pKa NA <i>K</i> _p , cm/h ^f 0.0747 Log <i>K</i> _p ^g -1.126 WS, g/L (1.93E-4) 7.96E-4	Fat 70.74 Brain 14.52 Rapid 4.62 Kidney 5.48 Liver 6.02 Slow 3.34 Skin 7.71	32.97 8.95 2.17 3.37 5.58 3.42 4.18
2	4'-OH fenpropathrin Cyclopropanecarboxylic acid, 2,2,3,3-tetramethyl-, cyano[3-(4-hydroxyphenoxy)phenyl]methyl ester		CAS no. 66280-02-2 MW, g/mol 365.42 Exp Kow @ pH 7.4 NA Log <i>D</i> @ pH 7.4 4.49 Log <i>P</i> 4.49 pKa, MA 9.97 WS, g/L (7.31E-4) 3.38E-3	Fat 81.78 Brain 14.50 Rapid 4.61 Kidney 5.48 Liver 6.02 Slow 3.34 Skin 7.70	39.68 8.99 2.18 3.39 5.61 3.44 4.20
3	2'-OH fenpropathrin Cyclopropanecarboxylic acid, 2,2,3,3-tetramethyl-, cyano[3-(2-hydroxyphenoxy)phenyl]methyl ester		CAS no. 155913-61-4 MW, g/mol 365.42 Exp Kow @ pH 7.4 NA Log <i>D</i> @ pH 7.4 4.64 Log <i>P</i> 4.64 pKa, MA 9.22 WS, g/L (5.44E-4) 2.04E-3	Fat 79.33 Brain 14.51 Rapid 4.62 Kidney 5.48 Liver 6.02 Slow 3.34 Skin 7.71	37.95 8.98 2.18 3.38 5.60 3.43 4.19
4	2-OH methyl fenpropathrin Cyclopropanecarboxylic acid, 2-(hydroxymethyl)-2,3,3-trimethyl-, cyano(3-phenoxyphenyl)methyl ester		CAS no. 66403-98-3 MW, g/mol 365.42 Exp Kow @ pH 7.4 NA Log <i>D</i> @ pH 7.4 3.71 Log <i>P</i> 3.71 pKa, MA 15.1 WS, g/L (3.39E-3) 8.71E-3	Fat 80.20 Brain 14.24 Rapid 4.55 Kidney 5.40 Liver 5.92 Slow 3.30 Skin 7.57	47.32 9.13 2.23 3.45 5.70 3.50 4.27

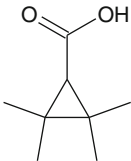
(continued)

Table D8 (continued)

No. ^a	Chemical structure ^b	Pesticide metabolism and physical and chemical properties ^{c, d}	Partition coefficients ^e				
			Tissue	Rat	Human		
5	2-carboxyl fenpropathrin 1,2-cyclopropanedicarboxylic acid, 1,3,3-trimethyl-, 2-[cyano(3-phenoxyphenyl)methyl] ester		CAS no. MW, g/mol Exp Kow @ pH 7.4 Log <i>D</i> @ pH 7.4 Log <i>P</i> p <i>K</i> _a , MA WS, g/L (9.57E-1)	NA 379.41 NA 0.74 3.76 4.29 4.13	Fat Brain Rapid Kidney Liver Slow Skin	0.20 0.89 0.69 0.71 0.67 0.65 0.65	0.22 0.94 0.68 0.74 0.80 0.72 0.71
6	4'-OH, 2-OH methyl fenpropathrin Cyclopropanecarboxylic acid, 2-(hydroxymethyl)-2,3,3-trimethyl-, cyano[3-(4-hydroxyphenoxy)phenyl]methyl ester		CAS no. MW, g/mol Exp Kow @ pH 7.4 Log <i>D</i> @ pH 7.4 Log <i>P</i> p <i>K</i> _a , MA WS, g/L (1.28E-2)	97280-62-1 381.42 NA 2.92 2.92 9.97 2.49E-2	Fat Brain Rapid Kidney Liver Slow Skin	28.26 11.54 3.80 4.47 4.88 2.80 6.18	23.12 8.61 2.17 3.31 5.41 3.36 4.07
7	2'-OH, 2-OH methyl fenpropathrin Cyclopropanecarboxylic acid, 2-(hydroxymethyl)-2,3,3-trimethyl-, cyano[3-(2-hydroxyphenoxy)phenyl]methyl ester		CAS no. MW, g/mol Exp Kow @ pH 7.4 Log <i>D</i> @ pH 7.4 Log <i>P</i> p <i>K</i> _a , MA WS, g/L (9.5E-3)	97280-61-0 381.42 NA 3.07 3.07 9.22 2.22E-2	Fat Brain Rapid Kidney Liver Slow Skin	38.16 12.49 4.07 4.80 5.26 2.98 6.68	29.67 8.92 2.23 3.41 5.59 3.46 4.20
	Hydrolysis Products: Alcohol Leaving groups, metabolites and conjugates See Cyhalothrin data						
8-1	Cyanohydrin of PB aldehyde Benzeneacetonitrile, α-hydroxy-3-phenoxy-						
9-2	Cyanohydrin of 4'-OH PB aldehyde Benzeneacetonitrile, α-hydroxy-3-(4-hydroxyphenoxy)- CAS no. 82186-81-0						
10-3	Cyanohydrin of 2'-OH PB aldehyde Benzeneacetonitrile, α-hydroxy-3-(2-hydroxyphenoxy)- CAS no. NA						
11-4	PB aldehyde Benzaldehyde, 3-phenoxy- CAS no. 39515-51-0						
12-5	4'-OH PB aldehyde Benzaldehyde, 3-(4-hydroxyphenoxy)- CAS no. NA						
13-6	2'-OH PB aldehyde Benzaldehyde, 3-(2-hydroxyphenoxy)- CAS no. NA						

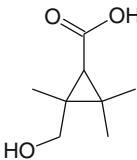
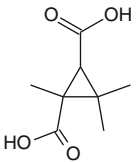
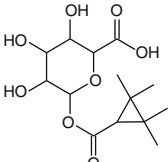
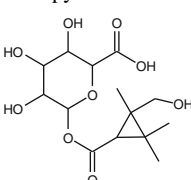
(continued)

Table D8 (continued)

No. ^a	Chemical structure ^b	Pesticide metabolism and physical and chemical properties ^{c, d}	Partition coefficients ^e		
			Tissue	Rat	Human
14-7	PB alcohol				
	Benzenemethanol, 3-phenoxy- CAS no. 13826-35-2				
15-8	4'-OH PB alcohol				
	Benzenemethanol, 3-(4-hydroxyphenoxy)- CAS no. 63987-19-9				
16-9	2'-OH PB alcohol				
	Benzenemethanol, 3-(2-hydroxyphenoxy)- CAS no. 63987-17-7				
17-10	PB acid				
	Benzoic acid, 3-phenoxy- CAS no. 3739-38-6				
18-11	4'-OH PB acid				
	Benzoic acid, 3-(4-hydroxyphenoxy)- CAS no. 35065-12-4				
19-12	2'-OH PB acid				
	Benzoic acid, 3-(2-hydroxyphenoxy)- CAS no. 35101-26-9				
20-13	PB alcohol glucuronic acid				
	Hexopyranosiduronic acid, (3-phenoxyphenyl)methyl CAS no. 65658-93-7				
21-14	4'-OH PB alcohol glucuronic acid				
	Hexopyranosiduronic acid, [3-(4-hydroxyphenoxy)phenyl]methyl CAS no. NA				
22-15	2'-OH PB alcohol glucuronic acid				
	Hexopyranosiduronic acid, [3-(2-hydroxyphenoxy)phenyl]methyl CAS no. NA				
23-16	PB acid glucuronide				
	β -D-Glucopyranuronic acid, 1-(3-phenoxybenzoate) CAS no. 57991-35-2				
24-17	PB acid glycine				
	Glycine, N-(3-phenoxybenzoyl)- CAS no. 57991-36-3				
25-18	4'-OH PB acid glucuronide				
	β -D-Glucopyranuronic acid, 1-[3-(4-hydroxyphenoxy)benzoate] CAS no. 66856-01-7				
26-19	4'-OH PB acid sulfate				
	Benzoic acid, 3-[4-(sulfoxy)phenoxy]- CAS no. 58218-91-0				
27-20	2'-OH PB acid glucuronide				
	Hexopyranuronic acid, 1-[3-(2-hydroxyphenoxy)benzoate] CAS no. NA				
28-21	2'-OH PB acid sulfate				
	Benzoic acid, 3-[2-(sulfoxy)phenoxy]- CAS no. 61183-26-4				
	Hydrolysis Products: Acid Leaving Groups, metabolites and conjugates				
29-1	TetraMeCPCA				
	Cyclopropanecarboxylic acid, 2,2,3,3-tetramethyl-				
					
	CAS no.	15641-58-4	Fat	0.15	0.20
	MW, g/mol	142.2	Brain	0.90	0.92
	Exp Kow @ pH 7.4	NA	Rapid	0.82	0.82
	Log <i>D</i> @ pH 7.4	0.02	Kidney	0.83	0.85
	Log <i>P</i>	1.9	Liver	0.76	0.85
	p <i>K</i> _a , MA	5.52	Slow	0.79	0.82
	WS, g/L (78.8)	446.31	Skin	0.71	0.80
30-2	2-OH, TriMe CPCA				
	Cyclopropanecarboxylic acid, 2-(hydroxymethyl)-2,3,3-trimethyl-				
	CAS no.	97280-65-4	Fat	0.12	0.19
	MW, g/mol	158.2	Brain	0.90	0.90

(continued)

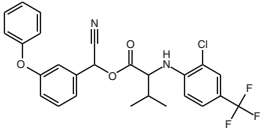
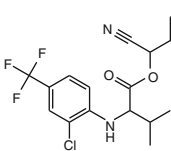
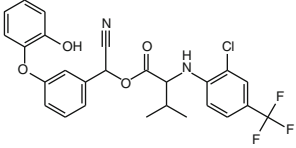
Table D8 (continued)

No. ^a	Chemical structure ^b	Pesticide metabolism and physical and chemical properties ^{c, d}		Partition coefficients ^e		
				Tissue	Rat	Human
31-3		Exp Kow @ pH 7.4	NA	Rapid	0.86	0.86
		Log <i>D</i> @ pH 7.4	-1.65	Kidney	0.86	0.89
		Log <i>P</i>	0.46	Liver	0.79	0.86
		p <i>K</i> _a , MA	5.16	Slow	0.83	0.85
		WS, g/L (1,789.0)	1,000.0	Skin	0.72	0.81
32-4		CAS no.	17219-45-3	Fat	0.13	0.20
		MW, g/mol	172.18	Brain	0.92	0.92
		Exp Kow @ pH 7.4	NA	Rapid	0.88	0.88
		Log <i>D</i> @ pH 7.4	-3.45	Kidney	0.88	0.90
		Log <i>P</i>	0.6	Liver	0.81	0.88
		p <i>K</i> _a , MA	4.54	Slow	0.85	0.87
		WS, g/L (53,065.0)	1,000.0	Skin	0.74	0.83
33-5		CAS no.	NA	Brain	0.13	0.19
		MW, g/mol	318.32	Rapid	0.91	0.92
		Exp Kow @ pH 7.4	NA	Kidney	0.87	0.87
		Log <i>D</i> @ pH 7.4	-2.61	Liver	0.87	0.90
		Log <i>P</i>	1.11	Slow	0.80	0.87
		p <i>K</i> _a , MA	2.68	Skin	0.84	0.86
		WS, g/L (1,623.4)	1,000.0		0.73	0.82
33-5		CAS no.	NA	Brain	0.13	0.20
		MW, g/mol	334.42	Rapid	0.94	0.94
		Exp Kow @ pH 7.4	NA	Kidney	0.89	0.89
		Log <i>D</i> @ pH 7.4	-4.18	Liver	0.89	0.92
		Log <i>P</i>	-0.46	Slow	0.82	0.89
		p <i>K</i> _a , MA	2.68	Skin	0.87	0.89
		WS, g/L (28,538.7)	1,000.0		0.75	0.84

^a Parent chemical or metabolite number for cross-reference to Table E8 ([Appendix E](#), Fenprothrin)

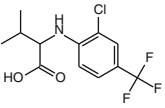
^{b-g} Metabolism source, Kaneko and Miyamoto (2001) and Kaneko (2010). See footnotes in Table D1 ([Appendix D](#))

Table D9 Chemical structure, physical and chemical properties, and tissue partition coefficients for fluvalinate and resulting metabolites

No. ^a	Chemical structure ^b	Pesticide metabolism and physical and chemical properties ^{c, d}	Partition coefficients ^e		
			Tissue	Rat	Human
1	Fluvalinate Valine, N-[2-chloro-4-(trifluoromethyl)phenyl]-, cyano(3-phenoxyphenyl)methyl ester				
		CAS no.	69409-94-5	Fat	68.06
		MW, g/mol	502.91	Brain	14.52
		Exp Kow @ pH 7.4	NA	Rapid	4.62
		Log D @ pH 7.4	5.93	Kidney	5.48
		Log P	5.93	Liver	6.02
		pKa	NA	Slow	3.34
		K _p , cm/h ^f	0.0272	Skin	7.71
		Log K _p ^g	-1.565		4.18
		WS, g/L (5.92E-6)	1.10E-5		
2	4'-OH Fluvalinate Valine, N-[2-chloro-4-(trifluoromethyl)phenyl]-, cyano[3-(4-hydroxyphenoxy)phenyl]methyl ester				
		CAS no.	82186-78-5	Fat	71.52
		MW, g/mol	518.91	Brain	14.52
		Exp Kow @ pH 7.4	NA	Rapid	4.62
		Log D @ pH 7.4	5.15	Kidney	5.48
		Log P	5.15	Liver	6.02
		pKa, MA	9.96	Slow	3.34
		WS, g/L (2.16E-5)	3.08E-5	Skin	7.71
3	2'-OH Fluvalinate Valine, N-[2-chloro-4-(trifluoromethyl)phenyl]-, cyano[3-(2-hydroxyphenoxy)phenyl]methyl ester				
		CAS no.	NA	Fat	71.52
		MW, g/mol	518.91	Brain	14.52
		Exp Kow @ pH 7.4	NA	Rapid	4.62
		Log D @ pH 7.4	5.29	Kidney	5.48
		Log P	5.3	Liver	6.02
		pKa, MA	9.22	Slow	3.34
		WS, g/L (1.64E-5)	2.76E-5	Skin	7.71
	Hydrolysis Products: Alcohol Leaving groups, metabolites and conjugates				
	See Cyhalothrin for data				
4-1	Cyanohydrin of PB aldehyde				
	Benzeneacetone nitrile, α-hydroxy-3-phenoxy- CAS no. 39515-47-4				
5-2	Cyanohydrin of 4'-OH PB aldehyde				
	Benzeneacetone nitrile, α-hydroxy-3-(4-hydroxyphenoxy)- CAS no. 82186-81-0				
6-3	Cyanohydrin of 2'-OH PB aldehyde				
	Benzeneacetone nitrile, α-hydroxy-3-(2-hydroxyphenoxy)- CAS no. NA				
7-4	PB aldehyde				
	Benzaldehyde, 3-phenoxy- CAS no. 39515-51-0				
8-5	4'-OH PB aldehyde				

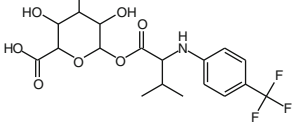
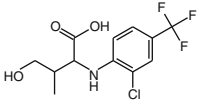
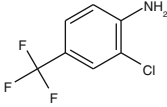
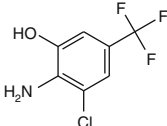
(continued)

Table D9 (continued)

No. ^a	Chemical structure ^b	Pesticide metabolism and physical and chemical properties ^{c, d}	Partition coefficients ^e		
			Tissue	Rat	Human
9-6	Benzaldehyde, 3-(4-hydroxyphenoxy)-	CAS no. NA			
10-7	2'-OH PB aldehyde				
11-8	Benzaldehyde, 3-(2-hydroxyphenoxy)-	CAS no. NA			
12-9	PB alcohol				
13-10	Benzenemethanol, 3-phenoxy-	CAS no. 13826-35-2			
14-11	4'-OH PB alcohol				
15-12	Benzenemethanol, 3-(4-hydroxyphenoxy)-	CAS no. 63987-19-9			
16-13	2'-OH PB alcohol				
17-14	Benzenemethanol, 3-(2-hydroxyphenoxy)-	CAS no. 63987-17-7			
18-15	PB acid				
19-16	Benzoic acid, 3-phenoxy-	CAS no. 3739-38-6			
20-17	4'-OH PB acid				
21-18	Benzoic acid, 3-(4-hydroxyphenoxy)-	CAS no. 35065-12-4			
22-19	2'-OH PB acid				
23-20	Benzoic acid, 3-(2-hydroxyphenoxy)-	CAS no. 35101-26-9			
24-21	PB alcohol glucuronic acid				
25-1	Hexopyranosiduronic acid, (3-phenoxyphenyl)methyl	CAS no. 65658-93-7			
	4'-OH PB alcohol glucuronic acid				
	Hexopyranosiduronic acid, [3-(4-hydroxyphenoxy)phenyl]methyl	CAS no. NA			
	2'-OH PB alcohol glucuronic acid				
	Hexopyranosiduronic acid, [3-(2-hydroxyphenoxy)phenyl]methyl	CAS no. NA			
	PB acid glucuronide				
	β -D-Glucopyranuronic acid, 1-(3-phenoxybenzoate)	CAS no. 57991-35-2			
	PB acid glycine				
	Glycine, N-(3-phenoxybenzoyl)-	CAS no. 57991-36-3			
	4'-OH PB acid glucuronide				
	β -D-Glucopyranuronic acid, 1-[3-(4-hydroxyphenoxy)benzoate]	CAS no. 66856-01-7			
	2'-OH PB acid glucuronide				
	Hexopyranuronic acid, 1-[3-(2-hydroxyphenoxy)benzoate]	CAS no. NA			
	4'-OH PB acid sulfate				
	Benzoic acid, 3-[4-(sulfooxy)phenoxy]-	CAS no. 58218-91-0			
	2'-OH PB acid sulfate				
	Benzoic acid, 3-[2-(sulfooxy)phenoxy]-	CAS no. 61183-26-4			
	Hydrolysis Products: Acid Leaving groups, metabolites and conjugates				
	No common name or abbreviation				
	Valine, N-[2-chloro-4-(trifluoromethyl)phenyl]-				
					
	CAS no.	76338-73-3	Fat	0.11	0.15
	MW, g/mol	295.69	Brain	0.79	0.80
	Exp Kow @ pH 7.4	NA	Rapid	0.73	0.73
	Log <i>D</i> @ pH 7.4	-0.11	Kidney	0.74	0.76
	Log <i>P</i>	3.12	Liver	0.68	0.74
	p <i>K</i> _a , MA	3.84	Slow	0.70	0.73
	WS, g/L (16.15)	73.9	Skin	0.62	0.70

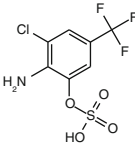
(continued)

Table D9 (continued)

No. ^a	Chemical structure ^b	Pesticide metabolism and physical and chemical properties ^{c, d}	Partition coefficients ^e		
			Tissue	Rat	Human
26-2	No common name or abbreviation Hexopyranuronic acid, 1-O-[N-[4-(trifluoromethyl)phenyl]valyl]-				
		CAS no. NA	Fat	0.12	0.19
		MW, g/mol 437.36	Brain	0.89	0.89
		Exp Kow @ pH 7.4 NA	Rapid	0.85	0.85
		Log <i>D</i> @ pH 7.4 -1.73	Kidney	0.85	0.88
		Log <i>P</i> 1.99	Liver	0.78	0.85
		p <i>K</i> _a , MA 2.67	Slow	0.82	0.84
		WS, g/L (53.74) 1,000.0	Skin	0.71	0.80
27-3	No common name or abbreviation Valine, N-[2-chloro-4-(trifluoromethyl)phenyl]-4-hydroxy-				
		CAS no. 82186-86-5	Fat	0.11	0.17
		MW, g/mol 311.68	Brain	0.84	0.84
		Exp Kow @ pH 7.4 NA	Rapid	0.80	0.80
		Log <i>D</i> @ pH 7.4 -1.35	Kidney	0.80	0.83
		Log <i>P</i> 2.01	Liver	0.74	0.80
		p <i>K</i> _a , MA 3.66	Slow	0.77	0.80
		WS, g/L (149.13) 738.27	Skin	0.67	0.75
28-4	Trifluoromethyl chloroaniline Benzenamine, 2-chloro-4-(trifluoromethyl)-				
		CAS no. 39885-50-2	Fat	60.01	46.20
		MW, g/mol 195.57	Brain	13.23	9.37
		Exp Kow @ pH 7.4 NA	Rapid	4.30	2.34
		Log <i>D</i> @ pH 7.4 3.1	Kidney	5.08	3.58
		Log <i>P</i> 3.1	Liver	5.56	5.87
		p <i>K</i> _a , MB 0.82	Slow	3.15	3.63
		WS, g/L (1.04E-1) 0.18	Skin	7.07	4.41
29-5	Hydroxy, trifluorochloroaniline Phenol, 2-amino-3-chloro-5-(trifluoromethyl)-				
		CAS no. 84960-10-1	Fat	73.33	54.84
		MW, g/mol 211.57	Brain	13.58	9.46
		Exp Kow @ pH 7.4 NA	Rapid	4.40	2.35
		Log <i>D</i> @ pH 7.4 3.17	Kidney	5.20	3.60
		Log <i>P</i> 3.3	Liver	5.70	5.92
		p <i>K</i> _a , MA 7.79	Slow	3.22	3.66
		WS, g/L (7.48E-2) 0.32	Skin	7.25	4.45
30-6	Hydroxy, trifluorochloroaniline sulfate Phenol, 2-amino-3-chloro-5-(trifluoromethyl)-, hydrogen sulfate (ester)				
		CAS no. NA	Fat	0.13	0.19
		MW, g/mol 291.63	Brain	0.91	0.91
		Exp Kow @ pH 7.4 NA	Rapid	0.87	0.87

(continued)

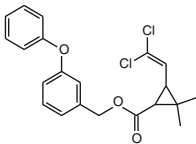
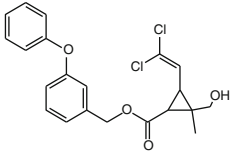
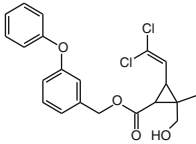
Table D9 (continued)

No. ^a	Chemical structure ^b	Pesticide metabolism and physical and chemical properties ^{c, d}		Partition coefficients ^e		
				Tissue	Rat	Human
		Log <i>D</i> @ pH 7.4	-1.33	Kidney	0.87	0.89
Log <i>P</i>		2.17	Liver	0.80	0.87	
p <i>K</i> _a , MA		-5.46	Slow	0.84	0.86	
WS, g/L (187.8)		358.55	Skin	0.73	0.82	

^a Parent chemical or metabolite number for cross-reference to Table E9 (Appendix E, Fluvalinate)

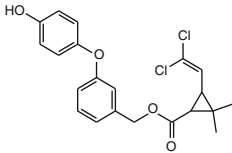
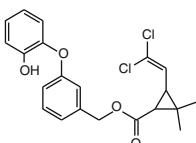
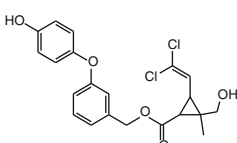
^{b-g} Metabolism source, Kaneko and Miyamoto (2001) and Kaneko (2010). See footnotes in Table D1 (Appendix D)

Table D10 Chemical structure, physical and chemical properties, and tissue partition coefficients for cis/trans-permethrin and resulting metabolites

No. ^a	Chemical structure ^b	Pesticide metabolite and physical and chemical properties ^{c, d}		Partition coefficient ^e			
				Tissue	Rat	Human	
1	(Cis, trans)-permethrin Cyclopropanecarboxylic acid, 3-(2,2-dichloroethenyl)-2,2-dimethyl-(3-phenoxyphenyl) methyl ester-		CAS no.	52645-53-1	Fat	67.40	31.21
MW, g/mol	391.29		Brain	14.52	8.94		
Exp Kow @ pH 7.4	NA		Rapid	4.62	2.17		
Log <i>D</i> @ pH 7.4	7.64		Kidney	5.48	3.36		
Log <i>P</i>	7.64		Liver	6.02	5.57		
p <i>K</i> _a , MA,	NA		Slow	3.34	3.42		
<i>K</i> _p (cm/h) ^f	1.967		Skin	7.71	4.18		
Log <i>K</i> _p ^g	0.294						
WS, g/L (1.04E-6)	3.77E-5						
2	trans- 2-OH, (cis, trans)-permethrin Cyclopropanecarboxylic acid, 3-(2,2-dichloroethenyl)-2-(hydroxymethyl)-2-methyl-, (3-phenoxyphenyl)methyl ester, (1 <i>R</i> ,2 <i>R</i> ,3 <i>R</i>)-rel. ^h		CAS no.	64024-17-5	Fat	67.72	31.38
MW, g/mol	407.3		Brain	14.52	8.94		
Exp Kow @ pH 7.4	NA		Rapid	4.61	2.17		
Log <i>D</i> @ pH 7.4	6.22		Kidney	5.48	3.36		
Log <i>P</i>	6.22		Liver	6.02	5.57		
p <i>K</i> _a , MA,	15.1		Slow	3.34	3.42		
WS, g/L (1.35E-5)	3.64E-4		Skin	7.71	4.18		
3	Cis-2-OH, (cis, trans)-permethrin Cyclopropanecarboxylic acid, 3-(2,2-dichloroethenyl)-2-(hydroxymethyl)-2-methyl-, (3-phenoxyphenyl)methyl ester, (1 <i>R</i> ,2 <i>R</i> ,3 <i>S</i>)-rel. ^h		CAS no.	64024-16-4	Fat	67.72	31.38
MW, g/mol	407.3		Brain	14.52	8.94		
Exp Kow @ pH 7.4	NA		Rapid	4.62	2.17		
Log <i>D</i> @ pH 7.4	6.22		Kidney	5.48	3.36		
Log <i>P</i>	6.22		Liver	6.02	5.57		

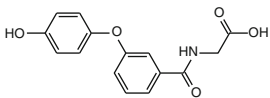
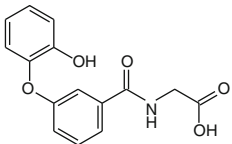
(continued)

Table D10 (continued)

No. ^a	Chemical structure ^b	Pesticide metabolite and physical and chemical properties ^{c, d}		Partition coefficient ^e		
				Tissue	Rat	Human
		pKa, MA,	15.1	Slow	3.34	3.42
		WS, g/L (1.35E-5)	3.64E-4	Skin	7.71	4.18
4	4'-OH-(cis, trans)-permethrin Cyclopropanecarboxylic acid, 3-(2,2-dichloroethenyl)-2,2-dimethyl-, [3-(4-hydroxyphenoxy) phenyl] methyl ester					
		CAS no.	67328-58-9	Fat	67.46	31.24
		MW, g/mol	407.3	Brain	14.52	8.94
		Exp Kow @ pH 7.4	NA	Rapid	4.62	2.17
		Log <i>D</i> @ pH 7.4	6.85	Kidney	5.48	3.36
		Log <i>P</i>	6.85	Liver	6.02	5.57
		pKa, MA,	10.04	Slow	3.34	3.42
		WS, g/L (3.9E-6)	1.08E-4	Skin	7.71	4.18
5	2'-OH, (cis, trans)-permethrin Cyclopropanecarboxylic acid, 3-(2,2-dichloroethenyl)-2,2-dimethyl-, [3-(2-hydroxyphenoxy)phenyl]methyl ester					
		CAS no.	NA	Fat	67.44	31.23
		MW, g/mol	407.3	Brain	14.52	8.94
		Exp Kow @ pH 7.4	NA	Rapid	4.62	2.17
		Log <i>D</i> @ pH 7.4	6.99	Kidney	5.48	3.36
		Log <i>P</i>	7.00	Liver	6.02	5.57
		pKa, MA,	9.31	Slow	3.34	3.42
		WS, g/L (2.96E-6)	9.59E-5	Skin	7.71	4.18
6	4'-OH-trans-2-OH-cis-permethrin Cyclopropanecarboxylic acid, 3-(2,2-dichloroethenyl)-2-(hydroxymethyl)-2-methyl-, [3-(4-hydroxyphenoxy)phenyl]methyl ester					
		CAS no.	64024-20-0	Fat	69.80	32.47
		MW, g/mol	423.29	Brain	14.52	8.95
		Exp Kow @ pH 7.4	NA	Rapid	4.62	2.17
		Log <i>D</i> @ pH 7.4	5.43	Kidney	5.48	3.37
		Log <i>P</i>	5.43	Liver	6.02	5.58
		pKa, MA,	10.04	Slow	3.34	3.42
		WS, g/L (5.06E-5)	1.04E-3	Skin	7.71	4.18
	Hydrolysis Products: Alcohol Leaving group, metabolites and conjugates					
	See cyhalothrin					
7-1	PB alcohol					
	Benzenemethanol, 3-phenoxy- CAS no. 13826-35-2					
8-2	4'-OH-PB alcohol					
	Benzenemethanol, 3-(4-hydroxyphenoxy)- CAS no. 63987-19-9					
9-3	2'-OH PB alcohol					
	Benzenemethanol, 3-(2-hydroxyphenoxy)- CAS no. 63987-17-7					
10-4	PB aldehyde					
	Benzaldehyde, 3-phenoxy- CAS no. 39515-51-0					
11-5	4'-OH PB aldehyde					
	Benzaldehyde, 3-(4-hydroxyphenoxy)- CAS no. NA					
12-6	2'-OH PB aldehyde					
	Benzaldehyde, 3-(2-hydroxyphenoxy)- CAS no. NA					

(continued)

Table D10 (continued)

No. ^a	Chemical structure ^b	Pesticide metabolite and physical and chemical properties ^{c, d}	Partition coefficient ^e			
			Tissue	Rat	Human	
13-7	PB alcohol glucuronic acid Hexopyranosiduronic acid, (3-phenoxyphenyl)methyl CAS no. 65658-93-7					
14-8	4'-OH PB alcohol glucuronic acid Hexopyranosiduronic acid, [3-(4-hydroxyphenoxy)phenyl]methyl CAS no. NA					
15-9	2'-OH PB alcohol glucuronic acid Hexopyranosiduronic acid, [3-(2-hydroxyphenoxy)phenyl]methyl CAS no. NA					
16-10	PB acid Benzoic acid, 3-phenoxy- CAS no. 3739-38-6					
17-11	4'-OH PB acid Benzoic acid, 3-(4-hydroxyphenoxy)- CAS no. 35065-12-4					
18-12	2'-OH PB acid Benzoic acid, 3-(2-hydroxyphenoxy)- CAS no. 35101-26-9					
19-13	PB acid glucuronide β -D-glucopyranuronic acid, 1-(3-phenoxybenzoate) CAS no. 57991-35-2					
20-14	PB acid glycine Glycine, N-(3-phenoxybenzoyl)- CAS no. 57991-36-3					
21-15	4'-OH PB acid glucuronide β -D-Glucopyranuronic acid, 1-[3-(4-hydroxyphenoxy)benzoate] CAS no. 66856-01-7					
22-16	4'-OH PB acid glycine Glycine, N-[3-(4-hydroxyphenoxy)benzoyl]- 	CAS no. MW, g/mol Exp Kow @ pH 7.4 Log <i>D</i> @ pH 7.4 Log <i>P</i> p <i>K</i> _a , MA, WS, g/L (445.6)	74857-94-6 287.27 NA -1.74 1.76 3.62 1,000.0	Fat Brain Rapid Kidney Liver Slow Skin	0.14 0.98 0.94 0.94 0.86 0.91 0.79	0.22 0.99 0.94 0.97 0.94 0.93 0.88
23-17	4'-OH PB acid sulfate Benzoic acid, 3-[4-(sulfooxy) phenoxy] CAS no. 58218-91-0					
24-18	2'-OH PB acid glucuronide Hexopyranuronic acid, 1-[3-(2-hydroxyphenoxy)benzoate] CAS no. NA					
25-19	2'-OH PB acid glycine Glycine, N-[3-(2-hydroxyphenoxy)benzoyl]- 	CAS no. MW, g/mol Exp Kow @ pH 7.4 Log <i>D</i> @ pH 7.4 Log <i>P</i> p <i>K</i> _a , A, WS, g/L (345.1)	NA 287.27 NA -1.61 1.91 3.63 1,000.0	Fat Brain Rapid Kidney Liver Slow Skin	0.15 0.98 0.94 0.94 0.86 0.91 0.79	0.22 0.99 0.94 0.97 0.94 0.93 0.88
26-20	2'-OH PB acid sulfate Benzoic acid, 3-[2-(sulfooxy)phenoxy]- CAS no. 61183-26-4 Hydrolysis Products: Acid Leaving groups, metabolites and conjugates					
27-1	(cis, trans)-Permethrinic acid (DCCA) Cyclopropanecarboxylic acid, 3-(2,2-dichloroethenyl)-2,2-dimethyl- CAS no. 55701-05-8					

(continued)

Table D10 (continued)

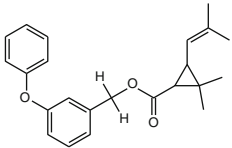
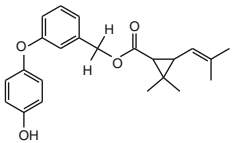
No. ^a	Chemical structure ^b	Pesticide metabolite and physical and chemical properties ^{c, d}	Partition coefficient ^e		
			Tissue	Rat	Human
28-2	(cis, trans)-2-OH methyl-(cis, trans)-Permethrinic acid (2OH-methyl DCCA) Cyclopropanecarboxylic acid, 3-(2,2-dichloroethenyl)-2-(hydroxymethyl)-2-methyl- CAS no. 64162-73-8				
29-3	(cis, trans)-DCCA glucuronic acid (DCCAG) Hexopyranuronic acid, 1-O-[[3-(2,2-dichloroethenyl)-2,2-dimethylcyclopropyl]carbonyl]- CAS no. 80446-46-4				
30-4	(cis, trans)-2-OH methyl, (cis, trans)-DCCA glucuronic acid Hexopyranuronic acid, 1-O-[[3-(2,2-dichloroethenyl)-2-(hydroxymethyl)-2-methylcyclopropyl]carbonyl]- CAS no. 61183-31-1				
31-5	cis-2-OH methyl-(cis, trans)-DCCA lactone 3-oxabicyclo[3.1.0] hexano-2-one, 6-(2,2-dichloroethenyl)-5-methyl- CAS no. NA				

^a Parent chemical or metabolite number for cross-reference to Tables E10 and E11 ([Appendix E](#), trans and cis-permethrin)

^{b-g} Metabolism source, Kaneko and Miyamoto (2001) and Kaneko (2010). See footnotes in Table D1 ([Appendix D](#))

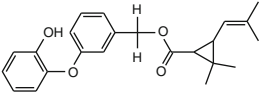
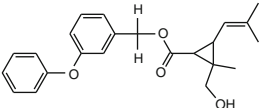
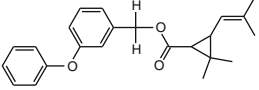
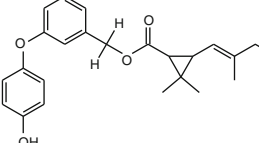
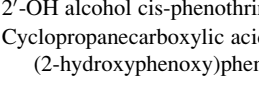
^{h, i} CAS nos. for generic structures unavailable

Table D11 Chemical structure, physical and chemical properties, and tissue partition coefficients for (cis, trans)-phenothrin and resulting metabolites

No. ^a	Chemical structure ^b	Pesticide metabolism and physical and chemical properties ^{c, d}	Partition coefficients ^e			
			Tissue	Rat	Human	
1	(cis, trans)-phenothrin Cyclopropanecarboxylic acid, 2,2-dimethyl-3-(2-methyl-1-propenyl)-, (3-phenoxyphenyl) methyl ester					
		CAS no.	26002-80-2	Fat	67.40	31.21
		MW, g/mol	350.5	Brain	14.52	8.94
		Exp K_{ow} @ pH 7.4	NA	Rapid	4.62	2.17
		Log D @ pH 7.4	7.68	Kidney	5.48	3.36
		Log P	7.68	Liver	6.02	5.57
		pKa	NA	Slow	3.34	3.42
		K_p , cm/h ^f	3.724	Skin	7.71	4.18
		Log K_p ^g	0.571			
		WS, g/L (1.7E-6)	1.20E-4			
2	4'-OH cis-phenothrin Cyclopropanecarboxylic acid, 2,2-dimethyl-3-(2-methyl-1-propen-1-yl)-, [3-(4-hydroxyphenoxy)phenyl]methyl ester					
		CAS no.	NA	Fat	67.45	31.24
		MW, g/mol	366.5	Brain	14.52	8.94
		Exp K_{ow} @ pH 7.4	NA	Rapid	4.62	2.17
		Log D @ pH 7.4	6.89	Kidney	5.48	3.36
		Log P	6.89	Liver	6.02	5.57
		pKa, MA	10.04	Slow	3.34	3.42
		WS, g/L (6.43E-6)	3.43E-4	Skin	7.71	4.18

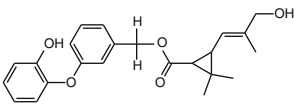
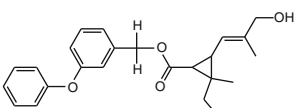
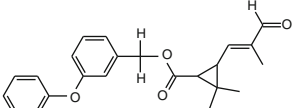
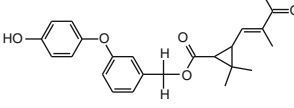
(continued)

Table D11 (continued)

No. ^a	Chemical structure ^b	Pesticide metabolism and physical and chemical properties ^{c, d}	Partition coefficients ^e			
			Tissue	Rat	Human	
3	2'-OH cis-phenothrin Cyclopropanecarboxylic acid, 2,2-dimethyl-3-(2-methyl-1-propen-1-yl)-, [3-(2-hydroxyphenoxy)phenyl]methyl ester		CAS no. MW, g/mol Exp K _{ow} @ pH 7.4 Log D @ pH 7.4 Log P pKa, MA WS, g/L (4.79E-6)	NA 366.5 NA 7.04 7.04 9.31 3.06E-4	Fat Brain Rapid Kidney Liver Slow Skin	67.43 31.23 14.52 8.94 4.62 2.17 5.48 3.36 6.02 5.57 3.34 3.42 7.71 4.18
4	(cis, trans)-2-OH methyl-cis-phenothrin Cyclopropanecarboxylic acid, 2-(hydroxymethyl)-2-methyl-3-(2-methyl-1-propen-1-yl)-, (3-phenoxyphenyl)methyl ester		CAS no. MW, g/mol Exp K _{ow} @ pH 7.4 Log D @ pH 7.4 Log P pKa, MA WS, g/L (2.22E-5)	NA 366.45 NA 6.26 6.26 15.1 1.16E-3	Fat Brain Rapid Kidney Liver Slow Skin	67.69 31.36 14.52 8.94 4.62 2.17 5.48 3.36 6.02 5.57 3.34 3.42 7.71 4.18
5	(cis, trans)-Alcohol (cis, trans)-phenothrin Cyclopropanecarboxylic acid, 3-(3-hydroxy-2-methyl-1-propen-1-yl)-2,2-dimethyl-, (3-phenoxyphenyl)methyl ester		CAS no. MW, g/mol Exp K _{ow} @ pH 7.4 Log D @ pH 7.4 Log P pKa, MA WS, g/L (3.85E-5)	NA 366.5 NA 5.98 5.98 14.83 1.44E-3	Fat Brain Rapid Kidney Liver Slow Skin	68.00 31.52 14.52 8.94 4.62 2.17 5.48 3.36 6.02 5.57 3.34 3.42 7.71 4.18
6	4'-OH alcohol cis-phenothrin Cyclopropanecarboxylic acid, 3-(3-hydroxy-2-methyl-1-propen-1-yl)-2, 2-dimethyl-, [3-(4-phenoxy)phenyl]methyl ester		CAS no. MW, g/mol Exp K _{ow} @ pH 7.4 Log D @ pH 7.4 Log P pKa, MA WS, g/L (1.45E-4)	NA 382.45 NA 5.19 5.19 10.04 4.12E-3	Fat Brain Rapid Kidney Liver Slow Skin	71.56 33.41 14.52 8.95 4.62 2.17 5.48 3.37 6.02 5.58 3.34 3.42 7.71 4.18
7	2'-OH alcohol cis-phenothrin Cyclopropanecarboxylic acid, 3-(3-hydroxy-2-methyl-1-propen-1-yl)-2,2-dimethyl-, [3-(2-hydroxyphenoxy)phenyl]methyl ester		CAS no. MW, g/mol	NA 382.45	Fat Brain	70.34 32.76 14.52 8.95

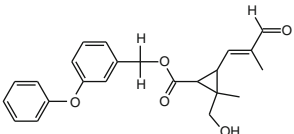
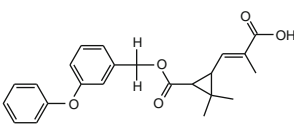
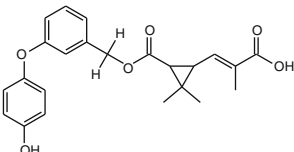
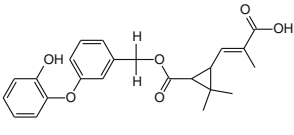
(continued)

Table D11 (continued)

No. ^a	Chemical structure ^b	Pesticide metabolism and physical and chemical properties ^{c, d}		Partition coefficients ^c		
				Tissue	Rat	Human
8		Exp K_{ow} @ pH 7.4	NA	Rapid	4.62	2.17
		Log D @ pH 7.4	5.34	Kidney	5.48	3.37
		Log P	5.34	Liver	6.02	5.58
		pKa, MA	9.31	Slow	3.34	3.42
		WS, g/L (1.08E-4)	3.68E-3	Skin	7.71	4.18
		Cyclopropanecarboxylic acid, 2-(hydroxymethyl)-3-[3-hydroxy-2-methyl-1-propen-1-yl]-2-methyl-, (3-phenoxyphenyl)methyl				
9		CAS no.	NA	Fat	80.67	38.86
		MW, g/mol	382.45	Brain	14.51	8.99
		Exp K_{ow} @ pH 7.4	NA	Rapid	4.62	2.18
		Log D @ pH 7.4	4.56	Kidney	5.48	3.38
		Log P	4.56	Liver	6.02	5.60
		pKa, MA	14.83	Slow	3.34	3.43
WS, g/L (5.01E-4)	4.65E-3	Skin	7.70	4.20		
10		CAS no.	NA	Fat	67.72	31.38
		MW, g/mol	364.43	Brain	14.52	8.94
		Exp K_{ow} @ pH 7.4	NA	Rapid	4.62	2.17
		Log D @ pH 7.4	6.22	Kidney	5.48	3.36
		Log P	6.22	Liver	6.02	5.57
		pKa, MA	10.04	Slow	3.34	3.42
WS, g/L (2.47E-5)	4.64E-4	Skin	7.71	4.18		
11		CAS no.	NA	Fat	69.09	32.10
		MW, g/mol	380.43	Brain	14.52	8.95
		Exp K_{ow} @ pH 7.4	NA	Rapid	4.62	2.17
		Log D @ pH 7.4	5.57	Kidney	5.48	3.37
		Log P	5.58	Liver	6.02	5.58
		pKa, MA	9.31	Slow	3.34	3.42
WS, g/L (7.08E-5)	1.18E-3	Skin	7.71	4.18		

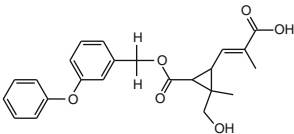
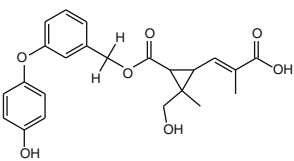
(continued)

Table D11 (continued)

No. ^a	Chemical structure ^b	Pesticide metabolism and physical and chemical properties ^{c, d}	Partition coefficients ^c				
			Tissue	Rat	Human		
12	2-OH methyl aldehyde cis phenothrin Cyclopropanecarboxylic acid, 2-(hydroxymethyl)-2-methyl-3-[2-methyl-3-oxo-1-propenyl]-, (3-phenoxyphenyl)methyl ester		CAS no.	NA	Fat	76.70	36.30
		MW, g/mol	380.43	Brain	14.52	8.97	
		Exp K_{ow} @ pH 7.4	NA	Rapid	4.62	2.18	
		Log D @ pH 7.4	4.8	Kidney	5.48	3.38	
		Log P	4.8	Liver	6.02	5.59	
		pKa, MA	15.1	Slow	3.34	3.43	
		WS, g/L (3.22E-4)	4.49E-3	Skin	7.71	4.19	
13	2-carboxy (cis, trans)-phenothrin Cyclopropanecarboxylic acid, 3-[2-carboxy-1-propen-1-yl]-2,2-dimethyl-, (3-phenoxyphenyl)methyl ester (1R-cis, 79897-38-4)		CAS no.	79897-38-4	Fat	70.19	40.75
		MW, g/mol	380.43	Brain	14.18	9.07	
		Exp K_{ow} @ pH 7.4	NA	Rapid	4.53	2.21	
		Log D @ pH 7.4	3.75	Kidney	5.37	3.42	
		Log P	6.14	Liver	5.90	5.66	
		pKa, MA	4.99	Slow	3.29	3.47	
		WS, g/L (2.54E-3)	5.25E-2	Skin	7.54	4.24	
14	2-carboxy 4'OH cis-phenothrin Cyclopropanecarboxylic acid, 3-[2-carboxy-1-propen-1-yl]-2,2-dimethyl-, [3-(4-hydroxyphenoxy)phenyl]methyl ester (1R-cis, 79861-56-6)		CAS no.	79861-56-6	Fat	25.37	20.49
		MW, g/mol	396.43	Brain	11.46	8.44	
		Exp K_{ow} @ pH 7.4	NA	Rapid	3.76	2.12	
		Log D @ pH 7.4	2.96	Kidney	4.43	3.24	
		Log P	5.35	Liver	4.84	5.30	
		pKa, MA	4.99	Slow	2.77	3.29	
		WS, g/L (9.56E-3)	0.15	Skin	6.13	3.99	
15	2-carboxy 2'OH cis-phenothrin Cyclopropanecarboxylic acid, 3-[2-carboxy-1-propen-1-yl]-2,2-dimethyl-, [3-(2-hydroxyphenoxy)phenyl]methyl ester		CAS no.	NA	Fat	33.13	25.47
		MW, g/mol	396.43	Brain	12.33	8.74	
		Exp K_{ow} @ pH 7.4	NA	Rapid	4.01	2.18	
		Log D @ pH 7.4	3.1	Kidney	4.74	3.34	
		Log P	5.53	Liver	5.18	5.47	
		pKa, MA	4.99	Slow	2.94	3.38	
		WS, g/L (7.26E-3)	0.13	Skin	6.59	4.11	

(continued)

Table D11 (continued)

No. ^a	Chemical structure ^b	Pesticide metabolism and physical and chemical properties ^{c, d}	Partition coefficients ^e			
			Tissue	Rat	Human	
16	Carboxy 2-OH methyl cis-phenothrin Cyclopropanecarboxylic acid, 3-[2-carboxyl-1-propen-1-yl]-2-(hydroxymethyl)-2-methyl-, (3-phenoxyphenyl)methyl ester					
		CAS no.	NA	Fat	5.77	5.29
		MW, g/mol	396.43	Brain	6.00	5.58
		Exp K _{ow} @ pH 7.4	NA	Rapid	2.16	1.57
		Log D @ pH 7.4	2.32	Kidney	2.50	2.28
		Log P	4.72	Liver	2.67	3.58
		pKa, MA	4.99	Slow	1.66	2.30
		WS, g/L (3.36E-2)	0.51	Skin	3.29	2.74
17	Carboxy 2-OH methyl 4'-OH cis phenothrin Cyclopropanecarboxylic acid, 3-[2-carboxyl-1-propen-1-yl]-2-(hydroxymethyl)-2-methyl-, [3-(4-hydroxyphenoxy)phenyl]methyl ester					
		CAS no.	NA	Fat	0.86	0.84
		MW, g/mol	412.43	Brain	1.85	2.04
		Exp K _{ow} @ pH 7.4	NA	Rapid	0.94	0.86
		Log D @ pH 7.4	1.54	Kidney	1.02	1.08
		Log P	3.93	Liver	1.03	1.44
		pKa, MA	4.99	Slow	0.81	1.07
		WS, g/L (0.124)				
	Hydrolysis Products: Alcohol Leaving groups, metabolites and conjugates					
	See permethrin for data					
18-1	PB alcohol					
	Benzenemethanol, 3-phenoxy-	CAS no. 13826-35-2				
19-2	4'-OH PB alcohol					
	Benzenemethanol, 3-(4-hydroxyphenoxy)-	CAS no. 63987-19-9				
20-3	2'-OH PB alcohol					
	Benzenemethanol, 3-(2-hydroxyphenoxy)-	CAS no. 63987-17-7				
21-4	PB aldehyde					
	Benzaldehyde, 3-phenoxy-	CAS no. 39515-51-0				
22-5	4'-OH PB aldehyde					
	Benzaldehyde, 3-(4-hydroxyphenoxy)-	CAS no. NA				
23-6	2'-OH PB aldehyde					
	Benzaldehyde, 3-(2-hydroxyphenoxy)-	CAS no. NA				
24-7	PB acid					
	Benzoic acid, 3-phenoxy-	CAS no. 3739-38-6				
25-8	4'-OH PB acid					
	Benzoic acid, 3-(4-hydroxyphenoxy)-	CAS no. 35065-12-4				
26-9	2'-OH PB acid					
	Benzoic acid, 3-(2-hydroxyphenoxy)-	CAS no. 35101-26-9				
27-10	PB alcohol glucuronic acid					
	Hexopyranosiduronic acid, (3-phenoxyphenyl)methyl	CAS no. 65658-93-7				
28-11	4'-OH PB alcohol glucuronic acid					
	Hexopyranosiduronic acid, [3-(4-hydroxyphenoxy)phenyl]methyl	CAS no. NA				

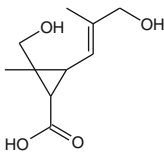
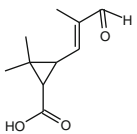
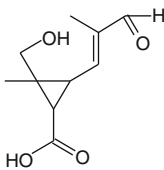
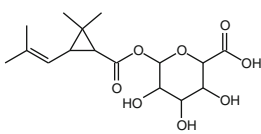
(continued)

Table D11 (continued)

No. ^a	Chemical structure ^b	Pesticide metabolism and physical and chemical properties ^{c, d}	Partition coefficients ^e		
			Tissue	Rat	Human
29-12	2'-OH PB alcohol glucuronic acid Hexopyranosiduronic acid, [3-(2-hydroxyphenoxy)phenyl]methyl CAS no. NA				
30-13	PB acid glucuronide β -D-Glucopyranuronic acid, 1-(3-phenoxybenzoate) CAS no. 57991-35-2				
31-14	PB acid glycine Glycine, N-(3-phenoxybenzoyl)- CAS no. 57991-36-3				
32-15	4'-OH PB acid glucuronide β -D-Glucopyranuronic acid, 1-[3-(4-hydroxyphenoxy)benzoate] CAS no. 66856-01-7				
33-16	4'-OH PB acid sulfate Benzoic acid, 3-[4-(sulfoxy)phenoxy]- CAS no. 58218-91-0				
34-17	2'-OH PB acid glucuronide β -D-Glucopyranuronic acid, 1-[3-(2-hydroxyphenoxy)benzoate] CAS no. 66856-01-7				
35-18	2'-OH PB acid sulfate Benzoic acid, 3-[2-(sulfoxy)phenoxy]- CAS no. 61183-26-4 Hydrolysis Products, Acid Leaving groups, metabolites and conjugates				
36-1	(cis, trans)-chrysanthemic acid (CPCA) Cyclopropanecarboxylic acid, 2,2-dimethyl-3-(2-methyl-1-propen-1-yl)- CAS no. 10453-89-1	MW, g/mol 168.23 Exp K_{ow} @ pH 7.4 NA Log D @ pH 7.4 0.11 Log P 2.19 pKa, MA 5.31 WS, g/L (50.5) 272.34	Fat 0.13 Brain 0.85 Rapid 0.76 Kidney 0.77 Liver 0.72 Slow 0.74 Skin 0.66	0.18 0.87 0.76 0.80 0.80 0.77 0.74	
37-2	3-OH methyl (cis, trans)-chrysanthemic acid (3-OHMCPCA) Cyclopropanecarboxylic acid, 3-[3-hydroxy-2-methyl-1-propen-1-yl]-2,2-dimethyl- CAS no. 22413-48-5	MW, g/mol 184.23 Exp K_{ow} @ pH 7.4 NA Log D @ pH 7.4 -1.82 Log P 0.49 pKa, MA 5.03 WS, g/L (1,881.2) 1,000.0	Fat 0.12 Brain 0.87 Rapid 0.83 Kidney 0.83 Liver 0.76 Slow 0.80 Skin 0.70	0.18 0.87 0.83 0.85 0.83 0.82 0.78	
38-3	2-OH methyl cis-chrysanthemic acid Cyclopropanecarboxylic acid, 2-(hydroxymethyl)-2-methyl-3-(2-methyl-1-propen-1-yl)- CAS no. NA	MW, g/mol 184.23 Exp K_{ow} @ pH 7.4 NA Log D @ pH 7.4 -1.75 Log P 0.9 pKa, MA 4.62 WS, g/L (1,639.3) 1,000	Fat 0.14 Brain 0.98 Rapid 0.94 Kidney 0.94 Liver 0.86 Slow 0.91 Skin 0.79	0.22 0.99 0.94 0.97 0.94 0.93 0.88	

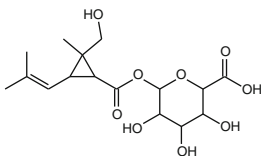
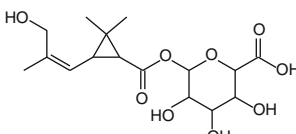
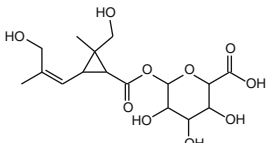
(continued)

Table D11 (continued)

No. ^a	Chemical structure ^b	Pesticide metabolism and physical and chemical properties ^{c, d}		Partition coefficients ^e			
				Tissue	Rat	Human	
39-4	2-OH methyl-3-OH cis-chrysanthemic acid (2, 3-OH-Me-CPCA) Cyclopropanecarboxylic acid, 2-(hydroxymethyl)-3-[3-hydroxy-2-methyl-1-propen-1-yl]-methyl-		CAS no.	NA	Fat	0.14	0.22
			MW, g/mol	200.23	Brain	0.98	0.99
			Exp K _{ow} @ pH 7.4	NA	Rapid	0.94	0.94
			Log D @ pH 7.4	-3.51	Kidney	0.94	0.97
			Log P	-0.8	Liver	0.86	0.94
			pKa, MA	4.52	Slow	0.91	0.93
			WS, g/L (43,354.0)	1,000	Skin	0.79	0.88
40-5	3-aldehyde (cis, trans)-chrysanthemic acid (3-ACPCA) Cyclopropanecarboxylic acid, 2,2-dimethyl-3-[2-methyl-3-oxo-1-propen-yl]-		CAS no.	874301-57-2	Fat	0.12	0.18
			MW, g/mol	182.22	Brain	0.87	0.87
			Exp K _{ow} @ pH 7.4	NA	Rapid	0.83	0.83
			Log D @ pH 7.4	-1.73	Kidney	0.83	0.86
			Log P	0.78	Liver	0.76	0.83
			pKa, MA	4.87	Slow	0.80	0.82
			WS, g/L (1,612.3)	1,000.0	Skin	0.70	0.78
41-6	3-aldehyde-2-OH methyl cis chrysanthemic acid Cyclopropanecarboxylic acid, 2-(hydroxymethyl)-2-methyl-3-[2-methyl-3-oxo-1-propen-1-yl]-		CAS no.	NA	Fat	0.14	0.22
			MW, g/mol	198.22	Brain	0.98	0.99
			Exp K _{ow} @ pH 7.4	NA	Rapid	0.94	0.94
			Log D @ pH 7.4	-3.38	Kidney	0.94	0.97
			Log P	-0.52	Liver	0.86	0.94
			pKa, MA	4.39	Slow	0.91	0.93
			WS, g/L (34,405.3)	1,000.0	Skin	0.79	0.88
42-7	2-carboxyl (cis, trans)-chrysanthemic acid (CCPCA) Cyclopropanecarboxylic acid, 3-[2-carboxy-1-propen-1-yl]-2,2-dimethyl-		CAS no.	497-95-0			
43-8	(cis, trans) 2-carboxy (cis, trans)-2-OH methyl (cis, trans)-chrysanthemic acid (2-OH methyl-CCPCA) Cyclopropanecarboxylic acid, 3-[2-carboxy-1-propen-1-yl]-2-(hydroxymethyl)-2-methyl-		CAS no.	NA			
44-9	(cis, trans)-CPCA glucuronic acid Hexopyranuronic acid, 1-O-[[2,2-dimethyl-3-(2-methyl-1-propen-1-yl)cyclopropyl]carbonyl]-		CAS no.	NA	Fat	0.12	0.19
			MW, g/mol	344.36	Brain	0.90	0.90
			Exp K _{ow} @ pH 7.4	NA	Rapid	0.85	0.86
			Log D @ pH 7.4	-1.44	Kidney	0.86	0.88
			Log P	2.28	Liver	0.79	0.86
			pKa, MA	2.68	Slow	0.83	0.85
			WS, g/L (113.7)	1,000.0	Skin	0.72	0.81

(continued)

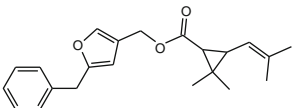
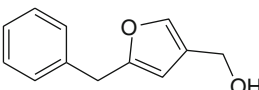
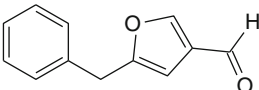
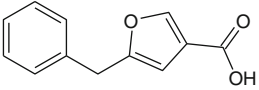
Table D11 (continued)

No. ^a	Chemical structure ^b	Pesticide metabolism and physical and chemical properties ^{c, d}	Partition coefficients ^c				
			Tissue	Rat	Human		
45-10	2-OH methyl CPCA glucuronic acid Hexopyranuronic acid, 1-O-[[2-(hydroxymethyl)-2-methyl-3-(2-methyl-1-propen-1-yl)cyclopropyl]carbonyl]-		CAS no.	NA	Fat	0.14	0.22
		MW, g/mol	360.36	Brain	0.98	0.99	
		Exp K_{ow} @ pH 7.4	NA	Rapid	0.94	0.94	
		Log D @ pH 7.4	-2.86	Kidney	0.94	0.97	
		Log P	0.86	Liver	0.86	0.94	
		pKa, MA	2.68	Slow	0.91	0.93	
		WS, g/L (1,485.1)	1,000.0	Skin	0.79	0.88	
46-11	3-OH methyl (cis, trans)-CPCA glucuronic acid Hexopyranuronic acid, 1-O-[[3-[3-hydroxy-2-methyl-1-propen-1-yl]-2,2-dimethylcyclopropyl]carbonyl]-		CAS no.	NA	Fat	0.13	0.20
		MW, g/mol	360.36	Brain	0.93	0.93	
		Exp K_{ow} @ pH 7.4	NA	Rapid	0.89	0.89	
		Log D @ pH 7.4	-3.14	Kidney	0.89	0.92	
		Log P	0.58	Liver	0.82	0.89	
		pKa, MA	2.68	Slow	0.86	0.88	
		WS, g/L (2,575.5)	1,000.0	Skin	0.75	0.84	
47-12	2-OH-methyl-3-OH CPCA glucuronide Hexopyranuronic acid, 1-O-[[2-(hydroxymethyl)-3-[3-hydroxy-2-methyl-1-propen-1-yl]-2-methyl cyclopropyl]carbonyl]-		CAS no.	NA	Fat	0.14	0.22
		MW, g/mol	376.36	Brain	0.98	0.99	
		Exp K_{ow} @ pH 7.4	NA	Rapid	0.94	0.94	
		Log D @ pH 7.4	-4.56	Kidney	0.94	0.97	
		Log P	-0.84	Liver	0.86	0.94	
		pKa, MA	2.68	Slow	0.91	0.93	
		WS, g/L (33,569.3)	1,000.0	Skin	0.79	0.88	
48-13	(cis, trans)-CCPCA glucuronic acid Hexopyranuronic acid, 1-O-[[3-[2-carboxy-1-propen-1-yl]-2,2-dimethylcyclopropyl]carbonyl]- CAS no. NA						
49-15	2-OH methyl CCPCA glucuronic acid Hexopyranuronic acid, 1-O-[[3-[(1Z)-2-carboxy-1-propen-1-yl]-2-(hydroxymethyl)-2-methylcyclopropyl]carbonyl]-						

^a Parent chemical or metabolite number for cross-reference to Tables E12 and E13 ([Appendix E](#), trans and cis phenothrin)

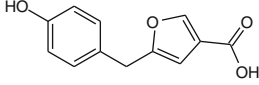
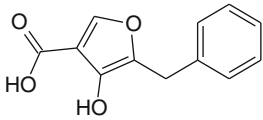
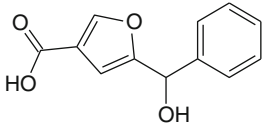
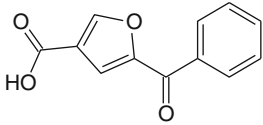
^{b-g} Metabolism source, Kaneko and Miyamoto (2001) and Kaneko (2010). See footnotes in Table D1 ([Appendix C](#))

Table D12 Chemical structure, physical and chemical properties, and tissue partition coefficients for (cis, trans)-resmethrin and resulting metabolites

No. ^a	Chemical structure ^b	Pesticide metabolite and physical and chemical properties ^{c, d}	Partition coefficient ^e		
			Tissue	Rat	Human
1	(cis, trans)-resmethrin Cyclopropane carboxylic acid, 2,2-dimethyl-3-(2-methyl-1-propenyl)-[5-(phenylmethyl)-3-furanyl] methyl ester (CAS no. 10453-86-8)		CAS no. 33911-28-3 MW, g/mol 338.4 Exp Kow @ pH 7.4 NA Log D @ pH 7.4 6.63 Log P 6.63 pKa, NA K _p , cm/h ^f 0.793 Log K _p ^g -0.100 WS, g/L (1.58E-5) 8.28E-4	Fat 7.33 Brain 14.52 Rapid 4.62 Kidney 5.48 Liver 6.02 Slow 3.34 Skin 7.71	31.27 6.82 5.79 2.17 3.36 5.57 3.42 4.18
Hydrolysis Products: Alcohol Leaving groups, metabolites and conjugates					
2-1	BF Alcohol 3-furanmethanol, 5-(phenylmethyl)		CAS no. 20416-09-5 MW, g/mol 188.2 Exp Kow @ pH 7.4 NA Log D @ pH 7.4 2.18 Log P 2.18 pKa, MA 14.21 WS, g/L (0.690) 1.06	Fat 7.33 Brain 5.93 Rapid 2.22 Kidney 2.54 Liver 2.71 Slow 1.73 Skin 3.29	6.82 5.79 1.70 2.43 3.75 2.45 2.89
3-2	BF Aldehyde 3-furancarboxaldehyde, 5-(phenylmethyl)		CAS no. 34878-15-4 MW, g/mol 186.2 Exp Kow @ pH 7.4 NA Log D @ pH 7.4 2.5 Log P 2.5 pKa, NA NA WS, g/L (0.376) 0.11	Fat 17.13 Brain 8.99 Rapid 3.12 Kidney 3.63 Liver 3.92 Slow 2.35 Skin 4.88	15.37 7.82 2.10 3.11 4.97 3.15 3.77
4-3	BF Acid 3-furancarboxylic acid, 5-(phenylmethyl)		CAS no. 24313-22-2 MW, g/mol 202.2 Exp Kow @ pH 7.4 NA Log D @ pH 7.4 0.11 Log P 3.01 pKa, MA 4.12 WS, g/L (34.34) 143.52	Fat 0.14 Brain 0.87 Rapid 0.79 Kidney 0.80 Liver 0.81 Slow 0.76 Skin 0.78	0.19 0.89 0.80 0.82 0.82 0.79 0.76

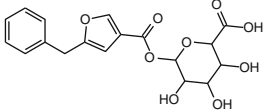
(continued)

Table D12 (continued)

No. ^a	Chemical structure ^b	Pesticide metabolite and physical and chemical properties ^{c, d}	Partition coefficient ^e				
			Tissue	Rat	Human		
5-4	4'-OH BF Acid 3-furancarboxylic acid, 5-[(4-hydroxyphenyl)methyl]-		CAS no.	37744-73-3	Fat	0.12	0.18
		MW, g/mol	218.2	Brain	0.86	0.86	
		Exp Kow @ pH 7.4	NA	Rapid	0.81	0.81	
		Log <i>D</i> @ pH 7.4	-0.63	Kidney	0.81	0.84	
		Log <i>P</i>	2.28	Liver	0.82	0.81	
		p <i>K</i> _a , MA	4.12	Slow	0.78	0.81	
		WS, g/L (121.4)	431.74	Skin	0.69	0.77	
6-5	4-OH BF Acid 3-furancarboxylic acid, 4-hydroxy-5-(phenylmethyl)-		CAS no.	57744-72-2	Fat	0.12	0.17
		MW, g/mol	218.21	Brain	0.83	0.84	
		Exp Kow @ pH 7.4	NA	Rapid	0.77	0.77	
		Log <i>D</i> @ pH 7.4	-0.22	Kidney	0.77	0.80	
		Log <i>P</i>	2.92	Liver	0.71	0.78	
		p <i>K</i> _a , MA	3.99	Slow	0.74	0.77	
		WS, g/L (54.2)	496.53	Skin	0.66	0.73	
7-6	α-OH-BF Acid 3-furan carboxylic acid, 5-(hydroxyphenylmethyl)		CAS no.	37744-70-0	Fat	1.35	1.34
		MW, g/mol	218.2	Brain	2.09	2.30	
		Exp Kow @ pH 7.4	NA	Rapid	1.18	1.11	
		Log <i>D</i> @ pH 7.4	1.37	Kidney	1.26	1.33	
		Log <i>P</i>	1.55	Liver	1.24	1.69	
		p <i>K</i> _a , MA	4.04	Slow	1.04	1.32	
		WS, g/L (2.38)	520.4	Skin	1.33	1.41	
8-7	α-keto-BF Acid 3-furancarboxylic acid, 5-benzoyl		CAS no.	37744-71-1	Fat	0.12	0.18
		MW, g/mol	216.2	Brain	0.88	0.89	
		Exp Kow @ pH 7.4	NA	Rapid	0.84	0.84	
		Log <i>D</i> @ pH 7.4	-1.18	Kidney	0.84	0.87	
		Log <i>P</i>	1.89	Liver	0.77	0.84	
		p <i>K</i> _a , MA	3.51	Slow	0.81	0.83	
		WS, g/L (367.0)	400.91	Skin	0.71	0.79	
9-8	BF Acid glucuronic acid B-D-glucopyranuronic acid, 1-[5-(phenylmethyl)-3-furancarboxylate	CAS no.	37744-75-5	Fat	0.13	0.20	
		MW, g/mol	378.33	Brain	0.92	0.92	

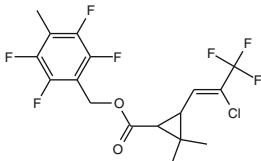
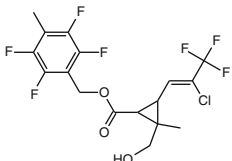
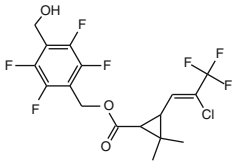
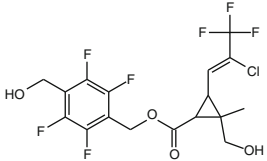
(continued)

Table D12 (continued)

No. ^a	Chemical structure ^b	Pesticide metabolite and physical and chemical properties ^{c, d}	Partition coefficient ^e		
			Tissue	Rat	Human
		Exp Kow @ pH 7.4 NA Log <i>D</i> @ pH 7.4 -0.69 Log <i>P</i> 3.04 pKa, MA 2.66 WS, g/L (16.18) 1,000.0	Rapid Kidney Liver Slow Skin	0.87 0.87 0.80 0.84 0.73	0.87 0.90 0.87 0.86 0.82
10-9	4'-OH BF Acid glucuronide Hexopyranuronic acid, 1-O-[[5-[(4-hydroxyphenyl)-3-furanyl]carbonyl]-	CAS no. NA MW, g/mol 394.33 Exp Kow @ pH 7.4 NA Log <i>D</i> @ pH 7.4 -3.06 Log <i>P</i> 0.66 pKa, MA 2.66 WS, g/L (1,362.6) 1,000.0	Fat Brain Rapid Kidney Liver Slow Skin	0.13 0.92 0.88 0.88 0.81 0.85 0.74	0.20 0.92 0.88 0.90 0.88 0.87 0.83
11-10	4'-OH-BF Acid sulfate 3-furancarboxylic acid, 5-[[4-(sulfooxy) phenyl]methyl]-	CAS no. 37744-74-4 MW, g/mol 298.27 Exp Kow @ pH 7.4 NA Log <i>D</i> @ pH 7.4 -3.34 Log <i>P</i> 1.16 pKa, MA -4.04 WS, g/L (8,944.0) 1,000.0	Fat Brain Rapid Kidney Liver Slow Skin	0.13 0.93 0.88 0.89 0.81 0.85 0.74	0.20 0.93 0.88 0.91 0.88 0.88 0.83
	Hydrolysis Products: Acid Leaving groups, metabolites and conjugates (taken from cis/trans-phenothrin)				
12-1	(cis, trans)-chrysanthemic acid (CPCA)	Cyclopropanecarboxylic acid, 2,2-dimethyl-3-(2-methyl-1-propen-1-yl)- CAS no. 10453-89-1			
13-2	3-OH methyl (cis, trans)-chrysanthemic acid (3-OHMeCPCA)	Cyclopropanecarboxylic acid, 3-[3-hydroxy-2-methyl-1-propen-1-yl]-2,2-dimethyl- CAS no. 22413-48-5)			
14-3	3-aldehyde (cis, trans)-chrysanthemic acid (3-ACPCA)	Cyclopropanecarboxylic acid, 2,2-dimethyl-3-[2-methyl-3-oxo-1-propen-yl]- CAS no. 874301-57-2			
15-4	2-carboxyl (cis, trans)-chrysanthemic acid (CCPCA)	Cyclopropanecarboxylic acid, 3-[2-carboxy-1-propen-1-yl]-2,2-dimethyl- CAS no. 497-95-0			
16-5	(cis, trans)-CPCA glucuronic acid	Hexopyranuronic acid, 1-O-[[2, 2-dimethyl-3-(2-methyl-1-propen-1-yl) cyclopropyl] carbonyl]-CAS no. NA			
17-6	3-OH methyl (cis, trans)-CPCA glucuronic acid	Hexopyranuronic acid, 1-O-[[3-[(1Z)-3-hydroxy-2-methyl-1-propen-1-yl]-2,2-dimethylcyclopropyl]carbonyl]- CAS no. NA			
18-7	2-carboxy (cis, trans)-CPCA (CCPCA) glucuronic acid	Hexopyranuronic acid, 1-O-[[3-[(1Z)-2-carboxy-1-propen-1-yl]-2,2-dimethylcyclopropyl] carbonyl]- CAS no. NA			

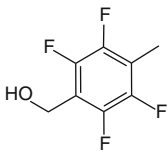
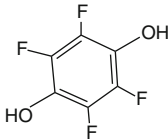
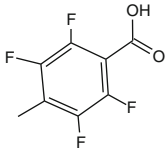
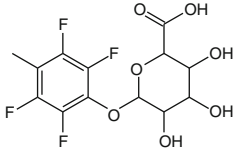
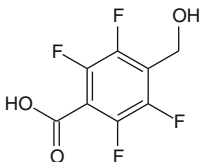
^a Parent chemical or metabolite number for cross-reference to Table E14 (Appendix E, Resmethrin)^{b-g} Metabolism source, Kaneko and Miyamoto (2001) and Kaneko (2010). See footnotes in Table D1 (Appendix D)

Table D13 Chemical structure, physical and chemical properties, and tissue partition coefficients for tefluthrin and resulting metabolites

No. ^a	Chemical structure ^b	Pesticide metabolism and physical and chemical properties ^{c, d}	Partition coefficients ^e			
			Tissue	Rat	Human	
1	Tefluthrin Cyclopropanecarboxylic acid, 3-[(1Z)-2-chloro-3,3,3-trifluoro-1-propen-1-yl]-2,2-dimethyl-, (2,3,5,6-tetrafluoro-4-methylphenyl)methyl ester					
		CAS no.	391634-71-2	Fat	71.14	33.2
		MW, g/mol	418.73	Brain	14.5	8.95
		Exp Kow @ pH 7.4	NA	Rapid	4.62	2.17
		Log <i>D</i> @ pH 7.4	5.17	Kidney	5.48	3.37
		Log <i>P</i>	5.17	Liver	6.02	5.58
		pKa	NA	Slow	3.34	3.42
		<i>K</i> _p , cm/h ^f	0.0236	Skin	7.71	4.18
		Log <i>K</i> _p ^g	-1.627			
		WS, g/L (9.0E-5)	5.69E-5			
2	2-OH Methyl Tefluthrin Cyclopropanecarboxylic acid, 3-[(1Z)-2-chloro-3,3,3-trifluoro-1-propen-1-yl]-2-(hydroxymethyl)-2-methyl-, [2,3,5,6-tetrafluoro-4-methylphenyl)methyl ester					
		CAS no.	120808-42-6	Fat	70.63	41.0
		MW, g/mol	434.73	Brain	14.19	9.07
		Exp Kow @ pH 7.4	NA	Rapid	4.53	2.21
		Log <i>D</i> @ pH 7.4	3.75	Kidney	5.37	3.42
		Log <i>P</i>	3.75	Liver	5.90	5.66
		pKa, MA	15.1	Slow	3.29	3.48
		WS, g/L (1.1E-3)	5.49E-4	Skin	7.54	4.24
3	4-OH methyl tefluthrin Cyclopropanecarboxylic acid, 3-[(1Z)-2-chloro-3,3,3-trifluoro-1-propen-1-yl]-2,2-dimethyl-, [2,3,5,6-tetrafluoro-4-(hydroxymethyl)phenyl)methyl ester					
		CAS no.	120851-77-6	Fat	70.17	40.73
		MW, g/mol	434.73	Brain	14.18	9.07
		Exp Kow @ pH 7.4	NA	Rapid	4.53	2.21
		Log <i>D</i> @ pH 7.4	3.75	Kidney	5.37	3.42
		Log <i>P</i>	3.75	Liver	5.90	5.66
		pKa, MA	12.81	Slow	3.29	3.47
		WS, g/L (1.17E-3)	5.42E-4	Skin	7.54	4.24
4	2-OH Methyl, 4-OH methyl tefluthrin Cyclopropanecarboxylic acid, 3-[(1Z)-2-chloro-3,3,3-trifluoro-1-propen-1-yl]-2-(hydroxymethyl)-2-methyl-, [2,3,5,6-tetrafluoro-4-(hydroxymethyl)phenyl)methyl ester					
		CAS no.	NA	Fat	7.48	6.85
		MW, g/mol	450.73	Brain	6.50	6.03
		Exp Kow @ pH 7.4	NA	Rapid	2.34	1.69
		Log <i>D</i> @ pH 7.4	2.33	Kidney	2.70	2.46
		Log <i>P</i>	2.33	Liver	2.89	3.86
		pKa, MA	NA	Slow	1.79	2.48
		WS, g/L (1.51E-2)	1.74E-3	Skin	3.57	2.95

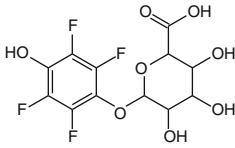
(continued)

Table D13 (continued)

No. ^a	Chemical structure ^b	Pesticide metabolism and physical and chemical properties ^{c, d}	Partition coefficients ^e		
			Tissue	Rat	Human
Hydrolysis products of esters: alcohol leaving groups, metabolites and conjugates					
5-1	Tefluthrin alcohol				
	Benzenemethanol, 2,3,5,6-tetrafluoro-4-methyl				
		CAS no.	79538-03-7	Fat	0.91 0.92
		MW, g/mol	194.13	Brain	1.71 1.88
		Exp Kow @ pH 7.4	NA	Rapid	1.02 0.96
		Log <i>D</i> @ pH 7.4	1.29	Kidney	1.08 1.14
		Log <i>P</i>	1.29	Liver	1.06 1.41
		p <i>K</i> _a , MA	12.95	Slow	0.91 1.12
		WS, g/L (3.71)	0.3	Skin	1.11 1.19
6-2	Tetrafluoro-1,4-benzenediol				
	1,4-benzenediol, 2,3,5,6-tetrafluoro-				
		CAS no.	142209-31-2	Fat	1.15 1.16
		MW, g/mol	182.07	Brain	1.92 2.12
		Exp Kow @ pH 7.4	NA	Rapid	1.13 1.07
		Log <i>D</i> @ pH 7.4	1.3	Kidney	1.20 1.28
		Log <i>P</i>	3.08	Liver	1.18 1.58
		p <i>K</i> _a , MA	5.9	Slow	1.01 1.25
		WS, g/L (4.17)	6.69	Skin	1.25 1.33
7-3	Tetrafluoro-4-methyl benzoic acid				
	Benzoic acid, 2,3,5,6-tetrafluoro-4-methyl				
		CAS no.	652-32-4	Fat	0.11 0.17
		MW, g/mol	208.11	Brain	0.85 0.86
		Exp Kow @ pH 7.4	NA	Rapid	0.81 0.81
		Log <i>D</i> @ pH 7.4	-0.89	Kidney	0.81 0.84
		Log <i>P</i>	2.26	Liver	0.75 0.81
		p <i>K</i> _a , MA	1.83	Slow	0.78 0.81
		WS, g/L (228.7)	64.21	Skin	0.68 0.77
8-4	Tetrafluoro-4-methylphenyl glucuronic acid				
	Hexopyranosiduronic acid, 2,3,5,6-tetrafluoro-4-methylphenyl				
		CAS no.	NA	Fat	0.13 0.19
		MW, g/mol	356.22	Brain	0.91 0.91
		Exp Kow @ pH 7.4	NA	Rapid	0.87 0.87
		Log <i>D</i> @ pH 7.4	-4.44	Kidney	0.87 0.90
		Log <i>P</i>	-0.72	Liver	0.80 0.87
		p <i>K</i> _a , MA	2.71	Slow	0.84 0.86
		WS, g/L (35,171.9)	1,000.0	Skin	0.73 0.82
9-5	Tetrafluoro-4-OH methyl benzoic acid				
	Benzoic acid, 2,3,5,6-tetrafluoro-4-(hydroxymethyl)-				
		CAS no.	107900-84-5	Fat	0.12 0.19
		MW, g/mol	224.11	Brain	0.90 0.91
		Exp Kow @ pH 7.4	NA	Rapid	0.86 0.86
		Log <i>D</i> @ pH 7.4	-2.31	Kidney	0.86 0.89
		Log <i>P</i>	0.84	Liver	0.79 0.86
		p <i>K</i> _a , MA	1.62	Slow	0.83 0.86
		WS, g/L (3,073.8)	645.71	Skin	0.73 0.81

(continued)

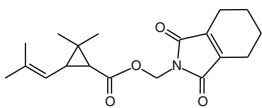
Table D13 (continued)

No. ^a	Chemical structure ^b	Pesticide metabolism and physical and chemical properties ^{c, d}		Partition coefficients ^e		
				Tissue	Rat	Human
10-6	Tetrafluoro-4-OH phenyl glucuronic acid Hexopyranosiduronic acid, 2,3,5,6-tetrafluoro-4-hydroxyphenyl	CAS no.	NA	Fat	0.13	0.20
		MW, g/mol	358.2	Brain	0.93	0.93
		Exp Kow @ pH 7.4	NA	Rapid	0.89	0.89
		Log <i>D</i> @ pH 7.4	-4.81	Kidney	0.89	0.92
		Log <i>P</i>	-0.11	Liver	0.82	0.89
		p <i>K</i> _a , A	5.65	Slow	0.86	0.88
		WS, g/L (70,822.2)	1,000.0	Skin	0.75	0.84
	Hydrolysis products: Acid leaving groups and conjugates, see bifenthrin, cyhalothrin					
11-1	TFP acid	Cyclopropanecarboxylic acid, 3-[2-chloro-3,3,3-trifluoro-1-propen-yl]-2,2-dimethyl-	CAS no. 74609-46-4			
12-2	2-OH methyl TFP acid	Cyclopropanecarboxylic acid, 3-[2-chloro-3,3,3-trifluoro-1-propen-1-yl]-2-(hydroxymethyl)-2-methyl-	CAS no. 107900-83-4			
13-3	TFP acid glucuronide	Hexopyranuronic acid, 1-O-[[3-[(1 <i>Z</i>)-2-chloro-3,3,3-trifluoro-1-propen-1-yl]-2,2-dimethylcyclopropyl]carbonyl]-	CAS no. 120851-78-7			
14-4	2-OH methyl TFP acid glucuronide	Hexopyranuronic acid, 1-O-[[3-[2-chloro-3,3,3-trifluoro-1-propen-1-yl]-2-(hydroxymethyl)-2-methylcyclopropyl]carbonyl]-	CAS no. NA			

^a Parent chemical or metabolite number for cross-reference to Table E15 (Appendix E, Tefluthrin)

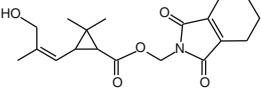
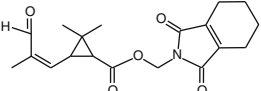
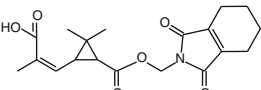
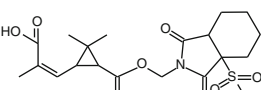
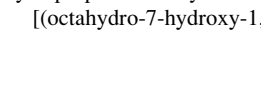
^{b-g} Metabolism source, Prout et al. (1985); Prout and Howard (1985). See footnotes in Table D1 (Appendix D)

Table D14 Chemical structure, physical and chemical properties, and tissue partition coefficients for *cis*, *trans*-tetramethrin and the resulting metabolites

No. ^a	Chemical structure ^b	Pesticide metabolite and physical and chemical properties ^{c, d}		Partition coefficient ^e		
				Tissue	Rat	Human
1	(<i>cis</i> , <i>trans</i>)-Tetramethrin Cyclopropane carboxylic acid, 2, 2-dimethyl-3-(2-methyl-1-propenyl)-, (1,3,4,5,6,7-hexahydro-1,3-dioxo-2 H-isindol-2-yl)methyl ester	CAS no.	7696-12-0	Fat	80.4	38.3
		MW, g/mol	331.41	Brain	14.5	8.98
		Exp Kow @ pH 7.4	NA	Rapid	4.62	2.18
		Log <i>D</i> @ pH 7.4	4.68	Kidney	5.48	3.38
		Log <i>P</i>	4.68	Liver	6.02	5.60
		p <i>K</i> _a , MB	-2.55	Slow	3.34	3.43
		<i>K</i> _p , cm/h ^f	0.036	Skin	7.71	4.19
		Log <i>K</i> _p ^g	-1.442			
		WS, g/L (8.07E-4)	4.59E-3			

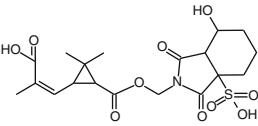
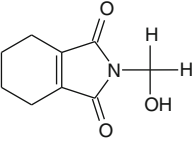
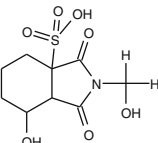
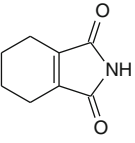
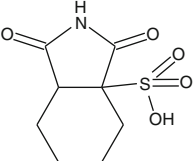
(continued)

Table D14 (continued)

No. ^a	Chemical structure ^b	Pesticide metabolite and physical and chemical properties ^{c, d}	Partition coefficient ^c				
			Tissue	Rat	Human		
2	(cis, trans)-3-OH-tetramethrin Cyclopropanecarboxylic acid, 3-[3-hydroxy-2-methyl-1-propen-1-yl]-2-dimethyl-, (1,3,4,5,6,7-hexahydro-1,3-dioxo-2 H-isoindol-2-yl) methyl ester		CAS no.	Fat	30.6	24.6	
		MW, g/mol	347.41	Brain	11.9	8.69	
		Exp Kow @ pH 7.4	NA	Rapid	3.89	2.18	
		Log <i>D</i> @ pH 7.4	2.98	Kidney	4.58	3.34	
		Log <i>P</i>	2.98	Liver	5.01	5.46	
		p <i>K</i> _a , MB	-2.55	Slow	2.86	3.38	
		WS, g/L (1.83E-2)	3.31E-2		6.35	4.11	
3	(cis, trans)-3-aldehyde-tetramethrin Cyclopropanecarboxylic acid, 2,2-dimethyl-3-(2-methyl-3-oxo-1-propen-1-yl)-, (1,3,4,5,6,7-hexahydro-1,3-dioxo-2 H-isoindol-2-yl) methyl ester		CAS no.	NA	Fat	47.8	35.0
		MW, g/mol	345.39	Brain	13.2	9.06	
		Exp Kow @ pH 7.4	NA	Rapid	4.25	2.24	
		Log <i>D</i> @ pH 7.4	3.22	Kidney	5.03	3.45	
		Log <i>P</i>	3.22	Liver	5.51	5.67	
		p <i>K</i> _a , MB	-2.56	Slow	3.11	3.50	
		WS, g/L (1.17E-2)	1.79E-2	Skin	7.01	4.26	
4	(cis, trans)-Acid NPY Cyclopropanecarboxylic acid, 3-[2-carboxy-1-propen-1-yl]-2,2-dimethyl-, 1-[(1,3,4,5,6,7-hexahydro-1,3-dioxo-2 H-isoindol-2-yl)methyl] ester		CAS no.	79672-53-0	Fat	0.25	0.29
		MW, g/mol	361.39	Brain	0.98	1.04	
		Exp Kow @ pH 7.4	NA	Rapid	0.77	0.75	
		Log <i>D</i> @ pH 7.4	0.75	Kidney	0.79	0.82	
		Log <i>P</i>	3.14	Liver	0.74	0.88	
		p <i>K</i> _a , MB	4.99	Slow	0.72	0.80	
		WS, g/L (1.21)	6.51	Skin	0.72	0.79	
5	(cis, trans)-Acid, NPY SA Cyclopropanecarboxylic acid, 3-[2-carboxy-1-propen-1-yl]-2,2-dimethyl-, (octahydro-1,3-dioxo-3a-sulfo-2 H-isoindol-2-yl)methyl ester		CAS no.	155915-28-9	Fat	0.14	0.22
		MW, g/mol	443.47	Brain	0.98	0.99	
		Exp Kow @ pH 7.4	NA	Rapid	0.94	0.94	
		Log <i>D</i> @ pH 7.4	-4.89	Kidney	0.94	0.97	
		Log <i>P</i>	-0.17	Liver	0.86	0.94	
		p <i>K</i> _a , MA	0.15	Slow	0.91	0.93	
		WS, g/L (24,573.3)	1,000.0	Skin	0.79	0.88	
6	(Cis, trans)-Acid, 7-OH-NPY-SA Cyclopropanecarboxylic acid, 3-[2-carboxy-1-propen-1-yl]-2,2-dimethyl-, 1-[(octahydro-7-hydroxy-1,3-dioxo-3a-sulfo-2 H-isoindol-2-yl)methyl] ester		CAS no.	155915-29-0	Fat	0.12	0.19
		MW, g/mol	459.47	Brain	0.90	0.91	

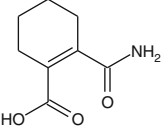
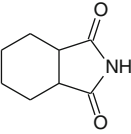
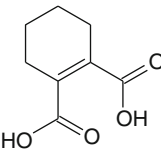
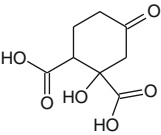
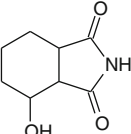
(continued)

Table D14 (continued)

No. ^a	Chemical structure ^b	Pesticide metabolite and physical and chemical properties ^{c, d}	Partition coefficient ^c		
			Tissue	Rat	Human
		Exp Kow @ pH 7.4 NA Log <i>D</i> @ pH 7.4 -6.33 Log <i>P</i> -1.61 pKa, MA 0.0 WS, g/L (330,472.7) 1,000.0	Rapid Kidney Liver Slow Skin	0.86 0.86 0.79 0.83 0.73	0.86 0.89 0.86 0.86 0.81
7-1	Hydrolysis Products: Alcohol Leaving groups, metabolites and conjugates MTI [N-(hydroxymethyl)-3,4,5,6-tetrahydrophthalimide] 1 H-isoindole-1,3(2 H)-dione, 4,5,6,7-tetrahydro-2-(hydroxymethyl)- 	CAS no. 4887-42-7 MW, g/mol 181.19 Exp Kow @ pH 7.4 NA Log <i>D</i> @ pH 7.4 0.62 Log <i>P</i> 0.62 pKa, MA 13.42 WS, g/L (16.05) 4.22	Fat Brain Rapid Kidney Liver Slow Skin	0.31 1.12 0.92 0.93 0.88 0.87 0.84	0.36 1.18 0.91 0.97 1.02 0.94 0.93
8-2	7-OH-MTI-SA 3aH-isoindole-3a-sulfonic acid, octahydro-7-hydroxy-2-(hydroxymethyl)-1,3,dioxo- 	CAS no. 155915-32-5 MW, g/mol 279.27 Exp Kow @ pH 7.4 NA Log <i>D</i> @ pH 7.4 -7.88 Log <i>P</i> -4.38 pKa, MA 9.22 WS, g/L (86,787,801) 1,000.0	Fat Brain Rapid Kidney Liver Slow Skin	0.14 0.97 0.93 0.96 0.85 0.90 0.78	0.22 0.97 0.93 0.96 0.92 0.92 0.87
9-3	TPI (3, 4, 5, 6-tetrahydrophthalimide) 1 H-isoindole-1,3(2 H)-dione, 4, 5, 6, 7-tetrahydro- 	CAS no. 4720-86-9 MW, g/mol 151.16 Exp Kow @ pH 7.4 NA Log <i>D</i> @ pH 7.4 1.11 Log <i>P</i> 1.12 pKa, MA 9.49 WS, g/L (8.45) 3.07	Fat Brain Rapid Kidney Liver Slow Skin	0.73 1.54 1.02 1.06 1.02 0.92 1.04	0.76 1.68 0.98 1.12 1.31 1.10 1.13
10-4	TPI-SA 3aH-isoindole-3a-sulfonic acid, octahydro-1,3-dioxo- 	CAS no. 155915-27-8 MW, g/mol 233.24 Exp Kow @ pH 7.4 NA Log <i>D</i> @ pH 7.4 -5.19 Log <i>P</i> -1.69 pKa, MA 0.14 WS, g/L (790,816.7) 1,000.0	Fat Brain Rapid Kidney Liver Slow Skin	0.14 0.95 0.91 0.84 0.92 0.88 0.76	0.21 0.95 0.91 0.94 0.91 0.90 0.85

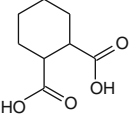
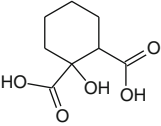
(continued)

Table D14 (continued)

No. ^a	Chemical structure ^b	Pesticide metabolite and physical and chemical properties ^{c, d}	Partition coefficient ^c		
			Tissue	Rat	Human
11-5	THAM 1-cyclohexene-1-carboxylic acid, 2-(aminocarbonyl)- 	CAS no. 81951-65-7 MW, g/mol 169.18 Exp Kow @ pH 7.4 NA Log <i>D</i> @ pH 7.4 -2.64 Log <i>P</i> 0.14 pKa, MA 4.64 WS, g/L (1,150.1) 1,000.0	Fat Brain Rapid Kidney Liver Slow Skin	0.13 0.91 0.87 0.87 0.80 0.84 0.73	0.19 0.92 0.87 0.90 0.87 0.87 0.82
12-6	HPI 1 H-isoindole-1,3(2 H)-dione, hexahydro- 	CAS no. 1444-94-6 MW, g/mol 153.18 Exp Kow @ pH 7.4 NA Log <i>D</i> @ pH 7.4 0.48 Log <i>P</i> 0.48 pKa, NA 11.97 WS, g/L (28.58) 10.39	Fat Brain Rapid Kidney Liver Slow Skin	0.23 1.01 0.86 0.87 0.81 0.82 0.77	0.29 1.06 0.85 0.91 0.93 0.88 0.86
13-7	THPA (3,4,5,6-tetrahydrophthalic acid) 1-cyclohexene-1,2-dicarboxylic acid 	CAS no. NA MW, g/mol 170.16 Exp Kow @ pH 7.4 NA Log <i>D</i> @ pH 7.4 -3.68 Log <i>P</i> 0.97 pKa, MA 3.94 WS, g/L (85,273.0) 1,000.0	Fat Brain Rapid Kidney Liver Slow Skin	0.13 0.93 0.88 0.89 0.81 0.86 0.74	0.20 0.93 0.88 0.91 0.88 0.88 0.83
14-8	1-OH-5-oxo-HPA 1,2-cyclohexanedicarboxylic acid, 1-hydroxy-5-oxo- 	CAS no. 155915-31-4 MW, g/mol 202.16 Exp Kow @ pH 7.4 NA Log <i>D</i> @ pH 7.4 -6.74 Log <i>P</i> -2.01 pKa, MA 3.4 WS, g/L (4,318,144.0) 1,000.0	Fat Brain Rapid Kidney Liver Slow Skin	0.13 0.94 0.90 0.90 0.83 0.87 0.76	0.21 0.94 0.90 0.93 0.90 0.89 0.85
15-9	4-OH-HPI-1-2 (3-hydroxy-cyclohexane-1,2-dicarboximide) 1-H-isoindole-1,3(2 H)-dione, hexahydro-4-hydroxy- 	CAS no. 169.18 MW, g/mol 169.18 Exp Kow @ pH 7.4 NA Log <i>D</i> @ pH 7.4 -0.43 Log <i>P</i> -0.43 pKa, MA 11.47 WS, g/L (144.5)	Fat Brain Rapid Kidney Liver Slow	0.13 0.90 0.84 0.85 0.78 0.81	0.19 0.90 0.84 0.87 0.85 0.84

(continued)

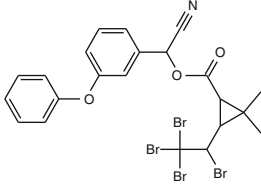
Table D14 (continued)

No. ^a	Chemical structure ^b	Pesticide metabolite and physical and chemical properties ^{c, d}	Partition coefficient ^c		
			Tissue	Rat	Human
16-10	TCDA (1,2-cyclohexanedicarboxylic acid) 1,2-cyclohexanedicarboxylic acid				
		CAS no. 1687-30-5	Fat	0.13	0.20
		MW, g/mol 172.18	Brain	0.92	0.93
		Exp Kow @ pH 7.4 NA	Rapid	0.88	0.88
		Log <i>D</i> @ pH 7.4 -3.68	Kidney	0.88	0.91
		Log <i>P</i> 0.61	Liver	0.81	0.88
		pKa, MA 4.18	Slow	0.85	0.87
		WS, g/L (83,412.7) 1,000.0	Skin	0.74	0.83
17-11	1-OH-HPA (1-hydroxy-1,2-cyclohexanedicarboxylic acid) 1,2-cyclohexanedicarboxylic acid, 1-hydroxy-				
		CAS no.	Fat	0.13	0.20
		MW, g/mol 188.18	Brain	0.92	0.92
		Exp Kow @ pH 7.4 NA	Rapid	0.88	0.88
		Log <i>D</i> @ pH 7.4 -4.58	Kidney	0.88	0.91
		Log <i>P</i> -2.66E-3	Liver	0.81	0.88
		pKa, MA 4.10	Slow	0.85	0.87
		WS, g/L (409,207.0) 1,000.0	Skin	0.74	0.83
		Hydrolysis Products: Acid Leaving groups, metabolites and conjugates			
18-1	(cis, trans)-chrysanthemic acid (CPCA) Cyclopropanecarboxylic acid, 2,2-dimethyl-3-(2-methyl-1-propen-1-yl)-	CAS no. 10453-89-1			
19-2	3-OH methyl (cis, trans) chrysanthemic acid (3-OHMe CPCA) Cyclopropanecarboxylic acid, 3-(3-hydroxy-2-methyl-1-propenyl)-2,2-dimethyl-	CAS no. 22413-48-5			
20-3	3-aldehyde (cis, trans)-chrysanthemic acid (3-ACPCA) Cyclopropanecarboxylic acid, 2,2-dimethyl-3-[2-methyl-3-oxo-1-propen-yl]-	CAS no. 874301-57-2			
21-4	2-carboxy (cis, trans)-chrysanthemic acid (CCPCA) Cyclopropanecarboxylic acid, 3-[2-carboxyl-1-propen-1-yl]-2,2-dimethyl-	CAS no. 497-95-0			
22-5	(cis, trans)-CPCA glucuronic acid Hexopyranuronic acid, 1-O-[[2,2-dimethyl-3-(2-methyl-1-propen-1-yl)cyclopropyl]carbonyl]-	CAS no. NA			
23-6	3-OH methyl (cis, trans)-CPCA glucuronic acid Hexopyranuronic acid, 1-O-[[3-[(1Z)-3-hydroxy-2-methyl-1-propen-1-yl]-2,2-dimethylcyclopropyl]carbonyl]-	CAS no. NA			
24-7	2-carboxy (cis, trans)-CPCA (CCPCA) glucuronic acid Hexopyranuronic acid, 1-O-[[3-[(1Z)-2-carboxy-1-propen-1-yl]-2,2-dimethylcyclopropyl]carbonyl]-	CAS no. NA			

^a Parent chemical or metabolite number for cross-reference to Table E16 ([Appendix E](#), Tetramethrin)

^{b-g} Metabolism source, Kaneko and Miyamoto (2001) and Kaneko (2010). See footnotes in Table D1 ([Appendix D](#))

Table D15 Chemical structure, physical and chemical properties, and tissue partition coefficients for tralomethrin and the resulting metabolites

No. ^a	Chemical structure ^b	Pesticide metabolite and physical and chemical properties ^{c, d}	Partition coefficient ^e		
			Tissue	Rat	Human
1	Tralomethrin (1R,3R, 1'S) Cyclopropanecarboxylic acid, 2,2-dimethyl-3-(1,2,2,2-tetrabromoethyl)-, cyano(3-phenoxyphenyl)methyl ester				
		CAS no. 66841-25-6 MW, g/mol 665.01 Exp Kow @ pH 7.4 NA Log <i>D</i> @ pH 7.4 7.11 Log <i>P</i> 7.11 p <i>K</i> _a NA <i>K</i> _p , cm/h ^f 0.0176 Log <i>K</i> _p ^g -1.752 WS, g/L (5.87E-6) 3.95E-6	Fat 67.42 Brain 14.52 Rapid 4.62 Kidney 5.48 Liver 6.02 Slow 3.34 Skin 7.71	31.23 8.94 2.17 3.36 5.57 3.42 4.18	
	Numbering based on deltamethrin				
1	Cis-Deltamethrin (1R,3R, 1'S) Cyclopropanecarboxylic acid, 3-(2,2-dibromoethyl)-2,2-dimethyl-,cyano(3-phenoxyphenyl)methyl ester- CAS no. 52918-63-5				
2	4'-OH Deltamethrin Cyclopropanecarboxylic acid, 3-(2,2-dibromoethyl)-2,2-dimethyl-,cyano[3-(4-hydroxyphenoxy)phenyl]methyl ester CAS no. 66855-89-8				
3	2'-OH Deltamethrin Cyclopropanecarboxylic acid, 3-(2,2-dibromoethyl)-2,2-dimethyl-,cyano[3-(2-hydroxyphenoxy)phenyl]methyl ester CAS no. 66855-88-7				
4	5-OH Deltamethrin Cyclopropanecarboxylic acid, 3-(2,2-dibromoethyl)-2,2-dimethyl-, cyanol(3-hydroxy-5-phenoxyphenyl)methyl ester CAS no. 66855-90-1				
5	trans-2-OH methyl deltamethrin Cyclopropanecarboxylic acid, 3-(2,2-dibromoethyl)-2-(hydroxymethyl)-2-methyl-, cyano(3-phenoxyphenyl)methyl ester CAS no. 69321-10-4				
6	4'-OH, trans-2-OH methyl deltamethrin Cyclopropanecarboxylic acid, 3-(2,2-dibromoethyl)-2-(hydroxymethyl)-2-methyl-, cyano[3-(4-hydroxyphenoxy)phenyl]methyl ester CAS no. 70080-85-2 Hydrolysis Products: Alcohol Leaving groups, metabolites and conjugates See cyhalothrin, cypermethrin, deltamethrin, fenvalerate, fenpropathrin, and fluvalinate				
7-1	Cyanohydrin of PB aldehyde Benzeneacetonitrile, α-hydroxy-3-phenoxy- CAS no. 39515-47-4				
8-2	Cyanohydrin of 4'-OH PB aldehyde Benzeneacetonitrile, α-hydroxy-3-(4-hydroxyphenoxy)- CAS no. 82186-81-0				
9-3	Cyanohydrin of 2'-OH PB aldehyde Benzeneacetonitrile, α-hydroxy-3-(2-hydroxyphenoxy)—CAS no. NA				
10-4	Cyanohydrin of 5-OH PB aldehyde Benzeneacetonitrile, α, 3-dihydroxy-5-phenoxy- CAS no. NA				
11-5	PB aldehyde Benzaldehyde, 3-phenoxy- CAS no. 39515-51-0				
12-6	4'OH PB aldehyde Benzaldehyde, 3-(4-hydroxyphenoxy)—CAS no. NA				

(continued)

Table D15 (continued)

No. ^a	Chemical structure ^b	Pesticide metabolite and physical and chemical properties ^{c, d}	Partition coefficient ^e		
			Tissue	Rat	Human
13-7	2'-OH PB aldehyde Benzaldehyde, 3-(2-hydroxyphenoxy)—CAS no. NA				
14-8	5-OH PB aldehyde Benzaldehyde, 3-hydroxy-5-phenoxy- (or Benzaldehyde, 5-hydroxy-3-phenoxy-) CAS no. NA				
15-9	PB alcohol Benzenemethanol, 3-phenoxy- CAS no. 13826-35-2				
16-10	4'-OH PB alcohol Benzenemethanol, 3-(4-hydroxyphenoxy)- CAS no. 63987-19-9				
17-11	2'-OH PB alcohol Benzenemethanol, 3-(2-hydroxyphenoxy)- CAS no. 63987-17-7				
18-12	5-OH PB alcohol Benzenemethanol, 3-hydroxy-5-phenoxy- (or Benzenemethanol, 5-hydroxy-3-phenoxy-) CAS no. NA				
19-13	PB acid Benzoic acid, 3-phenoxy- CAS no. 3739-38-6				
20-14	4'-OH PB acid Benzoic acid, 3-(4-hydroxyphenoxy)- CAS no. 35065-12-4				
21-15	2'-OH PB acid Benzoic acid, 3-(2-hydroxyphenoxy)- CAS no. 35101-26-9				
22-16	5-OH PB acid Benzoic acid, 3-hydroxy-5-phenoxy- (or Benzoic acid, 5-hydroxy-3-phenoxy-) CAS no. 63987-26-8				
23-17	PB alcohol glucuronic acid Hexopyranosiduronic acid, (3-phenoxyphenyl)methyl CAS no. 65658-93-7				
24-18	4'-OH PB alcohol glucuronic acid Hexopyranosiduronic acid, [3-(4-hydroxyphenoxy) phenyl] methyl CAS no. NA				
25-19	2'-OH PB alcohol glucuronic acid Hexopyranosiduronic acid, [3-(2-hydroxyphenoxy) phenyl] methyl CAS no. NA				
26-20	5-OH PB alcohol glucuronic acid Hexopyranosiduronic acid, (3-hydroxy-5-phenoxyphenyl) methyl CAS no. NA				
27-21	PB acid glucuronic acid β -D-Glucopyranuronic acid, 1-(3-phenoxybenzoate) CAS no. 57991-35-2				
28-22	PB acid glycine Glycine, N-(3-phenoxybenzoyl)- CAS no. 57991-36-3				
29-23	4'-OH PB acid glucuronic acid β -D-Glucopyranuronic acid, 1-[3-(4-hydroxyphenoxy)benzoate] CAS no. 66856-01-7				
30-24	5-OH PB acid glucuronic acid Hexopyranuronic acid, 1-(3-hydroxy-5-phenoxybenzoate) (or 1-(5-hydroxy-3-phenoxybenzoate) CAS no. 80405-64-7				
31-25	4'-OH PB acid sulfate Benzoic acid, 3-[4-(sulfooxy)phenoxy]- CAS no. 58218-91-0				
32-25	2'-OH PB acid sulfate Benzoic acid, 3-[2-(sulfooxy)phenoxy]- CAS no. 61183-26-4				

(continued)

Table D15 (continued)

No. ^a	Chemical structure ^b	Pesticide metabolite and physical and chemical properties ^{c, d}	Partition coefficient ^e		
			Tissue	Rat	Human
33-26	2'-OH PB acid glucuronic acid (not shown)	Hexopyranuronic acid, 1-[3-(2-hydroxyphenoxy) benzoate CAS no. NA			
34-27	5-OH PB acid sulfate (not shown)	Benzoic acid, 3-phenoxy-5-(sulfooxy)—CAS no. NA Hydrolysis Products: Acid Leaving groups, metabolites and conjugates			
35-1	(cis, trans)-decamethrinic acid (Dibromo-CPCA)	Cyclopropanecarboxylic acid, 3-(2,2-dibromoethenyl)-2,2-dimethyl CAS no. 59952-39-5			
36-2	(cis, trans)-hydroxymethyl-(cis, trans)-decamethrinic acid (Dibromo-CPCA)	Cyclopropanecarboxylic acid, 3-(2,2-dibromoethenyl)-2-(hydroxymethyl)-2-methyl- CAS no. 82079-71-8			
37-3	(cis, trans)-dibromo-CPCA glucuronic acid	Hexopyranuronic acid, 1-O-[[3-(2,2-dibromoethenyl)-2,2-dimethylcyclopropyl] carbonyl]- CAS no. 82079-70-7			
38-4	(cis, trans)-2-OH Me (cis, trans)-dibromo CPCA glucuronic acid	Hexopyranuronic acid, 1-O-[[3-(2,2-dibromoethenyl)-2-(hydroxymethyl)-2-methylcyclopropyl]carbonyl]- CAS no. 66856-00-6			

^a Parent chemical or metabolite number for cross-reference to Table E17 ([Appendix E](#), Tralomethrin)

^{b-g} Metabolism source, Kaneko and Miyamoto (2001) and Kaneko (2010). See footnotes in Table D1 ([Appendix D](#))

Appendix E: Metabolic Pathways and Preliminary Metabolic Rate Constants (V_{\max} and K_m) for the Metabolism of Parent Pyrethroids and Metabolites

Table E1 Biotransformation and elimination paths of Allethrin and the resulting metabolites and preliminary liver V_{\max} and K_m values^a

Biotransformation and elimination paths		
No. ^b	Initiating pesticide/metabolite ^c	Resulting metabolite
1	Allethrin	
	RAM 1	Allethrin alcohol
	RAM 18	Allethrin eliminated
2	Allethrin alcohol	
	RAM 2	Allethrin aldehyde
	RAM 19	Allethrin aldehyde eliminated
3	Allethrin aldehyde	
	RAM 3	Allethrin acid
	RAM 20	Allethrin acid eliminated
4	Allethrin acid	
	RAM 4	Allethrin hydroxymethyl acid
	RAM 5	Allethrin hydroxy acid
	RAM 6	Allethrin epoxide acid
	RAM 7	Allethrolone + CCPCA
	RAM 21	Allethrin acid eliminated
5	Allethrin hydroxymethyl acid	
	RAM 8	Allethrolone + 2-OH methyl CCPCA
	RAM 22	Allethrin hydroxymethyl acid eliminated
6	Allethrin hydroxy acid	
	RAM 9	Met B + CCPCA
	RAM 23	Allethrin hydroxy acid eliminated
7	Allethrin epoxide acid	
	RAM 10	Allethrin dihydroxy acid
	RAM 24	Allethrin epoxide acid eliminated
8	Allethrin dihydroxy acid	
	RAM 11	Met A + CCPCA
	RAM 25	Allethrin dihydroxy acid eliminated

(continued)

Table E1 (continued)

Biotransformation and elimination paths		
No. ^b	Initiating pesticide/metabolite ^c	Resulting metabolite
9	Allethrolone	
	RAM 12	Allethrolone glucuronic acid
	RAM 13	Allethrolone sulfate
	RAM 26	Allethrolone eliminated
10	Met B (hydrolysis product of allethrin hydroxy acid)	
	RAM 14	Met B glucuronic acid
	RAM 27	Met B eliminated
11	Met A (hydrolysis product of allethrin dihydroxy acid)	
	RAM 15	Met A glucuronic acid
	RAM 28	Met A eliminated
12	Allethrolone glucuronic acid	
	RAM 29	Allethrolone glucuronic acid eliminated
13	Allethrolone sulfate	
	RAM 30	Allethrolone sulfate eliminated
14	Met B glucuronic acid	
	RAM 31	Met B glucuronic acid eliminated
15	Met A glucuronic acid	
	RAM 32	Met A glucuronic acid eliminated
16	CCPCA (formed from RAM 7, 9, 11)	
	RAM 16	CCPCA glucuronic acid
	RAM 33	CCPCA eliminated
17	2-OH methyl CCPCA (formed from RAM 8)	
	RAM 17	2-OH methyl CCPCA glucuronic acid
	RAM 34	2-OH methyl methyl CCPCA eliminated
18	CCPCA glucuronic acid	
	RAM 35	CCPCA glucuronic acid eliminated
19	2-OH methyl CCPCA glucuronic acid	
	RAM 36	2-OH methyl CCPCA glucuronic acid eliminated

^a Preliminary estimates of liver V_{\max} ($\mu\text{mol h}^{-1} \text{kg}^{-1}$ bwt, unscaled) and K_m (μM) are equal to 10.0

^b Parent chemical or metabolite number for cross-reference in Table D1 ([Appendix D](#), Allethrin)

^c Refer to Table D1 for structure based on number

Table E2 Biotransformation and elimination paths of Bifenthrin and the resulting metabolites and preliminary liver V_{\max} and K_m values^a

Biotransformation and elimination paths		
No. ^b	Initiating pesticide/metabolite ^c	Resulting metabolite
1	Bifenthrin	
	RAM 1	4'-OH bifenthrin
	RAM 2	2'-OH bifenthrin
	RAM 3	2-OH methyl bifenthrin
	RAM 4	2-methyl BP alcohol + TFP acid
	RAM 29	Bifenthrin eliminated
2	4'-OH bifenthrin	
	RAM 5	4'-OH, 2-OH methyl bifenthrin
	RAM 6	4'-OH, 2-methyl BP alcohol + TFP acid
	RAM 30	4'OH bifenthrin eliminated

(continued)

Table E2 (continued)

Biotransformation and elimination paths		
No. ^b	Initiating pesticide/metabolite ^c	Resulting metabolite
3	3'-OH-bifenthrin	
	RAM 7	3'-OH, 2-OH methyl bifenthrin
	RAM 8	3'-OH, 2-methyl BP alcohol + TFP acid
4	RAM 31	3'-OH bifenthrin
	2-OH methyl bifenthrin	
	RAM 9	4'OH, 2-OH methyl bifenthrin
	RAM 10	3'OH, 2-OH methyl bifenthrin
5	RAM 11	2-methyl BP alcohol + 2-OH methyl TFP acid
	RAM 32	2-OH methyl bifenthrin eliminated
	4'-OH, 2-OH methyl bifenthrin	
	RAM 12	4'-OH, 2-methyl BP alcohol + 2-OH methyl TFP acid
6	RAM 33	4'-OH, 2-OH methyl bifenthrin eliminated
	3'-OH, 2-OH methyl bifenthrin	
7	RAM 13	3'-OH, 2-methyl BP alcohol + 2-OH methyl TFP acid
	RAM 34	3'-OH, 2-OH methyl bifenthrin eliminated
	2-methyl BP alcohol	
8	RAM 14	2-methyl BP aldehyde
	RAM 15	2-methyl BP alcohol glucuronic acid
	RAM 35	2-methyl PB alcohol eliminated
	4'-OH, 2-methyl BP alcohol	
9	RAM 16	4'-OH, 2-methyl BP aldehyde
	RAM 17	4'-OH, 2-methyl BP alcohol glucuronic acid
	RAM 36	4'-OH, 2-methyl BP alcohol eliminated
	3'-OH, 2-methyl BP alcohol	
10	RAM 18	3'-OH, 2-methyl BP aldehyde
	RAM 19	3'-OH, 2-methyl BP alcohol glucuronic acid
	RAM 37	3'-OH, 2-methyl BP alcohol eliminated
11	2-methyl BP aldehyde	
	RAM 20	2-methyl BP acid
	RAM 38	2-methyl BP aldehyde eliminated
12	4'-OH, 2-methyl BP aldehyde	
	RAM 21	4'-OH, 2-methyl BP acid
	RAM 39	4'-OH, 2-methyl BP aldehyde eliminated
13	3'-OH, 2-methyl BP aldehyde	
	RAM 22	3'-OH, 2-methyl BP acid
	RAM 40	3'-OH, 2-methyl BP aldehyde eliminated
14	2-methyl BP alcohol glucuronic acid	
	RAM 41	2-methyl BP alcohol glucuronic acid eliminated
15	4'-OH, 2-methyl BP alcohol glucuronic acid	
	RAM 42	4'-OH, 2-methyl BP alcohol glucuronic acid eliminated
16	3'-OH, 2-methyl alcohol glucuronic acid	
	RAM 43	3'-OH, 2-methyl alcohol glucuronic acid eliminated
16	2-methyl BP acid	
	RAM 23	2-methyl BP acid glycine

(continued)

Table E2 (continued)

Biotransformation and elimination paths		
No. ^b	Initiating pesticide/metabolite ^c	Resulting metabolite
	RAM 24	2-methyl BP acid glucuronide
	RAM 44	2-methyl PB acid eliminated
17	4'-OH, 2-methyl BP acid	
	RAM 25	4'-OH, 2-methyl BP acid glucuronide
	RAM 26	4'-OH, 2-methyl BP acid sulfate
	RAM45	4'-OH, 2-methyl BP acid eliminated
18	3'-OH, 2-methyl BP acid	
	RAM 27	3'-OH, 2-methyl BP acid glucuronide
	RAM 28	3'-OH, 2-methyl BP acid sulfate
	RAM 46	3'-OH, 2-methyl BP acid eliminated
19	2-methyl BP acid glycine	
	RAM 47	2-methyl BP acid glycine eliminated
20	2-methyl BP acid glucuronide	
	RAM 48	2-methyl BP acid glucuronide eliminated
21	4'-OH, 2-methyl BP acid glucuronide	
	RAM 49	4'-OH, 2-methyl BP acid glucuronide eliminated
22	4'-OH, 2-methyl BP acid sulfate	
	RAM 50	4'-OH, 2-methyl BP acid sulfate eliminated
23	3'-OH, 2-methyl BP acid glucuronide	
	RAM 51	3'-OH, 2-methyl BP acid glucuronide eliminated
24	3'-OH, 2-methyl BP acid sulfate	
	RAM 52	3'-OH, 2-methyl BP acid sulfate eliminated
25	TFP acid (formed from RAM 4, 6, 8)	
	RAM 29	TFP acid glucuronide
	RAM 53	TFP acid eliminated
26	2-OH methyl TFP acid (formed from RAM 11, 12, 13)	
	RAM 30	2-OH methyl TFP acid glucuronide
	RAM 54	2-OH methyl TFP acid eliminated
27	TFP acid glucuronide	
	RAM 55	TFP acid glucuronide eliminated
28	2-OH methyl TFP acid glucuronide	
	RAM 56	2-OH methyl TFP acid glucuronide eliminated

^a Preliminary estimates of liver V_{\max} ($\mu\text{mol h}^{-1} \text{kg}^{-1}$ bwt, unscaled) and K_m (μM) are equal to 10.0

^b Parent chemical or metabolite number for cross-reference in Table D2 ([Appendix D](#), Bifenthrin)

^c Refer to Table D2 for structure based on number

Table E3 Biotransformation and elimination paths of Cyfluthrin and the resulting metabolites and preliminary liver V_{\max} and K_m values^a

Biotransformation and elimination paths		
No. ^b	Initiating pesticide/metabolite ^c	Resulting metabolite
1	Cyfluthrin	
	RAM 1	4'-OH cyfluthrin
	RAM 2	2'-OH cyfluthrin
	RAM 3	5-OH cyfluthrin
	RAM 4	2-OH methyl cyfluthrin

(continued)

Table E3 (continued)

Biotransformation and elimination paths		
No. ^b	Initiating pesticide/metabolite ^c	Resulting metabolite
2	RAM5	Cyanohydrin of 4-fluoro-PB aldehyde + DCCA
	RAM37	Cyfluthrin eliminated
	4'-OH cyfluthrin	
	RAM 6	4'-OH, 2-OH methyl cyfluthrin
3	RAM 7	Cyanohydrin of 4'-OH, 4-fluoro-PB aldehyde + DCCA
	RAM 38	4'-OH cyfluthrin eliminated
	2'-OH cyfluthrin	
	RAM 8	Cyanohydrin of 2'-OH, 4-fluoro-PB aldehyde + DCCA
4	RAM 39	2'-OH cyfluthrin eliminated
	5-OH cyfluthrin	
	RAM 9	Cyanohydrin of 5-OH, 4-fluoro-PB aldehyde + DCCA
5	RAM 40	5-OH cyfluthrin eliminated
	2-OH methyl cyfluthrin	
	RAM 10	4'-OH, 2-OH methyl cyfluthrin
	RAM 11	Cyanohydrin of 4-fluoro-PB aldehyde + 2-OH methyl DCCA
6	RAM 41	2-OH methyl cyfluthrin eliminated
	4'-OH, 2-OH methyl cyfluthrin	
	RAM 12	Cyanohydrin of 4'-OH, 4-fluoro-PB aldehyde + 2-OH methyl DCCA
7	RAM 42	4'-OH, 2-OH methyl cyfluthrin eliminated
	Cyanohydrin of 4-fluoro-PB aldehyde	
	RAM 13	4-fluoro-PB aldehyde
8	RAM 43	Cyanohydrin of 4-fluoro-PB aldehyde eliminated
	Cyanohydrin of 4'-OH, 4-fluoro-PB aldehyde	
	RAM 14	4'-OH, 4-fluoro-PB aldehyde
	RAM 44	Cyanohydrin of 4'-OH, 4-fluoro-PB aldehyde eliminated
9	Cyanohydrin of 2'-OH, 4-fluoro-PB aldehyde	
	RAM 15	2'-OH, 4-fluoro-PB aldehyde
	RAM 45	Cyanohydrin of 2'-OH, 4-fluoro-PB aldehyde eliminated
10	Cyanohydrin of 5-OH, 4-fluoro-PB aldehyde	
	RAM 16	5-OH, 4-fluoro-PB aldehyde
	RAM 46	Cyanohydrin of 5-OH, 4-fluoro-PB aldehyde eliminated
11	4-fluoro-PB aldehyde	
	RAM 17	4-fluoro-PB acid
	RAM 18	4-fluoro-PB alcohol
	RAM 47	4-fluoro-PB aldehyde eliminated
12	4'-OH, 4-fluoro-PB aldehyde	
	RAM 19	4'-OH, 4-fluoro-PB acid
	RAM 20	4'-OH, 4-fluoro-PB alcohol
	RAM 48	4'-OH, 4-fluoro-PB aldehyde eliminated

(continued)

Table E3 (continued)

Biotransformation and elimination paths		
No. ^b	Initiating pesticide/metabolite ^c	Resulting metabolite
13	2'-OH, 4-fluoro-PB aldehyde	
	RAM 21	2'-OH, 4-fluoro-PB acid
	RAM 22	2'-OH, 4-fluoro-PB alcohol
	RAM 49	2'-OH, 4-fluoro-PB aldehyde eliminated
14	5-OH, 4-fluoro-PB aldehyde	
	RAM 23	5-OH, 4-fluoro-PB acid
	RAM 24	5-OH, 4-fluoro-PB alcohol
	RAM50	5-OH, 4-fluoro-PB aldehyde
15	4-fluoro-PB alcohol	
	RAM 25	4-fluoro-PB alcohol glucuronic acid
	RAM 51	4-fluoro-PB alcohol eliminated
16	4'-OH, 4-fluoro-PB alcohol	
	RAM 26	4'-OH, 4-fluoro-PB alcohol glucuronic acid
	RAM 52	4'-OH, 4-fluoro-PB alcohol eliminated
17	2'-OH, 4-fluoro-PB alcohol	
	RAM 27	2'-OH, 4-fluoro-PB alcohol glucuronic acid
	RAM 53	2'-OH, 4-fluoro-PB alcohol eliminated
18	5-OH, 4-fluoro-PB alcohol	
	RAM 28	5-OH, 4-fluoro-PB alcohol glucuronic acid
	RAM 54	5-OH, 4-fluoro-PB alcohol eliminated
19	4-fluoro-PB acid	
	RAM 29	4-fluoro-PB acid glucuronide
	RAM 30	4-fluoro-PB acid sulfate
	RAM 55	4-fluoro-PB acid eliminated
20	4'-OH, 4-fluoro-PB acid	
	RAM 31	4'-OH, 4-fluoro-PB acid glucuronide
	RAM 32	4'-OH, 4-fluoro-PB acid sulfate
	RAM 56	4'-OH, 4-fluoro-PB acid eliminated
21	2'-OH, 4-fluoro-PB acid	
	RAM 33	2'-OH, 4-fluoro-PB acid glucuronide
	RAM 34	2'-OH, 4-fluoro-PB acid sulfate
	RAM 57	2'-OH, 4-fluoro-PB acid eliminated
22	5-OH, 4-fluoro-PB acid	
	RAM 35	5-OH, 4-fluoro-PB acid glucuronide
	RAM 36	5-OH, 4-fluoro-PB acid sulfate
	RAM 58	5-OH, 4-fluoro-PB acid eliminated
23	4-fluoro-PB alcohol glucuronic acid	
	RAM 59	4-fluoro-PB alcohol glucuronic acid eliminated
24	4-OH, 4-fluoro-PB alcohol glucuronic acid	
	RAM 60	4'-OH, 4-fluoro-PB alcohol glucuronic acid eliminated
25	2'-OH, 4-fluoro-PB alcohol glucuronic acid	
	RAM 61	2'-OH, 4-fluoro-PB alcohol glucuronic acid eliminated
26	5-OH, 4-fluoro-PB alcohol glucuronic acid	
	RAM 62	5-OH, 4-fluoro-PB alcohol glucuronic acid eliminated

(continued)

Table E3 (continued)

Biotransformation and elimination paths		
No. ^b	Initiating pesticide/metabolite ^c	Resulting metabolite
27	4-fluoro-PB acid glucuronide RAM 63	4-fluoro-PB acid glucuronide eliminated
28	4-fluoro-PB acid glycine RAM 64	4-fluoro-PB acid glycine eliminated
29	4'-OH, 4-fluoro-PB acid glucuronide RAM 65	4'-OH, 4- Fluoro-PB acid glucuronide eliminated
30	2'-OH, 4-fluoro-PB acid glucuronide RAM 66	2'-OH, 4-fluoro-PB acid glucuronide
31	4'-OH, 4-fluoro-PB acid sulfate RAM 67	4'-OH, 4-fluoro-PB acid sulfate eliminated
32	2'OH, 4-fluoro-PB acid sulfate RAM 68	2'-OH, 4-fluoro-PB acid sulfate
33	5-OH, 4-fluoro-PB acid glucuronide RAM 69	5-OH, 4-fluoro-PB acid glucuronide eliminated
34	5-OH, 4-fluoro-PB acid sulfate RAM 70	5-OH, 4-fluoro-PB acid sulfate eliminated
35	DCCA (from RAM 5,7, 8, 9) RAM 37 RAM 71	DCCA glucuronic acid DCCA eliminated
36	2-OH methyl DCCA (from RAM 11, 12) RAM 38 RAM 72	2-OH methyl DCCA glucuronic acid 2-OH methyl DCCA eliminated
37	DCCA glucuronic acid RAM 73	DCCA glucuronic acid eliminated
38	2-OH methyl DCCA glucuronic acid RAM 74	2-OH methyl DCCA glucuronic acid eliminated

^a Preliminary estimates of liver V_{\max} ($\mu\text{mol h}^{-1} \text{kg}^{-1}$ bwt, unscaled) and K_m (μM) are equal to 10.0

^b Parent chemical or metabolite number for cross-reference in Table D3 ([Appendix D](#), Cyfluthrin)

^c Refer to Table D3 for structure based on number

Table E4 Biotransformation and elimination paths of Cyhalothrin and the resulting metabolites and preliminary liver V_{\max} and K_m values^a

Biotransformation and elimination paths		
No. ^b	Initiating pesticide/metabolite ^c	Resulting metabolite
1	Cyhalothrin RAM 1 RAM 2 RAM 3 RAM 4 RAM 5 RAM 35	4'-OH cyhalothrin 2'-OH cyhalothrin 5-OH cyhalothrin 2-OH methyl cyhalothrin Cyanohydrin of PB aldehyde + TFP acid Cyhalothrin eliminated
2	4'-OH cyhalothrin RAM 6 RAM 7 RAM 36	4'-OH, 2-OH Me, cyhalothrin Cyanohydrin of 4'-OH PB aldehyde + TFP acid 4'-OH cyhalothrin eliminated
3	2'-OH cyhalothrin RAM 8 RAM 37	Cyanohydrin of 2'-OH PB aldehyde + TFP acid 2'-OH cyhalothrin eliminated

(continued)

Table E4 (continued)

Biotransformation and elimination paths		
No. ^b	Initiating pesticide/metabolite ^c	Resulting metabolite
4	5-OH cyhalothrin	
	RAM 9	Cyanohydrin of 5-OH PB aldehyde + TFP acid
	RAM 38	5-OH cyhalothrin eliminated
5	2-OH methyl cyhalothrin	
	RAM 10	Cyanohydrin of 2-OH Me, 4'-OH
	RAM 11	Cyanohydrin of PB aldehyde + 2 OH Me TFP acid
	RAM 39	2-OH methyl cyhalothrin eliminated
6	2-OH Me, 4'-OH cyhalothrin	
	RAM 12	Cyanohydrin of 4'-OH PB aldehyde + 2 OH Me TFP acid
	RAM 40	2-OH Me, 4'-OH cyhalothrin eliminated
7	Cyanohydrin of PB aldehyde	
	RAM 13	PB aldehyde
8	Cyanohydrin of 4'-OH PB aldehyde	
	RAM 14	4'-OH PB aldehyde
9	Cyanohydrin of 2'-OH PB aldehyde	
	RAM 15	2'-OH PB aldehyde
10	Cyanohydrin of 5-OH PB aldehyde	
	RAM 16	5-OH PB aldehyde
11	PB aldehyde	
	RAM 17	PB alcohol
	RAM 18	PB acid
12	4'-OH PB aldehyde	
	RAM 19	4'-OH PB alcohol
	RAM 20	4'-OH PB acid
13	2'-OH PB aldehyde	
	RAM 21	2'-OH PB alcohol
	RAM 22	2'-OH PB acid
14	5-OH PB aldehyde	
	RAM 23	5-OH PB alcohol
	RAM 24	5-OH PB acid
15	PB alcohol	
	RAM 25	PB alcohol glucuronide
	RAM 41	PB alcohol eliminated
16	4'-OH PB alcohol	
	RAM 26	4'-OH PB alcohol glucuronide
	RAM 42	4'-OH PB alcohol eliminated
17	2'-OH PB alcohol	
	RAM 27	2'-OH PB alcohol glucuronide
	RAM 43	2'-OH PB alcohol eliminated
18	5-OH PB alcohol	
	RAM 28	5-OH PB alcohol glucuronide
	RAM 44	5-OH PB alcohol eliminated
19	PB acid	
	RAM 29	PB acid glucuronide
	RAM 30	PB acid glycine
	RAM 45	PB acid eliminated

(continued)

Table E4 (continued)

Biotransformation and elimination paths		
No. ^b	Initiating pesticide/metabolite ^c	Resulting metabolite
20	4'-OH PB acid	
	RAM 31	4'-OH PB acid glucuronide
	RAM 32	4'-OH PB acid sulfate
	RAM 46	4'-OH PB acid eliminated
21	2'-OH PB acid	
	RAM 33	2'-OH PB acid sulfate
	RAM 47	2'-OH PB acid eliminated
22	5-OH PB acid	
	RAM 34	5-OH PB acid glucuronide
	RAM 48	5-OH PB acid eliminated
23	PB alcohol glucuronide	
	RAM 49	PB alcohol glucuronide eliminated
24	4'-OH PB alcohol glucuronide	
	RAM 50	4'-OH PB alcohol glucuronide eliminated
25	2'-OH PB alcohol glucuronide	
	RAM 51	2'-OH PB alcohol glucuronide eliminated
26	5-OH PB alcohol glucuronide	
	RAM 52	5-OH PB alcohol glucuronide eliminated
27	PB acid glucuronide	
	RAM 53	PB acid glucuronide eliminated
28	PB acid glycine	
	RAM 54	PB acid glycine eliminated
29	4'-OH PB acid glucuronide	
	RAM 55	4'-OH PB acid glucuronide eliminated
30	4'-OH PB acid sulfate	
	RAM 56	4'-OH PB acid sulfate eliminated
31	2'-OH PB acid sulfate	
	RAM 57	2'-OH PB acid sulfate eliminated
32	5-OH PB acid glucuronide	
	RAM 58	5-OH PB acid glucuronide eliminated
33	5-OH PB acid sulfate	
	RAM 59	5-OH PB acid sulfate eliminated
34	TFP acid (RAM 5 + 7 + 8 + 9)	
	RAM 1A	2-OH Me TFP acid
	RAM 2A	TFP acid glucuronide
	RAM 60	TFP acid eliminated
35	2-OH Me TFP acid (RAM 11 + 12) + (RAM 1A)	
	RAM 3A	2-OH Me TFP acid glucuronide
	RAM 61	2-OH Me TFP acid eliminated
36	TFP acid glucuronide	
	RAM 62	TFP acid glucuronide eliminated
37	2-OH Me TFP acid glucuronide	
	RAM 63	2-OH Me TFP acid glucuronide eliminated

^a Preliminary estimates of liver V_{\max} ($\mu\text{mol h}^{-1} \text{kg}^{-1} \text{bwt}$, unscaled) and K_m (μM) are equal to 10.0

^b Parent chemical or metabolite number for cross-reference in Table D4 ([Appendix D](#), Cyhalothrin)

^c Refer to Table D4 for structure based on number

Table E5 Biotransformation and elimination paths of Cypermethrin and the resulting metabolites and preliminary liver V_{\max} and K_m values^a

Biotransformation and elimination paths		
No. ^b	Initiating pesticide/metabolite ^c	Resulting metabolite
1	Cypermethrin	
	RAM 1	4'-OH cypermethrin
	RAM 2	2'-OH cypermethrin
	RAM 3	5-OH cypermethrin
	RAM 4	2-OH methyl cypermethrin
	RAM 5	Cyanohydrin of PB aldehyde + DCCA
	RAM 35	Cypermethrin eliminated
2	4'-OH cypermethrin	
	RAM 6	2-OH Me, 4'-OH cypermethrin
	RAM 7	Cyanohydrin of 4'-OH PB aldehyde + DCCA
	RAM 36	4'-OH cypermethrin eliminated
3	2'-OH cypermethrin	
	RAM 8	Cyanohydrin of 2'-OH PB aldehyde + DCCA
	RAM 37	2'-OH cypermethrin eliminated
4	5-OH cypermethrin	
	RAM 9	Cyanohydrin of 5-OH PB aldehyde + DCCA
	RAM 38	5-OH cypermethrin eliminated
5	2-OH methyl cypermethrin	
	RAM 10	2-OH Me, 4'-OH cypermethrin
	RAM 11	Cyanohydrin of PB aldehyde+ 2 OH Me, DCCA
	RAM 39	2-OH methyl cypermethrin eliminated
6	2-OH Me, 4'-OH cypermethrin	
	RAM 12	4'-OH PB cyanohydrin +2 OH Me, DCCA
	RAM 40	2-OH Me, 4'-OH cypermethrin eliminated
7	Cyanohydrin of PB aldehyde	
	RAM 13	PB aldehyde
8	Cyanohydrin of 4'-OH PB aldehyde	
	RAM 14	4'-OH PB aldehyde
9	Cyanohydrin of 2'-OH PB aldehyde	
	RAM 15	2'-OH PB aldehyde
10	Cyanohydrin of 5-OH PB aldehyde	
	RAM 16	5-OH PB aldehyde
11	PB aldehyde	
	RAM 17	PB alcohol
	RAM 18	PB acid
12	4'-OH PB aldehyde	
	RAM 19	4'-OH PB alcohol
	RAM 20	4'-OH PB acid
13	2'-OH PB aldehyde	
	RAM 21	2'-OH PB alcohol
	RAM 22	2'-OH PB acid
14	5-OH PB aldehyde	
	RAM 23	5-OH PB alcohol
	RAM 24	5-OH PB acid

(continued)

Table E5 (continued)

Biotransformation and elimination paths		
No. ^b	Initiating pesticide/metabolite ^c	Resulting metabolite
15	PB alcohol	
	RAM 25	PB alcohol glucuronide
	RAM 41	PB alcohol eliminated
16	4'-OH PB alcohol	
	RAM 26	4'-OH PB alcohol glucuronide
	RAM 42	4'-OH PB alcohol eliminated
17	2'-OH PB alcohol	
	RAM 27	2'-OH PB alcohol glucuronide
	RAM 43	2'-OH PB alcohol eliminated
18	5-OH PB alcohol	
	RAM 28	5-OH PB alcohol glucuronide
	RAM 44	5-OH PB alcohol eliminated
19	PB acid	
	RAM 29	PB acid glucuronide
	RAM 30	PB acid glycine
	RAM 45	PB acid eliminated
20	4'-OH PB acid	
	RAM 31	4'-OH PB acid glucuronide
	RAM 32	4'-OH PB acid sulfate
	RAM 46	4'-OH PB acid eliminated
21	2'-OH PB acid	
	RAM 33	2'-OH PB acid sulfate
	RAM 47	2'-OH PB acid eliminated
22	5-OH PB acid	
	RAM 34	5-OH PB acid glucuronide
	RAM 48	5-OH PB acid eliminated
23	PB alcohol glucuronide	
	RAM 49	PB alcohol glucuronide eliminated
24	4'-OH PB alcohol glucuronide	
	RAM 50	4'-OH PB alcohol glucuronide eliminated
25	2'-OH PB alcohol glucuronide	
	RAM 51	2'-OH PB alcohol glucuronide eliminated
26	5-OH PB alcohol glucuronide	
	RAM 52	5-OH PB alcohol glucuronide eliminated
27	PB acid glucuronide	
	RAM 53	PB acid glucuronide eliminated
28	PB acid glycine	
	RAM 54	PB acid glycine eliminated
29	4'-OH PB acid glucuronide	
	RAM 55	4'-OH PB acid glucuronide eliminated
30	4'-OH PB acid sulfate	
	RAM 56	4'-OH PB acid sulfate eliminated
31	2'-OH PB acid sulfate	
	RAM 57	2'-OH PB acid sulfate eliminated
32	5-OH PB acid glucuronide	
	RAM 58	5-OH PB acid glucuronide eliminated

(continued)

Table E5 (continued)

Biotransformation and elimination paths		
No. ^b	Initiating pesticide/metabolite ^c	Resulting metabolite
33	DCCA (RAM 5+7+8+9)	
	RAM 1A	DCCA glucuronide
	RAM 2A	2 OH Me DCCA
	RAM 3A	Lactone
	RAM 59	DCCA eliminated
34	2 OH Me DCCA (RAM 11+12) + (RAM 2A)	
	RAM 4A	2 OH Me DCCA glucuronide
	RAM 60	2 OH Me DCCA eliminated
35	DCCA glucuronide	
	RAM 61	DCCA glucuronide eliminated
36	2-OH Me DCCA glucuronide	
	RAM 62	2-OH Me DCCA glucuronide eliminated
37	Lactone	
	RAM 63	Lactone eliminated

^a Preliminary estimates of liver V_{\max} ($\mu\text{mol h}^{-1} \text{kg}^{-1} \text{bwt}$, unscaled) and K_m (μM) are equal to 10.0

^b Parent chemical or metabolite number for cross-reference in Table D5 (Appendix D, Cypermethrin)

^c Refer to Table D5 for structure based on number

Table E6 Biotransformation and elimination paths of Deltamethrin and the resulting metabolites and preliminary liver V_{\max} and K_m values^a

Biotransformation and elimination paths		
No. ^b	Initiating pesticide/ metabolite ^c	Resulting metabolite
1	Deltamethrin	
	RAM 1	4'-OH deltamethrin
	RAM 2	2'-OH deltamethrin
	RAM 3	5-OH deltamethrin
	RAM 4	2-OH methyl deltamethrin
	RAM 5	Cyanohydrin of PB aldehyde + dibromo CPCA
	RAM 38	Deltamethrin eliminated
2	4'-OH deltamethrin	
	RAM 6	4'-OH, 2-OH Me, deltamethrin
	RAM 7	Cyanohydrin of 4'-OH PB aldehyde + dibromo CPCA
	RAM 39	4'-OH deltamethrin eliminated
3	2'-OH deltamethrin	
	RAM 8	Cyanohydrin of 2'-OH PB aldehyde + dibromo CPCA
	RAM 40	2'-OH deltamethrin eliminated
4	5-OH deltamethrin	
	RAM 9	Cyanohydrin of 5-OH PB aldehyde + dibromo CPCA
	RAM 41	5-OH deltamethrin eliminated
5	2-OH methyl deltamethrin	
	RAM 10	2-OH Me, 4'-OH deltamethrin
	RAM 11	Cyanohydrin of PB aldehyde + 2-OH Me dibromo CPCA
	RAM 42	2-OH methyl deltamethrin eliminated

(continued)

Table E6 (continued)

Biotransformation and elimination paths		
No. ^b	Initiating pesticide/ metabolite ^c	Resulting metabolite
6	4'-OH, 2-OH Me deltamethrin	
	RAM 12	Cyanohydrin of 4'-OH PB aldehyde + 2-OH Me dibromo CPCA
	RAM 43	2-OH Me, 4'-OH deltamethrin eliminated
7	Cyanohydrin of PB aldehyde	
	RAM 13	PB aldehyde
8	Cyanohydrin of 4'-OH PB aldehyde	
	RAM 14	4'-OH PB aldehyde
9	Cyanohydrin of 2'-OH PB aldehyde	
	RAM 15	2'-OH PB aldehyde
10	Cyanohydrin of 5-OH PB aldehyde	
	RAM 16	5-OH PB aldehyde
11	PB aldehyde	
	RAM 17	PB alcohol
	RAM 18	PB acid
12	4'-OH PB aldehyde	
	RAM 19	4'-OH PB alcohol
	RAM 20	4'-OH PB acid
13	2'-OH PB aldehyde	
	RAM 21	2'-OH PB alcohol
	RAM 22	2'-OH PB acid
14	5-OH PB aldehyde	
	RAM 23	5-OH PB alcohol
	RAM 24	5-OH PB acid
15	PB alcohol	
	RAM 25	PB alcohol glucuronic acid
	RAM 44	PB alcohol eliminated
16	4'-OH PB alcohol	
	RAM 26	4'-OH PB alcohol glucuronic acid
	RAM 45	4'-OH PB alcohol eliminated
17	2'-OH PB alcohol	
	RAM 27	2'-OH PB alcohol glucuronic acid
	RAM 46	2'-OH PB alcohol eliminated
18	5-OH PB alcohol	
	RAM 28	5-OH PB alcohol glucuronic acid
	RAM 47	5-OH PB alcohol eliminated
19	PB acid	
	RAM 29	PB acid glucuronide
	RAM 30	PB acid glycine
	RAM 48	PB acid eliminated

(continued)

Table E6 (continued)

Biotransformation and elimination paths		
No. ^b	Initiating pesticide/ metabolite ^c	Resulting metabolite
20	4'-OH PB acid	
	RAM 31	4'-OH PB acid glucuronide
	RAM 32	4'-OH PB acid sulfate
	RAM 49	4'-OH PB acid eliminated
21	2'-OH PB acid	
	RAM 34	2'-OH PB acid glucuronide
	RAM 35	2'-OH PB acid sulfate
	RAM 50	2'-OH PB acid eliminated
22	5-OH PB acid	
	RAM 36	5-OH PB acid glucuronide
	RAM 37	5-OH PB acid sulfate
	RAM 51	5-OH PB acid eliminated
23	PB alcohol glucuronic acid	
	RAM 52	PB alcohol glucuronic acid eliminated
24	4'-OH PB alcohol glucuronic acid	
	RAM 53	4'-OH PB alcohol glucuronic acid eliminated
25	2'-OH PB alcohol glucuronic acid	
	RAM 54	2'-OH PB alcohol glucuronic acid eliminated
26	5-OH PB alcohol glucuronic acid	
	RAM 55	5-OH PB alcohol glucuronic acid eliminated
27	PB acid glucuronide	
	RAM 56	PB acid glucuronide eliminated
28	PB acid glycine	
	RAM 57	PB acid glycine eliminated
29	4'-OH PB acid glucuronide	
	RAM 60	4'-OH PB acid glucuronide eliminated
30	5-OH PB acid glucuronide	
	RAM 61	5-OH PB acid glucuronide eliminated
31	4'-OH PB acid sulfate	
	RAM 62	4'-OH PB acid sulfate eliminated
32	2'-OH PB acid sulfate	
	RAM 63	2'-OH PB acid sulfate eliminated
33	2'-OH PB acid glucuronide	
	RAM 64	2'-OH PB acid glucuronide eliminated
34	5-OH PB acid sulfate	
	RAM 65	5-OH PB acid sulfate eliminated
35	Dibromo-CPCA (RAM 5 + 7 + 8 +9)	
	RAM 1A	Dibromo CPCA glucuronide
	RAM 2A	2-OH Me dibromo CPCA
	RAM 66	Dibromo-CPCA eliminated

(continued)

Table E6 (continued)

Biotransformation and elimination paths		
No. ^b	Initiating pesticide/ metabolite ^c	Resulting metabolite
36	2-OH Me dibromo CPCA (RAM 11 + 12) + (RAM 2A)	
	RAM 3A	2-OH Me dibromo CPCA glucuronide
	RAM 67	2-OH Me dibromo CPCA eliminated
37	Dibromo CPCA glucuronide	
	RAM 68	Dibromo CPCA glucuronide eliminated
38	2-OH Me dibromo CPCA glucuronide	
	RAM 69	2-OH Me dibromo CPCA glucuronide eliminated

^a Preliminary estimates of liver V_{\max} ($\mu\text{mol h}^{-1} \text{kg}^{-1}$ bwt, unscaled) and K_m (μM) are equal to 10.0

^b Parent chemical or metabolite number for cross-reference in Table D6 ([Appendix D](#), Deltamethrin)

^c Refer to Table D6 for structure based on number

Table E7 Biotransformation and elimination paths of Fenvalerate and the resulting metabolites and preliminary liver V_{\max} and K_m values^a

Biotransformation and elimination paths		
No. ^b	Initiating pesticide/metabolite ^c	Resulting metabolite
1	Fenvalerate	
	RAM 1	4'-OH fenvalerate
	RAM 2	2'-OH fenvalerate
	RAM 3	2-OH methyl fenvalerate
	RAM 4	Cyanohydrin of PB aldehyde + CPIA
	RAM 32	Fenvalerate eliminated
2	4'-OH fenvalerate	
	RAM 5	4'-OH, 2-OH Me fenvalerate
	RAM 6	Cyanohydrin of 4'-OH PB aldehyde + CPIA
	RAM 33	4'-OH fenvalerate eliminated
3	2'-OH fenvalerate	
	RAM 7	2'-OH, 2-OH Me fenvalerate
	RAM 8	Cyanohydrin of 2'-OH PB aldehyde + CPIA
	RAM 34	2'-OH fenvalerate eliminated
4	2-OH methyl fenvalerate	
	RAM 9	4'-OH, 2-OH Me fenvalerate
	RAM 10	2'-OH, 2-OH Me fenvalerate
	RAM 11	Cyanohydrin of PB aldehyde + 2-OH Me CPIA
	RAM 35	2-OH methyl fenvalerate eliminated
5	4'-OH, 2-OH Me fenvalerate	
	RAM 12	Cyanohydrin of 4'-OH PB aldehyde + 2-OH Me CPIA
	RAM 36	4'-OH, 2-OH Me fenvalerate eliminated
6	2'-OH, 2-OH Me fenvalerate	
	RAM 13	Cyanohydrin of 2'-OH PB aldehyde + 2-OH Me CPIA
	RAM 37	2'-OH, 2-OH Me fenvalerate eliminated
7	Cyanohydrin of PB aldehyde	
	RAM 14	PB aldehyde

(continued)

Table E7 (continued)

Biotransformation and elimination paths		
No. ^b	Initiating pesticide/metabolite ^c	Resulting metabolite
8	Cyanohydrin of 4'-OH PB aldehyde RAM 15	4'-OH PB aldehyde
9	Cyanohydrin of 2'-OH PB aldehyde RAM 16	2'-OH PB aldehyde
10	PB aldehyde RAM 17 RAM 18	PB alcohol PB acid
11	4'-OH PB aldehyde RAM 19 RAM 20	4'-OH PB alcohol 4'-OH PB acid
12	2'-OH PB aldehyde RAM 21 RAM 22	2'-OH PB alcohol 2'-OH PB acid
13	PB alcohol RAM 23 RAM 38	PB alcohol glucuronide PB alcohol eliminated
14	4'-OH PB alcohol RAM 24 RAM 39	4'-OH PB alcohol glucuronide 4'-OH PB alcohol eliminated
15	2'-OH PB alcohol RAM 25 RAM 40	2'-OH PB alcohol glucuronide 2'-OH PB alcohol eliminated
16	PB acid RAM 26 RAM 27 RAM 41	PB acid glucuronide PB acid glycine PB acid eliminated
17	4'-OH PB acid RAM 28 RAM 29 RAM 42	4'-OH PB acid glucuronide 4'-OH PB acid sulfate 4'-OH PB acid eliminated
18	2'-OH PB acid RAM 30 RAM 31 RAM 43	2'-OH PB acid glucuronide 2'-OH PB acid sulfate 2'-OH PB acid eliminated
19	PB alcohol glucuronide RAM 44	PB alcohol glucuronide eliminated
20	4'-OH PB alcohol glucuronide RAM 45	4'-OH PB alcohol glucuronide eliminated
21	2'-OH PB alcohol glucuronide RAM 46	2'-OH PB alcohol glucuronide eliminated
22	PB acid glucuronide RAM 47	PB acid glucuronide eliminated

(continued)

Table E7 (continued)

Biotransformation and elimination paths		
No. ^b	Initiating pesticide/metabolite ^c	Resulting metabolite
23	PB acid glycine RAM 48	PB acid glycine eliminated
24	4'-OH PB acid glucuronide RAM 49	4'-OH PB acid glucuronide eliminated
25	4'-OH PB acid sulfate RAM 50	4'-OH PB acid sulfate eliminated
26	2'-OH PB acid glucuronide RAM 51	2'-OH PB acid glucuronide eliminated
27	2'-OH PB acid sulfate RAM 52	2'-OH PB acid sulfate eliminated
28	CPIA (RAM 4 + 6 + 8) RAM 1A RAM 2A RAM 53	CPIA glucuronic acid 2-OH methyl CPIA CPIA eliminated
29	2-OH methyl CPIA (RAM 11 + 12 + 13) + (RAM 2A) RAM 3A RAM 4A RAM 5A RAM 54	4-OH methyl CPIA glucuronic acid α -OH, 2-OH methyl CPIA 3-OH CPIA-Lactone (not in Table D7) 2-OH methyl CPIA eliminated
30	α -OH, 2-OH methyl CPIA RAM 6A RAM 7A RAM 8A RAM 55	α -OH, 2-OH methyl CPIA glucuronic acid 2-OH methylethylidene CPIA α -OH, CPIA lactone (metabolite not in Table D7) α -OH, 2-OH methyl CPIA eliminated
31	2-OH methylethylidene CPIA RAM 9A RAM 10A RAM 56	CPdiB CPdiB acid lactone (metabolite not in Table D7) 2-OH methylethylidene CPIA eliminated
32	CPIA glucuronic acid RAM 57	CPIA glucuronic acid eliminated
33	4-OH methyl CPIA glucuronic acid RAM 58	4-OH methyl CPIA glucuronic acid eliminated
34	α -OH, 2-OH methyl CPIA glucuronic acid RAM 59	α -OH, 2-OH CPIA glucuronic acid eliminated

^a Preliminary estimates of liver V_{\max} ($\mu\text{mol h}^{-1} \text{kg}^{-1} \text{bwt}$, unscaled) and K_m (μM) are equal to 10.0

^b Parent chemical or metabolite number for cross-reference in Table D7 ([Appendix D](#), Fenvalerate)

^c Refer to Table D7 for structure based on number

Table E8 Biotransformation and elimination paths of Fenpropathrin and the resulting metabolites and preliminary liver V_{\max} and K_m values^a

Biotransformation and elimination paths		
No. ^b	Initiating pesticide/metabolite ^c	Resulting metabolite
1	Fenpropathrin	
	RAM 1	4'-OH fenpropathrin
	RAM 2	2'-OH fenpropathrin
	RAM 3	2-OH methyl fenpropathrin
	RAM 4	Cyanohydrin of PB aldehyde + TetraMeCPCA
	RAM 35	Fenpropathrin eliminated
2	4'-OH fenpropathrin	
	RAM 5	4'-OH, 2-OH Me fenpropathrin
	RAM 6	Cyanohydrin of 4'-OH PB aldehyde + TetraMeCPCA
	RAM 36	4'-OH fenpropathrin eliminated
3	2'-OH fenpropathrin	
	RAM 7	2'-OH, 2-OH Me fenpropathrin
	RAM 8	Cyanohydrin of 2'-OH PB aldehyde + TetraMeCPCA
	RAM 37	2'-OH fenpropathrin eliminated
4	2-OH methyl fenpropathrin	
	RAM 9	2-carboxy-fenpropathrin
	RAM 10	Cyanohydrin of PB aldehyde + 2-OH, TriMeCPCA
	RAM 38	2-OH methyl fenpropathrin eliminated
5	2-carboxy fenpropathrin	
	RAM 11	Cyanohydrin of PB aldehyde + TriMe CPDCA
	RAM 39	2-carboxy fenpropathrin eliminated
6	4'-OH, 2-OH Me fenpropathrin	
	RAM 12	Cyanohydrin of 4'-OH PB aldehyde + 2-OH, TriMeCPCA
	RAM 40	4'-OH, 2-OH Me fenpropathrin eliminated
7	2'-OH, 2-OH Me fenpropathrin	
	RAM 13	Cyanohydrin of 2'-OH PB aldehyde + 2-OH, TriMeCPCA
	RAM 41	2'-OH, 2-OH Me fenpropathrin eliminated
8	Cyanohydrin of PB aldehyde	
	RAM 14	PB aldehyde
9	Cyanohydrin of 4'-OH PB aldehyde	
	RAM 15	4'-OH PB aldehyde
10	Cyanohydrin of 2'-OH PB aldehyde	
	RAM 16	2'-OH PB aldehyde
11	PB aldehyde	
	RAM 17	PB alcohol
	RAM 18	PB acid
12	4'-OH PB aldehyde	
	RAM 19	4'-OH PB alcohol
	RAM 20	4'-OH PB acid
13	2'-OH PB aldehyde	
	RAM 21	2'-OH PB alcohol
	RAM 22	2'-OH PB acid
14	PB alcohol	
	RAM 23	PB alcohol glucuronide
	RAM 42	PB alcohol eliminated

(continued)

Table E8 (continued)

Biotransformation and elimination paths		
No. ^b	Initiating pesticide/metabolite ^c	Resulting metabolite
15	4'-OH PB alcohol	
	RAM 24	4'-OH PB alcohol glucuronide
	RAM 43	4'-OH PB alcohol eliminated
16	2'-OH PB alcohol	
	RAM 25	2'-OH PB alcohol glucuronide
	RAM 44	2'-OH PB alcohol eliminated
17	PB acid	
	RAM 26	PB acid glucuronide
	RAM 27	PB acid glycine
	RAM 45	PB acid eliminated
18	4'-OH PB acid	
	RAM 28	4'-OH PB acid glucuronide
	RAM 29	4'-OH PB acid sulfate
	RAM 46	4'-OH PB acid eliminated
19	2'-OH PB acid	
	RAM 30	2'-OH PB acid glucuronide
	RAM 31	2'-OH PB acid sulfate
	RAM 47	2'-OH PB acid eliminated
20	PB alcohol glucuronide	
	RAM 48	PB alcohol glucuronide eliminated
21	4'-OH PB alcohol glucuronide	
	RAM 49	4'-OH PB alcohol glucuronide eliminated
22	2'-OH PB alcohol glucuronide	
	RAM 50	2'-OH PB alcohol glucuronide eliminated
23	PB acid glucuronide	
	RAM 51	PB acid glucuronide eliminated
24	PB acid glycine	
	RAM 52	PB acid glycine eliminated
25	4'-OH PB acid glucuronide	
	RAM 53	4'-OH PB acid glucuronide eliminated
26	4'-OH PB acid sulfate	
	RAM 54	4'-OH PB acid sulfate eliminated
27	2'-OH PB acid glucuronide	
	RAM 55	2'-OH PB acid glucuronide eliminated
28	2'-OH PB acid sulfate	
	RAM 56	2'-OH PB acid sulfate eliminated
29	TetraMeCPCA (from RAM 4, 6, 8)	
	RAM 32	2-OH, TriMeCPCA
	RAM 33	TetraMeCPCA glucuronic acid
	RAM 57	TetraMeCPCA eliminated
30	2-OH, TriMeCPCA (from RAM 10, 12, 13)	
	RAM 34	TriMe CPDCA
	RAM 35	2-OH, TriMe CPCA glucuronic acid
	RAM 58	2-OH, TriMeCPCA eliminated

(continued)

Table E8 (continued)

Biotransformation and elimination paths		
No. ^b	Initiating pesticide/metabolite ^c	Resulting metabolite
31	TriMe CPDCA (from RAM 11) RAM 59	TriMe CPDCA eliminated
32	TetraMeCPCA glucuronic acid RAM 60	TetraMeCPCA glucuronic acid eliminated
33	2-OH, TriMe CPCA glucuronic acid RAM 61	2-OH, TriMe CPCA glucuronic acid eliminated

^a Preliminary estimates of liver V_{\max} ($\mu\text{mol h}^{-1} \text{kg}^{-1}$ bwt, unscaled) and K_m (μM) are equal to 10.0

^b Parent chemical or metabolite number for cross-reference in Table D8 ([Appendix D](#), Fenpropathrin)

^c Refer to Table D8 for structure based on number

Table E9 Biotransformation and elimination paths of Fluvalinate and the resulting metabolites and preliminary liver V_{\max} and K_m values^a

Biotransformation and elimination paths		
No. ^b	Initiating pesticide/ metabolite ^c	Resulting metabolite
1	Fluvalinate	
	RAM 1	4'-OH Fluvalinate
	RAM 2	2'-OH Fluvalinate
	RAM 3	Cyanohydrin of PB aldehyde + valine, N-[2-chloro-4-(trifluoromethyl)phenyl]-
	RAM 23	Fluvalinate eliminated
2	4'-OH Fluvalinate	
	RAM 4	Cyanohydrin of 4'-OH PB aldehyde + valine, N-[2-chloro-4-(trifluoromethyl)phenyl]-
	RAM 24	4'-OH Fluvalinate eliminated
3	2'-OH Fluvalinate	
	RAM 5	Cyanohydrin of 2'-OH PB aldehyde + valine, N-[2-chloro-4-(trifluoromethyl)phenyl]-
	RAM 25	4-OH methyl Fluvalinate eliminated
4	Cyanohydrin of PB aldehyde	
	RAM 6	PB aldehyde
5	Cyanohydrin of 4'-OH PB aldehyde	
	RAM 7	4'-OH PB aldehyde
6	Cyanohydrin of 2'-OH PB aldehyde	
	RAM 8	2'-OH PB aldehyde
7	PB aldehyde	
	RAM 9	PB alcohol
	RAM 10	PB acid
8	4'-OH PB aldehyde	
	RAM 11	4'-OH PB alcohol
	RAM 12	4'-OH PB acid
9	2'-OH PB aldehyde	
	RAM 13	2'-OH PB alcohol
	RAM 14	2'-OH PB acid

(continued)

Table E9 (continued)

Biotransformation and elimination paths		
No. ^b	Initiating pesticide/ metabolite ^c	Resulting metabolite
10	PB alcohol	
	RAM 15	PB alcohol glucuronic acid
	RAM 26	PB alcohol eliminated
11	4'-OH PB alcohol	
	RAM 16	4'-OH PB alcohol glucuronic acid
	RAM 27	4'-OH PB alcohol eliminated
12	2'-OH PB alcohol	
	RAM 17	2'-OH PB alcohol glucuronic acid
	RAM 28	2'-OH PB alcohol eliminated
13	PB acid	
	RAM 17	PB acid glucuronide
	RAM 18	PB acid glycine
	RAM 29	PB acid eliminated
14	4'-OH PB acid	
	RAM 19	4'-OH PB acid glucuronide
	RAM 20	4'-OH PB acid sulfate
	RAM 30	4'-OH PB acid eliminated
15	2'-OH PB acid	
	RAM 21	2'-OH PB acid glucuronide
	RAM 22	2'-OH PB acid sulfate
	RAM 31	2'-OH PB acid eliminated
16	PB alcohol glucuronic acid	
	RAM 32	PB alcohol glucuronic acid eliminated
17	4'-OH PB alcohol glucuronic acid	
	RAM 33	4'-OH PB alcohol glucuronic acid eliminated
18	2'-OH PB alcohol glucuronic acid	
	RAM 34	2'-OH PB alcohol glucuronic acid eliminated
19	PB acid glucuronide	
	RAM 35	PB acid glucuronide eliminated
20	PB acid glycine	
	RAM 36	PB acid glycine eliminated
21	4'-OH PB acid glucuronide	
	RAM 37	4'-OH PB acid glucuronide eliminated
22	2'-OH PB acid glucuronide	
	RAM 38	2'-OH PB acid glucuronide eliminated
23	4'-OH PB acid sulfate	
	RAM 39	4'-OH PB acid sulfate eliminated
24	2'-OH PB acid sulfate	
	RAM 40	4'-OH acid sulfate eliminated
25	Valine N-[2-chloro-4-(trifluoromethyl)phenyl]- (RAM 3 + 4 + 5)	
	RAM 1A	Hexopyranuronic acid, 1-O-[N-[4-trifluoromethyl)phenyl]vinyl]-
	RAM 2A	Valine, N-[2-chloro-4-(trifluoromethyl)phenyl]4-hydroxy
	RAM 3A	Trifluoromethyl chloroaniline
	RAM 41	Valine N-[2-chloro-4-(trifluoromethyl)phenyl]- eliminated

(continued)

Table E9 (continued)

Biotransformation and elimination paths		
No. ^b	Initiating pesticide/ metabolite ^c	Resulting metabolite
26	Hexopyranuronic acid, 1-O-[N-[4-trifluoromethyl]phenyl]vinyl]- RAM 42	Hexopyranuronic acid, 1-O-[N-[4-trifluoromethyl]phenyl]vinyl]- eliminated
27	Valine, N-[2-chloro-4-(trifluoromethyl)phenyl]-4-hydroxy- RAM 43	Valine, N-[2-chloro-4-(trifluoromethyl)phenyl]-4-hydroxy- eliminated
28	Trifluoromethyl chloroaniline RAM 4A	Hydroxy, trifluorochloroaniline
	RAM 44	Trifluoromethyl chloroaniline eliminated
29	Hydroxy, trifluorochloroaniline RAM 5A	Hydroxy, trifluorochloroaniline sulfate
	RAM 45	Hydroxy, trifluorochloroaniline eliminated
30	Hydroxy, trifluorochloroaniline sulfate RAM 46	Hydroxy, trifluorochloroaniline sulfate eliminated

^a Preliminary estimates of liver V_{\max} ($\mu\text{mol h}^{-1} \text{kg}^{-1}$ bwt, unscaled) and K_m (μM) are equal to 10.0

^b Parent chemical or metabolite number for cross-reference in Table D9 ([Appendix D](#), Fluvalinate)

^c Refer to Table D9 for structure based on number

Table E10 Biotransformation and elimination paths of trans-permethrin and the resulting metabolites and preliminary liver V_{\max} and K_m values^a

Biotransformation and elimination paths		
No. ^b	Initiating pesticide/metabolite ^c	Resulting metabolite
1	trans-Permethrin RAM 1	trans-2-OH-trans-permethrin
	RAM 2	cis-2-OH-trans-permethrin
	RAM 3	4'-OH-trans-permethrin
	RAM 4	2'-OH-trans-permethrin (not shown)
	RAM 5	PB alcohol + trans DCCA
	RAM 27	trans-permethrin eliminated
2	trans-2-OH-trans-permethrin RAM 6	PB alcohol + trans-2-OH-trans DCCA
	RAM 28	trans-2-OH-trans-permethrin eliminated
3	cis-2-OH-trans-permethrin RAM 7	PB alcohol + cis-2-OH-trans DCCA
	RAM 29	cis-2-OH-trans-permethrin eliminated
4	4'-OH-trans-permethrin RAM 8	4'-OH PB alcohol + trans DCCA
	RAM 30	4'-OH-trans-permethrin eliminated
5	2'-OH-trans-permethrin RAM 9	2'-OH PB alcohol + trans DCCA
	RAM 31	2'-OH, trans-permethrin eliminated
6	4'-OH-(trans)-2-OH cis-permethrin (not reported)	

(continued)

Table E10 (continued)

Biotransformation and elimination paths		
No. ^b	Initiating pesticide/metabolite ^c	Resulting metabolite
7	PB alcohol	
	RAM 10	PB aldehyde
	RAM 11	PB alcohol glucuronic acid
	RAM 32	PB alcohol eliminated
8	4'-OH PB alcohol	
	RAM 12	4'-OH PB aldehyde
	RAM 13	4'-OH PB alcohol glucuronic acid
	RAM 33	4'-OH PB alcohol eliminated
9	2'-OH PB alcohol	
	RAM 14	2'-OH PB aldehyde
	RAM 15	2'-OH PB alcohol glucuronic acid
	RAM 34	2'-OH PB alcohol eliminated
10	PB aldehyde	
	RAM 16	PB acid
11	4'-OH PB aldehyde	
	RAM 17	4'-OH PB acid
12	2'-OH PB aldehyde	
	RAM 18	2'-OH PB acid
13	PB alcohol glucuronic acid	
	RAM 35	PB alcohol glucuronic acid eliminated
14	4'-OH PB alcohol glucuronic acid	
	RAM 36	4'-OH PB alcohol glucuronic acid eliminated
15	2'-OH PB alcohol glucuronic acid	
	RAM 37	2'-OH PB alcohol glucuronic acid eliminated
16	PB acid	
	RAM 19	PB acid glucuronide
	RAM 20	PB acid glycine
	RAM 38	PB acid eliminated
17	4'-OH PB acid	
	RAM 21	4'-OH PB acid glucuronide
	RAM 22	4'-OH PB acid glycine
	RAM 23	4'-OH PB acid sulfate
	RAM 39	4'-OH PB acid eliminated
18	2'-OH PB acid	
	RAM 24	2'-OH PB acid glucuronide
	RAM 25	2'-OH PB acid glycine
	RAM 26	2'-OH PB acid sulfate
	RAM 40	2'-OH PB acid eliminated
19	PB acid glucuronide	
	RAM 41	PB acid glucuronide eliminated
20	PB acid glycine	
	RAM 42	PB acid glycine eliminated
21	4'-OH PB acid glucuronide	
	RAM 43	4'-OH PB acid glucuronide eliminated

(continued)

Table E10 (continued)

Biotransformation and elimination paths		
No. ^b	Initiating pesticide/metabolite ^c	Resulting metabolite
22	4'-OH PB acid glycine RAM 44	4'-OH PB acid glycine eliminated
23	4'-OH PB acid sulfate RAM 45	4'-OH PB acid sulfate eliminated
24	2'-OH PB acid glucuronide RAM 46	4'-OH PB acid glucuronide eliminated
25	2'-OH PB acid glycine RAM 47	2'-OH PB acid glycine eliminated
26	2'-OH PB acid sulfate RAM 48	2'-OH PB acid sulfate eliminated
27	trans-DCCA (RAM 5 + 8 + 9) RAM 1A RAM 49	trans-DCCA glucuronide trans-DCCA eliminated
28	trans-2-OH Me-trans-DCCA (RAM 6) RAM 2A RAM 50	trans-2-OH Me, trans-DCCA glucuronide trans-2-OH Me trans-DCCA eliminated
29	cis-2-OH Me-trans-DCCA (RAM 7) RAM 3A RAM 51	cis-2-OH-Me-trans-DCCA lactone cis-2-OH-Me-trans-DCCA eliminated
30	DCCA glucuronide RAM 52	trans-DCCA glucuronide eliminated
31	trans-2-OH Me, trans-DCCA glucuronide RAM 53	trans-OH Me, trans-DCCA glucuronide eliminated
32	cis-2-OH Me trans-DCCA lactone RAM 54	cis-OH Me-trans-DCCA lactone eliminated

^a Preliminary estimates of liver V_{\max} ($\mu\text{mol h}^{-1} \text{kg}^{-1}$ bwt, unscaled) and K_m (μM) are equal to 10.0

^b Parent chemical or metabolite number for cross-reference in Table D10 ([Appendix D](#), cis/trans-Permethrin)

^c Refer to Table D10 for structure based on number

Table E11 Biotransformation and elimination paths of cis-permethrin and the resulting metabolites and preliminary liver V_{\max} and K_m values^a

Biotransformation and elimination paths		
No. ^b	Initiating pesticide/metabolite ^c	Resulting metabolite
1	<i>cis</i> -Permethrin RAM 1 RAM 2 RAM 3 RAM 4 RAM 5 RAM 31	t-OH, <i>cis</i> -permethrin c-OH, <i>cis</i> -permethrin 4'-OH, <i>cis</i> -permethrin 2'-OH, <i>cis</i> -permethrin PB alcohol + c-DCCA <i>Cis</i> -permethrin eliminated
2	t-OH, <i>cis</i> -permethrin RAM 6 RAM 7 RAM 32	4'-OH, t-OH, <i>cis</i> -permethrin PB alcohol + t-OH c-DCCA Trans-OH, <i>cis</i> -permethrin eliminated

(continued)

Table E11 (continued)

Biotransformation and elimination paths		
No. ^b	Initiating pesticide/metabolite ^c	Resulting metabolite
3	c-OH, <i>cis</i> -permethrin	
	RAM 8	4'-OH, t-OH, c-permethrin
	RAM 9	PB alcohol + <i>cis</i> OH c-DCCA
4	4'-OH, <i>cis</i> -permethrin	
	RAM 10	4'-OH, t-OH, <i>cis</i> -permethrin
	RAM 11	4'-OH PB alcohol + c-DCCA
5	2'-OH, <i>cis</i> -permethrin	
	RAM 12	4'-OH, <i>cis</i> -permethrin eliminated
	RAM 34	
6	4'-OH, t-OH, <i>cis</i> -permethrin	
	RAM 13	2'-OH PB alcohol + c-DCCA
	RAM 35	2'-OH, <i>cis</i> -permethrin eliminated
7	PB alcohol	
	RAM 14	4'-OH, t-OH, <i>cis</i> -permethrin eliminated
	RAM 36	
8	4'-OH PB alcohol	
	RAM 15	PB aldehyde
	RAM 37	PB alcohol glucuronide
9	2'-OH PB alcohol	
	RAM 16	PB alcohol eliminated
	RAM 17	
10	PB aldehyde	
	RAM 18	4'-OH PB aldehyde
	RAM 19	4'-OH PB alcohol glucuronide
11	4'-OH PB aldehyde	
	RAM 20	4'-OH PB alcohol eliminated
	RAM 38	
12	2'-OH PB aldehyde	
	RAM 21	2'-OH PB aldehyde
	RAM 22	2'-OH PB alcohol glucuronide
13	PB alcohol glucuronide	
	RAM 40	2'-OH PB alcohol eliminated
	RAM 41	
14	4'-OH PB alcohol glucuronide	
	RAM 42	PB acid
	RAM 43	
15	2'-OH PB alcohol glucuronide	
	RAM 23	4'-OH PB acid
	RAM 24	
16	PB acid	
	RAM 25	2'-OH PB acid
	RAM 26	
17	4'-OH PB acid	
	RAM 27	PB alcohol glucuronide eliminated
	RAM 28	4'-OH PB alcohol glucuronide eliminated
18	PB acid glucuronide	
	RAM 29	2'-OH PB alcohol glucuronide eliminated
	RAM 30	
19	PB acid glycine	
	RAM 31	PB acid glucuronide
	RAM 32	4'-OH PB glycine
20	PB acid eliminated	
	RAM 33	
	RAM 39	

(continued)

Table E11 (continued)

Biotransformation and elimination paths		
No. ^b	Initiating pesticide/metabolite ^c	Resulting metabolite
	RAM 27	4'-OH PB acid sulfate
	RAM 44	4'-OH PB acid eliminated
18	2-OH PB acid	
	RAM 28	2'-OH PB acid glucuronide
	RAM 29	2'-OH PB acid glycine
	RAM 30	2'-OH PB acid sulfate
	RAM 45	2'-OH PB acid eliminated
19	PB acid glucuronide	
	RAM 46	PB acid glucuronide eliminated
20	PB acid glycine	
	RAM 47	PB acid glycine eliminated
21	4'-OH PB acid glucuronide	
	RAM 48	4'-OH PB acid glucuronide eliminated
22	4'-OH PB acid glycine	
	RAM 49	4'-OH PB acid glycine eliminated
23	4'-OH PB acid sulfate	
	RAM 50	4'-OH PB acid sulfate eliminated
24	2'-OH PB acid glucuronide	
	RAM 51	2'-OH PB acid glucuronide eliminated
25	2'-OH PB acid glycine	
	RAM 52	2'-OH PB acid glycine eliminated
26	2'-OH PB acid sulfate	
	RAM 53	2'-OH PB acid sulfate eliminated
27	<i>cis</i> -DCCA (RAM 5 + 11 + 12)	
	RAM 1A	<i>cis</i> -DCCA glucuronic acid
	RAM 54	<i>cis</i> -DCCA eliminated
28	<i>trans</i> -OH methyl- <i>cis</i> -DCCA (RAM 7 + 13)	
	RAM 2A	<i>trans</i> OH Me, <i>cis</i> -DCCA glucuronic acid
	RAM 55	<i>trans</i> -hydroxymethyl- <i>cis</i> -DCCA eliminated
29	<i>cis</i> -OH methyl- <i>cis</i> -DCCA (RAM 9)	
	RAM 3A	<i>cis</i> -OH Me- <i>cis</i> -DCCA lactone
	RAM 56	<i>cis</i> -hydroxymethyl- <i>cis</i> -DCCA eliminated
30	<i>cis</i> -DCCA glucuronic acid	
	RAM 57	<i>cis</i> -DCCA glucuronic acid eliminated
31	<i>trans</i> -OH Me, <i>cis</i> -DCCA glucuronic acid	
	RAM 58	<i>trans</i> -OH Me, <i>cis</i> -DCCA glucuronic acid eliminated
32	<i>cis</i> -OH Me <i>cis</i> DCCA lactone	
	RAM 59	<i>cis</i> -OH Me DCCA lactone eliminated

^a Preliminary estimates of liver V_{\max} ($\mu\text{mol h}^{-1} \text{kg}^{-1}$ bwt, unscaled) and K_m (μM) are equal to 10.0

^b Parent chemical or metabolite number for cross-reference in Table D10 ([Appendix D](#), *cis/trans*-Permethrin)

^c Refer to Table D10 for structure based on number

Table E12 Biotransformation and elimination paths of *trans*-phenothrin and the resulting metabolites and preliminary liver V_{\max} and K_m values^a

Biotransformation and elimination paths		
No. ^b	Initiating pesticide/metabolite ^c	Resulting metabolite
1	<i>trans</i> -Phenothrin	
	RAM 1	Alcohol t-phenothrin
	RAM 2	PB alcohol
	RAM 19	<i>trans</i> -phenothrin eliminated
2	Alcohol <i>trans</i> -phenothrin	
	RAM 3	Aldehyde t-phenothrin
	RAM 20	Alcohol t-phenothrin eliminated
3	Aldehyde <i>trans</i> -phenothrin	
	RAM 4	PB-alcohol + 3ACPCA
	RAM 5	2-carboxy <i>trans</i> -phenothrin
4	2-carboxy <i>trans</i> -phenothrin	
	RAM 6	PB alcohol + CCPCA
	RAM 21	2-Carboxy <i>trans</i> -phenothrin eliminated
5	PB alcohol	
	RAM 7	PB alcohol glucuronide
	RAM 8	PB aldehyde
	RAM 22	PB alcohol eliminated
6	PB aldehyde	
	RAM 9	PB acid
7	PB acid	
	RAM 10	PB acid glucuronide
	RAM 11	PB acid glycine
	RAM 12	PB acid sulfate
	RAM 13	4'-OH PB acid
	RAM 14	2'-OH PB acid
	RAM 23	PB acid eliminated
8	4'-OH PB acid	
	RAM 15	4'-OH PB acid glucuronide
	RAM 16	4'-OH PB acid sulfate
	RAM 24	4'-OH PB acid eliminated
9	2'-OH PB acid	
	RAM 17	2'-OH PB acid glucuronide
	RAM 18	2'-OH PB acid sulfate
	RAM 25	2'-OH PB acid eliminated
10	PB alcohol glucuronide	
	RAM 26	PB alcohol glucuronide eliminated
11	PB acid glucuronide	
	RAM 27	PB acid glucuronide eliminated
12	PB acid glycine	
	RAM 28	PB acid glycine eliminated
13	PB acid sulfate	
	RAM 29	PB acid sulfate eliminated
14	4'-OH PB acid glucuronide	
	RAM 30	4'-OH PB acid glucuronide eliminated

(continued)

Table E12 (continued)

Biotransformation and elimination paths		
No. ^b	Initiating pesticide/metabolite ^c	Resulting metabolite
15	4'-OH PB acid sulfate RAM 31	2'-OH PB acid sulfate eliminated
16	2'-OH PB acid glucuronide RAM 32	2'-OH PB acid glucuronide eliminated
17	2'-OH PB acid sulfate RAM 33	2'-OH PB acid sulfate eliminated
18	CPCA (from RAM 2) RAM 1A RAM 2A RAM 34	CPCA glucuronide 3-ACPCA CPCA eliminated
19	3-ACPCA (from RAM 12, 2A) RAM 3A	2-carboxyl cyclopropanecarboxylic acid (CCPCA)
20	CCPCA (from RAM 17, 3A) RAM 4A	CCPCA glucuronic acid
21	CPCA glucuronic acid RAM 35	CPCA glucuronic acid eliminated
22	CCPCA glucuronic acid RAM 36	CCPCA glucuronic acid eliminated

^a Preliminary estimates of liver V_{\max} ($\mu\text{mol h}^{-1} \text{kg}^{-1}$ bwt, unscaled) and K_m (μM) are equal to 10.0

^b Parent chemical or metabolite number for cross-reference in Table D11 ([Appendix D](#), cis/trans-Phenothrin)

^c Refer to Table D11 for structure based on number

Table E13 Biotransformation and elimination paths of *cis*-phenothrin and the resulting metabolites and preliminary liver V_{\max} and K_m values^a

Biotransformation and elimination paths		
No. ^b	Initiating pesticide/metabolite ^c	Resulting metabolite
1	<i>cis</i> -phenothrin RAM 1 RAM 2 RAM 3 RAM 4 RAM 5 RAM 51	4'-OH <i>cis</i> -phenothrin 2'-OH <i>cis</i> -phenothrin 2-OH methyl <i>cis</i> -phenothrin Alcohol <i>cis</i> -phenothrin PB alcohol + CPCA <i>cis</i> -phenothrin eliminated
2	4'-OH <i>cis</i> -phenothrin RAM 6 RAM 7 RAM 52	4'-OH alcohol <i>cis</i> -phenothrin 4'-OH PB alcohol + CPCA 4'-OH <i>cis</i> -phenothrin eliminated
3	2'-OH <i>cis</i> -phenothrin RAM 8 RAM 9 RAM 53	2'-OH-alcohol <i>cis</i> -phenothrin 2'-OH PB alcohol + CPCA 2'-OH <i>cis</i> -phenothrin eliminated
4	2-OH methyl <i>cis</i> -phenothrin RAM 10 RAM 11 RAM 54	2-OH methyl alcohol <i>cis</i> -phenothrin PB alcohol + 2 OH methyl CPCA 2-OH <i>c</i> -phenothrin

(continued)

Table E13 (continued)

Biotransformation and elimination paths		
No. ^b	Initiating pesticide/metabolite ^c	Resulting metabolite
5	Alcohol cis-phenothrin (alcohol, 3-OH position)	
	RAM 12	Aldehyde cis-phenothrin
	RAM 13	PB alcohol + 3-OH CPCA
	RAM 55	Alcohol cis-phenothrin eliminated
6	4'-OH- alcohol cis-phenothrin	
	RAM 14	4'-OH aldehyde cis-phenothrin
	RAM 15	4'-OH PB alcohol + 3-OH CPCA
	RAM 56	4'-OH alcohol cis-phenothrin eliminated
7	2'-OH alcohol cis-phenothrin	
	RAM 16	2'-OH-aldehyde cis-phenothrin
	RAM 17	2'-OH PB alcohol + 3-OH CPCA
	RAM 57	2'-OH alcohol cis-phenothrin eliminated
8	2-OH methyl alcohol cis-phenothrin	
	RAM 18	2-OH methyl aldehyde cis-phenothrin
	RAM 19	PB alcohol + 2-OH methyl-3-OH CPCA
	RAM 58	2-OH alcohol cis-phenothrin eliminated
9	Aldehyde cis-phenothrin	
	RAM 20	2-carboxy cis-phenothrin
	RAM 21	PB alcohol + 3-ACDCA
10	Aldehyde 4'-OH cis-phenothrin	
	RAM 22	2-carboxy 4'-OH cis-phenothrin
	RAM 23	4'-OH PB alcohol + 3-ACDCA
11	Aldehyde 2'-OH cis-phenothrin	
	RAM 24	2-carboxy 2'-OH cis-phenothrin
	RAM 25	2'-OH PB alcohol + 3ACPCA
12	2-OH methyl aldehyde cis-phenothrin	
	RAM 26	2-carboxy 2-OH methyl cis-phenothrin
	RAM 27	PB alcohol + 3-aldehyde-2-OH methyl CPCA
13	2-Carboxy cis-phenothrin	
	RAM 28	2-carboxy 4'-OH cis-phenothrin
	RAM 29	2-carboxy 2'-OH cis-phenothrin
	RAM 30	2-carboxy 2-OH methyl cis-phenothrin
	RAM 31	PB alcohol + carboxy CPCA
	RAM 59	2-carboxy cis-phenothrin eliminated
14	2-Carboxy 4'-OH cis-phenothrin	
	RAM 32	4'-OH PB alcohol + carboxy CPCA
	RAM 60	2-carboxy 4'-OH cis-phenothrin eliminated
15	2-Carboxy 2'-OH cis-phenothrin	
	RAM 33	2'-OH PB alcohol + carboxy CPCA
	RAM 61	2-carboxy 2'-OH cis-phenothrin eliminated
16	2-Carboxy 2-OH methyl cis-phenothrin	
	RAM 34	PB alcohol + carboxy 2-OH CPCA
	RAM 62	2-carboxy 2-OH methyl cis-phenothrin eliminated
17	2-Carboxy 2-OH methyl-4'-OH cis-phenothrin	
	RAM 35	4'-OH PB alcohol + carboxy 2-OH CPCA
	RAM 63	2-carboxy 2-OH methyl-4'-OH cis-phenothrin eliminated

(continued)

Table E13 (continued)

Biotransformation and elimination paths		
No. ^b	Initiating pesticide/metabolite ^c	Resulting metabolite
18	PB alcohol	
	RAM 36	PB alcohol glucuronide
	RAM 37	PB aldehyde
	RAM 64	PB alcohol eliminated
19	4'-OH PB alcohol	
	RAM 38	4'-OH PB alcohol glucuronide
	RAM 39	4'-OH PB aldehyde
	RAM 65	4'-OH PB alcohol eliminated
20	2'-OH PB alcohol	
	RAM 40	2'-OH PB alcohol glucuronide
	RAM 41	2'-OH PB aldehyde
	RAM 66	2'-OH PB alcohol eliminated
21	PB aldehyde	
	RAM 42	PB acid
22	4'OH PB aldehyde	
	RAM 43	4'-OH PB acid
23	2'-OH PB aldehyde	
	RAM 44	2'-OH PB acid
24	PB acid	
	RAM 45	PB acid glucuronide
	RAM 46	PB acid glycine
	RAM 67	PB acid eliminated
25	4'-OH PB acid	
	RAM 47	4'-OH PB acid glucuronide
	RAM 48	4'-OH PB acid sulfate
	RAM 68	4'-OH PB acid eliminated
26	2'-OH PB acid	
	RAM 49	2'-OH PB acid glucuronide
	RAM 50	2'-OH PB acid sulfate
	RAM 69	2'-OH PB acid eliminated
27	PB alcohol glucuronide	
	RAM 70	PB alcohol glucuronide eliminated
28	4'-OH PB alcohol glucuronide	
	RAM 71	4'-OH PB alcohol glucuronide eliminated
29	2'-OH PB alcohol glucuronide	
	RAM 72	2'-OH PB alcohol glucuronide eliminated
30	PB acid glucuronide	
	RAM 73	PB acid glucuronide eliminated
31	PB acid glycine	
	RAM 74	PB acid glycine eliminated
32	4'-OH PB acid glucuronide	
	RAM 75	4'-OH PB acid glucuronide eliminated
33	4'-OH PB acid sulfate	
	RAM 76	2'-OH PB acid sulfate eliminated

(continued)

Table E13 (continued)

Biotransformation and elimination paths		
No. ^b	Initiating pesticide/metabolite ^c	Resulting metabolite
34	2'-OH PB acid glucuronide RAM 77	2'-OH PB acid glucuronide eliminated
35	2'-OH PB acid sulfate RAM 78	2'-OH PB acid sulfate eliminated
36	CPCA (from RAM 5, 7, 9) RAM 1A RAM 79	CPCA glucuronide CPCA eliminated
37	2-OH methyl CPCA (from RAM 11) RAM 2A RAM 80	2-OH methyl CPCA glucuronide 2-OH methyl CPCA eliminated
38	3-OH methyl CPCA (from RAM 13, 15, 17) RAM 3A RAM 81	3-OH methyl CPCA glucuronide 3-OH methyl CPCA eliminated
39	2-OH methyl- 3-OH CPCA (from RAM 19) RAM 4A RAM 82	2-OH methyl-3-OH CPCA glucuronide 2-OH methyl-3-OH CPCA eliminated
40	3-Aldehyde CPCA (from RAM 21, 23, 25) RAM 5A	2-carboxy-CPCA
41	3-Aldehyde, 2-OH methyl CPCA (from RAM 27) RAM 6A	2-carboxy-2-OH methyl CPCA
42	2-Carboxy CPCA (from RAM 31, 32, 33, 5A) RAM 7A RAM 83	2-carboxy CPCA glucuronide 2-carboxy CPCA eliminated
43	2-Carboxy, 2-OH methyl CPCA (from RAM 34, 35, 6A) RAM 8A RAM 84	2-carboxy, 2-OH methyl CPCA glucuronide 2-carboxy, trans-2-OH methyl CPCA eliminated
44	CPCA glucuronide RAM 85	CPCA glucuronide eliminated
45	2-OH methyl CPCA glucuronide RAM 86	2-OH methyl CPCA glucuronide eliminated
46	3-OH methyl CPCA glucuronide RAM 87	3-OH methyl CPCA glucuronide eliminated
47	2-OH methyl-3-OH CPCA glucuronide RAM 88	2-OH methyl- 3-OH CPCA glucuronide eliminated
48	2-Carboxy CPCA glucuronide RAM 89	2-carboxy CPCA glucuronide eliminated
49	2-Carboxy, 2-OH methyl CPCA glucuronide RAM 90	2-carboxy, 2-OH methyl CPCA glucuronide eliminated

^a Preliminary estimates of liver V_{\max} ($\mu\text{mol h}^{-1} \text{kg}^{-1}$ bwt, unscaled) and K_m (μM) are equal to 10.0

^b Parent chemical or metabolite number for cross-reference in Table D11 ([Appendix D](#), cis/trans-Phenothrin)

^c Refer to Table D11 for structure based on number

Table E14 Biotransformation and elimination paths of Resmethrin and the resulting metabolites and preliminary liver V_{\max} and K_m values^a

Biotransformation and elimination paths		
No. ^b	Initiating pesticide/metabolite ^c	Resulting metabolite
1	Resmethrin	
	RAM1	BF alcohol + CPCA
	RAM 11	resmethrin eliminated
2	BF Alcohol	
	RAM 2	BF aldehyde
	RAM 12	BF alcohol eliminated
3	BF Aldehyde	
	RAM 3	BF acid
4	BF Acid	
	RAM 4	4'-OH BF acid
	RAM 5	4-OH BF acid
	RAM 6	α -OH BF acid
	RAM 7	BF acid glucuronide
	RAM 13	BF acid eliminated
5	4'-OH BF Acid	
	RAM 8	4'-OH BF acid glucuronide
	RAM 9	4'-OH BF acid sulfate
	RAM 14	4'-OH BF acid eliminated
6	4-OH BF Acid	
	RAM 15	4-OH BF acid eliminated
7	α -OH BF Acid	
	RAM 10	α -keto BF acid
	RAM 16	α -OH BF acid eliminated
8	α keto BF Acid	
	RAM 17	a-keto BF acid eliminated
9	BF Acid glucuronide	
	RAM 18	BF acid glucuronide eliminated
10	4'-OH BF Acid glucuronide	
	RAM 19	4'-OH BF acid glucuronide eliminated
11	4'-OH BF Acid sulfate	
	RAM 20	4'-OH BF acid sulfate eliminated
12	(<i>cis</i> or <i>trans</i>) CPCA (from RAM 1)	
	RAM 1A	3-OH methyl CPCA
	RAM 2A	CPCA glucuronic acid
	RAM 21	CPCA eliminated
13	3-OH methyl CPCA	
	RAM 3A	3-Aldehyde CPCA
	RAM 4A	3-OH methyl CPCA glucuronic acid
	RAM 22	3-OH methyl CPCA eliminated
14	3-Aldehyde CPCA	
	RAM 5A	2-carboxy CPCA (CCPCA)
15	(<i>cis</i> or <i>trans</i>) CCPCA	
	RAM 6A	CCPCA glucuronic acid
	RAM 23	CCPCA eliminated

(continued)

Table E14 (continued)

Biotransformation and elimination paths		
No. ^b	Initiating pesticide/metabolite ^c	Resulting metabolite
16	CPCA glucuronic acid RAM 24	CPCA glucuronic acid eliminated
17	3-OH methyl CPCA glucuronic acid RAM 25	3-OH methyl CPCA glucuronic acid eliminated
18	CCPCA glucuronic acid RAM 26	CCPCA glucuronic acid eliminated

^a Preliminary estimates of liver V_{\max} ($\mu\text{mol h}^{-1} \text{kg}^{-1}$ bwt, unscaled) and K_m (μM) are equal to 10.0

^b Parent chemical or metabolite number for cross-reference in Table D12 ([Appendix D](#), Resmethrin)

^c Refer to Table D12 for structure based on number

Table E15 Biotransformation and elimination paths of Tefluthrin and the resulting metabolites and preliminary liver V_{\max} , and K_m values^a

Biotransformation and elimination paths		
No. ^b	Initiating pesticide/ metabolite ^c	Resulting metabolite
1	Tefluthrin RAM 1 RAM 2 RAM 3 RAM 13	2-OH methyl tefluthrin 4-OH methyl tefluthrin Tefluthrin alcohol (+ TFP acid, RAM 3) Tefluthrin eliminated
2	2-OH methyl tefluthrin RAM 4 RAM 5 RAM 14	2-OH methyl, 4-OH methyl tefluthrin Tefluthrin alcohol (+ TFP OH methyl acid, RAM 5) 2-OH methyl tefluthrin eliminated
3	4-OH methyl tefluthrin RAM 6 RAM 15	2-OH methyl, 4-OH methyl tefluthrin 4-OH methyl tefluthrin eliminated
4	2-OH methyl, 4'-OH methyl tefluthrin RAM 7 RAM 8 RAM 16	Tetrafluoro-1,4-benzenediol (+ TFP OH methyl acid, RAM 7) Tetrafluoro-4-OH methyl benzoic acid (+ TFP OH methyl acid, RAM 8) 2-OH methyl, 4'-OH methyl tefluthrin eliminated
5	Tefluthrin alcohol (RAM 3 + RAM 5) (tetrafluoro-4-methyl-benzenemethanol) RAM 9 RAM 10 RAM 17	Tetrafluoro-4-methyl benzoic acid Tetrafluoro-4-methylphenyl glucuronic acid Tefluthrin alcohol eliminated
6	Tetrafluoro-1,4-benzenediol RAM 11 RAM 12 RAM 18	Tetrafluoro-4-OH methyl benzoic acid Tetrafluoro-4-OH-phenyl glucuronic acid Tetrafluoro-1,4-benzenediol eliminated
7	Tetrafluoro-4-methyl benzoic acid RAM 19	Tetrafluoro-4-methyl benzoic acid eliminated

(continued)

Table E15 (continued)

Biotransformation and elimination paths		
No. ^b	Initiating pesticide/ metabolite ^c	Resulting metabolite
8	Tetrafluoro-4-methylphenyl glucuronic acid RAM 20	Tetrafluoro-4-methylphenyl glucuronic acid eliminated
9	Tetrafluoro-4-OH methyl benzoic acid RAM 21	Tetrafluoro-4-OH methyl benzoic acid eliminated
10	Tetrafluoro-4-OH phenyl glucuronic acid RAM 22	Tetrafluoro-4-OH phenyl glucuronic acid eliminated
11	TFP acid (formed from RAM 3) RAM 1A RAM 23	Tefluthrin acid glucuronide Tefluthrin acid eliminated
12	2-OH methyl TFP acid (formed from RAM 5 + 7 + 8) RAM 2A RAM 24	2-OH methyl tefluthrin acid glucuronide 2-OH methyl tefluthrin acid eliminated
13	TFP acid glucuronide RAM 25	Tefluthrin acid glucuronide eliminated
14	2-OH methyl TFP acid glucuronide RAM 26	2-OH methyl tefluthrin acid glucuronide eliminated

^a Preliminary estimates of liver V_{\max} ($\mu\text{mol h}^{-1} \text{kg}^{-1}$ bwt, unscaled) and K_m (μM) are equal to 10.0

^b Parent chemical or metabolite number for cross-reference in Table D13 ([Appendix D](#), Tefluthrin)

^c Refer to Table D13 for structure based on number

Table E16 Biotransformation and elimination paths of cis, trans-Tetramethrin and the resulting metabolites and preliminary liver V_{\max} and K_m values^a

Biotransformation and elimination paths		
No. ^b	Initiating pesticide/ metabolite ^c	Resulting metabolite
1	(cis, trans)-Tetramethrin RAM 1 RAM 2 RAM 19	(cis, trans)-3-OH tetramethrin MTI + CPCA tetramethrin eliminated
2	(cis, trans) 3-OH tetramethrin RAM 3 RAM 20	cis, trans-3-aldehyde-tetramethrin cis, trans-3-OH NPY eliminated
3	(cis, trans)-3-aldehyde tetramethrin RAM 4	cis, trans-acid NPY
4	(cis, trans)-acid NPY (cis, trans-carboxy tetramethrin) RAM 5 RAM 21	(cis, trans)-acid NPY SA (cis, trans)-acid NPY eliminated
5	(cis, trans)-acid-NYP SA (trans-acid tetramethrin sulfonic acid) RAM 6 RAM 7 RAM 22	TPI-SA (cis, trans)-acid-7-OH NPY SA (cis, trans)-NPY SA eliminated
6	(cis, trans)-acid 7-OH NPY SA RAM 8 RAM 23	(cis, trans-carboxy, 7-OH-tetramethrin sulfonic acid) 7-OH-MTI-SA + 2-carboxy CPCA (cis, trans)-acid 7-OH NPY sulfonic acid eliminated

(continued)

Table E16 (continued)

Biotransformation and elimination paths		
No. ^b	Initiating pesticide/ metabolite ^c	Resulting metabolite
7	MTI (hydroxymethyl tetrahydrophthalimide)	
	RAM 9	TPI
	RAM 24	MTI eliminated
8	7-OH-MTI-SA (3-OH hydroxymethyl tetrahydrophthalimide sulfonic acid)	
	RAM 25	3-OH MTI SA eliminated
9	TPI (tetrahydrophthalimide)	
	RAM 10	TPI SA
	RAM 11	THAM
	RAM 12	HPI
	RAM 26	TPI eliminated
10	TPI-SA (tetrahydrophthalimide sulfonic acid)	
	RAM 27	TPI SA eliminated
11	THAM	
	RAM 13	THPA
	RAM 28	THAM eliminated
12	HPI (hydrophthalimide)	
	RAM 14	1-OH-5-OXO-HPA
	RAM 15	3-OH HPI-1-2
	RAM 16	TCDA
	RAM 29	HPI eliminated
13	THPA	
	RAM 17	TCDA
	RAM 18	3-OH HPI-1-2
	RAM 30	THPA eliminated
14	1-OH-5-oxo-HPA	
	RAM 31	1-OH-5-OXO-HPA eliminated
15	3-OH-HPI-1-2	
	RAM 32	3-OH-HPI-1-2 eliminated
16	TCDA (from RAM 15 + 16)	
	RAM 33	TCDA eliminated
17	1-OH-HPA	
	RAM 34	1-OH-HPA eliminated
18	(cis, trans)-CPCA (from RAM 2)	
	RAM 1A	3-OH methyl (cis, trans)-CPCA
	RAM 2A	(cis, trans)-CPCA glucuronic acid
	RAM 35	(cis, trans)-CPCA eliminated
19	3-OH methyl (cis, trans)-CPCA	
	RAM 3A	3-Aldehyde (cis, trans)-CPCA
	RAM 4A	3-OH methyl (cis, trans)-CPCA glucuronic acid
	RAM 36	3-OH methyl (cis, trans)-CPCA eliminated
20	3-Aldehyde (cis, trans)-CPCA	
	RAM 5A	2-Carboxy (cis, trans)-CPCA
	RAM 6A	3-Aldehyde (cis, trans)-CPCA glucuronic acid
	RAM 37	3-Aldehyde (cis, trans)-CPCA eliminated

(continued)

Table E16 (continued)

Biotransformation and elimination paths	
No. ^b	Initiating pesticide/ metabolite ^c
	Resulting metabolite
21	2-Carboxy (cis, trans)-CPCA (from RAM 7)
	RAM 7A 2-Carboxy (cis, trans)-CPCA glucuronic acid
	RAM 38 2-Carboxy (cis, trans)-CPCA eliminated
22	(cis, trans)-CPCA glucuronic acid
	RAM 39 (cis, trans)-CPCA glucuronic acid eliminated
23	3-OH methyl (cis, trans)-CPCA glucuronic acid
	RAM 40 3-OH methyl (cis, trans)-CPCA glucuronic acid eliminated
24	2-Carboxy (cis, trans)-CPCA glucuronide
	RAM 41 2-Carboxy (cis, trans)-CPCA glucuronic acid eliminated

^a Preliminary estimates of liver V_{\max} ($\mu\text{mol h}^{-1} \text{kg}^{-1}$ bwt, unscaled) and K_m (μM) are equal to 10.0

^b Parent chemical or metabolite number for cross-reference in Table D14 ([Appendix D](#), Tetramethrin)

^c Refer to Table D14 for structure based on number

Table E17 Biotransformation and elimination paths of Tralomethrin and the resulting metabolites and preliminary liver V_{\max} and K_m values^a

Biotransformation and elimination paths	
No. ^b	Initiating pesticide/ metabolite ^c
	Resulting metabolite
1	Tralomethrin
	RAM 1 Deltamethrin
	RAM 38 tralomethrin eliminated
1	Deltamethrin (numbering based on deltamethrin)
	RAM 2 4'-OH deltamethrin
	RAM 3 2'-OH deltamethrin
	RAM 4 5-OH deltamethrin
	RAM 5 2-OH methyl deltamethrin
	RAM 6 Cyanohydrin of PB aldehyde + dibromo CPCA
	RAM 39 Deltamethrin eliminated
2	4'-OH deltamethrin
	RAM 7 4'-OH, 2-OH Me, deltamethrin
	RAM 8 Cyanohydrin of 4'-OH PB aldehyde + dibromo CPCA
	RAM 40 4'-OH deltamethrin eliminated
3	2'-OH deltamethrin
	RAM 9 Cyanohydrin of 2'-OH PB aldehyde + dibromo CPCA
	RAM 41 2'-OH deltamethrin eliminated
4	5-OH deltamethrin
	RAM 10 Cyanohydrin of 5-OH PB aldehyde + dibromo CPCA
	RAM 42 5-OH deltamethrin eliminated
5	2-OH methyl deltamethrin
	RAM 11 2-OH Me, 4'-OH deltamethrin
	RAM 12 Cyanohydrin of PB aldehyde + 2-OH Me dibromo CPCA
	RAM 43 2-OH methyl deltamethrin eliminated
6	4'-OH, 2-OH Me deltamethrin
	RAM 13 Cyanohydrin of 4'-OH PB aldehyde + 2-OH Me dibromo CPCA
	RAM 44 2-OH Me, 4'-OH deltamethrin eliminated

(continued)

Table E17 (continued)

Biotransformation and elimination paths		
No. ^b	Initiating pesticide/ metabolite ^c	Resulting metabolite
7	Cyanohydrin of PB aldehyde RAM 14	PB aldehyde
8	Cyanohydrin of 4'-OH PB aldehyde RAM 15	4'-OH PB aldehyde
9	Cyanohydrin of 2'-OH PB aldehyde RAM 16	2'-OH PB aldehyde
10	Cyanohydrin of 5-OH PB aldehyde RAM 17	5-OH PB aldehyde
11	PB aldehyde RAM 18 RAM 19	PB alcohol PB acid
12	4'-OH PB aldehyde RAM 20 RAM 21	4'-OH PB alcohol 4'-OH PB acid
13	2'-OH PB aldehyde RAM 22 RAM 23	2'-OH PB alcohol 2'-OH PB acid
14	5-OH PB aldehyde RAM 24 RAM 25	5-OH PB alcohol 5-OH PB acid
15	PB alcohol RAM 26 RAM 45	PB alcohol glucuronic acid PB alcohol eliminated
16	4'-OH PB alcohol RAM 27 RAM 46	4'-OH PB alcohol glucuronic acid 4'-OH PB alcohol eliminated
17	2'-OH PB alcohol RAM 28 RAM 47	2'-OH PB alcohol glucuronic acid 2'-OH PB alcohol eliminated
18	5-OH PB alcohol RAM 29 RAM 48	5-OH PB alcohol glucuronic acid 5-OH PB alcohol eliminated
19	PB acid RAM 30 RAM 31 RAM 49	PB acid glucuronide PB acid glycine PB acid eliminated
20	4'-OH PB acid RAM 32 RAM 33 RAM 50	4'-OH PB acid glucuronide 4'-OH PB acid sulfate 4'-OH PB acid eliminated
21	2'-OH PB acid RAM 34 RAM 35 RAM 51	2'-OH PB acid glucuronide 2'-OH PB acid sulfate 2'-OH PB acid eliminated

(continued)

Table E17 (continued)

Biotransformation and elimination paths		
No. ^b	Initiating pesticide/ metabolite ^c	Resulting metabolite
22	5-OH PB acid	
	RAM 36	5-OH PB acid glucuronide
	RAM 37	5-OH PB acid sulfate
	RAM 52	5-OH PB acid eliminated
23	PB alcohol glucuronic acid	
	RAM 53	PB alcohol glucuronic acid eliminated
24	4'-OH PB alcohol glucuronic acid	
	RAM 54	4'-OH PB alcohol glucuronic acid eliminated
25	2'-OH PB alcohol glucuronic acid	
	RAM 55	2'-OH PB alcohol glucuronic acid eliminated
26	5-OH PB alcohol glucuronic acid	
	RAM 56	5-OH PB alcohol glucuronic acid eliminated
27	PB acid glucuronide	
	RAM 57	PB acid glucuronide eliminated
28	PB acid glycine	
	RAM 58	PB acid glycine eliminated
29	4'-OH PB acid glucuronide	
	RAM 59	4'-OH PB acid glucuronide eliminated
30	5-OH PB acid glucuronide	
	RAM 60	5-OH PB acid glucuronide eliminated
31	4'-OH PB acid sulfate	
	RAM 61	4'-OH PB acid sulfate eliminated
32	2'-OH PB acid sulfate	
	RAM 62	2'-OH PB acid sulfate eliminated
33	2-OH PB acid glucuronide	
	RAM 63	2-OH PB acid glucuronide eliminated
34	5-OH PB acid sulfate	
	RAM 64	5-OH PB acid sulfate eliminated
35	Dibromo-CPCA (from RAM 6, 8, 9 10)	
	RAM 1A	Dibromo CPCA glucuronide
	RAM 2A	2-OH Me dibromo CPCA
	RAM 65	Dibromo-CPCA eliminated
36	2-OH Me dibromo CPCA (RAM 12, 13) + (RAM 2A)	
	RAM 3A	2-OH Me dibromo CPCA glucuronide
	RAM 66	2-OH Me dibromo CPCA eliminated
37	Dibromo CPCA glucuronide	
	RAM 67	Dibromo CPCA glucuronide eliminated
38	2-OH Me dibromo CPCA glucuronide	
	RAM 68	2-OH Me dibromo CPCA glucuronide eliminated

^a Preliminary estimates of liver V_{\max} ($\mu\text{mol h}^{-1} \text{kg}^{-1}$ bwt, unscaled) and K_m (μM) are equal to 10.0

^b Parent chemical or metabolite number for cross-reference in Table D15 (Appendix D, Tralomethrin)

^c Refer to Table D15 for structure based on number

Appendix F: Allethrin PBPK/PD Model

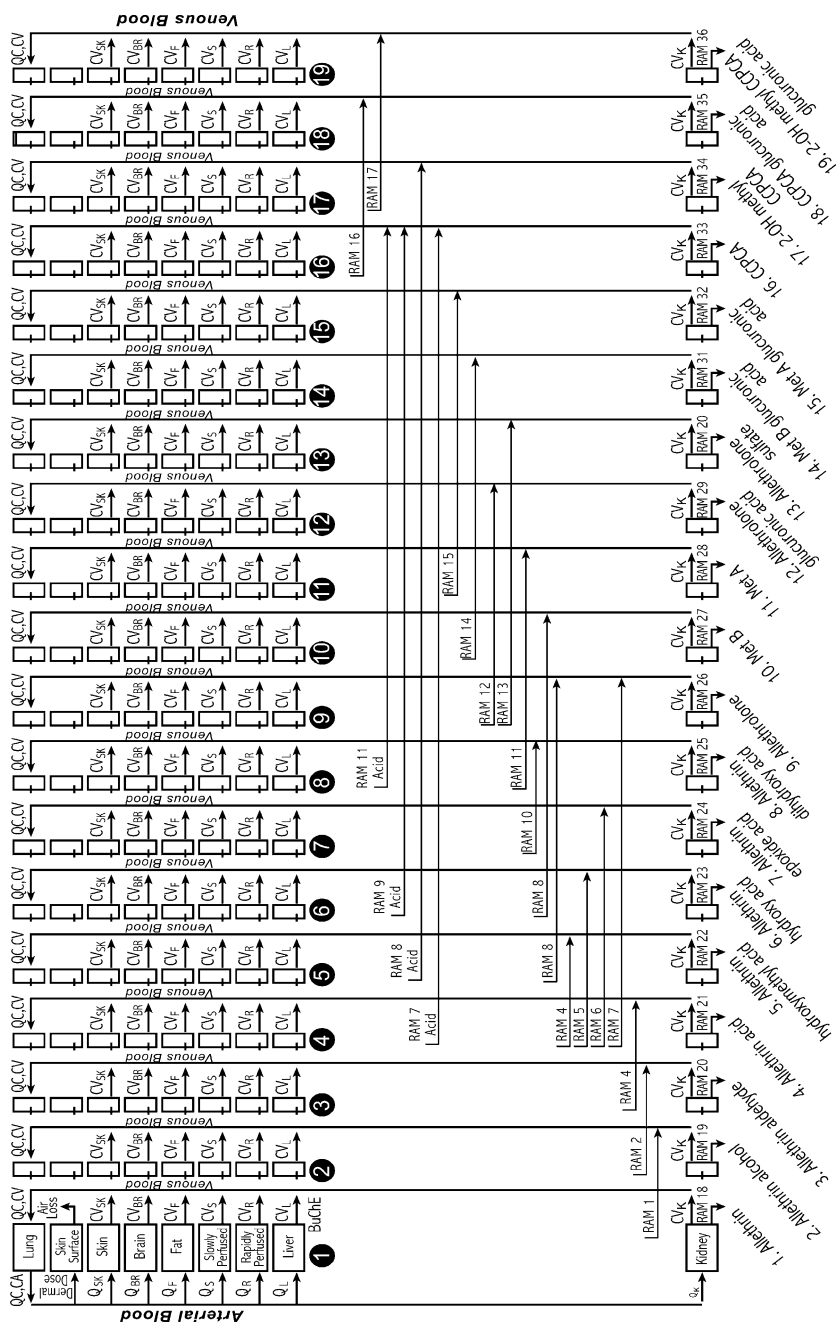


Fig. F1 Physiologically based pharmacokinetic/pharmacodynamic model for dermal exposure to allethrin

Index

Index for Rect Vol. 219

Abbreviations & acronyms, Appendix A, **219: 115**

Absorption modeling, GI (gastrointestinal) tract, **219: 24**

Absorption parameters, used in PBPK/PD models, **219: 24**

Acronyms & abbreviations, Appendix A, **219: 115**

Allethrin insecticide, water solubility vs. LogD (diag.), **219: 34**

Allethrin, in vivo metabolism, **219: 44**

Allethrin & metabolites, liver-blood partition coefficients, **219: 42**

Allethrin metabolites, water solubility vs. LogD (diag.), **219: 34**

Allethrin PBPK/PD model, depicted (Appendix F), **219: 251**

Analysis methods, chrysanthemic acids, **219: 18**

Analytical methods, for pyrethroid insecticide isomers, **219: 12**

Analyzing alcohol components, chrysanthemic acid derivatives, **219: 19**

Animal skin, chemical permeability, **219: 30**

Atomic force microscopy, biomembrane studies, **219: 82**

Bifenthrin, in vivo metabolism, **219: 44**

Biological parameters, assessing pyrethroid insecticide risk (table), **219: 2**

Biomembranes, ion channels, **219: 79**

Biomembranes, lipid structure, **219: 79**

Biomembranes, structure & drug permeability, **219: 79**

Biomembrane studies, atomic force microscopy, **219: 82**

Blood-partition coefficients, mechanistic models, **219: 33**

Calcium ion channels, pyrethroid insecticide neurotoxicity, **219: 87**

Carboxylesterase (hCE1) kinetics, deltamethrin hydrolysis (diag.), **219: 64**

Carboxylesterase hydrolysis, via hepatic microsomes (table), **219: 60**

Carboxylesterase kinetic parameters, deltamethrin hydrolysis (table), **219: 63**

Carboxylesterase (rat serum), stereoselective hydrolysis rates (table), **219: 76**

Carboxylesterases, metabolic enzymes, **219: 57**
Carboxylesterases, predicting liver & plasma activity, **219: 74**

Carboxylesterases, pyrethroid insecticide hydrolysis, **219: 59**

Carboxylesterases, their multiple forms, **219: 57**

Chemical expressions, Appendix A, **219: 118**

Chemicals, skin absorption, **219: 29**

Chiral components, pyrethrins & pyrethroid insecticides, **219: 17**

Chloride ion channels, pyrethroid insecticide neurotoxicity, **219: 87**

Chrysanthemic acid derivatives, analyzing alcohol components, **219: 19**

Chrysanthemic acid derivatives, pyrethroid insecticides (tables), **219: 19, 21**

Chrysanthemic acid derivatives, structures & names (table), **219: 19, 20**

Chrysanthemic acids, analytical chemistry, **219: 18**

Chrysanthemic acids, isomers, **219: 18**

Chrysanthemic acids, synthesis of pyrethroid insecticides, **219: 18**

- Cismethrin, sodium channel effect (diag.), **219: 83**
- Cyfluthrin, in vivo metabolism, **219: 45**
- Cyhalothrin effects, rotenone sensitive NADH (diag.), **219: 85**
- Cyhalothrin, in vivo metabolism, **219: 46**
- Cypermethrin, calculating tissue-blood partition coefficients, **219: 38**
- Cypermethrin insecticide, water solubility vs. LogD (diag.), **219: 35**
- Cypermethrin, in vivo metabolism, **219: 46**
- Cypermethrin & metabolites, liver-blood partition coefficients, **219: 43**
- Cypermethrin metabolites, water solubility vs. LogD (diag.), **219: 34**
- Cytochrome CYP 1A2 & 2C19 kinetic parameters, pyrethroid insecticides (table), **219: 70, 71**
- Cytochrome CYP 3A4 kinetic parameters, pyrethroid insecticides (table), **219: 72**
- Cytochrome P450 kinetic parameters, deltamethrin & esfenvalerate metabolism (table), **219: 65**
- Cytochrome P450s, metabolic enzymes, **219: 57**
- Cytochrome P450s, their multiple forms, **219: 58**
- DEET, pesticide absorption effects, **219: 32**
- Deltamethrin clearance, from liver microsomes (table), **219: 63**
- Deltamethrin hydrolysis, by enzymes (diag.), **219: 64**
- Deltamethrin hydrolysis, carboxylesterase kinetic parameters (table), **219: 63**
- Deltamethrin, in vivo metabolism, **219: 48**
- Deltamethrin, kinetic values compared, **219: 73**
- Deltamethrin metabolism, cytochrome P450 kinetic parameters (table), **219: 65**
- Deltamethrin, sodium channel effect (diag.), **219: 83**
- Dermal pesticide uptake, modeling, **219: 32**
- Discovery history, pyrethroid insecticides, **219: 6**
- Drug modeling, gut metabolism & transport, **219: 27**
- Drug permeability, biomembrane structure, **219: 79**
- Enterohepatic circulation, pesticide metabolism, **219: 27**
- Esfenvalerate clearance, from liver microsomes (table), **219: 63**
- Esfenvalerate metabolism, cytochrome P450 kinetic parameters (table), **219: 65**
- Fenpropathrin, in vivo metabolism, **219: 49**
- Fenvalerate, in vivo metabolism, **219: 49**
- Field reentry, pesticide exposure, **219: 30**
- Fluvalinate, in vivo metabolism, **219: 50**
- Gastrointestinal (GI) transit model, drug uptake (illus.), **219: 25**
- Gut metabolism, drug modeling, **219: 27**
- Gut transport, drug modeling, **219: 27**
- Human & rat liver microsomes, deltamethrin clearance rates (table), **219: 63**
- Human & rat liver microsomes, esfenvalerate clearance rates (table), **219: 63**
- Human risk assessment, QSAR & PBPK/PD models, **219: 1ff.**
- Hydrolase A kinetics, deltamethrin hydrolysis (diag.), **219: 64**
- Intestinal permeability, models, **219: 25**
- Intestinal permeability, pyrethroid insecticides, **219: 68**
- Ion channels, biomembranes, **219: 79**
- Ion permeation, lipid membranes (illus.), **219: 80**
- Kinetic parameters, deltamethrin & esfenvalerate metabolism (table), **219: 65**
- Kinetic parameters, in vitro *trans*-permethrin hydrolysis (table), **219: 61**
- Kinetics of activation, voltage dependence, **219: 81**
- Lipid membranes, ion permeation (illus.), **219: 80**
- Lipid structure, biomembranes, **219: 79**
- Liver-blood partition coefficients, allethrin & metabolites (diag.), **219: 42**
- Liver-blood partition coefficients, cypermethrin & metabolites (diag.), **219: 43**
- Liver cytochrome P450 hydroxylation, models, **219: 69**
- Liver & plasma enzyme activity, carboxylesterases, **219: 74**
- Mammalian targets, pyrethroid insecticides (table), **219: 80**
- Mammalian toxicity, pyrethroid insecticides, **219: 20**
- Mathematical expressions, Appendix A, **219: 118**
- Mechanisms, blood-partition coefficients, **219: 33**
- Mechanisms classed, pyrethroid insecticides (table), **219: 82**

- Mechanism studies, patch-clamp technique, **219: 81**
- Metabolic conjugation, pyrethroid insecticides, **219: 75**
- Metabolic enzymes, carboxylesterases, **219: 57**
- Metabolic hydrolysis, via hepatic microsomes (table), **219: 60**
- Metabolism in vitro parameters, pyrethroid insecticides (table), **219: 62**
- Metabolism in vitro, permethrin insecticide (table), **219: 61**
- Metabolism in vitro, pyrethroid insecticides, **219: 61**
- Metabolism in vivo, allethrin, **219: 44**
- Metabolism in vivo, bfenethrin, **219: 44**
- Metabolism in vivo, cyfluthrin, **219: 45**
- Metabolism in vivo, cyhalothrin, **219: 46**
- Metabolism in vivo, cypermethrin, **219: 46**
- Metabolism in vivo, deltamethrin, **219: 48**
- Metabolism in vivo, fenprothrin, **219: 49**
- Metabolism in vivo, fenvalerate, **219: 49**
- Metabolism in vivo, fluralinate, **219: 50**
- Metabolism in vivo, permethrin, **219: 50**
- Metabolism in vivo, phenothrin, **219: 52**
- Metabolism in vivo, pyrethroid insecticides, **219: 42**
- Metabolism in vivo, resmethrin, **219: 53**
- Metabolism in vivo, tefluthrin, **219: 54**
- Metabolism in vivo, tetramethrin, **219: 55**
- Metabolism in vivo, tralomethrin, **219: 56**
- Metabolism modeling, GI tract, **219: 24**
- Microsomes, substrate binding rates, **219: 64**
- Mitochondrial complex, pyrethroid neurotoxicity, **219: 84**
- Modeling dermal uptake, permethrin, **219: 32**
- Modeling GI absorption/metabolism, pyrethroid insecticides, **219: 24**
- Modeling hydroxylation, liver cytochrome P450, **219: 69**
- Models, tissue-blood partition coefficients, **219: 36**
- Models, tissue partition coefficients, **219: 33**
- Neurotoxicity effects, mitochondrial complex, **219: 84**
- Neurotoxicity of pyrethroids, sodium, calcium & chloride channels, **219: 87**
- Neurotoxicity, pyrethroid insecticides, **219: 86**
- Parameters defined, pyrethroid insecticide risk assessment, **219: 1**
- Parameters for risk assessment, QSAR-PBPK/PD models, **219: 1**
- Partition coefficient calculations, pyrethroid insecticides, **219: 41**
- Patch-clamp technique, mechanism studies, **219: 81**
- PBPK/PD models, parameters for human risk assessment, **219: 1ff.**
- PBPK/PD parameters, QSAR models, **219: 67**
- PBPK/PD (physiologically based pharmacokinetic/pharmacodynamic) models, derived absorption parameters, **219: 24**
- Permethrin effects, rat liver mitochondria (diag.), **219: 85**
- Permethrin effects, rotenone sensitive NADH (diag.), **219: 85**
- Permethrin insecticide, in vitro hydrolysis (table), **219: 61**
- Permethrin, in vivo metabolism, **219: 50**
- Pesticide absorption effects, DEET, **219: 32**
- Pesticide metabolism, enterohepatic circulation, **219: 27**
- Pesticide skin absorption, vehicle effects, **219: 31**
- Pesticides, skin absorption, **219: 32**
- Phenothrin, in vivo metabolism, **219: 52**
- Pyrethrin insecticide, description, **219: 2**
- Pyrethrin I & II, structures (diag.), **219: 5**
- Pyrethrin I, stereochemistry depicted (illus.), **219: 9**
- Pyrethrins I, stereodescriptors (diag.), **219: 8**
- Pyrethrins, chiral components described, **219: 17**
- Pyrethroid effects, mitochondrial complex, **219: 84**
- Pyrethroid insecticide acids, structures & names (table), **219: 19**
- Pyrethroid insecticide alcohols, structures & names (table), **219: 21**
- Pyrethroid insecticide analysis, isomer methods **219: 12**
- Pyrethroid insecticide binding to protein, QSAR models, **219: 67**
- Pyrethroid insecticide hydrolysis, carboxylesterases, **219: 59**
- Pyrethroid insecticide hydrolysis, carboxylesterases (table), **219: 60**
- Pyrethroid insecticide metabolism, aromatic leaving groups, **219: 75**
- Pyrethroid insecticide metabolism, conjugation, **219: 75**
- Pyrethroid insecticide neurotoxicity, sodium, calcium & chloride channels, **219: 87**
- Pyrethroid insecticide neurotoxicity, sodium channels, **219: 87**

- Pyrethroid insecticide risk, model parameters (table), **219**: 2
- Pyrethroid insecticides, acute rat toxicities (table), **219**: 22
- Pyrethroid insecticides, acute rat toxicity (illus.), **219**: 23
- Pyrethroid insecticides, calculated QikProp 3.0 values (table), **219**: 68
- Pyrethroid insecticides, calculating partition coefficients, **219**: 41
- Pyrethroid insecticides, chiral components described, **219**: 17
- Pyrethroid insecticides, chirality, isomers, technical products described (Appendix B), **219**: 121-129
- Pyrethroid insecticides, cytochrome CYP 1A2 & 2C19 kinetic parameters (table), **219**: 70
- Pyrethroid insecticides, cytochrome CYP 2C9 & 2D6 kinetic parameters (table), **219**: 71
- Pyrethroid insecticides, cytochrome CYP 3A4 kinetic parameters (table), **219**: 72
- Pyrethroid insecticides, description, **219**: 2
- Pyrethroid insecticides, discovery traced, **219**: 6
- Pyrethroid insecticides, human risk assessment models, **219**: 1ff.
- Pyrethroid insecticides, in vitro metabolism, **219**: 61
- Pyrethroid insecticides, intestinal permeability, **219**: 68
- Pyrethroid insecticides & isomers, chromatographic separation methods (Appendix C), **219**: 131-212
- Pyrethroid insecticides, isomers & technical products, **219**: 7
- Pyrethroid insecticides, mechanism classed (table), **219**: 82
- Pyrethroid insecticides, metabolic pathways (Appendix E), **219**: 213-250
- Pyrethroid insecticides, metabolism, **219**: 42
- Pyrethroid insecticides, modeling GI absorption/metabolism, **219**: 24
- Pyrethroid insecticides, multiple mammalian targets (table), **219**: 80
- Pyrethroid insecticides, neurotoxicity, **219**: 86
- Pyrethroid insecticides, QSAR & PBPK/PD models, **219**: 1ff.
- Pyrethroid insecticides, rat liver microsomal metabolism (table), **219**: 62
- Pyrethroid insecticides, skin permeation constants, **219**: 77
- Pyrethroid insecticides, skin permeation constants (table), **219**: 78
- Pyrethroid insecticides, stereochemistry, **219**: 9
- Pyrethroid insecticides, structures (table), **219**: 3
- Pyrethroid insecticide synthesis, alcohol components, **219**: 20
- Pyrethroid insecticide turnover numbers, rat vs. human carboxylesterases (diag.), **219**: 63
- Pyrethroid metabolism & neurotoxicity, discussion, **219**: 88-95
- QikProp 3.0 model values, pyrethroid insecticides (table), **219**: 68
- QSAR models, PBPK/PD parameters, **219**: 67
- QSAR models, pyrethroid binding to proteins, **219**: 67
- QSAR models, tissue-blood partition coefficients, **219**: 78
- QSAR-PBPK/PD (quantitative structure-activity relationship-physiologically based pharmacokinetic/pharmacodynamic) models, risk assessment, **219**: 1
- QSAR (quantitative structure-activity relationship) models, for human risk assessment, **219**: 1ff.
- Rat liver mitochondria, permethrin effects (diag.), **219**: 85
- Resmethrin, in vivo metabolism, **219**: 53
- Risk assessment models, pyrethroid insecticides, **219**: 1ff.
- Rotenone sensitive NADH, cyhalothrin effects (diag.), **219**: 85
- Rotenone sensitive NADH, permethrin effects (diag.), **219**: 85
- Skin absorption, chemicals, **219**: 29
- Skin absorption, factors affecting pesticide uptake, **219**: 32
- Skin absorption, pesticides, **219**: 32
- Skin-blood partitioning, process, **219**: 31
- Skin permeability, among animals, **219**: 30
- Skin permeation constants, pyrethroid insecticides, **219**: 77
- Skin permeation constants, pyrethroid insecticides (table), **219**: 78
- Sodium channel, concentration-dependent effects, **219**: 83
- Sodium channel effect, cismethrin & deltamethrin (diag.), **219**: 83

- Sodium channel effects, concentrations, **219**: 82
- Sodium channels, pyrethroid insecticide neurotoxicity, **219**: 87
- Stereochemistry described, pyrethroid insecticides, **219**: 9
- Stereoselective hydrolysis rates, rat serum carboxylesterase (table), **219**: 76
- Substrate binding rates, microsomes & P450s (diag.), **219**: 64
- Tefluthrin, in vivo metabolism, **219**: 54
- Tetramethrin, in vivo metabolism, **219**: 55
- Tissue-blood partition coefficients, cypermethrin (table), **219**: 38
- Tissue-blood partition coefficients, modeling, **219**: 36
- Tissue-blood partition coefficients, QSAR models, **219**: 78
- Tissue partition coefficients, modeling, **219**: 33
- Toxicity modeling, description, **219**: 67
- Toxicity to rats, pyrethroid insecticides, (illus.), **219**: 22
- Toxicity to rats, pyrethroid insecticides (table), **219**: 22
- Tralomethrin, in vivo metabolism, **219**: 56
- Vehicle effects, pesticide skin absorption, **219**: 31
- Voltage dependence, kinetics of activation, **219**: 81
- Worker exposure, pesticides from reentry, **219**: 30